doi:10.17596/0004154

R/V Mirai MR25-05C Cruise Report (MR25-Fujiwara)

Japan Agency for Marine-Earth Science and Technology
(JAMSTEC)

Contents

1. Cruise Summary

1.1 Cruise Information

Cruise ID: MR25-05C
Name of vessel: R/V Mirai
Title of project: Arctic Challenge for Sustainability III (ArCSIII)
Title of cruise: Observation cruise of ArCSIII
Chief Scientist: Amane Fujiwara [Japan Agency for Marine-Earth Science and Technology]
Cruise period: Aug 31 (Dutch Harbour, AK, USA) –Oct 5, 2025 (Shimizu, Shizuoka, Japan)
Ports of departure: Dutch Harbour / arrival: Shimizu
Research area: North Pacific, Bering Sea, Arctic Ocean
Research map

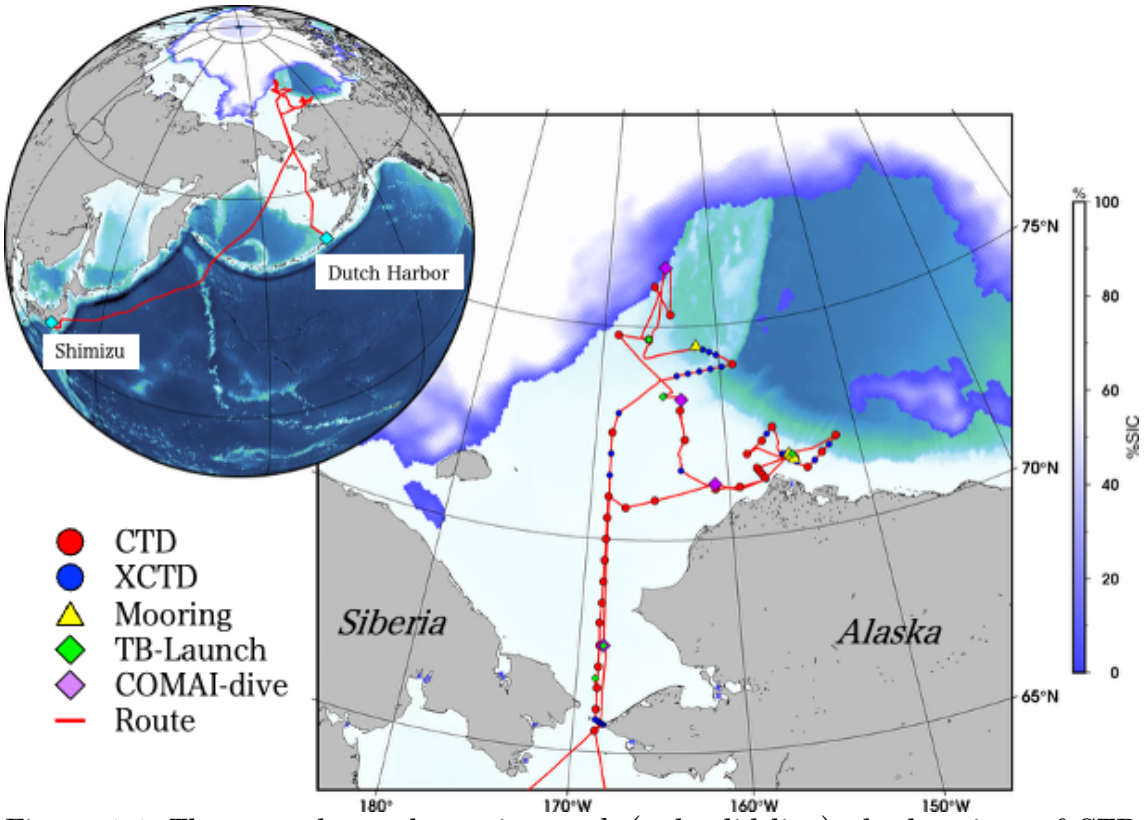

Figure 1-1. The map shows the cruise track (red solid line), the locations of CTD stations (red circle), XCTD deployment sites (blue circle), mooring deployment/recovery sites (yellow triangle), tethered balloon observation sites (green diamond), and underwater drone test dive sites (purple diamond). The white-blue color scale indicates the average sea-ice concentration from September 4 to 24 (during the observation period north of 65°N in the Arctic Ocean), derived from AMSR2/GCOM-W data.

1.2 Objectives

The Arctic Ocean is the area with the fastest rate of global oceanic warming in the world. The detailed research of the Research Vessel (R/V) MIRAI and other

icebreaker vessels, satellite observation and numerical modeling documented the impact of inflow of the Pacific origin water on Arctic sea ice decrease and the marine ecosystem, which is known as important sources of heat, nutrients, fresh water for the Arctic Ocean. Its impact is also getting greater and wide spreading into the entire Arctic. This cruise aims to develop the dataset that could allow for a synoptic view of the totality of hydrographic and ecosystem changes taking place in the Arctic Ocean and facilitate advancing model development to predict the future state of the Arctic.

In 2025, the R/V MIRAI conduct hydrographic, paleoenvironmental and biogeochemical surveys, including plankton, microplastic, and bottom sediment samplings, from the Chukchi, Beaufort, and East Siberian Seas to marginal ice zones of the Canada Basin. Moorings will be recovered and re-deployed on the pathway of the Pacific-origin water (Barrow Canyon and Northwind Abyssal Plain) to monitor its transport and impact on the marine ecosystem. In marginal ice zones, we will approach to sea-ice floes to measure marine environments by various sensors and to collect water, sea ice, plankton, and microplastic samples. An underwater drone (COMAI) will be launched from an ice-edge to ice-covered areas. Flying drones will be used to measure meteorological parameters and to assess the conditions of sea ice and waves. Various drifting buoys will be launched to measure the ocean waves, currents, and temperature.

1.3 Overview

We conducted meteorological and hydrographic surveys including marine biogeochemical samplings in the Pacific sector of the Arctic Ocean, the northern Bering Sea and the North Pacific Ocean on board the R/V Mirai from 31 August to 5 October 2025 under the framework of the Arctic Challenge for Sustainability III (ArCS III) Project (Figure 1-2). The research areas included the EEZ and the territorial sea of the USA. The observational activities consisted of CTD (Conductivity-Temperature-Depth) /water samplings, XCTD (eXpendable Conductivity-Temperature-Depth), bio-optical measurements, zooplankton net samplings, sediment samplings, incubation experiments, ship-board ocean current and surface water monitoring, sea ice sampling, meteorological measurements and samplings, aerosol observations, trials of an in-water drone, satellite observations, doppler radar, sea ice radar, sea bottom topography, gravity, and magnetic field measurements, and mooring and sediment trap recoveries and deployments (Figure 1-2).

In this cruise, we had 81 oceanographic stations (37 CTD and 44 XCTD stations), 24 zooplankton net sites, 16 sediment sampling sites, 4 sites for recoveries and deployments of hydrographic and sediment trap moorings. We also had 5 sites for tethered balloon launches and 22 sondes launch for meteorological and atmospheric observations. Continuous meteorological and oceanographic observations/samplings were carried out on the cruise track. We conducted the trial of an in-water drone, which is designed for oceanographic observation including under the sea ice (see section 3.4). We carried out a total of five YouTube livestreams to broadcast our onboard observations as part of our outreach activities (see section 3.6). These missions were successfully completed thanks to the great efforts made by the captain, ice pilot, officers, crews, and all the participants in this cruise (Photo 2-1). We would like to express our sincere appreciation to the United States Department of State

and the Alaska Fisheries Science Center of the NOAA National Marine Fisheries Service of the Department of Commerce of the United States for allowing us to conduct observations in the areas under their jurisdictions. Based on the data obtained in this cruise, we will be able to shed light on the Arctic change and its controlling factors and will contribute to global climate change studies.

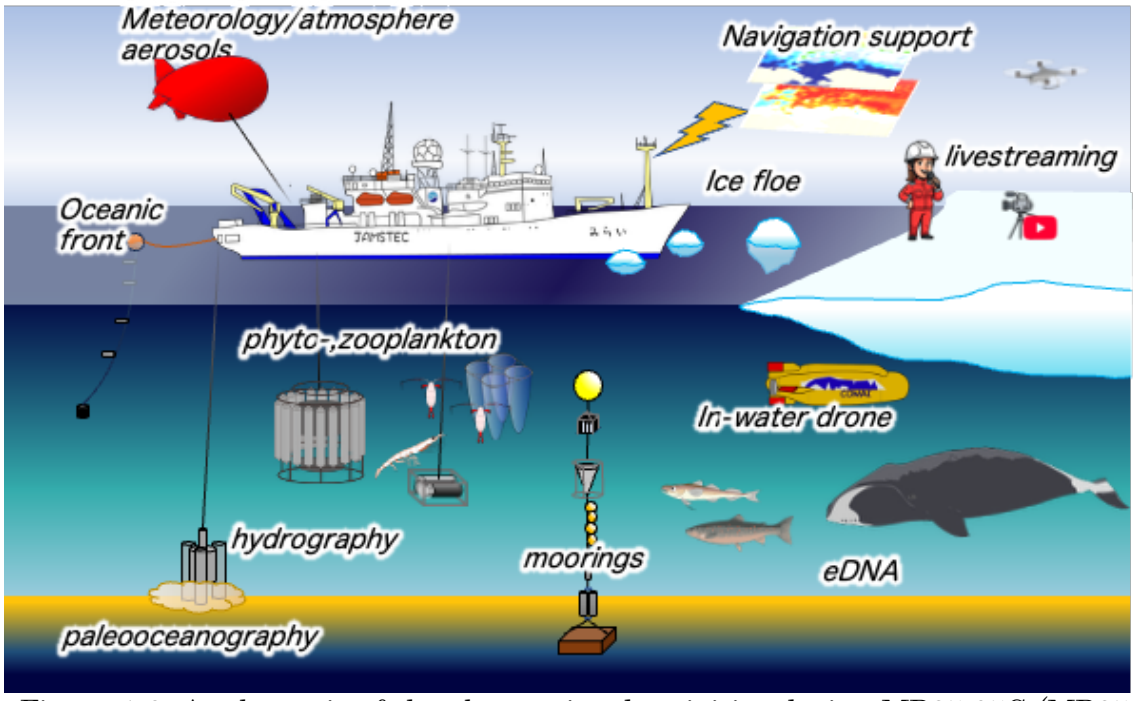

Figure 1-2: A schematic of the observational activities during MR25-05C (MR25-Fujiwara) cruise.

2. Research Proposal and Science Party

2.1 Title of proposal/Representative Personnel

1. Observational study of the Arctic environmental changes: Pacific-Arctic interaction, biogeochemical transport, mixing and marine ecosystem/Amane Fujiwara (JAMSTEC)
2. Research and development of under-ice observation technology/Hiroshi Yoshida (JAMSTEC)
3. Studies of elementary process at the Geochemical Atmosphere-Oceans cycle linking the climate change/Fumikazu Taketani
4. Quantification of the microplastic inventory in the waters of the western Arctic Ocean and microplastic influx from the Pacific Ocean/Takahito Ikenoue (JAMSTEC)
5. Feeding ecology of mesozooplankton analyzed by fatty acids/Kohei Matsuno (Hokkaido University)
6. Analysis of Arctic fish communities using environmental DNA/Akihide Kasai (Hokkaido University)
7. Effect of freshwater supply on pCO_2 and gas exchange process in the Arctic Ocean/Daiki Nomura (Hokkaido University)
8. Elucidation of carbon fixation from the surface water to the sediment/Takuhei Shiozaki (University of Tokyo)
9. Study on nutrient transport by Low-Density Pacific Water/Michiyo Kawai (Tokyo University of Marine Science and Technology)

2.2 Science Party

Table 2-1. List of onboard participants

Name	Affiliation	Occupation
FUJIWARA Amane	JAMSTEC	Chief Scientist/ Research Scientist
HATTA Mariko	JAMSTEC	Co-chief Scientist/ Senior Scientist
ONODERA Jonaotaro	JAMSTEC	Senior Scientist
KIMURA Satoshi	JAMSTEC	Research Scientist
SERVETAZ Aymeric	JAMSTEC	Research Scientist
FUKAI Yuri	JAMSTEC	Postdoctoral Researcher
MORI Akiko	National Institute of Polar Research	Assistant Professor
YAMAOKA Nobuyuki	MOL	Captain
YAMAGUCHI Taisei	JAMSTEC/The University of Tokyo	Research Assistant
YOSHIDA Hiroshi	JAMSTEC	Principal Scientist
ISHIBASHI Shojiro	JAMSTEC	Senior Scientist
TANAKA Kiyotaka	JAMSTEC	Project Senior Research Technician
SUGESAWA Makoto	JAMSTEC	Research Assistant
KINASE Takeshi	JAMSTEC	Project research technician
TAKETANI Fumikazu	JAMSTEC	Senior Researcher
IKENOUE Takahito*	JAMSTEC	Researcher
MATSUNO Kohei	Hokkaido University	Associate Professor
NOMURA Daiki	Hokkaido University	Professor
AKINO Ryota	Hokkaido University	Graduate Student
KAWAKAMI Tatsuya	Hokkaido University	Specially Appointed Associate Professor

KAMIYAMA Ikkan	Tokyo University of Marine Science and Technology	Graduate Student
SHIOZAKI Takuhei	The University of Tokyo	Associate Professor
MONTERO-SERRANO, Jean-Carlos	Université du Québec à Rimouski	Professor
SNIDER, David Duke	Martech Polar	Ice Pilot
OYAMA Ryo	Nippon Marine Enterprises	Chief Technical Staff
OGAWA Satomi	Nippon Marine Enterprises	Technical Staff
TAKAI Momoka	Nippon Marine Enterprises	Technical Staff
DOI Haruki	Nippon Marine Enterprises	Technical Staff
YOSHIDA Kazuhiro	Marine Works Japan	Chief Technical Staff
FUJIKI Nagisa	Marine Works Japan	Technical Staff
ARIHARA Ko	Marine Works Japan	Technical Staff
ORUI Masahiro	Marine Works Japan	Technical Staff
USHIROMURA Hiroki	Marine Works Japan	Technical Staff
YODA Aine	Marine Works Japan	Technical Staff
FUJIOKA Riho	Marine Works Japan	Technical Staff
ARII Yasuhiro	Marine Works Japan	Technical Staff
ARIGA Shiori	Marine Works Japan	Technical Staff
KUWAHARA Misato	Marine Works Japan	Technical Staff
MIYOSHI Yuko	Marine Works Japan	Technical Staff
IZUTSU Takuya	Marine Works Japan	Technical Staff
NAKAMURA Tomoki	Marine Works Japan	Technical Staff
FUJITA Kengo	Marine Works Japan	Technical Staff
SANO Mariko	Marine Works Japan	Technical Staff
KAZUNO Natsumi	Marine Works Japan	Technical Staff
ADACHI Nahoko	Marine Works Japan	Technical Staff

*canceled

Table 2-2. List of crew member

Name	Rank/Ratings
TSUJI Akihisa	Master
CHIBA Masato	Chief Officer
MATSUSHITA Hirosada	1st Officer
KANAYAMA Keiji	Jr.1st Officer
SAKURAI Natsuko	2nd Officer
KATO Hiroyuki	3rd Officer
FUNAE Koji	Chief Engineer
TAKAHASHI Jun	1st Engineer
TAKEYA Genta	2nd Engineer
KOGA Tomoya	3rd Engineer
MURAKAMI Masanori	Chief Radio Operator
KUDO Kazuyoshi	Boatswain
SATO Tsuyoshi	Quarter Master
KOMATA Shuji	Quarter Master
ISHII Yukito	Quarter Master
OKUBO Hideyuki	Quarter Master
TANIKAWA Masaya	Quarter Master
UEHARA Shohei	Quarter Master
ISOBE Keisuke	Quarter Master

SUMOMOZAWA Kazuya	Sailor
KUME Ryota	Sailor
HARADA Ryu	Sailor
TANIGUCHI Daisuke	No.1 Oiler
ANDO Kazuya	Oiler
WATANABE Takuya	Oiler
UCHIYAMA Tsuyoshi	Oiler
MARUYAMA Kyotaro	Assistant Oiler
AKIYOSHI Yuta	Assistant Oiler
MURAKAMI Toru	Chief Steward
ASANO Toshiyuki	Steward
SUZUKI Kentaro	Steward
MURAKAMI Kanjuro	Steward
KASHIWAGI Koichiro	Steward
HANGAI Yuta	Steward

Photo 2-1. Group photo of the MR25-05C cruise.

3. Research/Development Activities

3.1 Meteorology/Atmospheric Biogeochemistry

3.1.1 Reception experiment of GPS augmentation data by Quasi-Zenith Satellite - Evaluation of performance of the DFMC SBAS from QZSS

(1) Personnel
Toru Takahashi (ENRI)

(2) Objectives
The aviation and maritime activities in the Arctic are growing with the recession of the Arctic Sea ice. A model study suggested that the Global Navigation Satellite System (GNSS), which operates with the augmentation system such as the Satellite-based augmentation systems (SBAS) and Advanced Receiver Autonomous Integrity Monitoring (ARAIM), is effective for the navigation of aviation and maritime in the Arctic because of poor infrastructures (Reid et al., 2016). However, the current L1 SBAS broadcasts augmentation messages from geostationary (GEO) satellites, which are not available practically in the polar region at a latitude of 72 degrees or higher.
The Dual Frequency Multi Constellation Satellite Based Augmentation System (DFMC SBAS) has been standardized by the International Civil Aviation Organization (ICAO). Broadcasting augmentation messages from the Inclined Geosynchronous Orbit (IGSO) satellite is included in the future updates. The Electronic Navigation Research Institute (ENRI) developed the DFMC SBAS prototype based on the draft standards (Kitamura et al., 2018), and test messages are broadcasted from the Japanese Quasi-Zenith Satellite System (QZSS).
In the polar region, an auroral activity often generates the irregularity ionospheric plasma density and the ionospheric electric filed is intensified simultaneously. The carrier phase of the GNSS signal fluctuates by auroral activity. Since fluctuation sometimes causes the loss of lock on GNSS signals, the impact the auroral activity on the GNSS carrier phase should be investigated.
The main objective of this study is to evaluate the performance DFMC SBAS broadcasted from Japanese QZSS in the Arctic and high latitude regions. To test the DFMC SBAS in the Arctic, we installed the GNSS antenna, GNSS receivers, and DFMC SBAS receivers to oceanographic research vessel MIRAI.

(3) Activities (observation, sampling, development)
Signals from GNSS satellites and DFMC SBAS messages transmitted from the QZSS are recorded by GNSS receivers installed in MIRAI. Performance (accuracy and integrity) of the DFMC SBAS from QZSS is evaluated in the on-board environment in the Arctic region.

i. GNSS Receiver
A JAVAD DELTA receiver recorded signals from GPS, Galileo, GLONASS, BeiDou, and QZSS at the frequency of L1, L2, and L5 bands. The receiver recorded the observation message, including the pseudorange and carrier phase, with a sampling rate of 1 Hz. The navigation message, including the satellite obit information

ii. DFMC SBAS Message receivers
To obtain DFMC SBAS messages, a Furuno prototype DFMC SBAS receiver and CORE Cohac receivers were installed. The DFMC SBAS messages were generated by Electronic Navigation Research Institute (ENRI) and broadcasted from QZS02 and OZS04 satellites with a frequency of 1 Hz.

iii. Scintillation receiver
The GNSS signals are sometimes fluctuated by a combination of the ionospheric irregularity and electric field. The fluctuation is called scintillation and becomes a cause of the loss-of-lock GNSS signal. Since we need to receive the carrier phase with high and precise sampling to observe the scintillation, the Septentrio PolaRx5S, which records the GNSS signals with a sampling rate of 50

iv. GNSS Antenna
The GNSS antenna used was a Trimble GA830 capable of receiving L1, L2, and L5 bands. The antenna was designed for maritime and cold weather specifications.

The GNSS signals were successfully received by JAVAD DELTA and Septentrio PolaRx5S. The DFMC SBAS message was recorded by the Furuno prototype receiver and CORE Cohac, but the messages were not sometime recorded. This was likely to be caused by the ionospheric scintillation or visibility of the satellite.

(4) References
Kitamura, M., Aso, T., & Sakai, T. (2018) Wide Area Augmentation Performance of DFMC SBAS Using Global Monitoring Stations, The 16th IAIN World Congress 2018.
Reid, T., Walter, T., Blanch, J., & Enge, P. (2016) GNSS Integrity in The Arctic. NAVIGATION, 63: 469– 492. doi: 10.1002/navi.169.

(5) Data archives
These data obtained in this cruise will be submitted to the Data Management Group of JAMSTEC, and will be opened to the public via "Data Research System for Whole Cruise Information in JAMSTEC (DARWIN)" in JAMSTEC web site.
<https://www.godac.jamstec.go.jp/darwin/en/>

3.1.2. Surface Meteorological Observations

(1) Personnel

Amane Fujiwara	JAMSTEC -PI
Ryo Oyama	NME(Nippon Marine Enterprises, Ltd.)
Satomi Ogawa	NME
Haruki Doi	NME
Seika Takai	NME
Masanori Murakami	MIRAI Crew

(2) Objectives
Surface meteorological parameters are observed as a basic dataset of the meteorology. These parameters provide the temporal variation of the meteorological condition

surrounding the ship.

(3) Parameters
MIRAI Surface Meteorological (SMet) system measured parameters are listed in Table 3.1.2-1.

Table 3.1.2-1: Parameters of MIRAI SMet system

Parameter	Units	Remarks
1 Latitude	degree	
2 Longitude	degree	
3 Ship's speed	knot	MIRAI log
4 Ship's heading	degree	MIRAI gyro
5 Relative wind speed	m/s	6sec./10min. averaged
6 Relative wind direction	degree	6sec./10min. averaged
7 True wind speed	m/s	6sec./10min. averaged
8 True wind direction	degree	6sec./10min. averaged
9 Barometric pressure	hPa	adjusted to sea surface level 6sec. averaged
10 Air temperature (starboard)	degC	6sec. averaged
11 Air temperature (port)	degC	6sec. averaged
12 Dewpoint temperature (starboard)	degC	6sec. averaged
13 Dewpoint temperature (port)	degC	6sec. averaged
14 Relative humidity (starboard)	%	6sec. averaged
15 Relative humidity (port)	%	6sec. averaged
16 Sea surface temperature	degC	6sec. averaged
17 Precipitation intensity (optical rain gauge)	mm/hr	hourly accumulation
18 Precipitation (capacitive rain gauge)	mm/hr	hourly accumulation
19 Downwelling shortwave radiation	W/m^2	6sec. averaged
20 Downwelling infra-red radiation	W/m^2	6sec. averaged
21 Significant wave height (bow)	m	hourly
22 Significant wave height (stern)	m	hourly
23 Significant wave period (bow)	second	hourly
24 Significant wave period (stern)	second	hourly

Shipboard Oceanographic and Atmospheric Radiation (SOAR) system measured parameters are listed in Table 3.1.2-2.

Table 3.1.2-2: Parameters of SOAR system (JamMet)

Parameter	Units	Remarks
1 Latitude	degree	
2 Longitude	degree	
3 SOG	knot	
4 COG	degree	
5 Relative wind speed	m/s	
6 Relative wind direction	degree	
7 Barometric pressure	hPa	
8 Air temperature	degC	
9 Relative humidity	%	

10 Precipitation intensity (optical rain gauge)	mm/hr	
11 Precipitation (capacitive rain gauge)	mm/hr	reset at 50 mm
12 Down welling shortwave radiation	W/m^2	
13 Down welling infra-red radiation	W/m^2	
14 Defuse irradiance	W/m^2	
15 PAR	microE/cm^2/sec	
16 UV 305 nm	microW/cm^2/nm	
17 UV 320 nm	microW/cm^2/nm	
18 UV 340 nm	microW/cm^2/nm	
19 UV 380 nm	microW/cm^2/nm	

(4) Instruments and methods
In this cruise, the two systems for the observation were used.
SMet system
Instruments of SMet system are listed in Table 3.1.2-3. Data were collected and processed by KOAC-7800 weather data processor made by Koshin-Denki, Japan. The data set consists of 6 seconds averaged data.

Table 3.1.2-3: Instruments and installation locations of SMet system

Sensors	Type	Manufacturer	Location (altitude from surface)
Anemometer	KS-5900	Koshin Denki, Japan	Foremast (25 m)
Tair/RH with aspirated radiation shield	HMP155 43408 Gill	Vaisala, Finland R.M. Young, U.S.A.	Compass deck (21 m) starboard and port side
Thermometer: SST	RFN2-0	Koshin Denki, Japan	4th deck (-1m, inlet -5m)
Barometer	Model-370	Setra System, U.S.A.	Captain deck (13 m) Weather observation room
Capacitive rain gauge	50202	R. M. Young, U.S.A.	Compass deck (19 m)
Optical rain gauge	ORG-815DS	Osi, USA	Compass deck (19 m)
Radiometer (short wave)	MS-802	Eko Seiki, Japan	Radar mast (28 m)
Radiometer (long wave)	MS-202	Eko Seiki, Japan	Radar mast (28 m)
Wave height meter	WM-2	Tsurumi-seiki, Japan	Bow (10 m) Stern (8m)

SOAR measurement system
SOAR system designed by BNL (Brookhaven National Laboratory, USA) consists of major five parts.

a) Analog meteorological data sampling with CR1000 logger manufactured by Campbell Scientific Inc. Canada – wind, pressure, and rainfall (by a capacitive rain gauge) measurement.
b) Digital meteorological data sampling from individual sensors - air

temperature, relative humidity and precipitation (by optical rain gauge (ORG)) measurement.
c) Radiation data sampling with CR1000X logger manufactured by Campbell Inc. and radiometers with ventilation unit manufactured by Hukseflux Thermal Sensors B.V. Netherlands – short and long wave downward radiation measurement.
d) Photosynthetically Available Radiation (PAR) sensor manufactured by Biospherical Instruments Inc. (USA) - PAR measurement.
e) Scientific Computer System (SCS) developed by NOAA (National Oceanic and Atmospheric Administration, USA) - centralized data acquisition and logging of all data sets.

SCS recorded radiation, air temperature, relative humidity, CR1000 and ORG data. SCS composed Event data (JamMet) from these data and ship's navigation data every 6 seconds. Instruments and their locations are listed in Table 3.1.2-4.

Table 3.1.2-4: Instruments and installation locations of SOAR system

Sensors (Meteorological)	Type	Manufacturer	Location (altitude from surface)
Anemometer	05106	R.M. Young, USA	Foremast (25 m)
Barometer with pressure port	PTB210 61002 Gill	VAISALA, Finland R.M. Young, USA	Foremast (23 m)
Rain gauge	50202	R.M. Young, USA	Foremast (24 m)
Tair/RH with aspirated radiation shield	HMP155 43408 Gill	VAISALA, Finland R.M. Young, USA	Foremast (23 m)
Optical rain gauge	ORG-815DR	Osi, USA	Foremast (24 m)

Sensors (Radiation)	Type	Manufacturer	Location *
Radiometer (short wave) with ventilation unit	SR20 VU01	Hukseflux Thermal Sensors B.V., Netherlands	Foremast (25 m)
Radiometer (long wave) with ventilation unit	IR20 VU01	Hukseflux Thermal Sensors B.V., Netherlands	Foremast (25 m)

Sensor (PAR&UV)	Type	Manufacturer	Location (altitude from surface)
PAR&UV sensor	PUV-510	Biospherical Instrum ents Inc., USA	Navigation deck (18m)

For the quality control as post processing, we checked the following sensors, before and after the cruise.
Young Rain gauge (SMet and SOAR)
Inspect of the linearity of output value from the rain gauge sensor to change Input value by adding fixed quantity of test water.
Barometer (SMet and SOAR)
Comparison with the portable barometer value, PTB220, VAISALA
Thermometer (air temperature and relative humidity) (SMet and SOAR)

Comparison with the portable thermometer value, HM70, VAISALA

(5) Observation log
31 Aug. 2025 - 05 Oct. 2025

(6) Preliminary results
Figure. 3.1.2-1 shows the time series of the following parameters;
Wind (SMet)
Air temperature (SMet)
Relative humidity (SMet)
Precipitation (SOAR, ORG)
Short / Long wave radiation (SOAR)
Pressure (SMet)
Sea surface temperature (SMet)
Significant wave height (SMet)

(7) Data archives
These data obtained in this cruise will be submitted to the Data Management Group of JAMSTEC, and will be opened to the public via "Data Research System for Whole Cruise Information in JAMSTEC (DARWIN)" in JAMSTEC web site.
<https://www.godac.jamstec.go.jp/darwin/en/>

(8) Remarks
The following period, Sea surface temperature of SMet data were available.
00:29UTC 01 Sep. 2025 - 06:34UTC 03 Oct. 2025

The following time, increasing of SMet capacitive rain gauge data were invalid due to MF/HF radio transmission.
23:55UTC 31 Aug. 2025
01:12UTC 28 Sep. 2025

The following period, SMet wind speed/direction data were invalid.
06:52UTC 10 Sep. 2025 - 07:05UTC 10 Sep. 2025

The following period, SMet wind speed/direction were measured by the vane anemometer on the foremast.
03:00UTC 11 Sep. 2025 - 00:46UTC 24 Sep. 2025

The following periods, SOAR PAR and UV data were invalid due to system trouble.
18:29:22UTC 01 Sep. 2025 - 05:05:00UTC 02 Sep. 2025
06:15:24UTC - 08:23:01UTC 04 Sep. 2025
08:36:25UTC - 19:48:20UTC 04 Sep. 2025

The following periods, SOAR wind speed/direction data were invalid.
07:48UTC - 20:13UTC 13 Sep. 2025
05:32UTC - 10:37UTC 14 Sep. 2025
11:50UTC - 21:20UTC 19 Sep. 2025

The following periods, SOAR optical rain gauge data were doubtful due to the influence of rough wave splash and strong wind.
09:06UTC - 23:30UTC 27 Sep. 2025
00:22UTC - 01:36UTC 28 Sep. 2025
03:38UTC - 04:03UTC 28 Sep. 2025
06:53UTC - 08:55UTC 28 Sep. 2025

The following period, SOAR ORG, pressure, CRG and radiation data were invalid due to system trouble.
04:22UTC - 04:25UTC 04 Oct. 2025

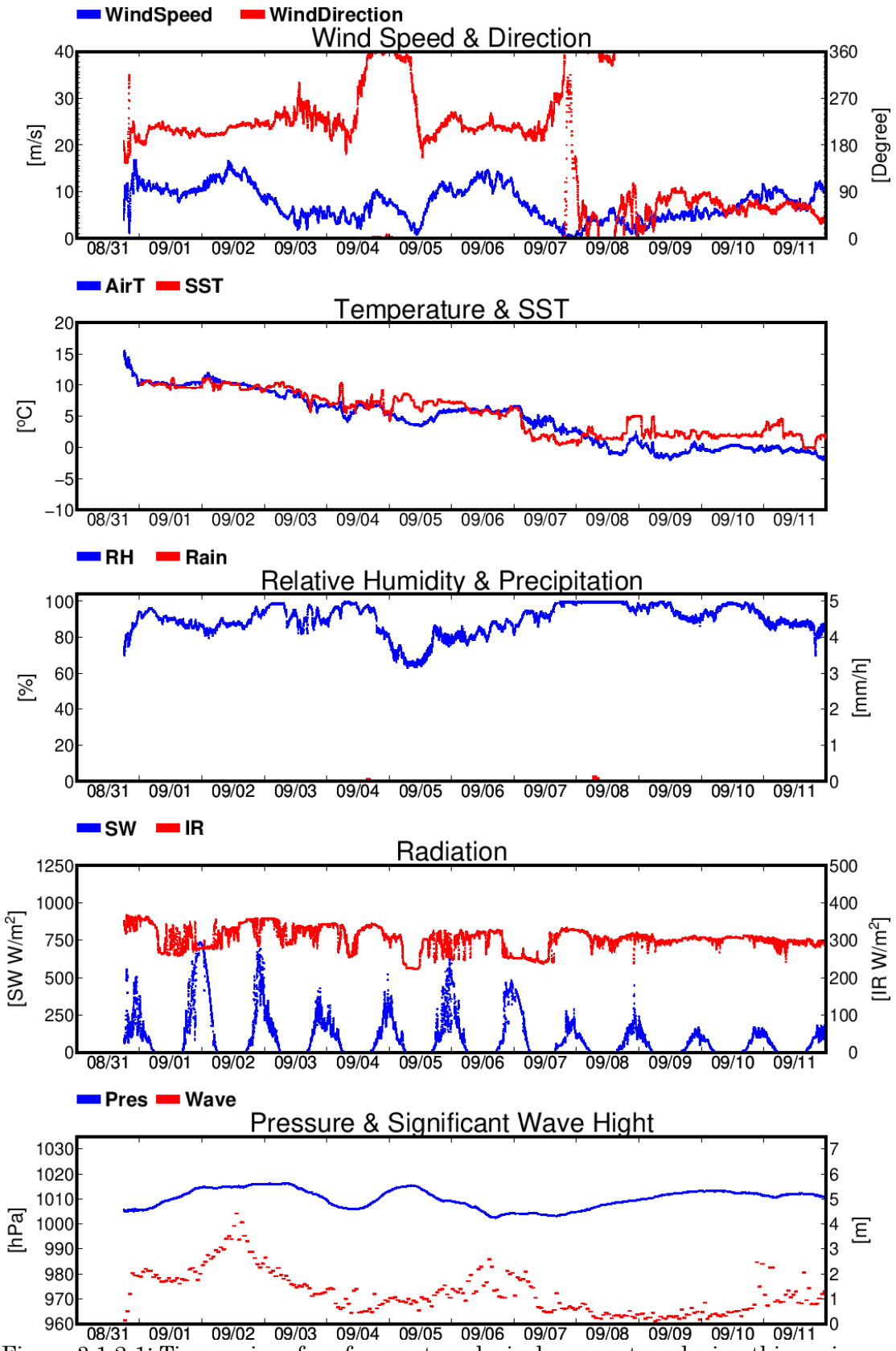

Figure 3.1.2-1: Time series of surface meteorological parameters during this cruise

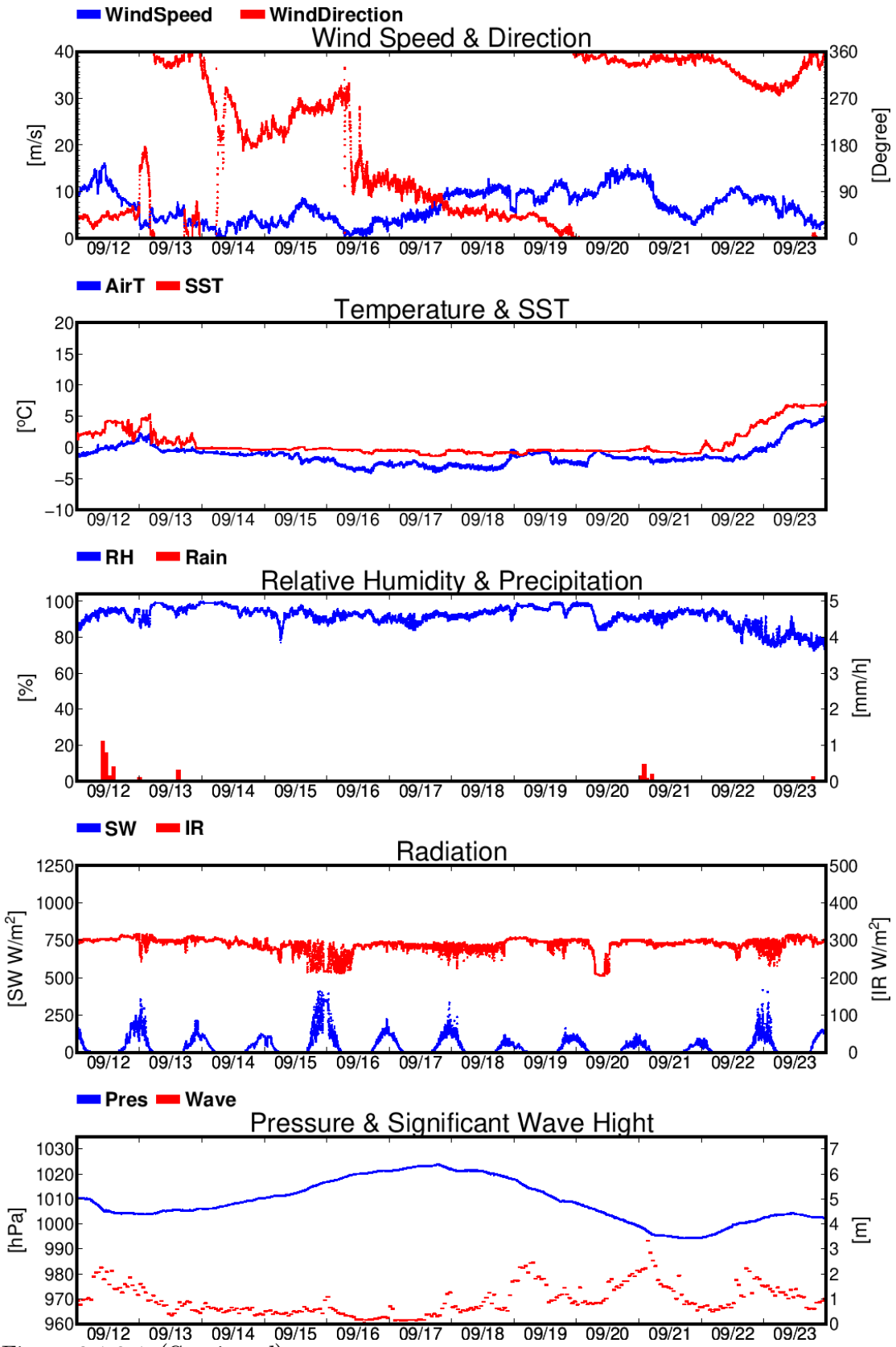

Figure 3.1.2-1: (Continued)

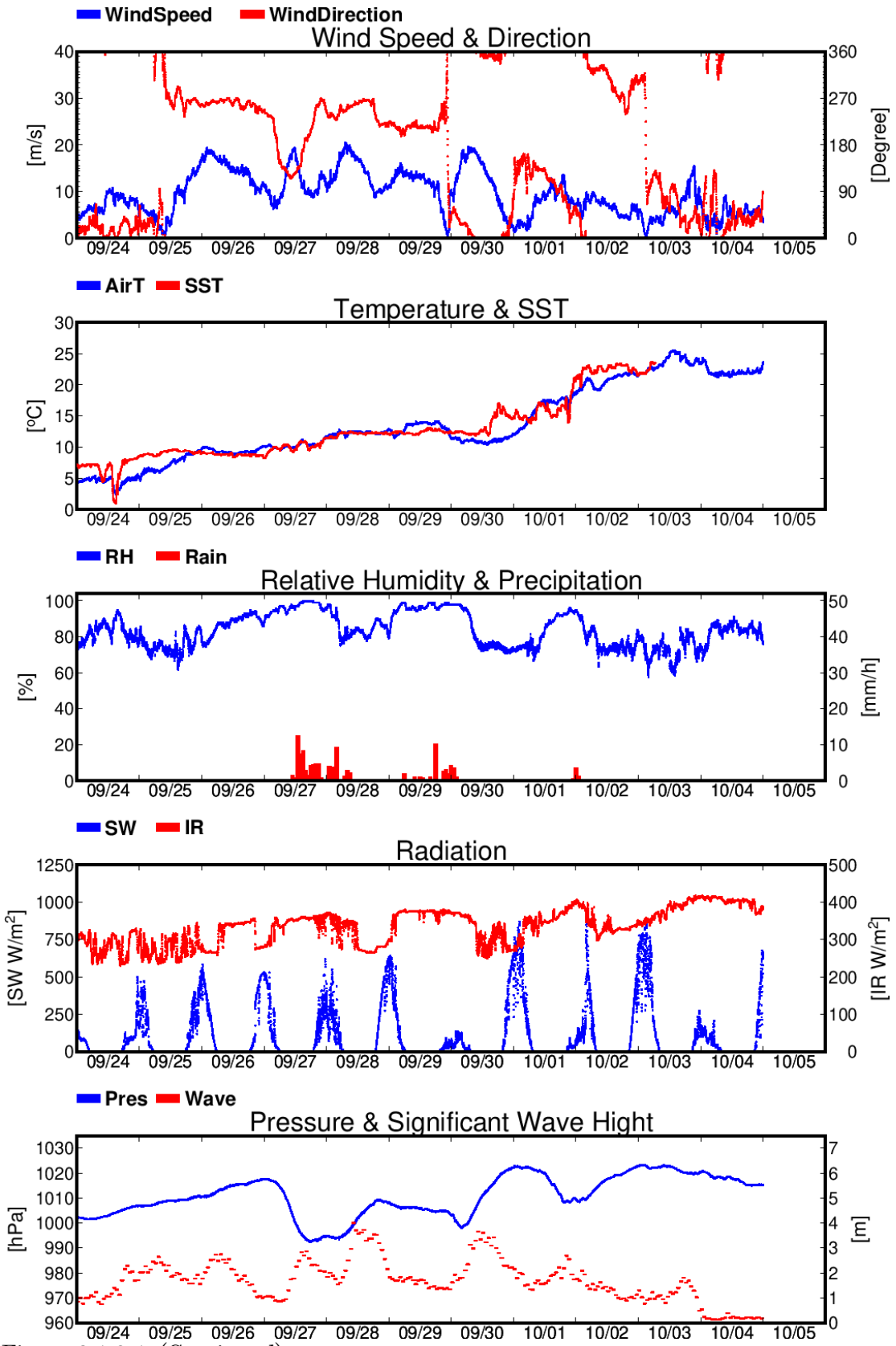

Figure 3.1.2-1: (Continued)

3.1.3. Ceilometer

(1) Personnel

Amane Fujiwara	JAMSTEC -PI
Ryo Oyama	NME(Nippon Marine Enterprises, Ltd.)
Satomi Ogawa	NME
Haruki Doi	NME
Seika Takai	NME
Masanori Murakami	MIRAI Crew

(2) Objectives

The information of cloud base height and the liquid water amount around cloud base is important to understand the process on formation of the cloud. As one of the methods to measure them, the ceilometer observation was carried out.

(3) Parameters

Cloud base height [m].
Backscatter profile, sensitivity and range normalized at 10 m resolution.
Estimated cloud amount [oktas] and height [m]; Sky Condition Algorithm.

(4) Instruments and methods

Cloud base height and backscatter profile were observed by ceilometer (CL51, VAISALA, Finland). The measurement configurations are shown in Table 3.1.3-1. On the archive dataset, cloud base height and backscatter profile are recorded with the resolution of 10 m.

Table 3.1.3-1: The measurement configurations

Property	Description
Laser source	Indium Gallium Arsenide (InGaAs) Diode
Transmitting center wavelength	910±10 nm at 25 degC
Transmitting average power	19.5 mW
Repetition rate	6.5 kHz
Detector	Silicon avalanche photodiode (APD)
Responsibility at 905 nm	65 A/W
Cloud detection range	0 ~ 13 km
Measurement range	0 ~ 15 km
Resolution	10 m in full range
Sampling rate	36 sec.
Sky Condition	Cloudiness in octas (0 ~ 9) 0 Sky Clear 1 Few 3 Scattered 5-7 Broken 8 Overcast 9 Vertical Visibility

(5) Observation log

31 Aug. 2025 - 05 Oct. 2025

(6) Preliminary results
Figure 3.1.3-1 shows the time-series of the lowest, second and third cloud base height during the cruise.

(7) Data archives
These data obtained in this cruise will be submitted to the Data Management Group of JAMSTEC, and will be opened to the public via "Data Research System for Whole Cruise Information in JAMSTEC (DARWIN)" in JAMSTEC web site.
<https://www.godac.jamstec.go.jp/darwin/en/>

(8) Remarks
Window cleaning
21:55UTC 05 Sep. 2025
19:29UTC 12 Sep. 2025
22:49UTC 19 Sep. 2025
01:33UTC 27 Sep. 2025
04:43UTC 03 Oct. 2025

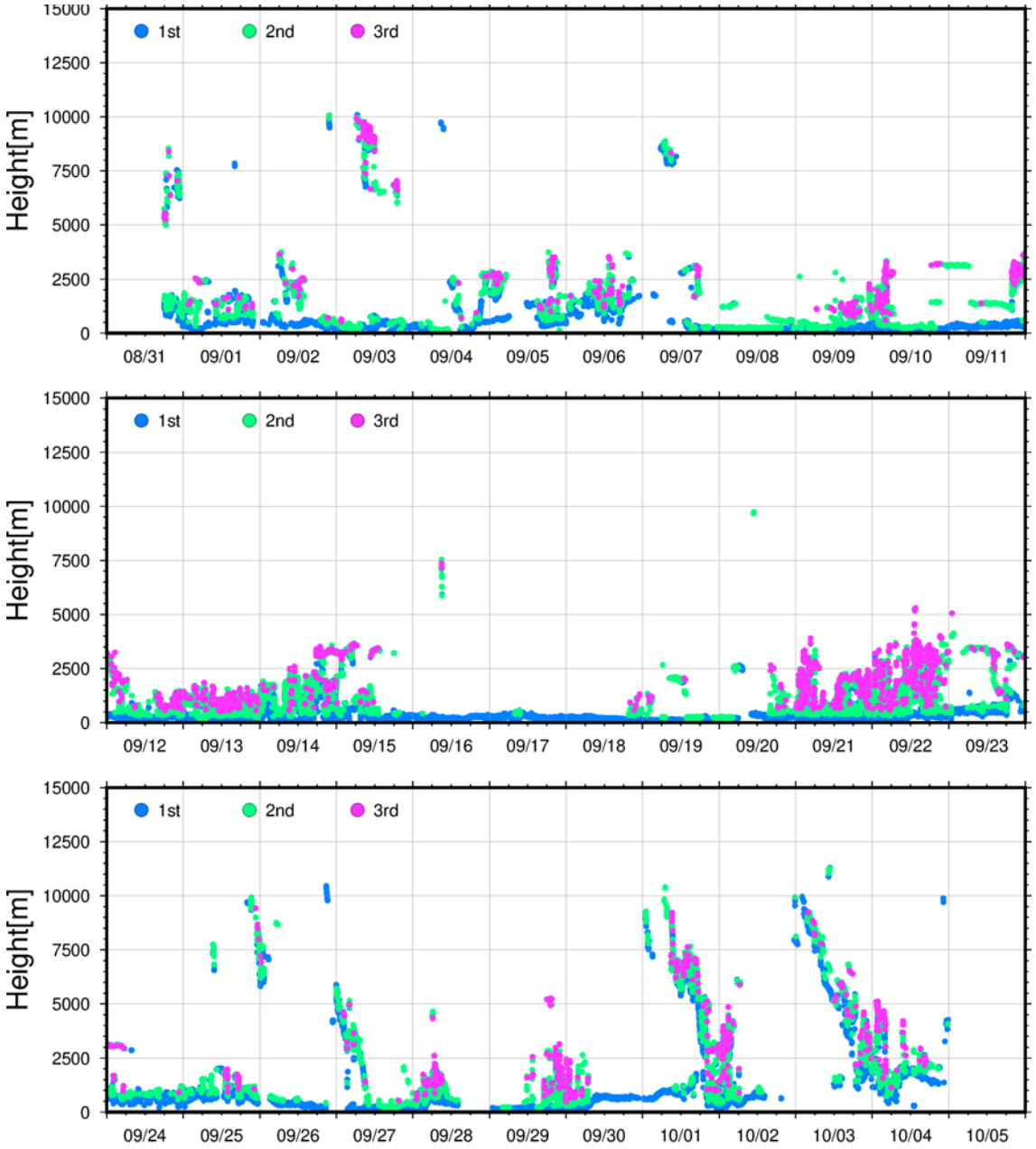

Figure 3.1.3-1: Time series of cloud base height during this cruise

3.1.4 Tropospheric gas and particles observation
3.1.4.1 Trace gases and aerosols in the marine boundary layer

(1) Personnel
Fumikazu Taketani (JAMSTEC RIGC)
Takeshi Kinase (JAMSTEC RIGC)
Takuma Miyakawa (JAMSTEC RIGC)
Hisahiro Takashima (JAMSTEC RIGC/Fukuoka Univ.)
Yugo Kanaya (JAMSTEC RIGC)
Masayuki Takigawa (JAMSTEC RIGC)
Yuzo Miyazaki (Hokkaido Univ.)
Yutaka Tobo (NIPR)
Atsushi Yoshida (NIPR)
Jun Uetake (Hokkaido Univ.)

(2) Objectives
We conducted shipborne observations of atmospheric compositions in the marine boundary layer to investigate variabilities of maritime aerosol physicochemical properties over the Arctic Ocean where the low cloud and sea fog prevail in summer season, and to investigate the role of processes (e.g., sea spraying, atmospheric secondary formation, and long-range transport) affecting the variabilities of aerosol particles. To achieve the objectives, we targeted the following parameters.
・ Particle number size distributions
・ Fluorescent aerosol particle number concentrations
・ Size-resolved chemical composition and particle mixing state
・ Vertical distributions of nitrogen dioxide (NO_2) and iodine monoxide (IO) in the troposphere
・ Surface carbon monoxide (CO) and ozone(O_3) mixing ratios

(3) Instruments and methods
(3-1) Continuous surface aerosol observations:
(3-1-1) Particle number size distributions (PSDs)
The size-resolved number concentration of particles was measured by a scanning mobility particle sizer (SMPS, model 3938, TSI) for the size range between 14 and 724 nm in diameter, and an optical particle counter (OPC) (9300P, ParticlePlus) for the size range between 0.3 and 5 μm in diameter. A custom-made heated inlet system (Miyakawa et al., 2023) was installed in front of the SMPS to measure the PSDs of total and non-volatile (at 300°C) aerosols. The particle sizing accuracy was validated before and after the cruise using standard particles (spherical polystyrene latex particles with known diameter).

(3-1-2) Fluorescence measurements of airborne particles
Fluorescent properties of aerosol particles (0.7–10 μm) were measured by a single particle fluorescence sensor, Waveband Integrated bioaerosol sensor (WIBS-4A, Droplet Measurement Technologies) (Taketani et al., 2025). Two pulsed xenon lamps emitting UV light (280 nm and 370 nm) were used for excitation. Fluorescence emitted from a single particle within 310–400 nm and 420–650 nm wavelength bands was detected by PMTs with the bandpass filters.

(3-1-3) Sampling air for the continuous observations
The sample air for particle measurements was commonly drawn from the rooftop of the environmental research room through a custom-made concentric tube-type inlet at the sampling rate of 31 L/min for sampling total suspended particulate matters (TSP) (Miyakawa et al., 2023;2025) to the SMPS and OPC. A part of the sampler air (~1.5 L/min) was isokinetically extracted and was dehumidified using a large diameter Nafion dryer (MD-700, Perma Pure, Inc.) to eliminate water vapor and liquid water contents of airborne particles (typical values of relative humidity (RH) at the exit of the dryer were lower than ~20% for Arctic region, and was subsequently introduced via flow splitters to those instruments installed in the environmental research room. Note that the WIBS4 were placed on the compass deck and directly measured particle size distributions of fluorescent aerosols at ambient RH.

(3-2) Aerosol sampling for chemical and physical analyses:
Samplings of aerosol particles in atmosphere were performed using various samplers on the compass deck and in the environmental research room.
(3-2-1) High-volume air sampling for the chemical composition analyses
Aerosol particles were collected on the filter along cruise track using two high-volume air samplers (HVS 1 and 2) located to the forefront of the compass deck to analyze the chemical composition (Miyakawa et al., 2025; Miyazaki et al., 2018). To avoid collecting particles derived from the research vessel's own exhaust, the pumping by the HVSs were automatically controlled using a "wind-direction selection system". All the samples will be analyzed in the laboratories at JAMSTEC and Hokkaido University. These sampling logs are listed in Tables 3.1.4.1-1 and 3.1.4.1-2.

HVS 1
A high volume air sampler (120SL, Kimoto Electric) with a 1-stage impactor (TE231, Tisch Environmental) was deployed for analyzing mode-segregated inorganic ions and trace metals of collected aerosols. Cellulose fiber filters (TE-241 (Tisch Environmental) for backup and TE-230-WH (Tisch Environmental) for 1 cascade stage) were used for the sampling. Size fractionated aerosol particles were separately collected on the filters at the sampling rate of approximately 1133 L/min and the fractionation specification is as follows.
Stage 1: 0.95 μm – TSP
Backup: ~0 μm – 0.95 μm

HVS 2
Another high volume air sampler (120SL, Kimoto Electric) with a 4-stage cascade impactor (TE234, Tisch Environmental) was deployed for analyzing mode-segregated carbonaceous components (elemental and organic carbons, water-soluble organic carbons, some specific molecular markers, and stable isotope of carbon) of collected aerosols. Pre-combusted quartz fiber filters (Pallflex Tissuquartz 2500QAT-UP (Cytiva, MA, US) for backup and TE-230-QZ (Tisch Environmental) for 4 cascade stages) was used for the sampling. Size fractionated aerosol particles were separately collected on the filters at the sampling rate of approximately 1133 L/min and the fractionation specification is as follows.
Stage 1: 7.2 μm – TSP

Stage 2: 3.0 μm – 7.2 μm
Stage 3: 1.5 μm – 3.0 μm
Stage 4: 0.95 μm – 1.5 μm
Backup: ~0 μm – 0.95 μm

(3-2-2) Air sampling for the individual particle analyses
Electron microscopic analyses, using Scanning Election Microscopy (SEM) and Transmission Electron Microscopy (TEM), will be performed in order to investigate the morphology and physicochemical properties of aerosol particles. For these purposes, aerosol particles were collected on a TEM grids (formvar) using the following impactors (impactor 1 and 2) (Miyakawa et al., 2025). All samples will be analyzed using SEM or TEM placed in a laboratory of JAMSTEC. These sampling logs are listed in Table 3.1.4.1-3 and Table 3.1.4.1-4.

Impactor 1
A two-stage impactor (AS-24W, ARIOS) was used for collecting fine particles to the TEM grid for the TEM analysis. Automated particle samplings were performed using the AS-24W for 20-60 min depending on the aerosol concentrations every 1 or 2 hours for the establishment of the highly time-resolved sampling of aerosol particles. The sampler air was drawn from the rooftop of the environmental research room to the AS-24W placed inside the room through the ~5-m long conductive silicon tube. The sampling flowrate was 2.2 lpm (i.e., the sum of the sampler and assist pump flow rates (1.2 lpm + 1 lpm)).

Impactor 2
A three-stage impactor (MPS-3, California Measurements) was used for collecting coarse particles to the TEM grid for the SEM analysis. Manual particle samplings were performed on the compass deck using the MPS-3 for 10-20 min depending on the aerosol concentrations. The sampling flowrate was 2.0 lpm and sizes of collected particles were >2 μm, 0.3–2 μm, and 0.05–0.3 μm.

(2-2-3) Aerosol sampling for investigating ice-nucleating particles, water-insoluble particles, and DNA
Aerosol particles were collected on filters along the cruise track using three hand-made air samplers (Sampler 1, 2, and 3) installed to the forefront of the compass deck to investigate ice-nucleating particles, water-insoluble particles (e.g., mineral dust, black carbon), and airborne DNA. To avoid collecting particles derived from the research vessel's own exhaust, each pump was automatically controlled using a "wind-direction selection system". These samples will be analyzed in the laboratories at NIPR and Hokkaido University. All filters were replaced at the same timing. Sampling logs are listed in Tables 3.1.4.1-5.

Sampler 1
A hand-made sampler with a pump (DA-241S, ULVAC) and a mass flow controller (MQV0050, Azbil) was deployed for analyzing DNA compositions. HEPA-type filters with were used for the sampling. Sampling flowrate was 26.0 L/min.

Sampler 2
A hand-made sampler with a pump (OSP-90W, Fuji Medical Instruments) and a

mass flow controller (MQV0020, Azbil) was deployed for analyzing INP concentrations. Polycarbonate filters with 0.2 μm pores (Nuclepore membrane, Whatman) were used for the sampling. Sampling flowrate was 9.6 L/min.

Sampler 3
A hand-made sampler with a pump (OSP-90W, Fuji Medical Instruments) and a mass flow controller (MQV0020, Azbil) was deployed for analyzing water-insoluble particles. olycarbonate filters with 0.2 μm pores (Nuclepore membrane, Whatman) were used for the sampling. Sampling flowrate was 9.6 L/min.

(3-3) MAX-DOAS:
Multi-Axis Differential Optical Absorption Spectroscopy (MAX-DOAS), a passive remote sensing technique measuring spectra of scattered visible and ultraviolet (UV) solar radiation, was used for atmospheric aerosol and gas profile measurements (Takashima et al., 2022). Our MAX-DOAS instrument consists of two main parts: an outdoor telescope unit and an indoor spectrometer (Acton SP-2358 with Princeton Instruments PIXIS-400B), connected to each other by a 14-m bundle optical fiber cable. The line of sight was in the directions of the portside of the vessel and the scanned elevation angles were 2, 4, 6, 10, 20, 30, 90 degrees in the 30-min cycle. The roll motion of the ship was measured to autonomously compensate additional motion of the prism, employed for scanning the elevation angle.
For the selected spectra recorded with elevation angles with good accuracy, DOAS spectral fitting was performed to quantify the slant column density (SCD) of NO_2 (and other gases) and O_4 (O_2-O_2, collision complex of oxygen) for each elevation angle. Then, the O_4 SCDs were converted to the aerosol optical depth (AOD) and the vertical profile of aerosol extinction coefficient (AEC) using an optimal estimation inversion method with a radiative transfer model. The tropospheric vertical column/profile of NO_2 and other gases (e.g., IO) were retrieved using derived aerosol profiles.

(3-4) CO and O_3:
Ambient air was continuously sampled on the compass deck and drawn through ~20-m-long Teflon tubes connected to a nondispersive infrared (NDIR) CO analyzer (Model 48i-TLE, Thermo Fisher Scientific) and a UV photometric ozone analyzer (model 205, 2B Technologies) (Kanaya et al., 2019), located in the environmental research room.

(4) Summary of the aerosol sampling
Aerosol samplings during MR25-05C were summarized in Tables 3.1.4.1-1 - 3.1.4.1-5.

Table 3.1.4.1-1: High-volume air samplings using HVS1 for aerosol composition analyses

ID	Data collected (Sampling start)				Latitude			Longitude		
	YYYY	MM	DD	hh:mm: (UTC)	Deg.	Min.	N/S	Deg.	Min.	E/W
MR2505C_J_B01	2025	9	1	15:30	55	39.5783	N	160	16.2063	W
MR2505C_J_B02	2025	9	17	18:15	75	56.77176	N	165	32.17538	W
MR2505C_J_B03	2025	10	2	2:29	40	8.22	N	147	42.12	E
MR2505C_J_S01	2025	9	1	21:16	55	39.5783	N	160	16.2063	W
MR2505C_J_S02	2025	9	3	21:54	64	35.04	N	168	12.83	W
MR2505C_J_S03	2025	9	5	21:27	68	59.99	N	168	44.89	W
MR2505C_J_S04	2025	9	9	16:34	71	47.79	N	155	25.89	W
MR2505C_J_S05	2025	9	9	16:34	71	47.79	N	155	25.89	W
MR2505C_J_S06	2025	9	11	18:22	71	55.1	N	158	27.71	W
MR2505C_J_S07	2025	9	13	16:49	72	3.16	N	163	36.85	W
MR2505C_J_S08	2025	9	15	16:30	73	21.27	N	163	11.09	W
MR2505C_J_S09	2025	9	17	18:42	75	56.79	N	165	32.08	W
MR2505C_J_S10	2025	9	19	17:43	74	30.53	N	162	6.54	W
MR2505C_J_S11	2025	9	21	18:40	74	3.48	N	158	51.71	W
MR2505C_J_S12	2025	9	23	16:31	67	30.03	N	168	30	W
MR2505C_J_S13	2025	9	25	18:40	59	54.17	N	177	55.13	W
MR2505C_J_S14	2025	9	27	3:27	55	21.56	N	175	1.62	E
MR2505C_J_S15	2025	9	29	22:39	47	5.07	N	160	30.21	E

Table 3.1.4.1-2: High-volume air sampling using HVS2 for aerosol composition analyses

ID	Data collected (Sampling start)				Latitude			Longitude		
	YYYY	MM	DD	hh:mm: (UTC)	Deg.	Min.	N/S	Deg.	Min.	E/W
MR2505C_H_B01	2025	9	1	15:30	55	39.5783	N	160	16.2063	W
MR2505C_H_B02	2025	9	17	18:15	75	56.77176	N	165	32.17538	W
MR2505C_H_B03	2025	10	2	2:29	40	8.22	N	147	42.12	E
MR2505C_H_S01	2025	9	1	21:16	55	39.5783	N	160	16.2063	W
MR2505C_H_S02	2025	9	3	21:54	64	35.04	N	168	12.83	W
MR2505C_H_S03	2025	9	5	21:27	68	59.99	N	168	44.89	W
MR2505C_H_S04	2025	9	9	16:34	71	47.79	N	155	25.89	W
MR2505C_H_S05	2025	9	9	16:34	71	47.79	N	155	25.89	W
MR2505C_H_S06	2025	9	11	18:22	71	55.1	N	158	27.71	W
MR2505C_H_S07	2025	9	13	16:49	72	3.16	N	163	36.85	W
MR2505C_H_S08	2025	9	15	16:30	73	21.27	N	163	11.09	W
MR2505C_H_S09	2025	9	17	18:42	75	56.79	N	165	32.08	W
MR2505C_H_S10	2025	9	19	17:43	74	30.53	N	162	6.54	W
MR2505C_H_S11	2025	9	21	18:40	74	3.48	N	158	51.71	W
MR2505C_H_S12	2025	9	23	16:31	67	30.03	N	168	30	W
MR2505C_H_S13	2025	9	25	18:40	59	54.17	N	177	55.13	W
MR2505C_H_S14	2025	9	27	3:27	55	21.56	N	175	1.62	E
MR2505C_H_S15	2025	9	29	22:39	47	5.07	N	160	30.21	E

Table 3.1.4.1-3: Aerosol sampling for TEM analyses

ID	Data collected (Sampling start)				Latitude			Longitude		
	YYYY	MM	DD	hh:mm: (UTC)	Deg.	Min.	N/S	Deg.	Min.	E/W
MR2505C-TEM-1	2025	9	1	18:15	55	42.54098	N	170	45.61303	W
MR2505C-TEM-2	2025	9	4	23:00	67	0.034448	N	169	14.68681	W
MR2505C-TEM-3	2025	9	7	4:00	71	7.068951	N	164	52.91714	W
MR2505C-TEM-4	2025	9	9	8:00	71	47.481	N	156	39.74577	W
MR2505C-TEM-5	2025	9	12	15:15	71	45.37162	N	156	55.4044	W
MR2505C-TEM-6	2025	9	15	17:00	73	21.42739	N	164	49.45385	W
MR2505C-TEM-7	2025	9	16	17:15	74	47.45194	N	169	20.49252	W
MR2505C-TEM-8	2025	9	18	16:05	76	23.11416	N	165	33.09772	W
MR2505C-TEM-9	2025	9	21	8:00	74	9.7368	N	160	39.84996	W
MR2505C-TEM-10	2025	9	23	6:00	69	30.89055	N	169	22.54011	W
MR2505C-TEM-11	2025	9	25	0:00	63	1.753035	N	174	13.17079	W
MR2505C-TEM-12	2025	9	27	18:17	53	20.28234	N	171	8.720363	E
MR2505C-TEM-13	2025	9	28	20:15	49	45.68077	N	167	22.85863	E
MR2505C-TEM-14	2025	10	1	3:00	43	17.48093	N	153	23.21021	E
MR2505C-TEM-15	2025	10	2	6:00	37	41.92963	N	142	9.146697	E

Table 3.1.4.1-4: Aerosol sampling for SEM experiments

ID	Data collected (Sampling end)				Latitude			Longitude		
	YYYY	MM	DD	hh:mm: (UTC)	Deg.	Min.	N/S	Deg.	Min.	E/W
MR2505C-ESEM-1	2025	9	3	6:41	61	44.45643	N	168	26.53409	W
MR2505C-ESEM-2	2025	9	3	22:03	64	38.14736	N	169	45.62879	W
MR2505C-ESEM-3	2025	9	4	4:04	65	30.70086	N	169	17.70548	W
MR2505C-ESEM-4	2025	9	4	14:25	66	31.41049	N	169	10.93381	W
MR2505C-ESEM-5	2025	9	5	1:53	67	16.9284	N	169	14.99736	W
MR2505C-ESEM-6	2025	9	5	21:27	69	0.005015	N	169	15.11452	W
MR2505C-ESEM-7	2025	9	6	4:30	69	29.99816	N	169	14.97092	W
MR2505C-ESEM-8	2025	9	6	7:51	69	59.99324	N	169	15.02857	W
MR2505C-ESEM-9	2025	9	6	16:05	71	0.007877	N	169	15.00965	W
MR2505C-ESEM-10	2025	9	6	19:24	70	45.17051	N	168	31.16738	W
MR2505C-ESEM-11	2025	9	6	23:48	70	56.15786	N	166	35.6685	W
MR2505C-ESEM-12	2025	9	7	16:28	71	17.09843	N	161	0.014366	W
MR2505C-ESEM-13	2025	9	8	0:38	71	13.33318	N	161	34.23247	W
MR2505C-ESEM-14	2025	9	8	15:55	71	47.68621	N	156	38.99351	W
MR2505C-ESEM-15	2025	9	9	18:34	71	44.15747	N	156	49.71822	W
MR2505C-ESEM-16	2025	9	9	2:34	71	49.19077	N	156	13.87059	W
MR2505C-ESEM-17	2025	9	10	19:34	72	1.851347	N	152	25.30668	W
MR2505C-ESEM-18	2025	9	11	3:38	71	25.70011	N	155	53.19776	W
MR2505C-ESEM-19	2025	9	11	18:28	71	55.10717	N	159	32.28859	W
MR2505C-ESEM-20	2025	9	11	22:19	72	11.35258	N	158	46.23392	W
MR2505C-ESEM-21	2025	9	12	1:36	72	29.04197	N	157	41.78024	W
MR2505C-ESEM-22	2025	9	12	16:05	71	45.25613	N	156	56.09201	W
MR2505C-ESEM-23	2025	9	12	21:36	71	34.65872	N	158	9.741951	W
MR2505C-ESEM-24	2025	9	13	8:39	71	10.08849	N	161	8.046139	W
MR2505C-ESEM-25	2025	9	13	16:56	72	6.100882	N	164	27.83569	W
MR2505C-ESEM-26	2025	9	15	20:42	73	21.6589	N	165	54.81015	W
MR2505C-ESEM-27	2025	9	16	20:42	74	43.26685	N	167	34.17679	W
MR2505C-ESEM-28	2025	9	17	21:38	75	32.85623	N	165	20.03798	W
MR2505C-ESEM-29	2025	9	18	1:59	75	19.8696	N	165	53.88547	W
MR2505C-ESEM-30	2025	9	18	16:45	76	23.35785	N	165	32.00211	W
MR2505C-ESEM-31	2025	9	19	17:51	74	31.28889	N	162	1.740666	W
MR2505C-ESEM-32	2025	9	20	16:11	74	28.49885	N	162	6.377247	W
MR2505C-ESEM-33	2025	9	21	18:46	74	3.486141	N	159	8.232648	W
MR2505C-ESEM-34	2025	9	22	4:50	73	48.37777	N	165	53.67256	W
MR2505C-ESEM-35	2025	9	22	9:52	73	15.17771	N	168	52.30069	W
MR2505C-ESEM-36	2025	9	22	14:47	72	30.00002	N	169	15.01322	W
MR2505C-ESEM-37	2025	9	23	1:52	70	27.67417	N	169	19.20496	W
MR2505C-ESEM-38	2025	9	23	16:37	67	30.01038	N	169	29.99249	W
MR2505C-ESEM-39	2025	9	24	1:48	66	48.4007	N	169	36.701	W
MR2505C-ESEM-40	2025	9	25	18:47	59	51.90829	N	178	2.011615	W
MR2505C-ESEM-41	2025	9	26	1:12	58	54.66489	N	180	45.41941	W
MR2505C-ESEM-42	2025	9	26	19:30	56	19.67992	N	177	15.43116	E
MR2505C-ESEM-43	2025	9	27	0:30	55	42.1653	N	175	50.71883	E

Table 3.1.4.1-5 Log of aerosol sampling by samplers 1, 2, and 3. Each filter was replaced at the same timing.

On board ID	Collection Date (start)					Latitude			Longitude		
	YYYY	MM	DD	hh:mm:ss	UTC/JST	Deg.	Min.	N/S	Deg.	Min.	E/W
MR2505C-#1	2025	9	1	21:16:00	UTC	55	39.5783	N	160	16.2063	W
MR2505C-#2	2025	9	3	21:54:00	UTC	64	35.04	N	168	12.83	W
MR2505C-#3	2025	9	5	21:27:00	UTC	68	59.99	N	168	44.89	W
MR2505C-#4	2025	9	9	16:34:00	UTC	71	47.79	N	155	25.89	W
MR2505C-#5	2025	9	9	16:34:00	UTC	71	47.79	N	155	25.89	W
MR2505C-#6	2025	9	11	18:22:00	UTC	71	55.1	N	158	27.71	W
MR2505C-#7	2025	9	13	16:49:00	UTC	72	3.16	N	163	36.85	W
MR2505C-#8	2025	9	15	16:30:00	UTC	73	21.27	N	163	11.09	W
MR2505C-#9	2025	9	17	18:42:00	UTC	75	56.79	N	165	32.08	W
MR2505C-#10	2025	9	19	17:43:00	UTC	74	30.53	N	162	6.54	W
MR2505C-#11	2025	9	21	18:40:00	UTC	74	3.48	N	158	51.71	W
MR2505C-#12	2025	9	23	16:31:00	UTC	67	30.03	N	168	30	W
MR2505C-#13	2025	9	25	18:40:00	UTC	59	54.17	N	177	55.13	W
MR2505C-#14	2025	9	27	3:27:00	UTC	55	21.56	N	175	1.62	E
MR2505C-#15	2025	9	29	22:39:00	UTC	47	5.07	N	160	30.21	E

(5) Preliminary results (WIBS-4A measurement)

Figure 3.1.4.1-1 (a) shows the temporal variations of number concentrations of fluorescent particles (FPs) and non-fluorescent (scattering) particles along the cruise route measured by WIBS-4A. Figures 3.1.4.1-1 (b) and (c) display the spatiotemporal distributions of number concentration of FPs and scattering particles, respectively. This indicates that concentrations vary significantly depending on location. We are going to compare this with other observed data in the future.

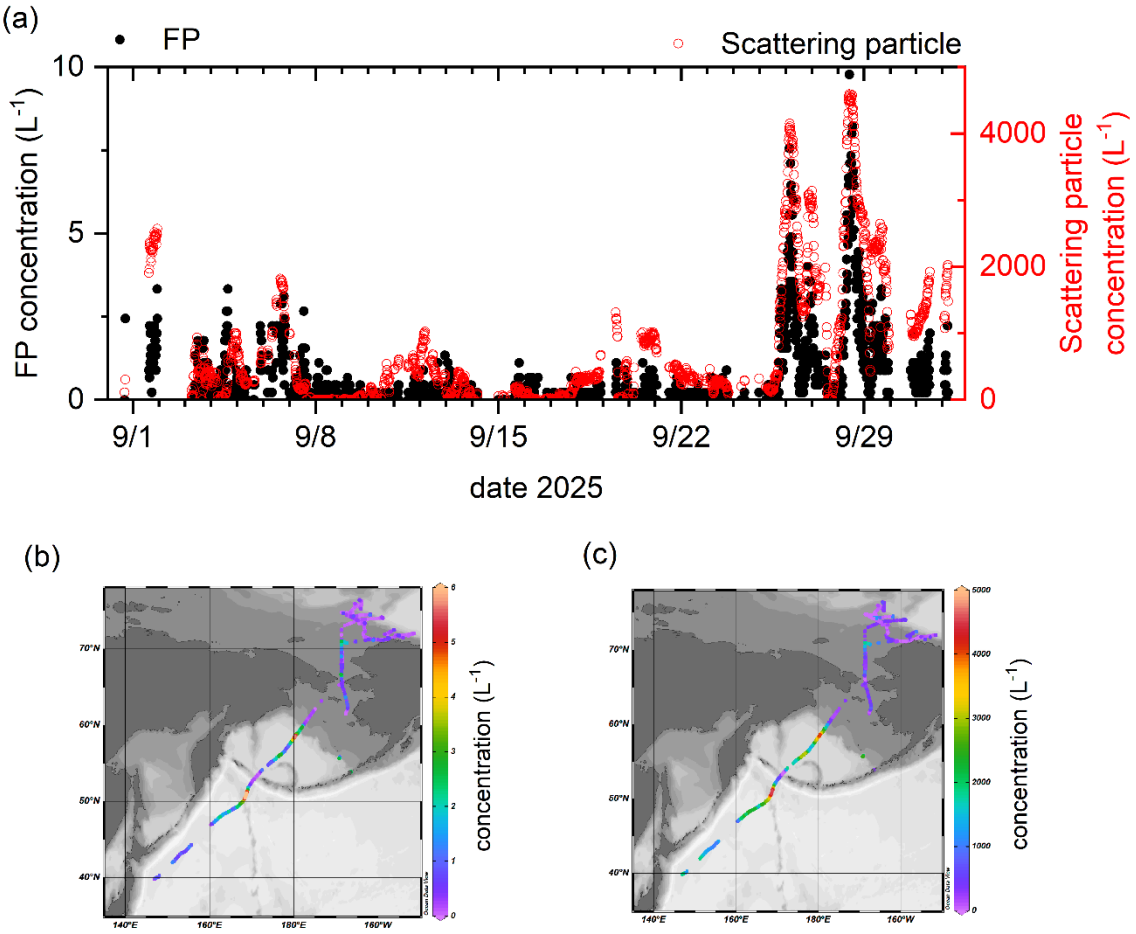

Figure 3.1.4.1-1: (a)Time series of concentrations of fluorescence particles (FPs) and scattering particles observed by WIBS-4A. Spatiotemporal distributions of concentrations of (b) FPs and (c) scattering particles.

(6) References:

Kanaya et al. (2019), Ozone and carbon monoxide observations over open oceans on R/V *Mirai* from 67° S to 75° N during 2012 to 2017: testing global chemical reanalysis in terms of Arctic processes, low ozone levels at low latitudes, and pollution transport, Atmos. Chem. Phys., 19, 7233–7254, https://doi.org/10.5194/acp-19-7233-2019

Kobayashi and Takegawa (2022), A new method to quantify particulate sodium and potassium salts (nitrate, chloride, and sulfate) by thermal desorption aerosol mass spectrometry, Atmos. Meas. Tech., 15, 833–844, https://doi.org/10.5194/amt-15-833-2022

Miyakawa et al. (2023), Measurements of aerosol particle size distributions and INPs over the Southern Ocean in the late austral summer of 2017 on board the R/V *Mirai*: Importance of the marine boundary layer structure, Earth Space Sci., 10, e2022EA002736, https://doi.org/10.1029/2022EA002736
Miyakawa et al. (2025), Natural and continental influence on aerosol distributions over the Northwestern Pacific Ocean in the late winter and early spring of 2021, accepted to Prog. Earth Planet. Sci.
Miyazaki et al. (2018), Chemical transfer of dissolved organic matter from surface seawater to sea spray water-soluble organic aerosol in the marine atmosphere, Sci Rep. 8, 14861, https://doi.org/10.1038/s41598-018-32864-7
Takashima et al. (2022), Full latitudinal marine atmospheric measurements of iodine monoxide, Atmos. Chem. Phys., 22, 4005–4018, https://doi.org/10.5194/acp-22-4005-2022
Taketani et al. (2025), Impact of Siberian Wildfires on Ice-Nucleating Particle Concentrations over the Northwestern Pacific, Environ. Sci. Technol., **59**, 5, 2565-2574, https://doi.org/10.1021/acs.est.4c04889

(7) Data archives

These data obtained in this cruise will be submitted to the Data Management Group of JAMSTEC, and will be opened to the public via "Data Research System for Whole Cruise Information in JAMSTEC (DARWIN)" in JAMSTEC web site.
<https://www.godac.jamstec.go.jp/darwin/en/>

3.1.4.2 Aerosol observations of the marine boundary layer by Tethered balloon

(1) Personnel

Fumikazu TAKETANI (JAMSTEC)
Takeshi KINASE (JAMSTEC)
Takuma MIYAKAWA (JAMSTEC)
Taisei YAMAGUCHI (JAMSTEC)
Ryo OYAMA (NME)
Haruki DOI (NME)
Seika TAKAI(NME)
Satomi OGAWA (NME)

(2) Objectives

To collect the aerosol samples and investigate vertical profiles of aerosol size distribution in/above the marine boundary layer.

(3) Instruments and methods

Tethered balloon observations were carried out by an airship-shaped balloon (15m^3, Kikyu-Seisakujo) connected to the portable winch installed at the upper deck (Photo 3.1.4.2-1) by the Kepler cable. We carried out 5 times tethered balloon observation in this cruise. The launching logs were listed in Table 3.1.4.2-1. A bag loaded several aerosol instruments and GPS sonde (RS-11g, Meisei) were connected below 5 m and 10 m from the balloon, respectively. Vertical profiles of particle number concentration and aerosol particle size distribution were measured by a condensation particle

counter (CPC) (Model 3007, TSI) and an optical particle counter (HHPC6+, Beckman coulter), respectively. Also, the video recording device (hero11, GoPro) was attached to the bottom of the bag. Aerosol particles were also sampled by a two-stage impactor (AS-16M, Arios) with a timer function. These samples will be analyzed in the laboratory after the cruise.

Photo 3.1.4.2-1: A photo of tethered balloon during observation. Below the balloon, an instrument box and a meteorological sonde are attached in sequence and connected to the portable winch installed on the deck.

Table 3.1.4.2-1: Launching logs

ID	Data collected (Sampling start)				Latitude			Longitude			Sampling height 1& time	Sampling height 2 & time	Sampling height 3 & time
	YYYY	MM	DD	hh:mm: (UTC)	Deg.	Min.	N/S	Deg.	Min.	E/W	m, min	m, min	m, min
MR2505C-TB-1	2025	9	4	17:35	66	37.7666	N	169	14.7162	W	100, 20	–	–
MR2505C-TB-2	2025	9	9	17:32	71	44.5104	N	156	48.2830	W	550, 30	150, 30	–
MR2505C-TB-3	2025	9	15	20:46	73	23.3484	N	165	29.0180	W	750, 25	350, 25	200, 10
MR2505C-TB-4	2025	9	16	20:50	74	43.0033	N	167	48.9358	W	850, 35	210, 10	–
MR2505C-TB-5	2025	9	23	19:20	67	28.0226	N	169	32.2773	W	1020, 30	500, 25	200, 5

(4) Preliminary result

Figure 3.1.4.2-1 shows the vertical profiles of concentrations of particles in diameters between 10–1000nm, 0.3–0.5μm, 0.5–1μm, 1–2μm, 2–5μm, and 5–10μm in the launching on 20:46(UTC) September 15, 2025. Temperature and relative humidity are also shown in this figure. In this case, the boundary height was estimated to be about 400m. We collected aerosol samples at 750m, 359m, and 200m.

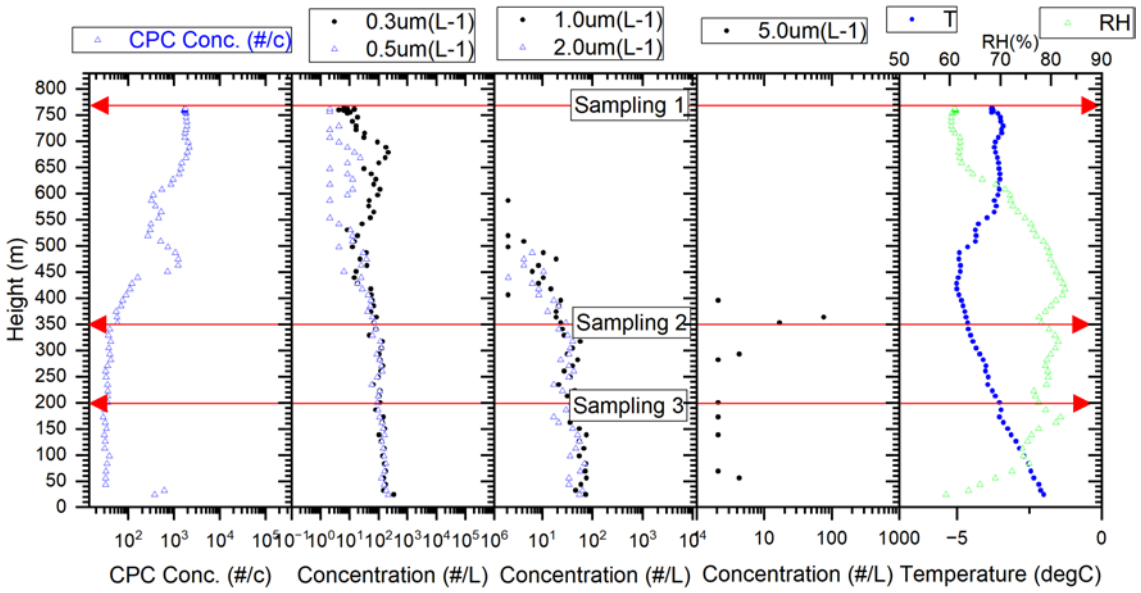

Figure 3.1.4.2-1: Vertical profiles of concentrations of (a) particles with diameters of 10–1000nm, (b) 0.3–0.5μm and 0.5–1μm, (c) 1–2μm and 2–5μm, and (d) 5–10μm, and (e) temperature and relative humidity in the launching on 20:46(UTC) September 15, 2025. Only data from the ballon ascent are shown in this figure.

(5) Data archive
These data obtained in this cruise will be submitted to the Data Management Group of JAMSTEC, and will be opened to the public via "Data Research System for Whole Cruise Information in JAMSTEC (DARWIN)" in JAMSTEC web site.<https://www.godac.jamstec.go.jp/darwin/en/>

3.1.4.3 Snow sampling

(1) Personnel
Fumikazu TAKETANI (JAMSTEC)
Takeshi KINASE (JAMSTEC)
Yuri FUKAI (JAMSTEC)
Amane FUJIWARA (JAMSTEC)

(2) Objectives
To investigate the nutrients in the snow over the Arctic Ocean
To investigate influence of the wet deposition to the marine ecosystem over the Arctic Ocean

(3) Parameters
・Chemical composition of snow

(4) Instruments and methods
Snow sampling was performed by a hand-made plastic sampler installed at the compass deck. The samples were collected in a plastic bottle(50ml), then dissolved in a refrigerator. These samples were analyzed in R/V Mirai and laboratory at JAMSTEC to investigate the chemical composition including nutrients. Sampling

logs are listed in Table 3.1.4.3-1.

(5) Data archives
All data obtained during this cruise will be submitted to Data Management Group (DMG) of JAMSTEC after the sample analysis and validation. The data will be opened to the public via "Data Research System for Whole Cruise Information (DARWIN)" in JAMSTEC web site.

Table 3.1.4.3-1 Sampling logs for snow.

On board ID	Collection Date (start)					Latitude			Longitude		
	YYYY	MM	DD	hh:mm:ss	UTC/ JST	Deg.	Min.	N/S	Deg.	Min.	E/W
MR2505C-snow001	2025	9	8	16:10:00	UTC	71	47.81	N	155	20.56	W
MR2505C-snow-002	2025	9	8	16:10:00	UTC	71	47.81	N	155	20.56	W
MR2505C-snow-003	2025	9	10	16:24:00	UTC	72	1.78	N	151	34.73	W
MR2505C-snow-004	2025	9	12	16:50:00	UTC	71	45.24	N	155	3.95	W
MR2505C-snow-005	2025	9	13	16:54:00	UTC	72	4.75	N	163	34.5	W
MR2505C-snow-006	2025	9	14	16:30:00	UTC	73	3.01	N	163	19	W
MR2505C-snow-007	2025	9	15	16:45:00	UTC	73	21.42	N	163	10.65	W
MR2505C-snow-008	2025	9	20	21:43:00	UTC	74	31.86	N	161	56.1	W
MR2505C-snow-009	2025	9	21	2:15:00	UTC	74	30.2	N	161	56.1	W
MR2505C-snow-010	2025	9	21	21:45:00	UTC	74	3.37	N	158	52.41	W

3.1.4.4 Vertical profiles of meteorological data measured by radio sonde

(1) Personnel
Fumikazu TAKETANI (JAMSTEC)
Takeshi KINASE (JAMSTEC)
Takuma MIYAKAWA (JAMSTEC)
Taisei YAMAGUCHI (JAMSTEC)
Masaki KATSUMATA (JAMSTEC)
Ryo OYAMA (NME)
Haruki DOI (NME)
Seika TAKAI(NME)
Satomi OGAWA (NME)

(2) Objectives
To obtain vertical profiles of air temperature, relative humidity, and wind speed/direction.

(3) Instruments and methods
Vaisala RS-41 was used as a sensor for radio sonde observation. The ground check device (RI41) operated by MW41 software prepared and calibrated the sensor. For the calibration reference, the value from a barometer (PTB-330) near RI41 was applied. The sensor and balloon (200, Kikyu-Seisakujo or TA-200, Totex) were placed in the shipboard balloon launcher for launch (Photo 3.1.4.4-1). Meteorological data which was continuously obtained at the foremast was referred as the surface condition at launch. MW41 also recorded and processed the sounding data, with a

processor (SPS-311), GPS antenna (GA20), and UHF antenna (RB21).

(4) Preliminary result
During this cruise, we carried out 23 radiosonde observations, as listed in Table 3.1.4.4-1.

(5) Data archive
These data obtained in this cruise will be submitted to the Data Management Group of JAMSTEC, and will be opened to the public via "Data Research System for Whole Cruise Information in JAMSTEC (DARWIN)" in JAMSTEC web site.<https://www.godac.jamstec.go.jp/darwin/en/>

Table 3.1.4.4-1: Radiosonde launch log, with latitude and longitude, surface observations, and maximum height.

SN	Data collected				Latitude			Longitude			Pressure	Temperature	RH	Wind direction	Wind speed	SST	Max height
	YYYY	MM	DD	hh:mm: (UTC)	Deg.	Min.	N/S	Deg.	Min.	E/W	hPa	℃	%	deg	m/s	℃	m
X0914241	2025	9	2	19:00	59	14.8884	N	167	47.3022	W	1013.57	9.9	87	221	12.3	9.64	23082
N2510149	2025	9	2	23:00	60	1.6026	N	168	17.8308	W	1013.67	9.3	91	214	8.3	9.32	22974
N2510150	2025	9	4	16:00	66	41.6964	N	168	53.6802	W	1005.16	6.3	97	355	7.3	6.16	23034
X0914280	2025	9	5	19:00	68	46.3740	N	168	44.7750	W	1007.65	5.8	83	208	10.9	7.67	24465
X0912297	2025	9	9	0:00	71	42.5172	N	154	51.8250	W	1007.21	1.1	99	23	4.9	5.04	12945
N2510141	2025	9	9	22:50	71	41.7672	N	154	59.1294	W	1010.8	0	89	96	3.8	1.91	21955.68
N2510140	2025	9	15	22:00	73	21.7500	N	164	34.6026	W	1013.97	−1.9	89	253	3.6	−0.2	20707
N2510148	2025	9	16	0:00	73	26.6142	N	164	15.5244	W	1014.67	−1.8	87	252	4.1	−0.2	2643.85
N2510143	2025	9	16	1:00	73	30.6258	N	164	6.1752	W	1014.77	−1.9	88	275	5.3	−0.2	21091
N2510144	2025	9	16	22:00	74	42.4734	N	166	3.0060	W	1018.96	−2.6	88	104	5	−0.5	22452.73
N2510350	2025	9	17	1:00	74	44.6874	N	166	33.4944	W	1018.96	−2.3	89	93	2.2	−0.5	22100
X0914282	2025	9	17	20:00	75	56.7906	N	165	32.2074	W	1021.34	−3.4	92	75	5.7	−1.3	23336
X0914289	2025	9	19	20:00	74	30.8946	N	161	57.4074	W	1006.69	−2.1	92	18	12.4	−0.5	18381
X0914279	2025	9	21	22:00	74	3.4692	N	158	51.7872	W	991.93	−1.7	92	321	3.1	−0.9	21219
X0912295	2025	9	22	4:00	73	53.2818	N	162	57.2154	W	993.12	−1.6	91	339	6.7	−0.1	21190
X0914276	2025	9	22	10:00	73	21.7962	N	166	40.1826	W	995.72	−1.8	93	328	7.8	0.73	20699.03
X0542728	2025	9	22	19:00	72	8.9688	N	168	45.1494	W	998.71	−1.1	87	294	7.1	2.69	22944
X0542362	2025	9	23	21:00	67	30.0450	N	168	30.1698	W	1000.55	3.9	75	348	2.7	6.73	24284
X0542738	2025	9	23	23:00	67	22.2744	N	168	20.3634	W	1000.16	4.4	75	356	4.3	6.91	24232
X0542364	2025	9	25	1:00	63	4.1256	N	173	43.5276	W	1004.55	5.3	82	22	6.4	8.68	24925
X0542736	2025	9	27	3:00	55	30.6840	N	175	24.8664	E	1014.97	10.3	92	237	10.6	9.6	12145
X0542347	2025	9	27	11:00	54	26.9358	N	173	3.1392	E	1002.7	9.9	96	120	15.2	9.38	12614
X0542346	2025	9	28	4:00	52	5.4978	N	169	22.5924	E	991.84	12.1	90	231	15.3	11.6	15774

SN: serial number of radio sonde

Photo 3.1.4.4-1: Shipboard balloon launcher

3.1.4.5 Analysis of Water-Insoluble Substances in the Seawater

(1) Personnel
Fumikazu Taketani (JAMSTEC RIGC)
Yutaka Tobo (NIPR)
Atsushi Yoshida (NIPR)

(2) Objectives
To investigate the composition and concentration of insoluble particles suspended in seawater, and to understand how these particles are released into the atmosphere as aerosols.
We targeted the following parameters.
・ Composition, particle size, and concentration of insoluble particles in seawater.

(3) Instruments and methods
Seawater sampling
Seawater samples were collected using a bucket and Niskin bottles or from laboratory water outlet (Table 3.1.6-1).

Filtering of seawater
To collect the particles from the sampled seawater, a two-stage filtration was performed using 10 μm and 0.4 μm pore size polycarbonate filters (Whatman). All filter samples will be analyzed in the laboratory.

(4) Data archives
These data obtained in this cruise will be submitted to the Data Management Group of JAMSTEC, and will be opened to the public via "Data Research System for Whole Cruise Information in JAMSTEC (DARWIN)" in JAMSTEC web site.
<https://www.godac.jamstec.go.jp/darwin/en/>

Table 3.1.6-1 Log of seawater sampling.

On board ID	Collection Date (start)					Latitude			Longitude			Depth (m)
	YYYY	MM	DD	hh:mm:ss	UTC/JST	Deg.	Min.	N/S	Deg.	Min.	E/W	
Stn.4-0m	2025	09	04	23:18:00	UTC	67	0.03	N	168	45.042	W	0
Stn.4-5m	2025	09	04	23:18:00	UTC	67	0.03	N	168	45.042	W	5
Stn.4-Chl	2025	09	04	23:18:00	UTC	67	0.03	N	168	45.042	W	10
Stn.4-TB	2025	09	04	23:18:00	UTC	67	0.03	N	168	45.042	W	39.9
Stn.4-B-5	2025	09	04	23:18:00	UTC	67	0.03	N	168	45.042	W	39.9
Stn.4-0m-bio	2025	09	04	23:18:00	UTC	67	0.03	N	168	45.042	W	0
Stn.8-0m	2025	09	05	21:06:00	UTC	69	0.012	N	168	44.898	W	0
Stn.8-5m	2025	09	05	21:06:00	UTC	69	0.012	N	168	44.898	W	5
Stn.8-Chl	2025	09	05	21:06:00	UTC	69	0.012	N	168	44.898	W	15.1
Stn.8-B-5	2025	09	05	21:06:00	UTC	69	0.012	N	168	44.898	W	47.1
Stn.8-0m-bio	2025	09	05	21:06:00	UTC	69	0.012	N	168	44.898	W	0
Stn.14-TB	2025	09	06	23:46:00	UTC	70	56.16	N	165	24.336	W	36.9
Stn.14-Chl	2025	09	06	23:46:00	UTC	70	56.16	N	165	24.336	W	20.1
Stn.15-0m	2025	09	08	22:13:00	UTC	71	41.742	N	154	55.428	W	0
Stn.15-5m	2025	09	08	22:13:00	UTC	71	41.742	N	154	55.428	W	4.8
Stn.15-Chl	2025	09	08	22:13:00	UTC	71	41.742	N	154	55.428	W	10
Stn.15-50m	2025	09	08	22:13:00	UTC	71	41.742	N	154	55.428	W	49.5
Stn.15-B-5	2025	09	08	22:13:00	UTC	71	41.742	N	154	55.428	W	105.7
Stn.16-2-0m	2025	09	09	19:29:00	UTC	72	1.842	N	151	34.692	W	0
Stn.16-2-5m	2025	09	09	19:29:00	UTC	72	1.842	N	151	34.692	W	34
Stn.16-2-Chl	2025	09	09	19:29:00	UTC	72	1.842	N	151	34.692	W	18.1
Stn.16-2-50m	2025	09	09	19:29:00	UTC	72	1.842	N	151	34.692	W	49.5
Stn.16-2-TB	2025	09	09	19:29:00	UTC	72	1.842	N	151	34.692	W	49.5
Stn.16-2-800m	2025	09	09	19:29:00	UTC	72	1.842	N	151	34.692	W	792.5
Stn.16-2-0m-bio	2025	09	09	19:29:00	UTC	72	1.842	N	151	34.692	W	0
Stn.17-TB1	2025	09	10	23:32:00	UTC	71	42.726	N	152	51.744	W	50.9
Stn.17-TB2	2025	09	10	23:32:00	UTC	71	42.726	N	152	51.744	W	148.8
Stn.19-0m	2025	09	11	18:10:00	UTC	71	55.11	N	158	27.726	W	0
Stn.19-5m	2025	09	11	18:10:00	UTC	71	55.11	N	158	27.726	W	5.1
Stn.19-10m	2025	09	11	18:10:00	UTC	71	55.11	N	158	27.726	W	10.1
Stn.19-Chl	2025	09	11	18:10:00	UTC	71	55.11	N	158	27.726	W	24.6
Stn.19-B-5	2025	09	11	18:10:00	UTC	71	55.11	N	158	27.726	W	50.7
Stn.19-0m-bio	2025	09	11	18:10:00	UTC	71	55.11	N	158	27.726	W	0
Stn.21-0m	2025	09	12	04:08:00	UTC	72	29.046	N	156	18.198	W	0
Stn.21-5m	2025	09	12	04:08:00	UTC	72	29.046	N	156	18.198	W	5
Stn.21-Chl	2025	09	12	04:08:00	UTC	72	29.046	N	156	18.198	W	34.6
Stn.21-50m	2025	09	12	04:08:00	UTC	72	29.046	N	156	18.198	W	50.1
Stn.21-TB	2025	09	12	04:08:00	UTC	72	29.046	N	156	18.198	W	99.6
Stn.21-800m	2025	09	12	04:08:00	UTC	72	29.046	N	156	18.198	W	790.1
Stn.21-0m-bio	2025	09	12	04:08:00	UTC	72	29.046	N	156	18.198	W	0
Stn.22-TB	2025	09	12	16:16:00	UTC	71	45.258	N	155	3.918	W	247.8
Stn.27-0m	2025	09	13	05:06:00	UTC	71	10.404	N	159	13.164	W	0
Stn.27-5m	2025	09	13	05:06:00	UTC	71	10.404	N	159	13.164	W	4.6
Stn.27-Chl	2025	09	13	05:06:00	UTC	71	10.404	N	159	13.164	W	32.4
Stn.27-50m	2025	09	13	05:06:00	UTC	71	10.404	N	159	13.164	W	49.9
Stn.27-TB	2025	09	13	05:06:00	UTC	71	10.404	N	159	13.164	W	74.5
Stn.27-B-5	2025	09	13	05:06:00	UTC	71	10.404	N	159	13.164	W	90.3
Stn.30-0m	2025	09	13	23:57:00	UTC	73	2.28	N	163	26.022	W	0
Stn.30-5m	2025	09	13	23:57:00	UTC	73	2.28	N	163	26.022	W	5.1
Stn.30-Chl	2025	09	13	23:57:00	UTC	73	2.28	N	163	26.022	W	34.9
Stn.30-50m	2025	09	13	23:57:00	UTC	73	2.28	N	163	26.022	W	49.8
Stn.30-TB	2025	09	13	23:57:00	UTC	73	2.28	N	163	26.022	W	
Stn.30-B-5	2025	09	13	23:57:00	UTC	73	2.28	N	163	26.022	W	96.5
Stn.30-0m-bio	2025	09	13	23:57:00	UTC	73	2.28	N	163	26.022	W	0
Stn.31-TB	2025	09	16	16:10:00	UTC	74	47.514	N	168	43.566	W	49.4
Stn.32-0m	2025	09	16	22:27:00	UTC	74	42.462	N	166	2.676	W	0
Stn.32-5m	2025	09	16	22:27:00	UTC	74	42.462	N	166	2.676	W	5
Stn.32-Chl	2025	09	16	22:27:00	UTC	74	42.462	N	166	2.676	W	41.6
Stn.32-50m	2025	09	16	22:27:00	UTC	74	42.462	N	166	2.676	W	49.5
Stn.32-TB	2025	09	16	22:27:00	UTC	74	42.462	N	166	2.676	W	59.4
Stn.32-B-5	2025	09	16	22:27:00	UTC	74	42.462	N	166	2.676	W	408.5
Stn.33-0m	2025	09	17	18:15:00	UTC	75	56.772	N	165	32.172	W	0
Stn.33-5m	2025	09	17	18:15:00	UTC	75	56.772	N	165	32.172	W	5.2
Stn.33-50m	2025	09	17	18:15:00	UTC	75	56.772	N	165	32.172	W	49.9
Stn.33-B-5	2025	09	17	18:15:00	UTC	75	56.772	N	165	32.172	W	431.1
Stn.34-0m	2025	09	18	00:30:00	UTC	75	16.962	N	164	6.438	W	0
Stn.34-5m	2025	09	18	00:30:00	UTC	75	16.962	N	164	6.438	W	5.3
Stn.34-50m	2025	09	18	00:30:00	UTC	75	16.962	N	164	6.438	W	49.5
Stn.34-TB	2025	09	18	00:30:00	UTC	75	16.962	N	164	6.438	W	29.6
Stn.34-B-5	2025	09	18	00:30:00	UTC	75	16.962	N	164	6.438	W	1386.6
Stn.34-0m-bio	2025	09	18	00:30:00	UTC	75	16.962	N	164	6.438	W	0
Stn.35-2-0m	2025	09	21	00:46:00	UTC	74	31.86	N	161	56.148	W	0
Stn.35-2-5m	2025	09	21	00:46:00	UTC	74	31.86	N	161	56.148	W	5.4
Stn.35-2-Chl	2025	09	21	00:46:00	UTC	74	31.86	N	161	56.148	W	39.8
Stn.35-2-50m	2025	09	21	00:46:00	UTC	74	31.86	N	161	56.148	W	50
Stn.35-2-TB	2025	09	21	00:46:00	UTC	74	31.86	N	161	56.148	W	99.1
Stn.35-2-800m	2025	09	21	00:46:00	UTC	74	31.86	N	161	56.148	W	789.9
Stn.35-2-0m-bio	2025	09	21	00:46:00	UTC	74	31.86	N	161	56.148	W	0
Stn.36-0m	2025	09	21	19:08:00	UTC	74	3.498	N	158	51.792	W	0
Stn.36-5m	2025	09	21	19:08:00	UTC	74	3.498	N	158	51.792	W	5.7
Stn.36-Chl	2025	09	21	19:08:00	UTC	74	3.498	N	158	51.792	W	57.5
Stn.36-50m	2025	09	21	19:08:00	UTC	74	3.498	N	158	51.792	W	49.7
Stn.36-500m	2025	09	21	19:08:00	UTC	74	3.498	N	158	51.792	W	492.9
Stn.36-1000m	2025	09	21	19:08:00	UTC	74	3.498	N	158	51.792	W	987.2
Stn.36-3000m	2025	09	21	19:08:00	UTC	74	3.498	N	158	51.792	W	2948.1
Stn.36-B-5	2025	09	21	19:08:00	UTC	74	3.498	N	158	51.792	W	3439.3
Stn.36-0m-bio	2025	09	21	19:08:00	UTC	74	3.498	N	158	51.792	W	0
Stn.37-0m	2025	09	22	14:44:00	UTC	72	29.994	N	168	44.916	W	0
Stn.37-5m	2025	09	22	14:44:00	UTC	72	29.994	N	168	44.916	W	5.7
Stn.37-20-m	2025	09	22	14:44:00	UTC	72	29.994	N	168	44.916	W	20.1
Stn.37-50m	2025	09	22	14:44:00	UTC	72	29.994	N	168	44.916	W	49.7
Stn.37-B-5	2025	09	22	14:44:00	UTC	72	29.994	N	168	44.916	W	52.4
Stn.37-0m-bio	2025	09	22	14:44:00	UTC	72	29.994	N	168	44.916	W	0
0911-ICE-1	2025	09	11	16:15:00	UTC	71	56	N	158	27	W	0
0911-ICE-2	2025	09	11	16:15:00	UTC	71	56	N	158	27	W	0
0917-ICE-1	2025	09	17	16:30:00	UTC	75	57	N	165	44	W	0
0917-ICE-2	2025	09	17	16:30:00	UTC	75	57	N	165	44	W	0
0921-ICE-1	2025	09	21	16:55:00	UTC	74	04	N	158	49	W	0
0921-ICE-2	2025	09	21	16:55:00	UTC	74	04	N	158	49	W	0

3.1.5 Mie/Raman Lidar Observation

(1) Personnel
Fumikazu TAKETANI (JAMSTEC)
Takeshi KINASE (JAMSTEC)
Takuma MIYAKAWA (JAMSTEC)
Masaki KATSUMATA (JAMSTEC)
Kyoko TANIGUCHI (JAMSTEC)
Ryo OYAMA (NME)
Haruki DOI (NME)
Seika TAKAI (NME)
Satomi OGAWA (NME)

(2) Objective
The objective of this observation is to capture the vertical distribution of clouds, aerosols, and water vapor in high spatio-temporal resolution.

(3) Parameters
355nm Mie scattering signal
532nm Mie scattering signal
1064nm Mie scattering signal
387nm Raman nitrogen scattering signal (nighttime only)
408nm Raman water vapor scattering signal (nighttime only)
607nm Raman nitrogen scattering signal (nighttime only)
660nm Raman water vapor scattering signal (nighttime only)

(4) Instruments and methods
The Mirai Lidar system transmits a 10-Hz pulse laser in three wavelengths: 1064nm, 532nm, 355nm. For cloud and aerosol observation, the system detects Mie scattering at these wavelengths. The separate detections of polarization components at 532 nm and 355 nm obtain additional characteristics of the targets. The system also detects Raman water vapor signals at 660 nm and 408nm, Raman nitrogen signals at 607 nm and 387nm at nighttime. Based on the signal ratio of Raman water vapor to Raman nitrogen, the system offers water vapor mixing ratio profiles.

(5) Preliminary Results
The lidar system observed the lower atmosphere throughout the cruise, except on EEZs and territorial waters without permission. All data will be reviewed after the cruise to maintain data quality.

(6) Data Archive
These data obtained in this cruise will be submitted to the Data Management Group of JAMSTEC, and will be opened to the public via "Data Research System for Whole Cruise Information in JAMSTEC (DARWIN)" in JAMSTEC web site.
<https://www.godac.jamstec.go.jp/darwin/en/>

3.1.6 Observation of atmospheric water vapor isotopes

(1) Personnel
Hotaek Park (JAMSTEC) Principal investigator

Background and objective
The declining Arctic sea-ice caused increasing open sea surface can result in larger evaporation from the surface, enforced by the warming climates. The evaporated water vapor wets the atmosphere, which then likely strengthenes water cycle in terrestrial regions as a larger precipitable water. Observations identified the increase of both autumnal precipitation and winter snow depth in the terrestrial regions, particularly at the northeastern Siberia. However, the observational data have provided little evidence representing the influence of the declined sea-ice on the intensified terrestrial water cycle. Isotope is a useful tool to identify the contribution of the Arctic Ocean sourced water to the terrestrial hydrology, tracking the origins of the terrestrial precipitation. Focused on the advantage of stable water isotope, a precipitation isotope observational network was constructed, sampling the precipitation water at the Arctic Ocean and land. As the observational activity using the network, the isotope of the atmospheric water vapor has been monitored at the MIRAI Arctic Ocean cruise from 2019. This document reports the isotopic properties of atmospheric water vapor monitored at the R/V MIRAI 2025 Arctic cruise.

(2) Parameters
Isotope ratios of oxygen and hydrogen and water vapor concentration

(3) Instrument and method
The isotopic ratios of atmospheric water vapor were monitored by a L2130-*i* Isotope and Gas Concentration Analyzer, which provides $\delta^{18}O$ and $\delta^{2}H$ values for isotopic H_2O with high-precision measurements of 1–2 Hz frequency, including water vapor concentration. The observed data are archived on the storage of the spectrometer. Two standard liquids, for example with isotopic values of -0.38/-1.30‰ and -31.24/-245.22‰ for $\delta^{18}O/\delta^{2}H$, are individually injected for 15 minutes every 12-hour, in which the derived linear regression equation is used to calibrate the values monitored by the spectrometer.

(4) Preliminary results
The monitored isotopic ratios were averaged to hourly time scales, exhibiting the temporal

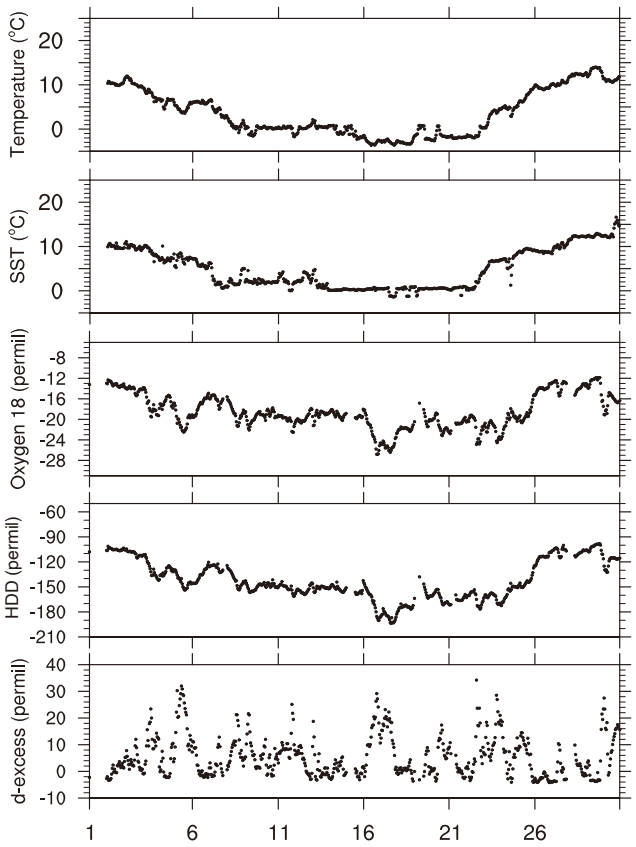

Fig. 1. The variability of air and sea surface temperature and atmospheric water vapor isotopic variables in September during MR-25 MIRAI cruise.

variability during the cruse period from September 1 to 30 of 2025, with air and sea surface temperature (Fig. 1). The isotopic ratios of $\delta^{18}O/\delta^{2}H$ showed higher values at the initial dates of the cruse, in which the vessel cruised relatively warm regions as identified by the warm air temperature. Then, the ratios gradually decreased and recorded the minimum values (i.e., -26.7‰ for $\delta^{18}O$ and -193.3 for $\delta^{2}H$) around Sep. 16 and 17, characterized by the colder air temperature. During the period from Sep. 15 to Sep. 25 as the vessel stayed over the northern Arctic Ocean, the air temperature recorded 0℃ below, and the sea surface temperature was also low, representing the spatial variability of the sea surface heat condition along the vessel cruising routes.

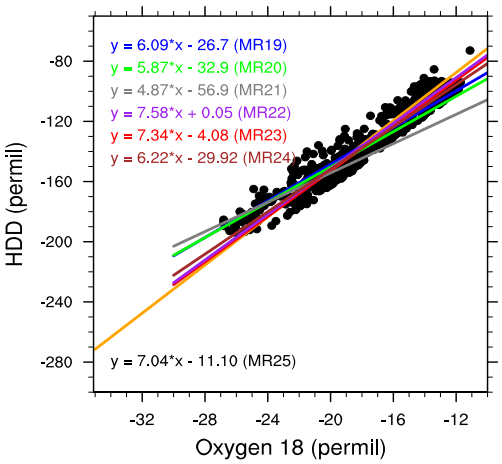

Fig. 2. Relationship between observed oxygen and hydrogen isotopes in individual cruise years from 2019 to 2025, represented by regression equations.

The isotopic ratios of $\delta^{18}O/\delta^{2}H$ significantly correlated with air temperature. The relationship has already identified at the previous cruise years (i.e., 2019–2024). The connectivity of the isotope ratios and air temperature is verified by the d-excess index that represents humidity and temperature conditions of the evaporated sea surface, exhibiting larger diurnal and daily variability at the range of approximately 35 ‰, relative to the lower variability of $\delta^{18}O$ and $\delta^{2}H$ (Fig. 1). The d-excess was correlated to the difference between sea surface and air temperature with larger scattering, as certified by the past cruise data. The water vapor recorded relatively lower isotopic ratios at cold temperature, resulting in higher d-excess values (Fig. 1). The larger difference between air and sea surface temperature represents higher atmospheric demand for evaporation, consequently higher evaporation with higher d-excess values.

The monitored $\delta^{18}O$ and $\delta^{2}H$ ratios indicated significantly higher correlation (Fig. 2), yielding the slope of 7.04. The slopes derived by the past six-year cruise, including this year, is lower than the value 8 of global meteoric water line (GMWL), representing the dependence of isotopic ratios on regional and temporal climatic conditions.

(5) Data archive

The data obtained in this cruise will be submitted to the Data Management Group of JAMSTEC, and will be opened to the public via "Data Research System for Whole Cruise Information in JAMSTEC (DARWIN)" in JAMSTEC web site. https://www.godac.jamstec.go.jp/darwin/en/

3.1.7 Microwave Radiometer

(1) Personnel

Fumikazu TAKETANI	(JAMSTEC)
Masaki KATSUMATA	(JAMSTEC)

Akira KUWANO-YOSHIDA (Kyoto Univ.)
Masahiro MINOWA (Furuno Electric Co., Ltd.)

(2) Objective
To retrieve the integrated and vertical profile of water vapor

(3) Method
The microwave radiometer (hereafter MWR; manufactured by Furuno Electric Co., Ltd.) is used. The MWR received natural microwave within the angle of 20 deg. from zenith. The MWR observes at the frequencies around 22 GHz, to retrieve the column integrated water vapor (or precipitable water), and the vertical profile of the water vapor. The observation was made approximately every 20 seconds except when periodic auto-calibration was on-going (once in several minutes). The rain sensor is equipped to identify the period of rainfall.
In addition to the MWR, the whole sky camera was installed beside the MWR. This is to monitor cloud cover, which also affects the microwave signals. The camera obtained the whole-sky image every 2 minutes.
All instruments were installed at the top of the roof of aft wheelhouse, as in Fig. 3.1.7-1. The data was continuously obtained all through the cruise period.

(4) Results
The data has been obtained all through the cruise. Further analyses will be carried out after the cruise.

(5) Data archive
The data will be submitted to the JAMSTEC Data Management Group (DMG).

(6) Acknowledgment
The observation was supported by the JSPS KAKENHI Grant 23H00519. Nippon Marine Enterprise Ltd. kindly supported the operation.

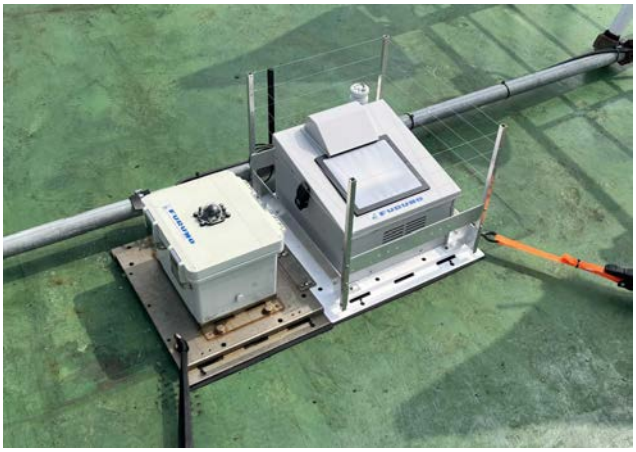

Fig. 3.1.7-1: Outlook of the instruments installed at the roof of the aft wheelhouse; the microwave radiometer for the air temperature (right), microwave radiometer for the water vapor (middle), and the whole-sky camera (left).

3.1.8. Ice radar

(1) Personnel
Amane Fujiwara JAMSTEC -PI

Ryo Oyama	NME(Nippon Marine Enterprises, Ltd.)
Satomi Ogawa	NME
Haruki Doi	NME
Seika Takai	NME
Masanori Murakami	MIRAI Crew

(2) Objectives
In the sea ice areas, marine radar provides an important tool for the detection of sea ice and icebergs. It is importance to monitor the sea ice daily and produce ice forecasts to assist ship traffic and other marine operations. In order to select route optimally, ice condition prediction technology is necessary, and image information of ice-sea radar is used for constructing a route selection algorithm.

(3) Parameters
Capture format: JPEG
Capture interval: 60 seconds
Resolution: 1,024×768 pixel
Color tone: 256 gradations

(4) Instruments and methods
R/V MIRAI is equipped with an Ice Navigation Radar, "sigma S6 Ice Navigator (Rutter Inc.)". The ice navigation radar, the analog signal from the x-band radar is converted by a modular radar interface and displayed as a digital video image (Figure 3.1.8-1). The sea ice radar is equipped with a screen capture function and saves at arbitrary time intervals.

(5) Observation log
04 Sep. 2025 - 23 Sep. 2025

(6) Data archives
These data obtained in this cruise will be submitted to the Data Management Group of JAMSTEC, and will be opened to the public via "Data Research System for Whole Cruise Information in JAMSTEC (DARWIN)" in JAMSTEC web site.
< https://www.godac.jamstec.go.jp/darwin/en/ >

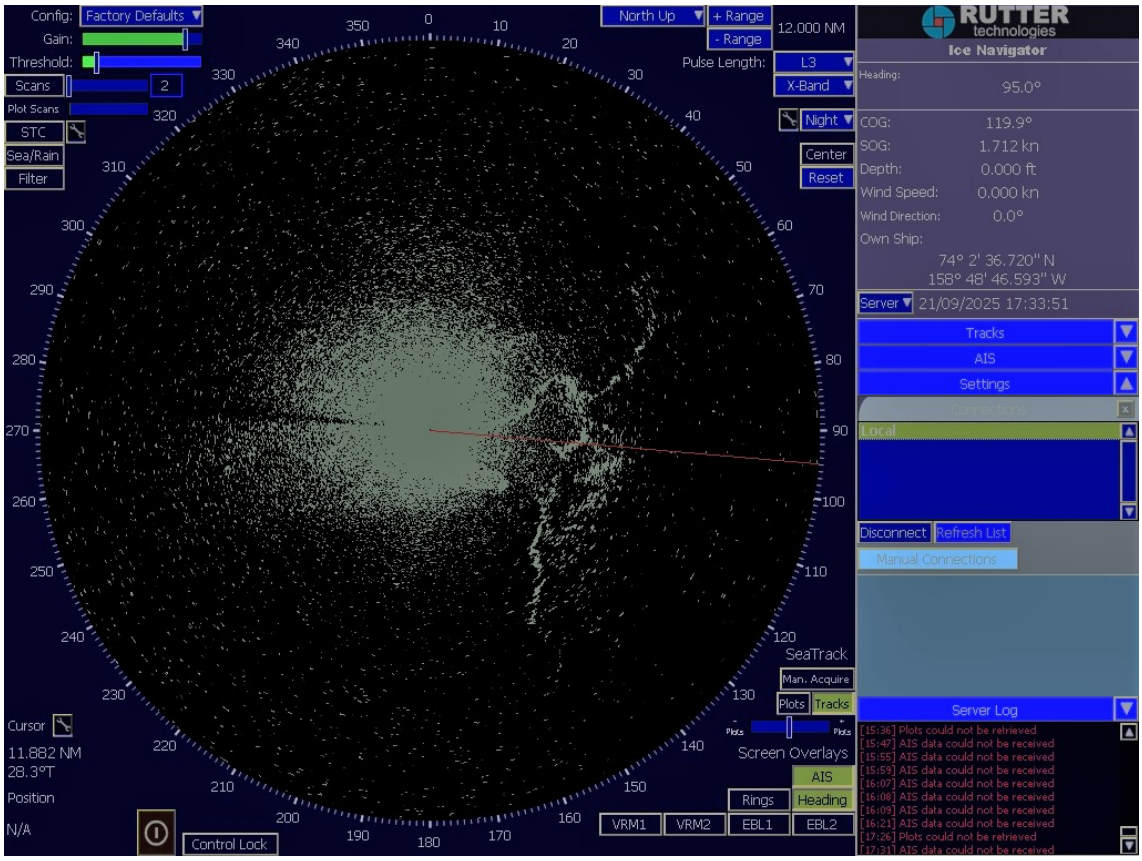

Figure 3.1.8-1: Image of sea ice from sea ice radar

3.2. Physical Oceanography

3.2.1. CTD cast and water samplings

(1) Personnel

Amane Fujiwara	JAMSTEC	- Principal Investigator
Riho Fujioka	MWJ	- Operation leader
Aine Yoda	MWJ	
Ko Arihara	MWJ	
Satoshi Kimura	JAMSTEC	
Yuri Fukai	JAMSTEC	
Taisei Yamaguchi	JAMSTEC	

(2) Objective

The $CTDO_2$/water sampling measurements were conducted to obtain vertical profiles of seawater properties by sensors and water sampling.

(3) Instruments and method

Instruments used in this cruise are as follows:

Winch and cable

Traction winch system (3.0 ton) (Dynacon, Inc., Bryan, Texas, USA)

Armored cable (φ = 9.5 mm)

Compact underwater slip ring swivel

Frame

592 kg stainless steel frame for 36-position 12-L water sample bottles

Aluminum rectangular fin (54 × 90 cm) to resist frame's rotation

Water sampler and sampling bottle

36-position carousel water sampler, SBE 32 (Sea-Bird Scientific, Washington, USA)

Serial no. 3254451-0826

12-L sample bottle, model OTE 110 (OceanTest Equipment, Inc., Fort Lauderdale, Florida, USA)

(No TEFLON coating, with Viton O-rings)

Deck unit

SBE11plus (Sea-Bird Scientific, Washington, USA)

Serial no. 11P39850-0705

Underwater unit

Pressure sensor, SBE 9plus (Sea-Bird Scientific, Washington, USA)

Serial no. 09P54451-1027 (117457) (calibration date: December 6, 2024)

Deep ocean standard thermometer, SBE 35 (Sea-Bird Scientific, Washington, USA)

Serial no. 0053 (calibration date: February 11, 2025)

Temperature sensor, SBE 3 (Sea-Bird Scientific, Washington, USA)

Primary, Serial no. 031525 (calibration date: Jun 14, 2024)

Secondary, Serial no. 034818 (calibration date: December 4, 2024)

Conductivity sensor, SBE 4C (Sea-Bird Scientific, Washington, USA)

Primary, Serial no. 043036 (calibration date: November 27, 2024)

Secondary, Serial no. 041088 (calibration date: Jun 6, 2024)

Dissolved oxygen sensor, Primary, RINKO III (JFE Advantech Co., Ltd., Hyogo, Japan)

Serial no. 0287, Sensing foil no. 163011BA (in situ calibrated on MR25-04cruise)

Dissolved oxygen sensor, Secondary, SBE 43 (Sea-Bird Scientific, Washington, USA)
Serial no. 430949 (calibration date: December 16, 2023)
Transmissometer, C-Star, (WET Labs, Inc., Philomath, Oregon, USA)
Serial no. 2532DR (in situ calibrated on MR25-04 cruise)
Turbidity Meter (Seapoint Sensors Inc., New Hampshire, USA)
Serial no. 14953 (Gain: 100 X, (0-25 FTU)
Chlorophyll fluorometer (Seapoint Sensors Inc., New Hampshire, USA)
Serial no. 4164, Gain: 10X (0-15 ug/L)
PAR sensor, PAR-Log ICSW (Sea-Bird Scientific, Washington, USA)
Serial no. 1026 (calibration date: July 06, 2015)
Altimeter, PSA-916T (Teledyne Benthos, Inc.)
Serial no. 1100
Pump, SBE 5T (Sea-Bird Scientific, Washington, USA)
Primary, Serial no. 054595
Secondary, Serial no. 053293
Bottom contact switch (Sea-Bird Scientific, Washington, USA)
Other additional sensors
Data logger (two 16 bit A/D channels and four serial [RS-232C] channels, JAMSTEC)
Software
Data acquisition software, SEASAVE-Win32, version 7.26.7.121
Data processing software, SBEDataProcessing-Win32, version 7.26.7.129 and some original modules

(4) Data Collection and processing
(4.1) Data collection
The CTD system was powered on at least 15 minutes in advance of the data acquisition to stabilize the pressure sensor. The data was acquired at least two minutes before and after the CTD cast to collect atmospheric pressure data on the ship's deck.
The CTD package was lowered into the water from the starboard side and held 10 m beneath the surface to activate the pump. After the pump was activated, the package was lifted to the surface and lowered at a rate of 1.0 m/s to 200 m (or 300m when significant wave height was high) then the package was stopped to operate the heave compensator of the crane. The package was lowered again and at 1.0m/s and after passing the depths where vertical gradient of water properties was large, it was lowered at a rate of 1.2m/s to the bottom. For the up cast, the package was lifted at a rate of 1.2 m/s except for bottle firing stops. As a rule, the bottle was fired after waiting from the stop for more than 30 seconds and the package was stayed at least 5 seconds for measurement of the SBE 35 at each bottle firing stops. For depths where vertical gradient of water properties was expected to be large, the bottle was fired after waiting from the stop for 60 seconds to enhance changing the water between inside and outside of the bottle. At 200m (or 300m) from the surface, the package was stopped to stop the heave compensator of the crane.

(4.2) Data collection problems
During cast 006M001, secondary conductivity data shifted from 50db to 31db and 11db to 1db during upcast, possibly due to jelly fish stuck in TC duct.
During cast 007M001, secondary conductivity data shifted from 40db to 1db to 1db

during upcast, possibly due to jelly fish stuck in TC duct.
During cast 035M002, turbidity data shifted 0 voltage from 359db downcast to 372db upcast. After this cast, turbidity sensor cable was checked and there was no problem. The cable and sensor connector were cleaned. After this cast, there was no problem.
During cast 021M001, RINKOⅢ data appeared to be noisy from 685db downcast to 1303db upcast.
After this cast, there was no problem. But during cast 035M002, RINKOⅢ data appeared to be noisy from 257db to 792db during downcast . After this cast, RINKO Ⅲ cable was checked and there was no problem. The cable and sensor connector were cleaned. After this cast, there was no problem.
More detailed information about the irregularities in data (noise, spike or shift, etc.) is recorded in remarks sheet included in data submission.
The definitions of these irregularities are as follows:
(1) noise: not singly but continuously detected outliers.
(2) spike: one-off outlier which is detected after data processing and is oceanographically impossible.
(3) shift: continuous data trend which is deviated from accurate ones.

(4.3) Data Processing
The following are the data processing software (SBEDataProcessing-Win32) and original software data processing module sequence and specifications used in reduction of CTD data in this cruise.
(The process in order)

DATCNV converted the raw data to engineering unit data. DATCNV also extracts bottle information where scans were marked with the bottle confirm bit during acquisition. The scan duration to be included in bottle file was set to 4.4 seconds, and the offset was set to 0.0 seconds. The hysteresis correction for the SBE 43 data (voltage) was applied for both profile and bottle information data. The tau correction for the SBE 43 data (voltage) was applied for deeper than 2000 dbar profile and bottle information data.
TCORP (original module, version 1.1) corrected the pressure sensitivity of the temperature (SBE3) sensor for both profile and bottle information data.
RINKOCOR (original module, 1.0) corrected the time-dependent, pressure-induced effect (hysteresis) of the RINKOIII profile data.
RINKOCORROS (original module) corrected the time-dependent, pressure-induced effect (hysteresis) of the RINKOIII bottle information data by using the hysteresis-corrected profile data.
BOTTLESUM created a summary of the bottle data. The data were averaged over 4.4 seconds.
ALIGNCTD converted the time-sequence of sensor outputs into the pressure sequence to ensure that all calculations were made using measurements from the same parcel of water. For a SBE 9plus CTD with the ducted temperature and conductivity sensors and a 3000-rpm pump, the typical net advance of the conductivity relative to the temperature is 0.073 seconds. So, the SBE 11plus deck unit was set to advance the primary and the secondary conductivity for 1.73 scans (1.75/24 = 0.073 seconds). Oxygen data are also systematically delayed with respect to depth mainly because of the long time constant of the oxygen sensor and of an additional delay from the transit time of water in the pumped plumbing line. This

delay was compensated by 4 seconds advancing the SBE 43 oxygen sensor output (voltage) relative to the temperature data. Delay of the RINKOIII data was also compensated by 1 second advancing sensor output (voltage) relative to the temperature data. Delay of the transmissometer data was also compensated by 2 seconds advancing sensor output (voltage) relative to the temperature data.
WILDEDIT marked extreme outliers in the data files. The first pass of WILDEDIT obtained the accurate estimate of the true standard deviation of the data. The data were read in blocks of 1000 scans. Data greater than 10 standard deviations were flagged. The second pass computed a standard deviation over the same 1000 scans excluding the flagged values. Values greater than 20 standard deviations were marked bad. This process was applied to pressure, depth, temperature, conductivity, and SBE 43 output.
CELLTM used a recursive filter to remove conductivity cell thermal mass effects from the measured conductivity. Typical values for SBE 9plus with TC duct and 3000 rpm pump which were 0.03 for thermal anomaly amplitude alpha and 7.0 for the time constant 1/beta were used.
FILTER performed a low-pass filter on pressure and depth with a time constant of 0.15 second. In order to produce zero phase lag (no time shift) the filter runs forward first then backward.
WFILTER performed as a median filter to remove spikes in transmissometer data, fluorometer data, and turbidity meter. A median value was determined by 49 scans of the window.
SECTIONU (original module, version 1.1) selected a time span of data based on scan number in order to reduce a file size. The minimum number was set to be the starting time when the CTD package was beneath the sea-surface after activation of the pump. The maximum number was set to be the end time when the depth of the package was 1 dbar below the surface. The minimum and maximum numbers were automatically calculated in the module.
LOOPEDIT marked scans where the CTD was moving less than the minimum velocity of 0.0 m/s (traveling backwards due to ship roll).
DESPIKE (original module, version 1.0) removed spikes of the data. A median and mean absolute deviation was calculated in 1-dbar pressure bins for both down and up cast, excluding the flagged values. Values greater than 4 mean absolute deviations from the median were marked bad for each bin. This process was performed twice for temperature, conductivity and RINKOIII output.
DERIVE was used to compute dissolved oxygen (SBE43), salinity, potential temperature, and sigma-theta.
BINAVG averaged the data into 1-decibar pressure bins and 1-sec time bins. The center value of the first bin was set equal to the bin size. The bin minimum and maximum values are the center values plus and minus half the bin size. Scans with pressures greater than the minimum and less than or equal to the maximum were averaged. Scans were interpolated so that a data recorded exist every dbar.
BOTTOMCUT (original module, version 0.1) deleted the deepest pressure bin when the averaged scan number of the deepest bin was smaller than the average scan number of the bin just above.
SPLIT was used to split data into down cast and up cast.

(5) Data archive
These data obtained in this cruise will be submitted to the Data Management Group

of JAMSTEC, and will be opened to the public via "Data Research System for Whole Cruise Information in JAMSTEC (DARWIN)" in JAMSTEC web site.

Table 3.1 MR25-05C CTD cast table

Stnnbr	Castno	Date(UTC)	Time(UTC)		BottomPosition		Depth	Wire	HT Above	Max	Max	CTD	Remark
		(mmddyy)	Start	End	Latitude	Longitude	(m)	Out (m)	Bottom (m)	Depth	Pressure	Filename	
001	001	090425	03:05	03:30	65-29.99N	168-44.99W	55.0	45.9	4.9	49.5	50.0	001M001	
002	001	090425	08:28	08:50	66-00.07N	168-44.88W	53.2	45.2	5.4	47.5	48.0	002M001	
003	001	090425	18:19	18:48	66-30.05N	168-45.19W	54.4	45.9	5.0	48.5	49.0	003M001	
004	001	090425	23:17	23:37	67-00.03N	168-45.04W	45.9	36.2	5.5	39.6	40.0	004M001	
005	001	090525	04:03	04:28	67-29.99N	168-45.01W	50.1	40.4	4.8	44.5	45.0	005M001	
006	001	090525	10:05	10:29	68-01.95N	168-49.97W	59.3	48.9	4.8	53.5	54.0	006M001	
007	001	090525	15:33	15:58	68-29.97N	168-45.03W	54.0	45.8	4.9	48.5	49.0	007M001	
008	001	090525	21:04	21:31	69-00.01N	168-44.89W	53.7	43.4	5.1	47.5	48.0	008M001	
009	001	090625	04:26	04:50	69-30.01N	168-45.03W	51.8	43.9	4.8	46.5	47.0	009M001	
010	001	090625	08:04	08:23	69-59.99N	168-44.98W	40.9	30.1	5.0	35.6	36.0	010M001	
011	001	090625	12:21	12:40	70-29.98N	168-45.08W	39.5	28.8	4.8	33.7	34.0	011M001	
012	001	090625	15:43	16:03	71-00.01N	168-44.90W	45.4	36.6	5.8	38.6	39.0	012M001	
013	001	090625	19:42	20:10	70-45.17N	167-28.81W	54.7	46.3	5.8	48.5	49.0	013M001	
014	001	090625	23:44	00:04	70-56.15N	165-24.33W	43.0	33.1	4.1	37.6	38.0	014M001	
015	001	090825	22:10	22:44	71-41.74N	154-55.43W	110.6	103.5	4.5	105.9	107.0	015M001	
016	001	091025	16:23	17:54	72-01.79N	151-34.75W	2413.0	2403.5	9.8	2397.1	2436.0	016M001	
016	002	091025	19:13	20:19	72-01.83N	151-34.69W	2426.0	794.6	-	792.3	802.0	016M002	
017	001	091025	23:28	00:09	71-42.72N	152-51.74W	229.0	221.2	4.6	224.6	227.0	017M001	
018	001	091125	04:19	04:39	71-25.69N	154-06.63W	41.6	31.4	5.4	33.7	34.0	018M001	
019	001	091125	18:07	18:31	71-55.11N	158-27.72W	57.3	48.7	5.7	50.5	51.0	019M001	
020	001	091125	22:17	22:44	72-11.35N	157-13.79W	121.7	111.0	5.5	114.8	116.0	020M001	
021	001	091225	01:38	02:33	72-29.04N	156-18.19W	1303.0	1288.7	10.0	1285.6	1303.0	021M001	
021	002	091225	03:53	05:04	72-29.05N	156-18.07W	1299.0	792.2	-	791.3	801.0	021M002	
022	001	091225	16:09	16:55	71-45.25N	155-03.91W	273.8	266.4	4.4	270.0	273.0	022M001	
023	001	091225	21:36	21:41	71-34.66N	157-50.27W	65.2	57.1	4.6	59.4	60.0	023M001	
024	001	091225	22:29	23:00	71-29.79N	157-40.13W	82.6	78.1	4.8	80.2	81.0	024M001	
025	001	091325	00:17	00:26	71-24.81N	157-29.91W	123.0	114.8	6.0	116.8	118.0	025M001	
026	001	091325	01:14	01:21	71-19.73N	157-19.97W	89.8	82.3	6.0	84.1	85.0	026M001	
027	001	091325	05:03	05:29	71-10.40N	159-13.16W	95.1	88.6	5.1	90.1	91.0	027M001	
028	001	091325	09:15	09:36	71-10.03N	160-59.85W	48.4	39.3	4.4	43.5	44.0	028M001	
029	001	091325	18:40	18:58	72-20.60N	163-07.63W	40.5	32.3	5.3	34.6	35.0	029M001	
030	001	091325	23:53	00:30	73-02.27N	163-26.02W	99.3	94.1	4.7	97.0	98.0	030M001	
031	001	091625	16:06	16:40	74-47.51N	168-43.56W	196.0	188.7	4.9	190.9	193.0	031M001	
032	001	091625	22:18	23:11	74-42.45N	166-02.67W	422.0	407.8	9.9	408.3	413.0	032M001	
033	001	091725	18:05	18:57	75-56.77N	165-32.17W	445.0	429.4	10.4	431.0	436.0	033M001	
034	001	091825	00:04	01:34	75-16.96N	164-06.44W	1419.0	1390.3	10.5	1386.7	1406.0	034M001	
035	001	092025	21:08	22:15	74-31.86N	161-56.14W	1688.0	1677.1	9.4	1675.6	1700.0	035M001	
035	002	092125	00:30	01:46	74-31.86N	161-56.92W	1686.0	790.0	9.2	791.2	801.0	035M002	
036	001	092125	18:14	20:39	74-03.49N	158-51.79W	3454.0	3451.5	9.8	3439.3	3504.0	036M001	
037	001	092225	14:41	15:04	72-29.99N	168-44.91W	58.4	48.1	5.6	52.4	53.0	037M001	

3.2.2. XCTD

(1) Personnel

Amane Fujiwara	JAMSTEC -PI
Ryo Oyama	NME(Nippon Marine Enterprises, Ltd.)
Satomi Ogawa	NME
Haruki Doi	NME
Seika Takai	NME
Masanori Murakami	MIRAI Crew

(2) Objectives

To obtain vertical profiles of sea water temperature and salinity (calculated from temperature, pressure (depth), and conductivity).

(3) Parameters

Conductivity [mS/cm]
Temperature [deg-C]

Depth [m] (XCTD-1N: 0 ~ 1000 m, XCTD-4A: 0 ~ 2000 m)

(4) Instruments and methods

We observed vertical profiles of sea water temperature and salinity measured by XCTD-1N and XCTD-4A probes manufactured by Tsurumi-Seiki Co. (TSK). The electric signal from the probe was converted by MK-150N (TSK), and was recorded by AL-12B software (Ver.1.8.0, TSK). We launched 45 probes by using the automatic launcher and the hand launcher. The XCTD observation log is shown in Table 3.2.2-1.

(5) Observation log

Table 3.2.2-1: XCTD observation log

No.	Station No.	Date [YYYY/MM/DD]	Time [hh:mm]	Latitude [deg]	Longitude [deg]	Depth [m]	SST [deg-C]	SSS [PSU]	Probe S/N
1	XCTD1	2025/09/01	00:04	54-44.7557N	167-28.2343W	598	-	-	22062269
2	Bering01	2025/09/04	05:22	65-38.8669N	168-16.3106W	45	10.259	25.597	25045607
3	Bering02	2025/09/04	05:38	65-40.2155N	168-21.8323W	50	10.267	25.514	25045608
4	Bering03	2025/09/04	05:55	65-41.5796N	168-27.5890W	53	10.227	26.770	25045605
5	Bering04	2025/09/04	06:12	65-42.9039N	168-33.2841W	51	8.084	30.102	25045606
6	Bering05	2025/09/04	06:29	65-44.2555N	168-38.9831W	51	6.616	30.931	25045603
7	Bering06	2025/09/04	06:50	65-45.5920N	168-44.6849W	52	5.850	31.171	25045604
8	Barrow01	2025/09/09	02:48	71-49.4985N	155-50.0761W	89	2.449	25.329	23118276
9	Barrow02	2025/09/09	03:19	71-48.9603N	155-35.7666W	119	2.837	25.491	25035499
10	Barrow03	2025/09/09	03:40	71-48.0606N	155-23.0147W	147	2.517	25.364	25035500
11	Barrow04	2025/09/09	03:56	71-45.9508N	155-17.0630W	202	1.917	25.079	25045602
12	Barrow05	2025/09/09	04:11	71-44.1099N	155-11.8657W	304	1.882	24.629	23118275
13	Barrow06	2025/09/09	04:26	71-42.0742N	155-05.9421W	178	1.549	24.303	25035498
14	Barrow07	2025/09/09	04:41	71-40.0389N	155-00.7315W	105	2.533	26.060	23118272
15	Barrow08	2025/09/09	04:56	71-37.8689N	154-55.0375W	55	4.477	27.603	25045601
16	Barrow09	2025/09/09	05:13	71-35.5312N	154-48.8377W	39	4.900	27.206	25035497
17	Sta.16 /XCTD17	2025/09/10	16:41	72-01.7956N	151-34.7389W	2414	2.002	25.038	25066604
18	XCTD18	2025/09/10	21:58	71-51.0092N	152-12.8300W	1857	2.035	24.715	23118274
19	XCTD19	2025/09/11	02:13	71-33.4842N	153-30.0683W	53	2.855	26.294	23118269
20	XCTD20	2025/09/11	23:50	72-20.3411N	156-46.8868W	275	1.817	25.450	23118277
21	Sta.21 /XCTD21	2025/09/12	01:52	72-29.0422N	156-18.2327W	1302	2.163	25.500	23118273
22	Sta.21 /XCTD22	2025/09/12	02:04	72-29.0442N	156-18.1975W	1300	2.153	25.513	25066605
23	XCTD23	2025/09/12	22:02	72-32.2308N	157-45.1484W	71	1.556	25.913	23118266
24	XCTD24	2025/09/12	23:37	71-27.3085N	157-34.9943W	109	2.540	27.745	23118270
25	XCTD25	2025/09/13	00:50	71-22.3279N	157-24.9228W	112	4.565	27.764	23118271
26	XCTD26	2025/09/13	01:43	71-17.2919N	157-14.8645W	57	4.536	27.384	23128448
27	XCTD27	2025/09/13	14:30	71-37.9883N	163-28.9510W	39	1.480	27.051	23118267
28	XCTD28	2025/09/15	22:54	73-23.0571N	164-43.3125W	77	-0.155	27.190	23118268
29	XCTD29	2025/09/17	00:17	75-16.9526N	164-06.4411W	1414	-0.463	27.134	25066603
30	XCTD30 /COMAI	2025/09/18	16:53	76-23.3545N	164-27.9941W	618	-0.828	27.345	23118206

31	XCTD31 /NAP	2025/09/20	21:22	74-31.8712N	161-56.1529W	1687	-0.411	25.174	25066602
32	XCTD32	2025/09/21	03:02	74-26.7741N	161-18.8039W	1682	0.122	25.206	25066601
33	XCTD33	2025/09/21	04:02	74-22.6116N	160-46.9420W	1500	-0.254	24.786	25066606
34	XCTD34	2025/09/21	05:01	74-18.2397N	160-12.9912W	525	-0.521	24.824	23118211
35	XCTD35	2025/09/21	18:33	74-03.4755N	158-51.6917W	3457	-0.977	24.997	25010012
36	XCTD36	2025/09/21	22:52	74-01.0347N	159-48.1175W	1076	-0.959	25.022	25010011
37	XCTD37	2025/09/22	00:08	73-59.1613N	160-46.1586W	544	-0.315	24.900	23118210
38	XCTD38	2025/09/22	01:25	73-56.6387N	161-43.1236W	343	0.492	25.197	23118207
39	XCTD39	2025/09/22	02:43	73-54.1232N	162-41.3527W	265	0.550	25.417	23118208
40	XCTD40	2025/09/22	04:19	73-51.1025N	163-38.6462W	227	-0.548	25.684	23118209
41	XCTD41	2025/09/22	12:12	72-57.6780N	168-19.7703W	60	0.611	28.409	23118214
42	XCTD42	2025/09/22	18:52	72-00.0007N	168-44.9888W	50	3.183	30.458	23118214
43	XCTD43	2025/09/22	21:11	71-30.0115N	168-45.0020W	48	3.836	29.665	23118212
44	XCTD44	2025/09/23	15:54	67-29.9963N	168-29.9943W	48	6.708	29.677	23118217
45	XCTD45	2025/09/26	22:36	55-57.5992N	176-25.5176E	3825	8.689	32.784	22062267

(6) Data archives

These data obtained in this cruise will be submitted to the Data Management Group of JAMSTEC, and will be opened to the public via "Data Research System for Whole Cruise Information in JAMSTEC (DARWIN)" in JAMSTEC web site.
< https://www.godac.jamstec.go.jp/darwin/en/ >

3.2.3. Shipboard ADCP

(1) Personnel

Amane Fujiwara	JAMSTEC -PI
Ryo Oyama	NME(Nippon Marine Enterprises, Ltd.)
Satomi Ogawa	NME
Haruki Doi	NME
Seika Takai	NME
Masanori Murakami	MIRAI Crew

(2) Objectives

To obtain continuous measurement data of the current profile along the ship's track.

(3) Parameters

Upper ocean current velocity: horizontal velocity (u), vertical velocity (v) and depth.

(4) Instruments and methods

Upper ocean current measurements were made during this cruise, using the hull-mounted Acoustic Doppler Current Profiler (ADCP) system. For most of its operation, the instrument was configured for water-tracking mode. Bottom-tracking mode, interleaved bottom-ping with water-ping, was made to get the calibration data for evaluating transducer misalignment angle in the shallow water. The system consists

of following components;

1. R/V MIRAI has installed the Ocean Surveyor for vessel-mount ADCP (frequency 76.8 kHz; Teledyne RD Instruments, USA). It has a phased-array transducer with single ceramic assembly and creates 4 acoustic beams electronically. We mounted the transducer head rotated to a ship-relative angle of 45 degrees azimuth from the keel.
2. For heading source, we use ship's gyro compass (Tokyo Keiki, Japan), continuously providing heading to the ADCP system directory. Additionally, we have Inertial Navigation Unit (Phins, Ixblue, France) which provide high-precision heading, attitude information, pitch and roll. They are stored in ".N2R" data files with a time stamp.
3. Differential GNSS system (StarPack-D, Fugro, Netherlands) providing precise ship's position.
4. We used VmDas software version 1.50.19(TRDI) for data acquisition.
5. To synchronize time stamp of ping with Computer time, the clock of the logging computer is adjusted to GPS time server by using NTP (Network Time Protocol).
6. Fresh water is charged in the sea chest to prevent bio fouling at transducer face.
7. The sound speed at the transducer does affect the vertical bin mapping and vertical velocity measurement, and that is calculated from temperature, salinity (constant value; 35.0 PSU) and depth (6.5 m; transducer depth) by equation in Medwin (1975).

Data were configured for "8 m" layer intervals starting about 23 m below sea surface. Data were recorded every ping as raw ensemble data (.ENR). Additionally, 15 or 60 seconds averaged data were recorded as short-term average (.STA). 300 seconds averaged data were long-term average (.LTA), respectively.

Major acquisition parameters for the measurement, Direct Command, are shown in Table 3.2.3-1.

Table 3.2.3-1: Major parameters

Bottom-Track Commands
BP = 001 Pings per Ensemble (almost less than 1,300 m depth)
Environmental Sensor Commands
EA = 04500 Heading Alignment (1/100 deg)
ED = 00065 Transducer Depth (0 - 65535 dm)
EF = +001 Pitch/Roll Divisor/Multiplier (pos/neg) [1/99 - 99]
EH = 00000 Heading (1/100 deg)
ES = 35 Salinity (0-40 pp thousand)
EX = 00000 Coordinate Transform (Xform:Type; Tilts; 3Bm; Map)
EZ = 10200010 Sensor Source (C; D; H; P; R; S; T; U)
C (1): Sound velocity calculates using ED, ES, ET (temp.)
D (0): Manual ED
H (2): External synchro
P (0), R (0): Manual EP, ER (0 degree)
S (0): Manual ES
T (1): Internal transducer sensor
U (0): Manual EU

EV = 0 Heading Bias (1/100 deg)
Timing Commands
TE = 00:00:02.00 Time per Ensemble (hrs:min:sec.sec/100)
TP = 00:02.00 Time per Ping (min:sec.sec/100)
Water-Track Commands
WA = 255 False Target Threshold (Max) (0-255 count)

WC = 120 Low Correlation Threshold (0-255)
WD = 111 100 000 Data Out (V; C; A; PG; St; Vsum; Vsum^2; #G; P0)
WE = 1000 Error Velocity Threshold (0-5000 mm/s)
WF = 0800 Blank After Transmit (cm)
WN = 100 Number of depth cells (1-128)
WP = 00001 Pings per Ensemble (0-16384)
WS = 800 Depth Cell Size (cm)
WV = 0390 Radial Ambiguity Velocity (cm/s)

(5) Observation log
31 Aug. 2025 - 05 Oct. 2025 (UTC)

(6) Preliminary results
Figures 3.2.3-1 show the current velocity of Barrow Canyon line.

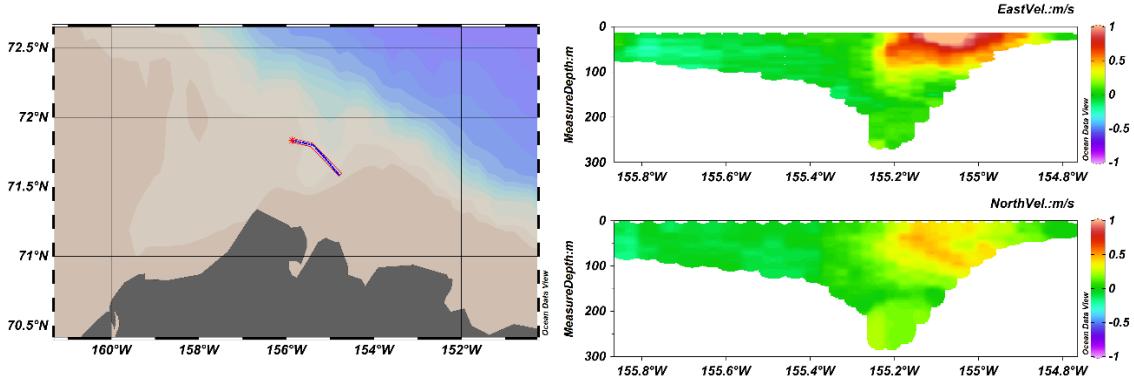

Figure 3.2.3-1: The current velocity of Barrow Canyon line at 9th September.

(7) Data archives
These data obtained in this cruise will be submitted to the Data Management Group of JAMSTEC, and will be opened to the public via "Data Research System for Whole Cruise Information in JAMSTEC (DARWIN)" in JAMSTEC web site.
< https://www.godac.jamstec.go.jp/darwin/en >

(8) Remarks
1) The following periods, data acquisition was suspended due to operating of the AUV "COMAI".
21:33UTC 07 Sep. 2025 - 23:07UTC 07 Sep. 2025
21:53UTC 14 Sep. 2025 - 22:45UTC 14 Sep. 2025
16:52UTC 15 Sep. 2025 - 18:06UTC 15 Sep. 2025
18:07UTC 18 Sep. 2025 - 19:17UTC 18 Sep. 2025
17:14UTC 23 Sep. 2025 - 18:30UTC 23 Sep. 2025

3.2.4. Moorings

Oceanographic moorings continuously measure oceanographic parameters (temperature, salinity, currents, oxygen, chlorophyll, pH, ice thickness) through the year. Three physical oceanographic moorings (BCE-24, BCC-24, BCW-24) in the Barrow Canyon and one sediment trap mooring (NAP-24t) in the Northwind Abyssal Plain are recovered. Three physical oceanographic moorings (BCE-25, BCC-25, BCW-25) are re-deployed in the Barrow Canyon and one sediment trap mooring (NAP-25t) is deployed in the Northwind Abyssal Plain.

3.2.4.1. Barrow Canyon Moorings

(1) Personnel

Motoyo Itoh*	JAMSTEC	- Principal Investigator
Jonaotaro Onodera	JAMSTEC	- On board Principal Investigator
Amane Fujiwara	JAMSTEC	- Chief Scientist

Hiroki Ushiromura as the leader of technical team for mooring operation of MWJ (Ushiromura, H., and Arihara, K.)
Ryo Oyama as the leader for SSBL acoustic survey team of NME (Oyama, R., Ogawa, S., Doi, H., and Takai, S.).

Ikkan Kamiyama	Tokyo University of Marine Science and Technology
Michiyo Yamamoto-Kawai*	Tokyo University of Marine Science and Technology
Tsubasa Kodaira*	The University of Tokyo

*: onshore members

(2) Objectives
The objective of mooring measurements in the Barrow Canyon is to monitor the variations of volume, heat and fresh water fluxes of Pacific-origin water through the Barrow Canyon. Barrow Canyon, in the northeast Chukchi Sea, is a major conduit through which the Pacific water enters the Arctic basin. JAMSTEC has conducted subsurface oceanographic mooring observations in the mouth of the Barrow Canyon since 2000.
We recovered three moorings (BCE-24, BCC-24, BCW-24) and re-deployed three similar configuration moorings (BCE-25, BCC-25, BCW-25) in the Barrow Canyon.

(3)Parameters
-Oceanic velocities
-Pressure, Temperature and Conductivity
-Dissolved oxygen
-Chlorophyll-a and turbidity
-Wave height
-Water sampling

(4) Instruments and methods
1) CTD, CT, T, P sensors
SBE37-SM (Sea-Bird Electronics Inc.)
A7CT-USB (JFE Advantech)
DEFI-T (JFE Advantech)
DEFI-D (JFE Advantech)

DEFI-CT (JFE Advantech)

2) Current meters
Workhorse ADCP 300 kHz Sentinel (Teledyne RD Instruments, Inc.)
Aquadopp Current Meter 2MHz (NORTEK AS)

3) Dissolved oxygen sensor
AROW-USB (JFE Advantech)

4) Chlorophyll-a and turbidity sensor
ACLW-USB (JFE Advantech)
MFL50W-USB (JFE Advantech)

5) Acoustic transponder
XT-6000, XT6001 (Teledyne Benthos, Inc.)

6) Acoustic releaser
8242XS (ORE offshore /EdgeTech)
865-A (Teledyne Benthos, Inc.)

7) Water sampler
RAS500 (McLANE)

8) Nitrate sensor
SUNA (Sea-Bird Electronics Inc.)

9) Wave height and current meter
Signature500 (NORTEK AS)

(5) Station list

Table 3.2.4.1-1: Moorings recovered by MR25-05C

Mooring Name	Recovered Time (UTC)	Latitude	Longitude
BCE-24	2025/09/08	71-40.4014'N	154-59.9036'W
BCC-24	2025/09/08	71-44.1010'N	155-09.6849'W
BCW-24	2025/09/08	71-47.8029'N	155-20.8307'W

Table 3.2.4.1-2: Moorings deployed by MR25-05C

Mooring Name	Deployed Time (UTC)	Latitude	Longitude	Depth (m)
BCE-25	2025/09/09	71-40.4029'N	154-59.8537'W	108
BCC-25	2025/09/09	71-44.1276'N	155-09.7512'W	292
BCW-25	2025/09/09	71-47.7959'N	155-20.7968'W	167

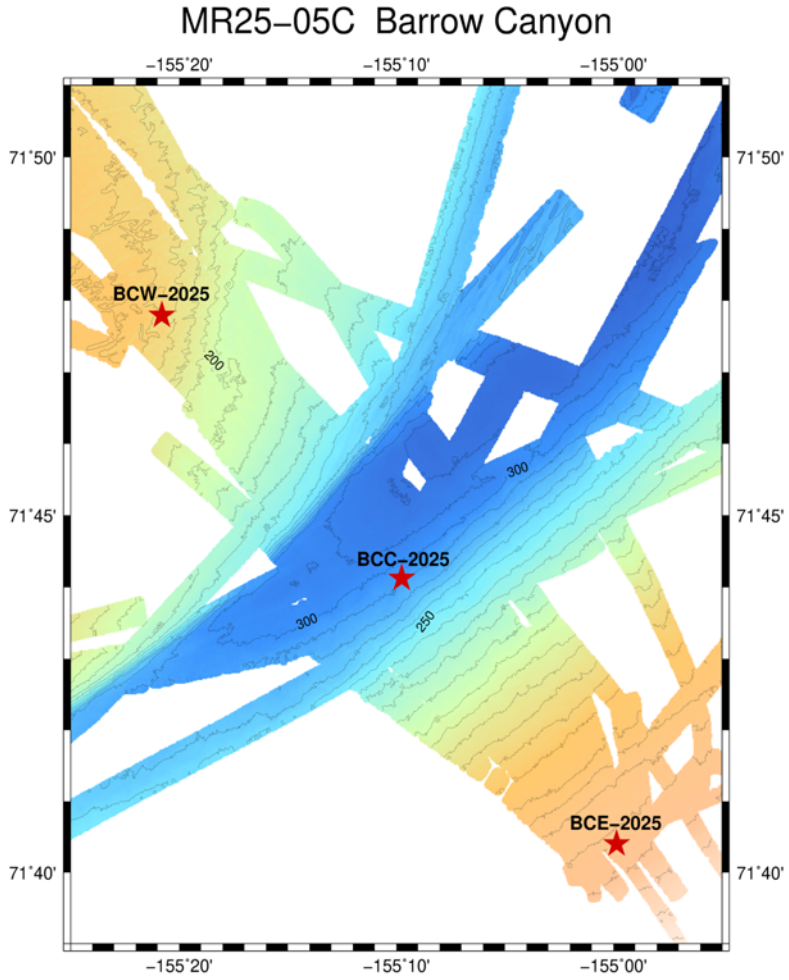

Figure 3.2.4.1-1: Positions of the moorings (BCE, BCC and BCW).

(7) Data archive

These mooring data will be opened to the public via a web site below.
<http://www.jamstec.go.jp/arctic/data_archive/mooring/mooring_index.html>

Figure 3.2.4.1-2: Deployed mooring diagrams.

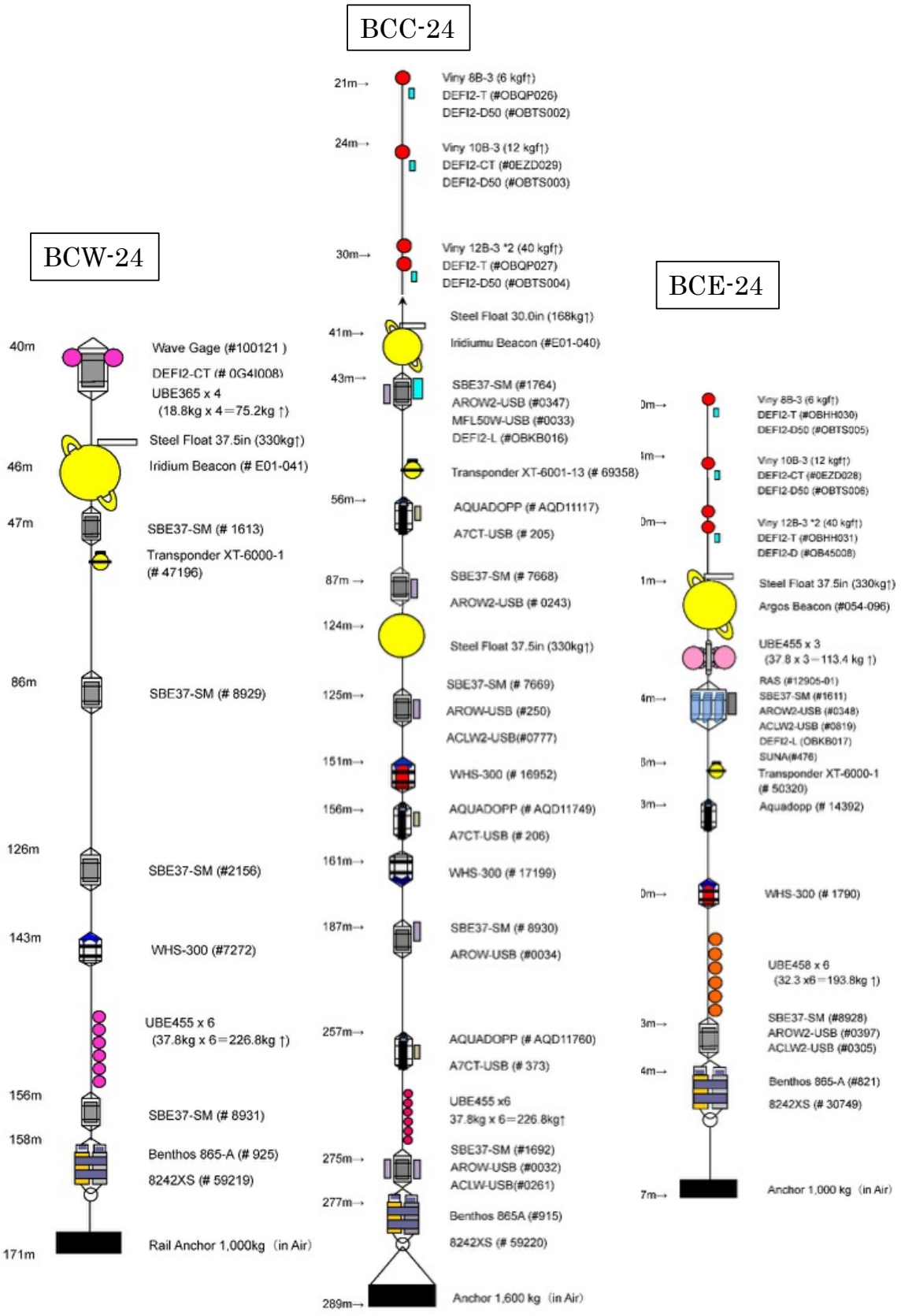

Figure 3.2.4.1-3: Recovered mooring diagrams.

3.2.4.2. Sediment Trap

(1) Personnel

Jonaotaro Onodera	JAMSTEC	- Principal Investigator
Motoyo Itoh*	JAMSTEC	
Yuichiro Tanaka*	AIST	
Atsushi Suzuki*	AIST	
Katsunori Kimoto*	JAMSTEC	
Eiji Watanabe*	JAMSTEC	
Takuhei Shiozaki	Tokyo Univ. AORI	

Hiroki Ushiromura as the leader of technical team for mooring operation of MWJ (Ushiromura, H., and Arihara, K.)
Ryo Oyama as the leader for SSBL acoustic survey team of NME (Oyama, R., Ogawa, S., Doi, H., and Takai, S.).
*: onshore members

(2) Objectives
- To understand lateral transportation of shelf-origin matter to basin with physical oceanographic condition from northern off Barrow Canyon to the Chukchi Borderland.
- To monitor hydrographic condition regarding to ocean acidification and warming.
- To investigate biodiversity in the study region.

(3) Parameters
Settling particles, water temperature, salinity, current, ice thickness, dissolved oxygen, CO2, turbidity, chlorophyll-a, PAR, pH

(4) Instruments and methods
<Instruments>
All instruments on recovered and deployed moorings are listed in Tables 3.2.4.2 -1 and -2. The designs of recovered and deployed mooring are shown in Figures 3.2.4.2 -1 to -3.

<Methods>
Acoustic communication of releasers to be deployed were examined at CTD test cast position in the eastern Bering Sea (55°39.58'N 169°16.19'W, 2456 m water depth) on Sep. 1, 2025. The releasers were mounted on CTD frame, and it was tested at 1000 m and 300 m depths using ship's acoustic ranging system. The Benthos 865A releaser was successful on the test at 1000 m depth. The Nichiyu LGCTi releaser might respond to call at 1000 m depth, but it was uncertain due to the ship's noise. The response of Nichiyu releaser was detected at 300 m depth and on deck. Therefore, this releaser was applied to the deployment of mooring NAP25t as planned.
For the deployment sensors, log file or photograph of configuration process were taken. Sample cups of sediment trap were filled-with filtered sea water taken at 1000 m depth in the southwestern Canada Basin in previous *Mirai* cruise. The water contains formalin (4v/v%) and sodium hydroborate for pH adjustment (pH ~8.2). The sampled duration of NAP25t will be about two years. The time-series sediment trap was scheduled with 14-days interval from September 21, 2025 to Sep. 20, 2026 (UTC), and from Aug. 9 to Aug. 8th, 2027, for the shallow and deep traps, respectively. The

scheduled time to change sample cup is 00:00 (UTC) of the event day.

Safety briefing by chief officer was conducted for all related staffs working on stern deck, just before the start of mooring operations. All staffs working on stern deck worn floating jackets, hard hat, safety shoes, and gloves. The "A" frame and capstan winch was applied for the mooring operation on the deck. Just in case, dragging tools, which are composed of hooks, weights, chains, shackles, TRITON wires and ropes, were loaded on the ship for mooring recovery. The ship track during the operation is in Fig. 3.2.4.2-4.

Recovery operation for NAP24t started from confirmation of the mooring existence using the water column image (Fig. 3.2.4.2.-5), and then acoustic communication between ship's transducer and the transducer of acoustic releaser. The deployed releaser of Benthos 865A was enabled, and release command was transmitted from ~260 m away (horizontal distance). The release was successful, and top buoy immediately found at sea surface. After the coming up of releaser's buoys at sea surface, the ship's zodiac went to the drifting top buoy, and connected a rope from stern to the top buoy. The rope was spooled on deck, and the mooring equipment was recovered on deck from the top buoy to acoustic releasers (Table 3.2.4.2.-1).

For deployment, all serial numbers of deploying equipment and connection of all parts were checked just before the deployment and/or during the deployment operation. Mooring deployment started from the throw-in of top buoy into water (Table 3.2.4.2-2). The ships go forward with slow speed (~1.0knot). Before the dropping sinker, the slow towing of mooring continued until the ship reaches at the planned target position of the mooring. Deepening and vanish of top buoy from sea surface was confirmed, and then reaching of sinker at ser floor was confirmed by ship's acoustic ranging system. The mooring position was determined using SSBL and transducer of Benthos 865A releaser. The water depth was determined by the depth value of the position in MBES topography map (Figure 3.2.4.2-4). The position, water depth, top depth, and recovery plan (season and ship) of the NAP24t will be noticed to AOOS and related persons.

The water of 60L taken at 1000m depth at CTD Station 35 (St. NAP) is to be used for treatment of recovered samples and waters for next sediment-trap deployment in 2027.

(5) Station list or Observation log

Table 3.2.4.2 -1. Summary on the recovery of NAP24t on September 19-20, 2025 (UTC).

NAP24t - Coordinates: 74°31.3763'N 161°56.1888'W, Water depth: 1680 m	
Transmitting the enable command of releaser Benthos 865A (~250 m away from NAP24t position)	18:26
Confirmation of response from the releaser	18:27
Transmission of the release command for Benthos 865A (~260 m away from NAP24t position)	21:01
Response of releasing completed	21:01
Finding of the deepest glass buoys with releasers at sea surface	21:20
Weather Condition: cloudy Air Temp. -2.3°C, Atmospheric Press. 1009 hPa, Wind Direction 26°, Wind Speed 9.2	21:01

m/s, SST -0.5°C, Wave 1.2 m (stern), Current 0.1 knot, Curr. Dir. 312°				
Zodiac boat on water				21:33
Connection of the ship's towing rope to top buoy by the clue on zodiac				21:48
Zodiac boat on deck				21:59
Start of spooling the towing rope connected to the top buoy				22:00
Recovered Mooring Instruments				
Item#	Type	Model	Serial Number	Time
1	Float Ice profiler CT DO Multi-Exciter PAR Iridium Beacon LED Flasher		ASL-SFFC-01 51123 0274 131 19 0F5I016 H01-001 J01-055	22:05
2	Floats Transponder	Benthos 17" x5 XT-6001	- 75683	22:05
3	CT	SBE37SM	13677	22:05
4	Float	Steel 30"	-	22:13
5	CT	SBE37SM	13678	22:19
6	ADCP	WH-300 (w/ BT)	24534	22:24
7	CT DO pH	SBE37SM ARO-USB SPS-14Ti +Battery Unit	15456 0136 40306167001	22:24
8	Float	Benthos 17" x5	-	22:27
9	ADCP CT	Aquadopp DW A7CT-USB	AQD15193 0799	22:36
10	CT	SBE37SM	1367	22:37
11	Logger ├ADCP ├ Pressure ├ DO └ CO2 CT	SeaGuard II DCS4520IW 4117E 4330IW CO2 A7CT-USB	1989 0691	22:41
12	Sediment trap CT DO ADCP	SMD26S-6000 A7CT-USB ARO-USB Aquadopp DW	26S034 0613 0219 9944	22:46
13	Floats	Benthos 17" x5	-	23:42
14	Sediment trap ADCP	SMD26S-6000 Aquadopp DW	26S035 9948	23:42
15	Floats	Benthos 17" x7	-	Sep. 20, 00:05
16	Releaser Releaser	Benthos 865A Nichiyu LGCTi	1078 005	00:05
End of recovery operation at 74°32.6803'N 161°56.2299'W				

Table 3.2.4.2 -2. Summary on the deployment of NAP25t on September 20, 2025 (UTC).

NAP25t

Planned Coordinates: 74°31.37' N 161°55.88' W, Water Depth: 1685 m				
Start of mooring deployment (74°28.4752'N 161°53.6206'W, 1619 m water depth)				16:23 (UTC)
Weather Condition: cloudy Air temp. -1.6°C, Atmospheric pressure 1002hPa, Wind direction 338°, Wind speed 11.6 m/s, SST -0.6°C, Current direction 304°, Current speed 0.2 knot				

Time of instruments and anchor in water				
Item#	Type	Model	Serial Number	Time
1	Float Ice profiler CT DO Multi-Exciter PAR Iridium Beacon LED Flasher	 IPS-5 A7CT2-USB ARO-USB MFL50W-USB DEFI2-L MMI-513-32000 MMF-523-12000	1002 51113 0310 0130 020 0BK0023 H01-001 J09-007	16:26
2	Floats Transponder	Benthos 17" x5 XT-6001	- 60645	16:26
3	CT	SBE37SM	6934	16:31
4	Float	Steel 30"	-	16:32
5	CT	SBE37SM	8858	16:38
6	ADCP	WH-300 (w/ BT)	15385	16:39
7	CT DO pH	SBE37SM ARO-USB SPS-14Ti +Battery Unit	8860 0135 40306169001	16:43
8	Float	Benthos 17" x5	-	16:48
9	Logger ├ADCP ├ Pressure ├ DO └ CO2 CT	SeaGuard II DCS4520IW 4117E 4330IW CO2 A7CT-USB	1958 0752	16:55
10	Sediment trap CT ADCP	SMD26S-6000 A7CT-USB Aquadopp DW	26S032 0626 6819	17:02
11	Floats	Benthos 17" x5	-	17:29
12	Sediment trap ADCP	SMD26S-6000 Aquadopp DW	26S033 6866	17:42
13	Floats	Benthos 17" x7	-	18:10
14	Releaser Releaser	Benthos 865A Nichiyu LGCTi	867 006	18:13
15	Anchor (74°31.4653'N 161°55.9471'W, 1684 m)	1000kg in air	-	18:26
Confirmation of anchor arrival at sea floor				18:39
Communication with releasers (Item#16) , away from ~500m of horizontal distance Benthos 865A ranging: successful Nichiyu LGCTi ranging: not successful Communication with transponder (Item#2): not successful			1078 006 75683	
SSBL transponder survey for Benthos 865A Position 74°31.2672'N 161°55.8818'W				

Water Depth	1680 m (SeaBeam depth of the position)
Estimated Top-buoy Depth	24 m

(6) Preliminary results

The deck works for the recovery and deployment were successful without any injures. On the recovery of the mooring NAP24t, there were some tangled ropes of deeper part in the recovered mooring, which were safely recovered. Sediment trap samples were successfully recovered (Fig. 3.2.4.2 -6). The samples will be analyzed onshore after the cruise. The hydrographic monitoring of the attached sensors was basically successful. The sensor guard of CT sensor at the top buoy was partly broken. The water immersion was found for the iridium beacon and LED flasher of the top buoy, and CT sensor mounted on the shallow sediment trap. The electric board of iridium beacon damaged by the accident, and it did not work when the NAP24t was recovered. The electric board of the LED flasher and CT sensor with water immersion was not damaged, and it is still available. The deployment work was smoothly operated. The water depth at the position of new mooring NAP25t was 5m shallower than the planned depth.

(7) Data archives

These data obtained in this cruise will be submitted to the Data Management Group of JAMSTEC, and will be opened to the public via "Data Research System for Whole Cruise Information in JAMSTEC (DARWIN)" in JAMSTEC web site.
<https://www.godac.jamstec.go.jp/darwin/en/>

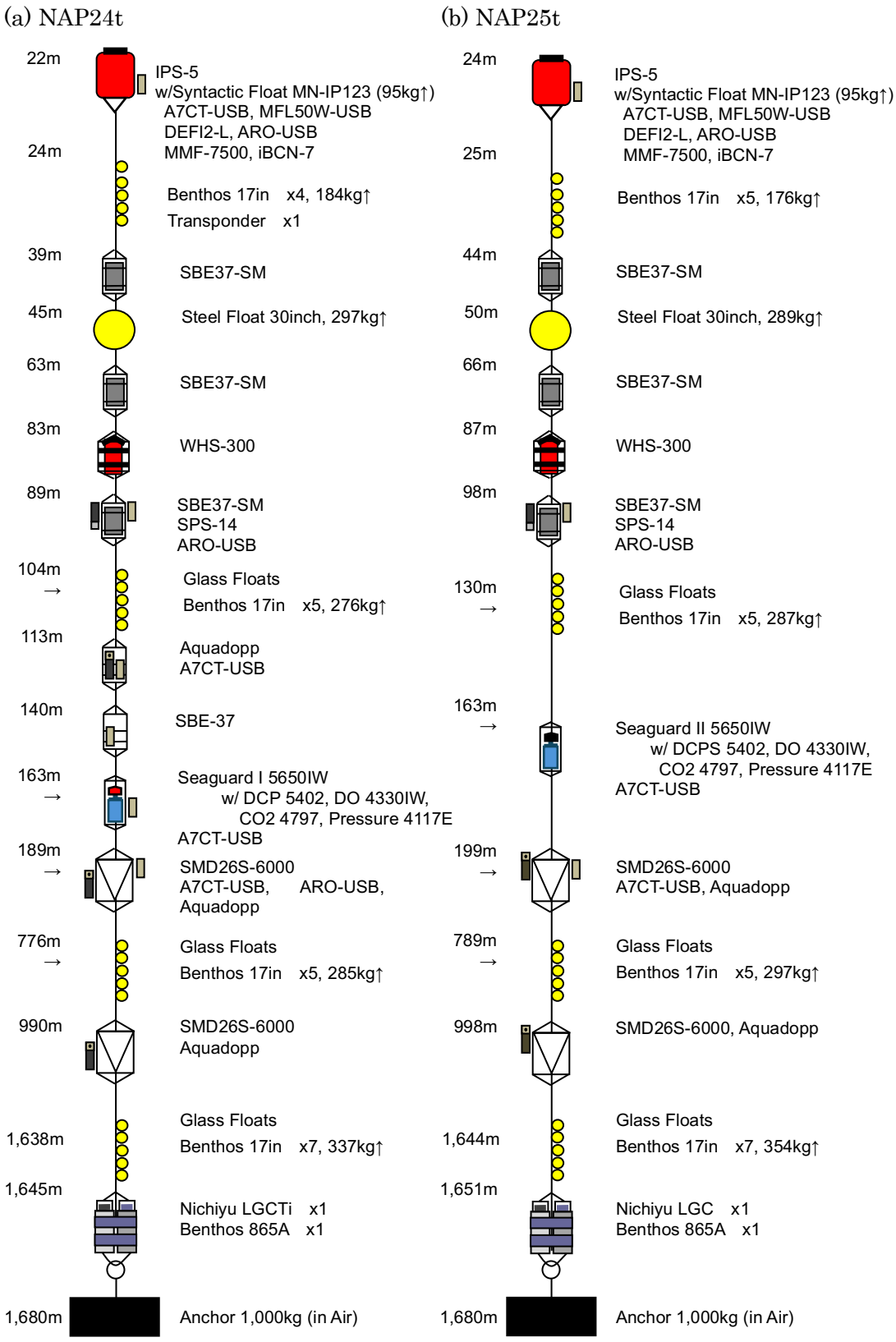

Figure 3.2.4.2 -1. The summary of mooring design for (a) NAP24t and (b) NAP25t. The equipment depths of NAP24t are median value during the deployment based on the retrieved data and the CTD calibration for the pressure of MFL50W at the top buoy.

Figure 3.2.4.2 -2. The mooring design of NAP24t for recovery.

Figure 3.2.4.2 -3. The mooring design of NAP25t for deployment.

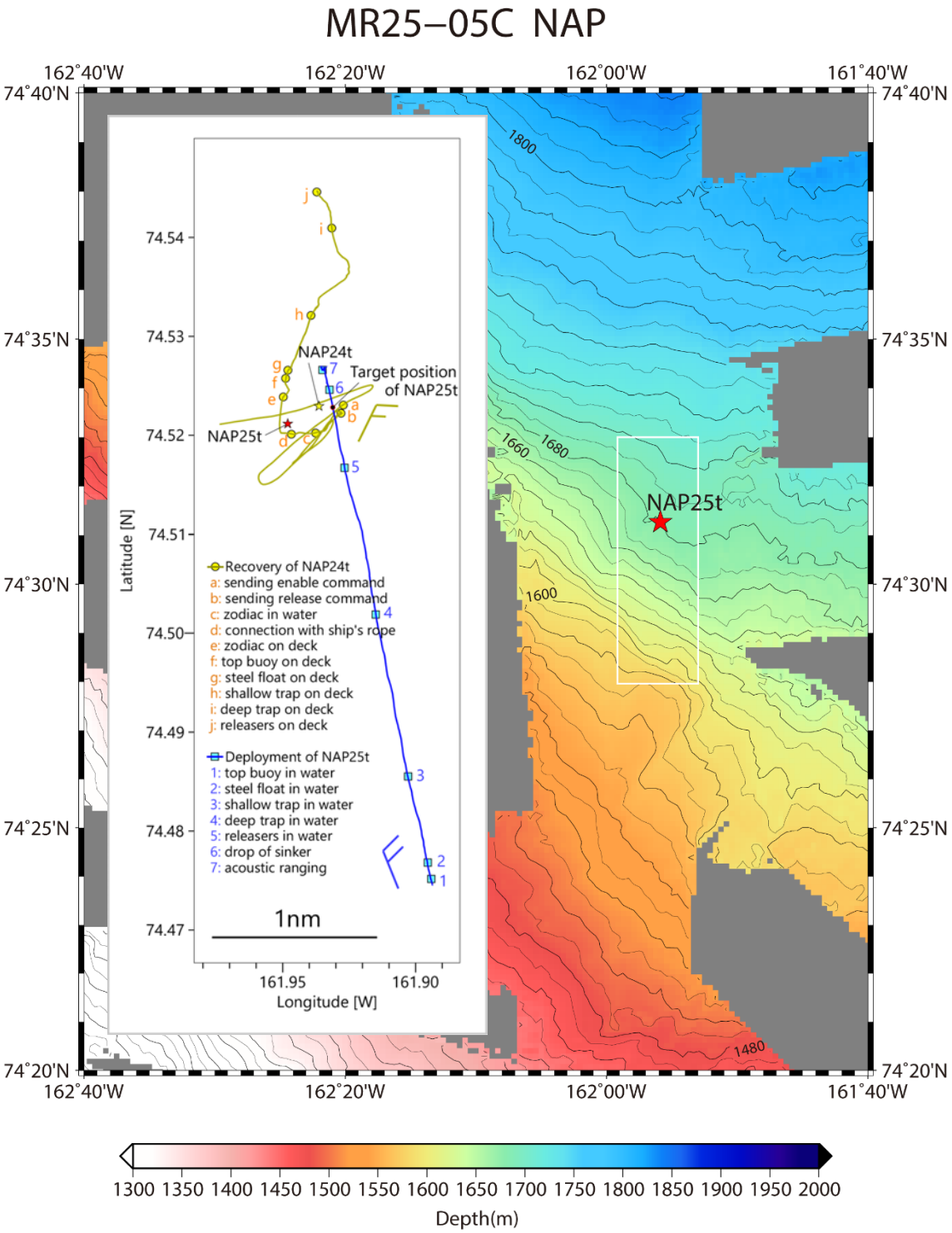

Figure 3.2.4.2 -4. The MBES topography map showing the mooring positions of NAP25t (star symbol in red). The white rectangular area was enlarged in the inside window for the ship track during the mooring operations of NAP24t recovery and NAP25t deployment with some operation events (circular and rectangular dot symbols) and the wind direction. The current condition was 0.2-0.3 knots for ~300° direction.

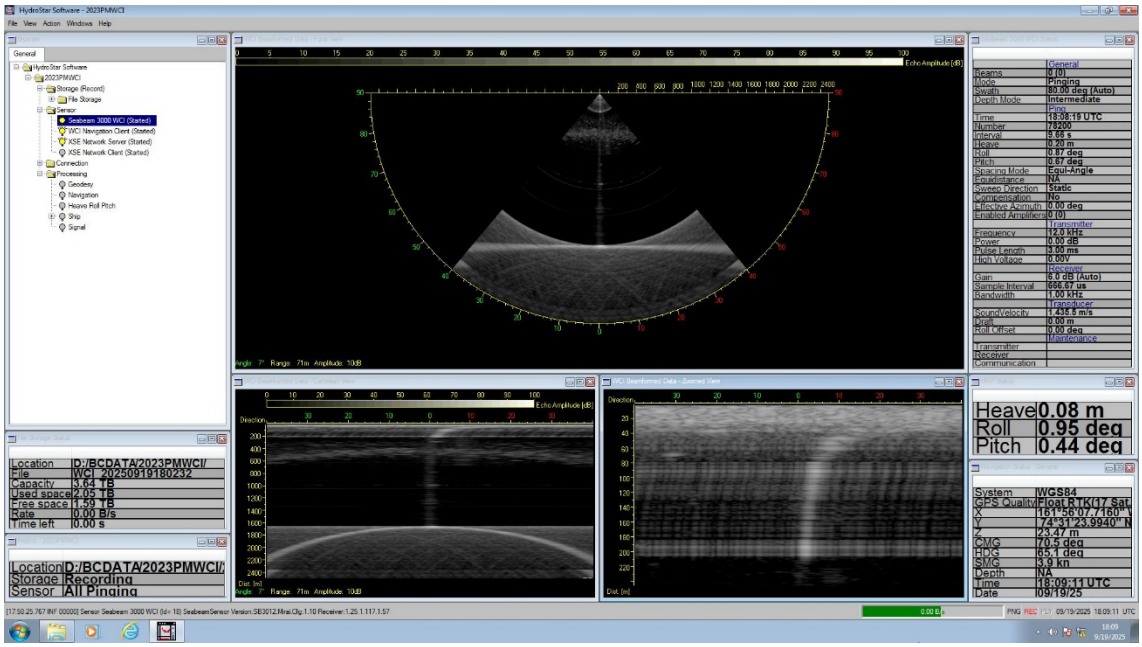

Figure 3.2.4.2 -5. The water column image of NAP24t taken before sending the enable command.

Figure 3.2.4.2 -6. The recovered sediment trap samples of NAP24t. The bottles with red and blue labels are from the shallow (nominally 200 m depth) and deep (1000 m depth) sediment traps, respectively.

3.2.5. Towed CTD chain

(1) Personnel

Satoshi KIMURA (JAMSTEC): Principal Investigator
Amane FUJIWARA (JAMSTEC)

Yuri FUKAI (JAMSTEC)

(2) Objectives

A vertical CTD profile is an established method in getting temperature and salinity structure from the ocean, whereas the horizontal profiling technique is not. With increasing interests in submesoscale ocean dynamics, horizontal profiles offer valuable insights into detecting such motions. In this study, horizontal profiles were obtained by towing a chain of CTDs using the A-frame and traction winch aboard the *Mirai* (Figure 3.2.5-1).

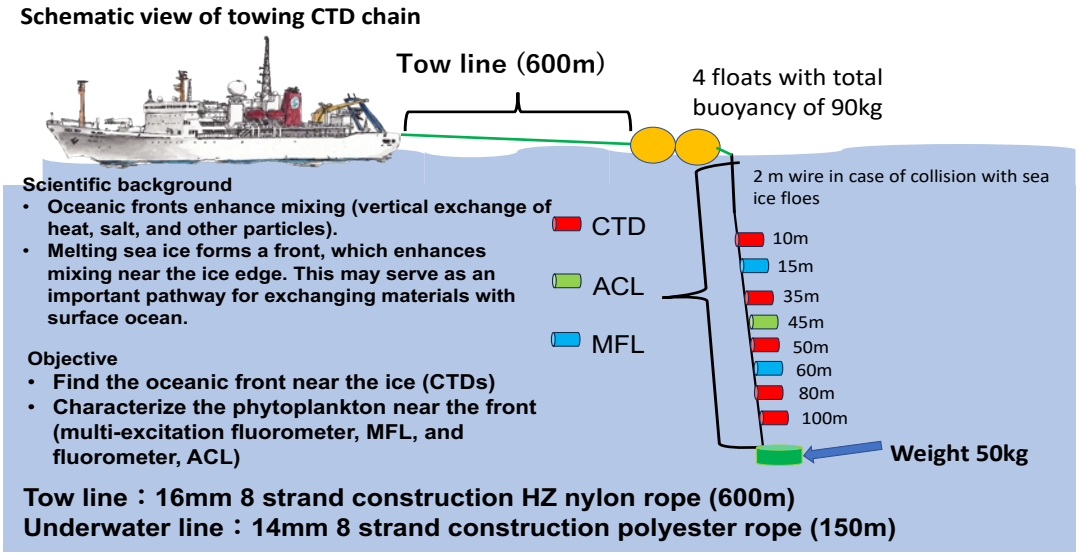

Figure 3.2.5-1 Schematic representation of towed instrument chain.

(3) Parameters

Temperature
Salinity
Pressure
Fluorescence

(4) Instruments and methods

We conducted one dive, DIVE01. The time and locations of the dive are in Table 3.2.5-1 and the locations are shown in Figure 3.2.5-2.

Table 3.2.5-1 Time and locations of DIVE01.

Dive name	Starting time [UTC]	Starting Longitude [decimal]	Starting Latitude [decimal]	Ending time [UTC]	Ending Longitude [decimal]	Ending Latitude [decimal]
DIVE01	9/18/2025 22:30:00	164.46° W	76.39° N	9/19/2025 00:45:00	164.62° W	76.33° N

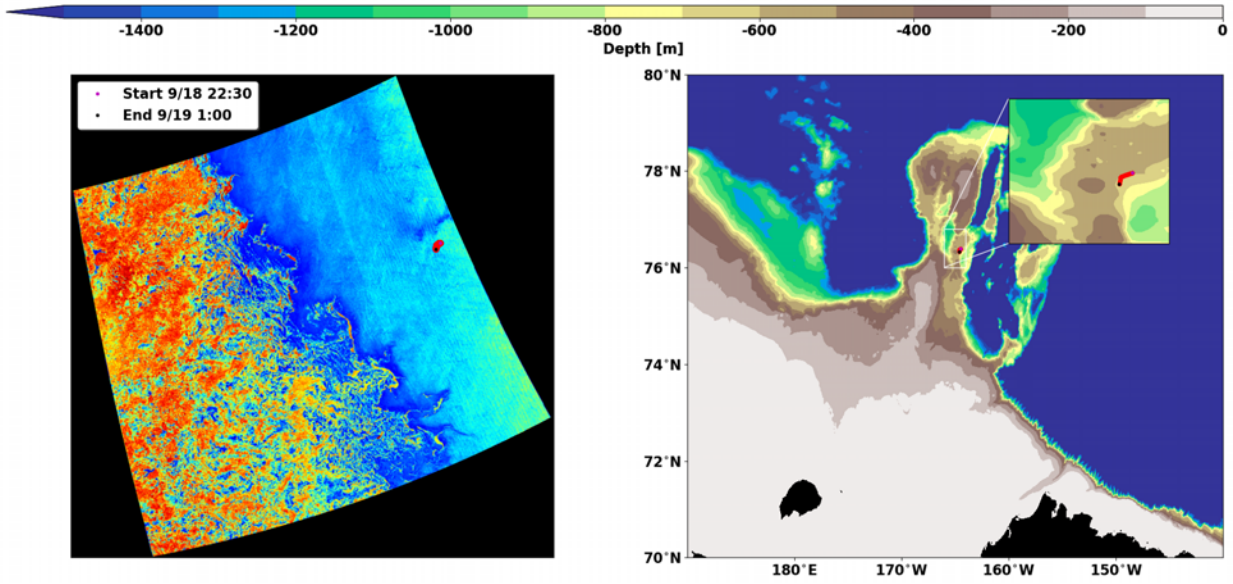

Figure 3.2.5-2 Left) Ice condition from SAR image and the ship location in reddots. Right) Ship location overlaying the bathymetry.We towed 5 CTDs, 2 MFL, and 1 ACL. The initial depths and instrument specifications are summarized in Table 3.9-2.

Table 3.2.5-2 List of instruments

DIVE01		
Initial depth [m]	Name of Instrument	Measured variables
10	JES10mini: SN019	S, T, P
15	MFL50W-USB	Fluorescence
35	JES10mini: SN036	S, T, P
45	ACLW-WF	Fluorescence
50	JES10mini: SN037	S, T, P
60	MFL50W-USB	Fluorescence
80	JES10mini: SN040	S, T, P
100	JES10mini: SN045	S, T, P

(5) Preliminary results

All instruments successfully recorded data, except for the pressure sensor in JES10mini (SN019), for which the issue is currently being addressed with the manufacturer. The dive is conducted near the ice edge (Figure 3.2.5-2). The dive traversed a front, as identified in the density from the towed CTD data (Figure 3.2.5-3). The ship's velocity was maintained at 1.5 knots relative to the water. The JES10mini CTD data reveal abrupt changes in water properties at the front. The instrument's depth decreased as the ship accelerated (Figure 3.2.5-2). The shipboard

ADCP data near the oceanic front reveals a slanted cell shape circulation, which appears to be a recirculation cell at the front (Figure 3.2.5-4).

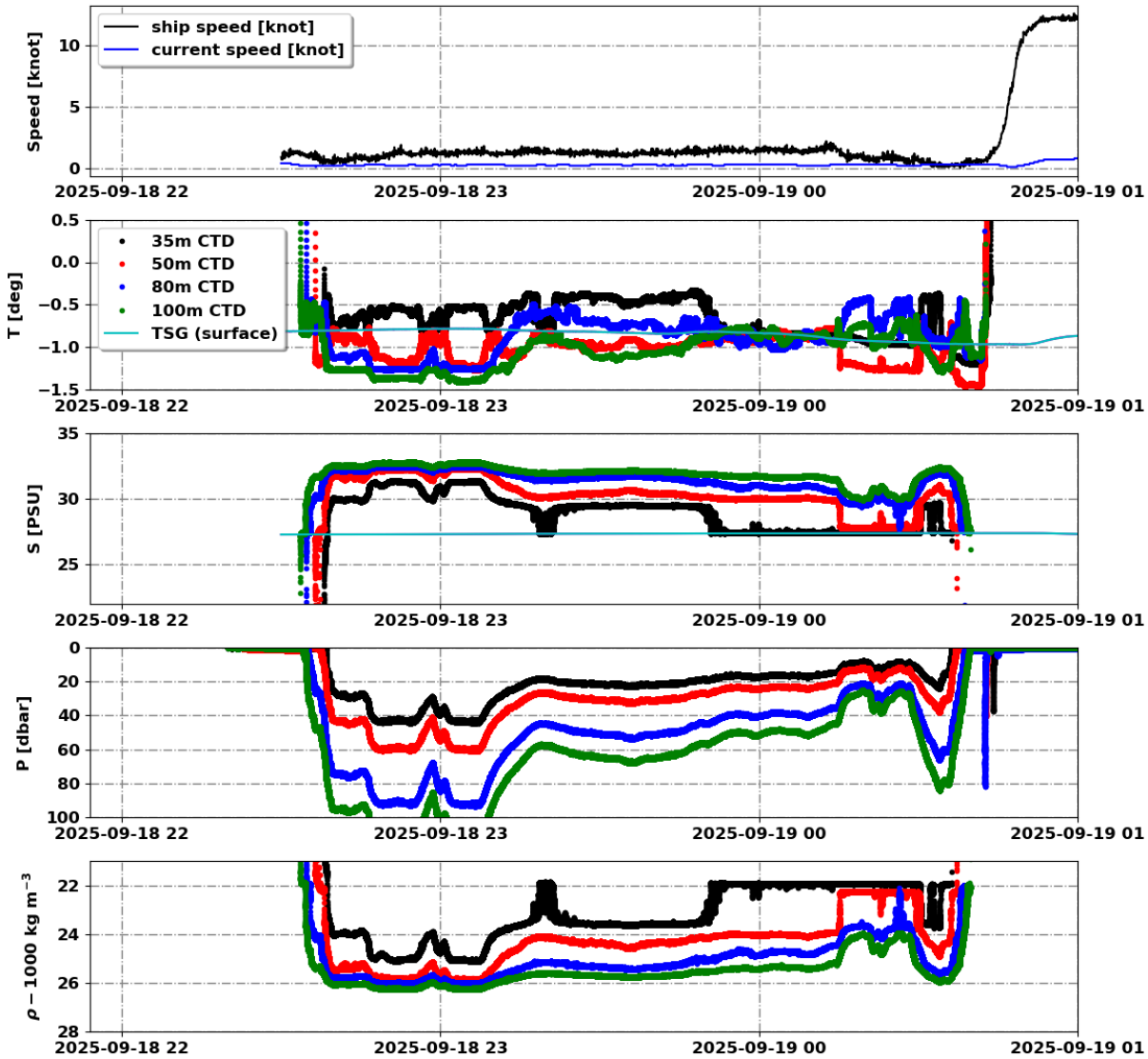

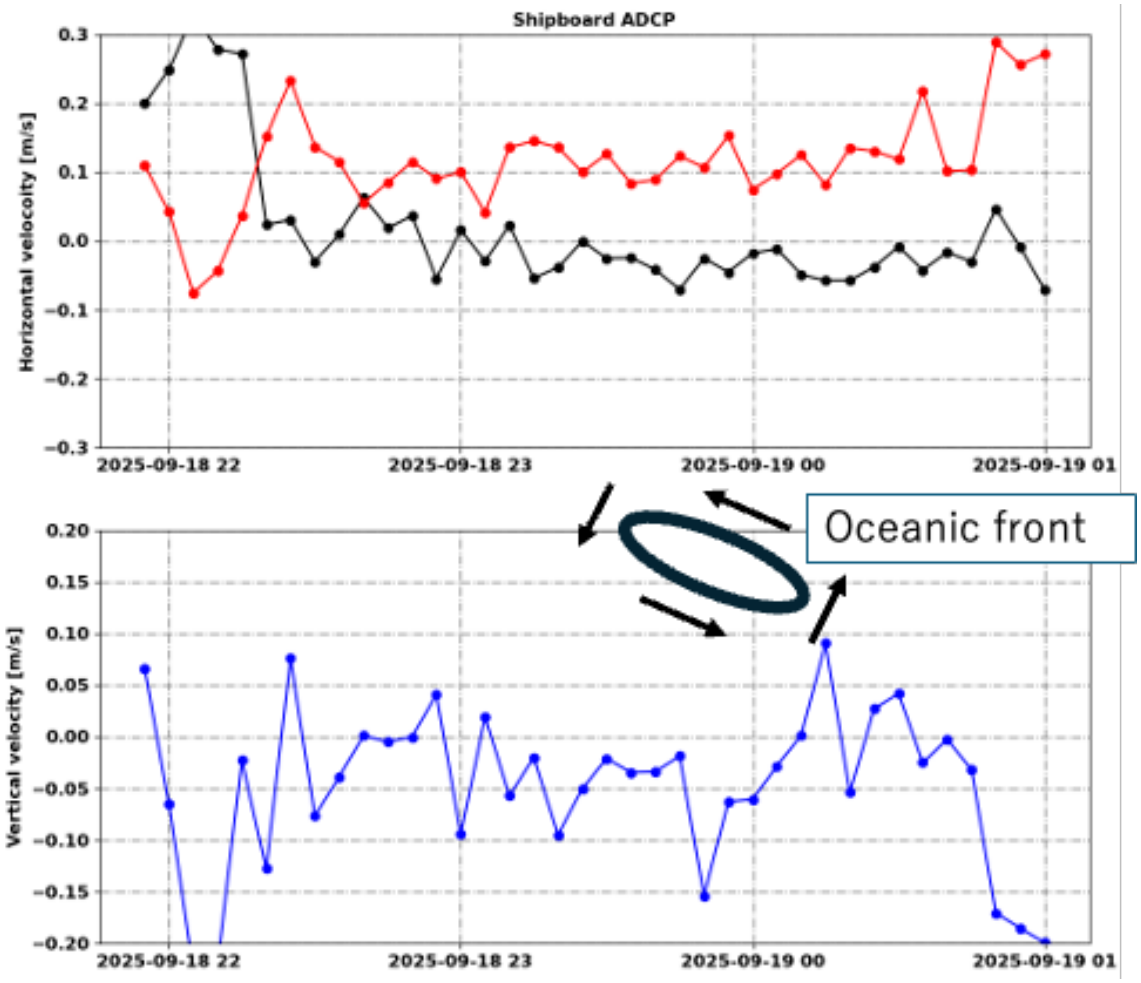

(6) Data archives

These data obtained in this cruise will be submitted to the Data Management Group of JAMSTEC, and will be opened to the public via "Data Research System for Whole Cruise Information in JAMSTEC (DARWIN)" in JAMSTEC web site.
<https://www.godac.jamstec.go.jp/darwin/en/>

3.2.6 Salinity

(1) Personnel

Amane Fujiwara	JAMSTEC	- Principal Investigator
Yasuhiro Arii	MWJ	- Operation leader

(2) Objectives

To calibrate the measurements of salinity collected from CTD casts, and to provide the data for bucket sampling and underway surface water monitoring system.

(3) Parameters

Salinity

(4) Instruments and methods

a. Sampling

Seawater samples were collected with 12 Liter water sampling bottles and underway surface water monitoring system. The salinity sample bottle of the 250 ml brown glass bottle with screw cap was used for collecting the sample water. Each bottle was rinsed 3 times with the sample water, and was filled with sample water to the bottle shoulder. Each bottle was stored for more than 24 hours in the laboratory before the salinity measurement.

The kind and number of samples taken are shown as follows;

Table 3.2.6-1. Kind and number of samples

Kind of Samples	Number of Samples
Samples for CTD	414
Samples for underway surface water monitoring system	28
Total	442

b. Instruments and Method

The salinity analysis was carried out on R/V MIRAI during the cruise of MR25-05C using the salinometer (Model 8400B "AUTOSAL"; Guildline Instruments Ltd.: S/N 62556) with an additional peristaltic-type intake pump (Ocean Scientific International, Ltd.). A pair of precision digital thermometers (1502A; FLUKE: S/N B78466 and B81549) were used for monitoring the ambient temperature and the bath temperature of the salinometer.

The specifications of the AUTOSAL salinometer and thermometer are shown as follows;

Salinometer (Model 8400B "AUTOSAL"; Guildline Instruments Ltd.)
Measurement Range : 0.005 to 42 (PSU)
Accuracy : Better than ± 0.002 (PSU) over 24 hours
Maximum Resolution : Better than ± 0.0002 (PSU) at 35 (PSU)
Thermometer (1502A: FLUKE)
Measurement Range : 16 to 30 deg C (Full accuracy)
Resolution : 0.001 deg C
Accuracy : 0.006 deg C (@ 0 deg C)

The measurement system was almost the same as Aoyama *et al.* (2002). The salinometer was operated in the air-conditioned ship's laboratory at a bath temperature of 24 deg C. The ambient temperature varied from approximately 22 deg C to 24 deg C, while the bath temperature was very stable and varied within +/- 0.002 deg C on rare occasion. The measurement for each sample was done with a double conductivity ratio and defined as the median of 34 readings of the salinometer. (Acquisition of the 34 readings took about 11 seconds when the function dial was turned to the 'read' setting) Data were taken after rinsed 5 times with the sample water. The double conductivity ratio of sample was calculated from average value of two measurements. And it was used to calculate the bottle salinity with the algorithm for the practical salinity scale, 1978 (UNESCO, 1981). In the case of the difference between the double conductivity ratio of these two measurements being greater than or equal to 0.00003, continue to be measured up to 3 times. The difference between the double conductivity ratio of these two measurements being smaller than 0.00002 were selected. The measurement was conducted in about 8

hours per day and the cell was cleaned with neutral detergent after the measurement of the day.

(5) Preliminary results

a. Standard Seawater

Standardization control of the salinometer was set to 627. The value of STANDBY was 24+5146 to 24+5148 and that of ZERO was 0.0±0001. The IAPSO Standard Seawater (SSW) batch P169 was used as the standard for salinity. 15 bottles of P169 were measured.

Figure 3.2.6-1 and 3.2.6-2 show the time series of the double conductivity ratio of the Standard Seawater batch P169. The average of the double conductivity ratio was 1.99966 and the standard deviation was 0.00001 which is equivalent to 0.0002 in salinity.

The specifications of SSW batch P169 used in this cruise are shown as follows;

Batch : P169
Conductivity ratio : 0.99983
Salinity : 34.993
Expiry : 9th Aug. 2027

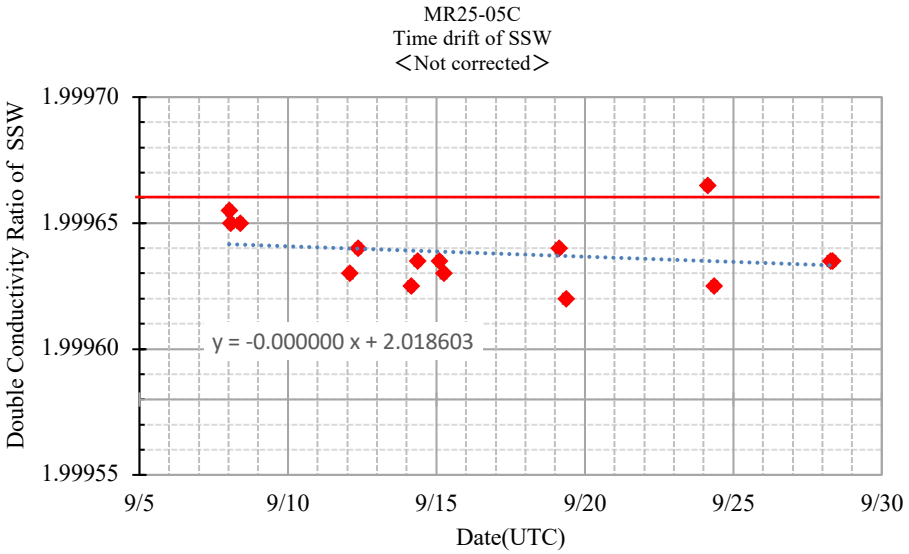

Figure 3.2.6-1: Time series of double conductivity ratio for the Standard Seawater (before correction)

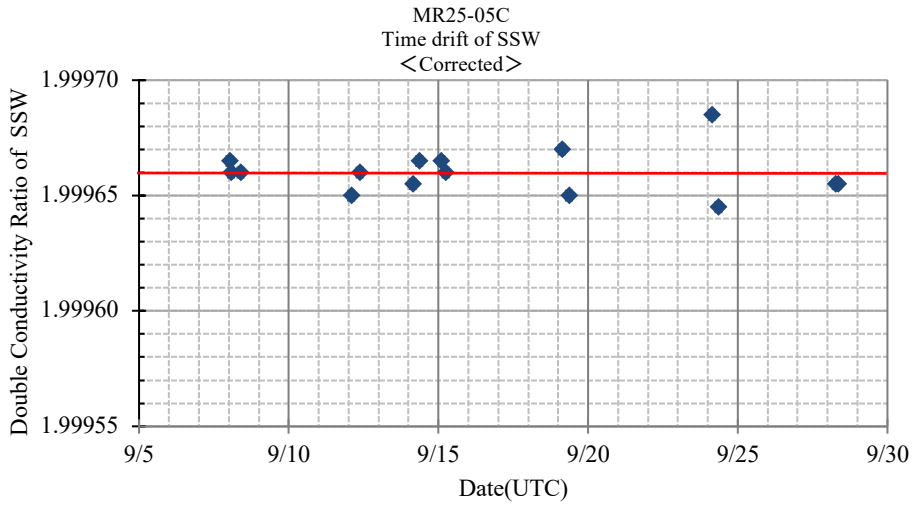

Figure 3.2.6-2: Time series of double conductivity ratio for the Standard Seawater (after correction)

b. Sub-Standard Seawater
Sub-standard seawater was made from surface sea water filtered by a pore size of 0.45 micrometer and stored in a 20 Liter container made of polyethylene and stirred for at least 24 hours before measuring. It was measured about every 10 samples in order to check for the possible sudden drifts of the salinometer.

c. Replicate Samples
We estimated the precision of this method using 40 pairs of replicate samples taken from the same water sampling bottle. The average and the standard deviation of absolute difference among 40 pairs of replicate samples were 0.0004 and 0.0004 in salinity, respectively.

(6) Data archives
These data obtained in this cruise will be submitted to the Data Management Group of JAMSTEC, and will be opened to the public via "Data Research System for Whole Cruise Information in JAMSTEC (DARWIN)" in JAMSTEC web site.
<https://www.godac.jamstec.go.jp/darwin/en/>

(7) References
M. Aoyama, T. Joyce, T. Kawano and Y. Takatsuki: Standard seawater comparison up to P129. Deep-Sea Research Part I, Vol. 49, 1103-1114, 2002.
UNESCO: Tenth report of the Joint Panel on Oceanographic Tables and Standards. UNESCO Tech. Papers in Mar. Sci., 36, 25 pp., 1981.

3.3. Biogeochemical Oceanography

3.3.1. Dissolved Oxygen

(1) Personnel

Mariko HATTA (JAMSTEC): Principal Investigator
Takuya IZUTSU (MWJ): Operation Leader
Yuko MIYOSHI (MWJ)
Misato KUWAHARA (MWJ)
Mariko SANO (MWJ)

(2) Objective

Determination of dissolved oxygen in seawater by Winkler titration.

(3) Parameters

Dissolved Oxygen

(4) Instruments and Methods

Following procedure is based on Winkler method (Dickson, 1996; Culberson, 1991).

a. Instruments

Burette for sodium thiosulfate and potassium iodate: Automatic piston burette (APB-510 / APB-610 / APB-620) manufactured by Kyoto Electronics Manufacturing Co., Ltd. / 10 cm^3 of titration vessel

Detector: Automatic photometric titrator (DOT-15X) manufactured by Kimoto Electric Co., Ltd.

Software: DOT Terminal Ver. 1.3.1

b. Reagents

Pickling Reagent I:
Manganese (II) chloride solution (3 mol dm^{-3})
Pickling Reagent II:
Sodium hydroxide (8 mol dm^{-3}) / Sodium iodide solution (4 mol dm^{-3})
Sulfuric acid solution (5 mol dm^{-3})
Sodium thiosulfate (0.025 mol dm^{-3})
Potassium iodate (0.001667 mol dm^{-3})

c. Sampling

Seawater samples were collected using sample bottles attached to the CTD/Carousel Water Sampling System (CTD system). Seawater for oxygen measurement was transferred from the bottle to a volume-calibrated flask (approximately 100 cm^3), with the flask overflowed three times volume to ensure complete rinsing. The temperature was measured simultaneously with a digital thermometer during the overflow process. After transferring the sample, two reagent solutions (Reagents I and II) of 1 cm^3 each were added immediately, and the flask was carefully stoppered. The flask was then shaken vigorously to mix the contents and to disperse the precipitate finely throughout. Once the precipitate has settled at least halfway down the flask, it was shaken again vigorously to redisperse the

precipitate. The flasks containing the fixed samples were stored in the laboratory until titration.

d. Sample measurement

For more than two hours after the re-shaking, the fixed samples were measured on board. A 1 cm^3 volume of sulfuric acid solution and a magnetic stirrer bar were placed into the sample flask, and the sample was stirred. The samples were titrated by a sodium thiosulfate solution, the morality of which had been determined using a potassium iodate solution. The temperature of the sodium thiosulfate during titration was recorded with a digital thermometer. Dissolved oxygen concentration ($\mu mol\ kg^{-1}$) was calculated based on the sample temperature during seawater collection, salinity, flask volume, and the titrated volume of sodium thiosulfate solution, excluding the blank. During this cruise, two sets of titration apparatus were used.

e. Standardization and determination of the blank

The concentration of the sodium thiosulfate titrant was determined using a potassium iodate solution. Pure potassium iodate was dried in an oven at 130 ºC, and 1.7835 g of it was dissolved in deionized water and diluted to final weight of 5 kg in a flask. To determine the titrant concentration, 10 cm^3 of the standard potassium iodate solution was transferred to another flask using a volume-calibrated dispenser. Then, 90 cm^3 of deionized water, 1 cm^3 of sulfuric acid solution, and 1 cm^3 each of fixing reagent solutions II and I were added in sequence. The volume of sodium thiosulfate required to titrate this diluted standard potassium iodate solution (usually averaged over five measurements) was used to calculate the morality of sodium thiosulfate titrant.

The oxygen present in the fixing reagents I (1 cm^3) and II (1 cm^3) was assumed to be 7.6×10^{-8} mol (Murray et al., 1968). The blank, due to sources other than oxygen, was determined as follows: 1 cm^3 and 2 cm^3 of the standard potassium iodate solution were added to separate flasks using a calibrated dispenser. Then, 100 cm^3 of deionized water, 1 cm^3 of sulfuric acid solution, 1 cm^3 of fixing reagent II, and the same volume of fixing reagent I were added sequentially. The blank was calculated as the difference between the titrated sodium thiosulfate volumes for 1 cm^3 and 2 cm^3 potassium iodate solutions. Each titration was preformed three times, and the average was taken as the blank value.

(5) Observation log

a. Standardization and determination of the blank

Table 3.1.1-1 shows results of the standardization and the blank determination during this cruise.

Table 3.1.1-1 Results of the standardization and the blank determinations during cruise

Date (yyyy/mm/dd)	Potassium iodate ID	Sodium thiosulfate ID	DOT-15X (No.9)		DOT-15X (No.10)		Stations
			E.P. (cm^3)	Blank (cm^3)	E.P. (cm^3)	Blank (cm^3)	
2025/09/01	K25E02	T-24G	3.980	-0.001	3.978	-0.001	001M001 002M001

							003M001 004M001 005M001 006M001 007M001 008M001
2025/09/06	K25E03	T-24G	3.979	0.000	3.976	-0.003	009M001 010M001 011M001 012M001 013M001 014M001 015M001
2025/09/09	K25E04	T-24G	3.977	0.000	3.976	-0.001	016M001 016M002 017M001 018M001 019M001 020M001 021M001 021M002 022M001 024M001 027M001 028M001 029M001 030M001
2025/09/15	K25E05	T-24G	3.978	0.001	3.976	-0.001	
2025/09/15	K25E05	T-24I	3.945	-0.002	3.945	-0.002	031M001 032M001 033M001 034M001
2025/09/19	K25E06	T-24I	3.945	-0.001	3.944	-0.002	035M001 035M002 036M001 037M001
2025/09/23	K24B01	T-24I	3.943	-0.001	3.942	-0.002	
2025/09/27	K24B02	T-24I	3.945	0.000	3.943	-0.003	

b. Repeatability of sample measurement

Replicate samples were taken at every CTD casts. The standard deviation of the replicate measurement (Dickson et al., 2007) was 0.11 µmol kg^{-1} (n=44).

(6) Data archives

These data obtained in this cruise will be submitted to the Data Management Group (DMG) of JAMSTEC,and will opened to the public via "Data Research System for Whole Cruise Information in JAMSTEC (DARWIN)" in JAMSTEC web site.
<https://www.godac.jamstec.go.jp/darwin/en/>

(7) References

Culberson, C. H. (1991). *Dissolved Oxygen.* WHPO Publication 91-1.

Dickson, A. G. (1996). Determination of dissolved oxygen in sea water by Winkler titration. In *WOCE Operations Manual*, Part 3.1.3 Operations & Methods, WHP Office Report WHPO 91-1.

Dickson, A. G., Sabine, C. L., & Christian, J. R. (Eds.), (2007). *Guide to best practices for ocean CO_2 measurements, PICES Special Publication 3*: North Pacific Marine Science Organization.

Murray, C. N., Riley, J. P., & Wilson, T. R. S. (1968). The solubility of oxygen in Winklerreagents used for the determination of dissolved oxygen. *Deep Sea Res.*, 15, 237-238.

3.3.2. Nutrients

(1) Personnel
Mariko HATTA [1)]: Principal Investigator
Shiori ARIGA [2)]: Operation Leader
Kengo FUJITA [2)]
Natsumi KAZUNO [2)]
1) Japan Agency for Marine-Earth Science and Technology
2) Marine Works Japan Ltd.

(2) Objectives
The objective of this document is to present the current status of nutrient measurements conducted during the R/V MIRAI cruise MR25-05C (EXPOCODE: 49NZ20250831) in the Arctic Ocean.

(3) Parameters
The measured parameters include nitrate, nitrite, silicate, phosphate, and ammonia in seawater.

(4) Instruments and methods
The analytical platform was upgraded from QuAAtro 2-HR to QuAAtro 39 in March 2021. However, following this replacement, several issues were reported with the QuAAtro 39 system (see the MR21-05C cruise report). In July 2022, to address these issues and improve analytical precision, the following modifications were made: (1) the pumps were replaced with a 14-tube pump (model number: TRA+B014-02, BL TEC K.K.), instead of the original 13-tube pump (model number: 166+B214-01, BL TEC K.K.); (2) the motor brackets were upgraded to new stainless models (model number: Motor-Braket-01-Rev-1 and Motor-Braket-02-Rev-1, BL TEC K.K.); and (3) the light source units were secured to reduce vibration. The modified platform, referred to as the "QuAAtro 39-J", was used for this cruise.
The analytical methods for nitrate, nitrite, silicate, and phosphate follow those described in the GO-SHIP Repeat Hydrography Nutrients Manual (Hydes et al., 2010; Becker et al., 2019). The method for ammonium follows the vaporization membrane permeability approach described by Kimura (2000).

(4.1) Nitrate + nitrite and nitrite

Nitrate + nitrite and nitrite were analyzed using a methodology modified from Grasshoff (1976). The flow diagrams are shown in Fig. 3.3.2.1 for nitrate + nitrite and Fig. 3.3.2.2 for nitrite. In the nitrate + nitrite analysis, samples were mixed with the alkaline imidazole buffer and then pushed through a cadmium coil coated with metallic copper. This step facilitated the reduction of nitrate to nitrite in the sample, allowing for the determination of total nitrate + nitrite in seawater. For the nitrite analysis, the samples were mixed with reagents without undergoing the reduction step. In the flow system, the seawater sample – either with or without the reduction step - was mixed with an acidic sulfanilamide reagent through a mixing coil to produce a diazonium ion. The mixture was then combined with the N-1-naphthylethylenediamine dihydrochloride (NED), producing a red azo dye. This azo dye was subsequently directed to the spectrophotometric detection to monitor the signal at 545 nm. Therefore, for the nitrite analysis, sample bypassed the Cd coil, and nitrate concentrations were calculated by the difference between nitrate + nitrite and nitrite concentrations.

Reagents

50 % Triton solution: 50 mL of Triton® X-100 (CAS No. 9002-93-1) was mixed with 50 mL of ethanol (99.5 %).

Imidazole (buffer), 0.06 M (0.4 % w/v): Dissolved 4 g of the imidazole (CAS No. 288-32-4) in 1000 mL ultra-pure water, and then added 2 mL of the hydrogen chloride (CAS No. 7647-01-0). After mixing, 1 mL of the 50 % triton solution was added.

Sulfanilamide, 0.06 M (1 % w/v) in 1.2 M HCl: Dissolved 10 g of 4-aminobenzenesulfonamide (CAS No. 63-74-1) in 900 mL of ultra-pure water, and then add 100 mL of the hydrogen chloride (CAS No. 7647-01-0). After mixing, 2 mL of the 50 % triton solution was added.

NED, 0.004 M (0.1 % w/v): Dissolved 1 g of N-(1-naphthalenyl)-1,2-ethanediamine dihydrochloride (CAS No. 1465-25-4) in 1000 mL of ultra-pure water and then added 10 mL of hydrogen chloride (CAS No. 7647-01-0). After mixing, 1 mL of the 50 % triton solution was added. This reagent was stored in a dark bottle.

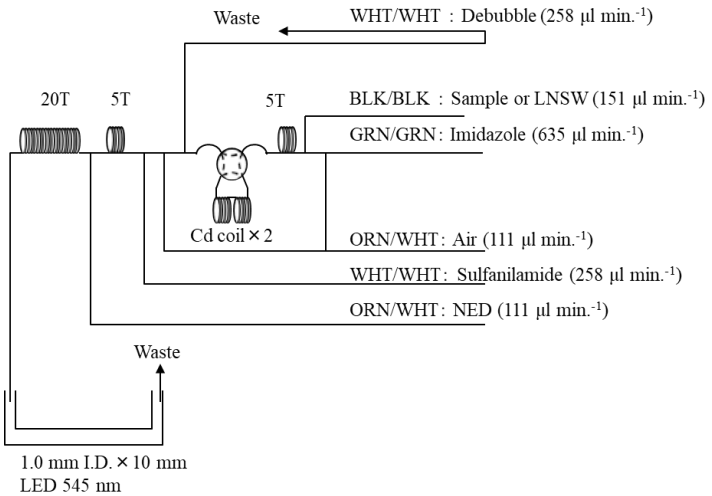

Figure 3.3.2.1 NO_3+NO_2 (1ch.) flow diagram.

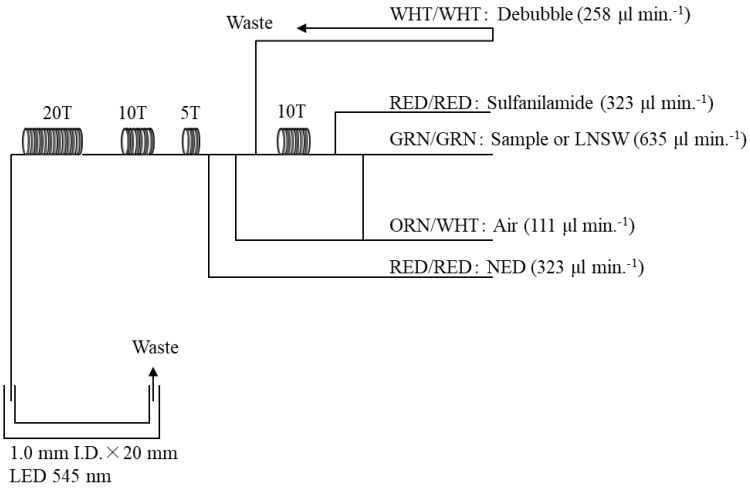

Figure 3.3.2.2 NO_2 (2ch.) flow diagram.

(4.2) Silicate

The method for silicate is analogous to that described for phosphate (4.3) and is essentially based on the method outlined by Grasshoff et al. (1999). The flow diagram is shown in Fig. 3.3.2.3. Silicomolybdic acid compound was first formed by mixing the silicate in the sample with the molybdic acid. This silicomolybdic acid was then reduced to silicomolybdous acid, known as "molybdenum blue," using L-ascorbic acid as the reductant. The signal was monitored at 630 nm.

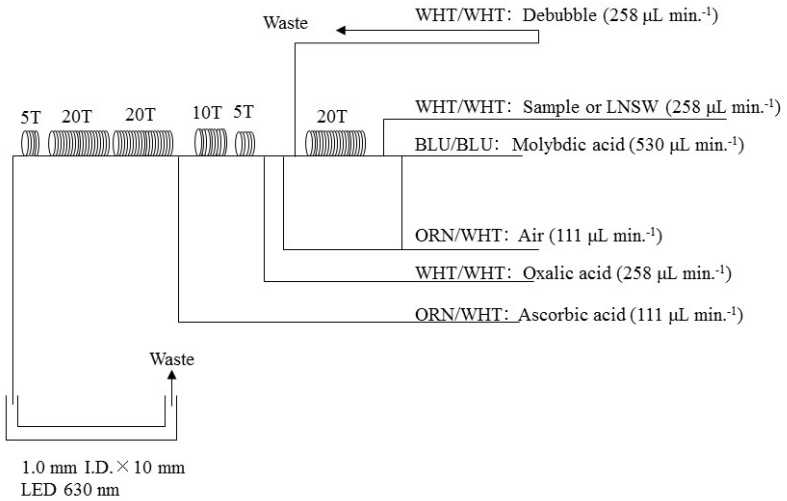

Figure 3.3.2.3 SiO_2 (3ch.) flow diagram.

Reagents

15 % Sodium dodecyl sulfate solution: 75 g of sodium dodecyl sulfate (CAS No. 151-21-3) was mixed with 425 mL ultra-pure water.

Molybdic acid, 0.03 M (1 % w/v): Dissolved 7.5 g of sodium molybdate dihydrate (CAS No. 10102-40-6) in 980 mL ultra-pure water, and then added 12 mL of 4.5M sulfuric acid. After mixing, 20 mL of the 15 % sodium dodecyl sulfate solution was added. Note that the amount of sulfuric acid was reduced from the previous report (MR19-03C) since we have modified the method of Grasshoff et al. (1999).

Oxalic acid, 0.6 M (5 % w/v): Dissolved 50 g of oxalic acid (CAS No. 144-62-7) in 950 mL of ultra-pure water.
Ascorbic acid, 0.01 M (3 % w/v): Dissolved 2.5 g of L-ascorbic acid (CAS No. 50-81-7) in 100 mL of ultra-pure water. This reagent was freshly prepared every day.

(4.3) Phosphate
The methodology for the phosphate analysis is a modified procedure based on Murphy and Riley (1962). The flow diagram is shown in Fig. 3.3.2.4. Molybdic acid was added to the seawater sample to form the phosphomolybdic acid compound, which was then reduced to phosphomolybdous acid using L-ascorbic acid as the reductant. The signal was monitored at 880 nm.

Reagents
15 % Sodium dodecyl sulfate solution: 75 g of sodium dodecyl sulfate (CAS No. 151-21-3) was mixed with 425 mL of ultra-pure water.
Stock molybdate solution, 0.03 M (0.8 % w/v): Dissolved 8 g of sodium molybdate dihydrate (CAS No. 10102-40-6) and 0.17 g of antimony potassium tartrate trihydrate (CAS No. 28300-74-5) in 950 mL of ultra-pure water, and then added 50 mL of sulfuric acid (CAS No. 7664-93-9).
PO_4 color reagent: Dissolved 1.2 g of L-ascorbic acid (CAS No. 50-81-7) in 150 mL of the stock molybdate solution. After mixing, 3 mL of the 15 % sodium dodecyl sulfate solution was added. This reagent was freshly prepared before every measurement.

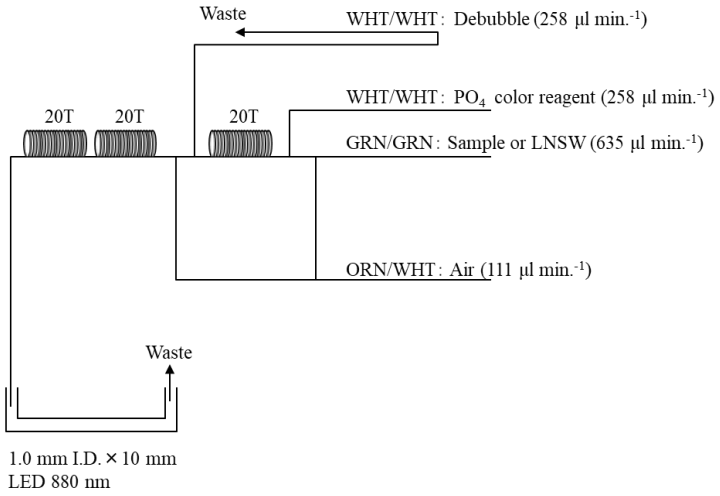

Figure 3.3.2.4 PO_4 (4ch.) flow diagram.

(4.4) Ammonia
The ammonia in seawater was determined using the flow diagrams shown in Fig. 3.3.2.5. The sample was mixed with an alkaline solution containing EDTA, which converted ammonia into its gaseous state. The ammonia gas was then absorbed in a sulfuric acid though a 0.5 µm pore-size membrane filter (ADVANTEC PTFE) at the dialyzer attached to the analytical system. The ammonia absorbed in sulfuric acid was subsequently determined by coupling it with phenol and hypochlorite to form indophenols blue, with the signal monitored at 630 nm.

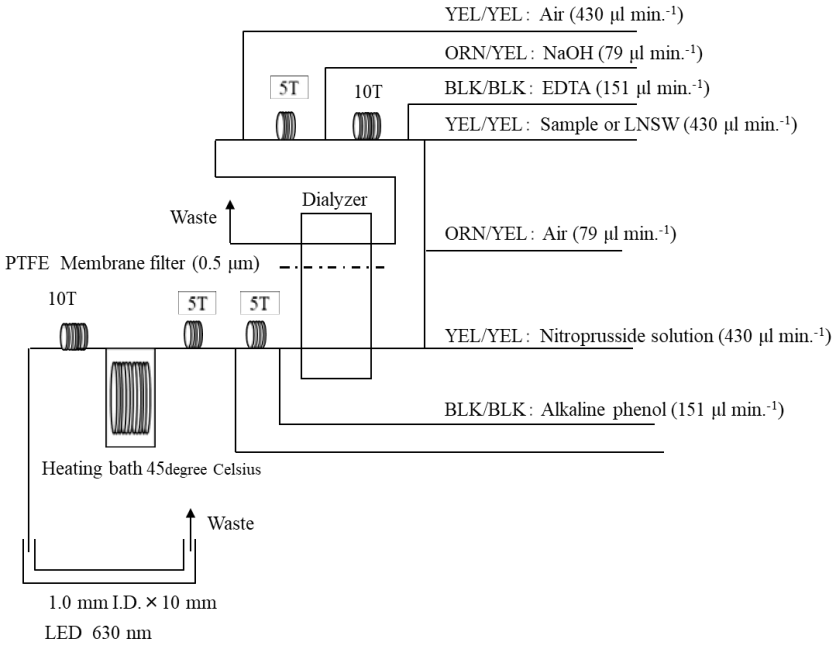

Figure 3.3.2.5 NH_4 (5ch.) flow diagram.

Reagents

30 % Triton solution: 30 mL of the Triton® X-100 (CAS No. 9002-93-1) was mixed with 70 mL ultra-pure water.

EDTA: Dissolved 41 g of tetrasodium;2-[2-[bis(carboxylatomethyl)amino]ethyl-(carboxylatemethyl)amino]acetate;tetrahydrate (CAS No. 13235-36-4) and 2 g of boric acid (CAS No. 10043-35-3) in 200 mL of ultra-pure water. After mixing, 1 mL of the 30 % triton solution was added. This reagent is prepared every week.

NaOH liquid: Dissolved 1.5 g of sodium hydroxide (CAS No. 1310-73-2) and 16 g of tetrasodium;2-[2-[bis(carboxylatomethyl)amino]ethyl-(carboxylatemethyl)amino]acetate;tetrahydrate (CAS No. 13235-36-4) in 100 mL of ultra-pure water. This reagent was prepared every week. Note that we reduced the amount of sodium hydroxide from 5 g to 1.5 g because pH of C standard solutions has been lowered 1 pH unit due to the change of recipe of B standards solution (the details of those standard solutions, see (6.4)).

Stock nitroprusside: Dissolved 0.25 g of sodium nitroferricyanide dihydrate (CAS No. 13755-38-9) in 100 mL of ultra-pure water, and then added 0.2 mL of 1M sulfuric acid. Stored in a dark bottle and prepared every month.

Nitroprusside solution: Added 4 mL of the stock nitroprusside and 4 mL of 1M sulfuric acid in 500 mL of ultra-pure water. After mixing, 2 mL of the 30 % triton solution was added. This reagent was stored in a dark bottle and prepared every 2 or 3 days.

Alkaline phenol: Dissolved 10 g of phenol (CAS No. 108-95-2), 5 g of sodium hydroxide (CAS No. 1310-73-2) and 2 g of sodium citrate dihydrate (CAS No. 6132-04-3) in 200 mL of ultra-pure water. Stored in a dark bottle and prepared every week.

NaClO solution: Mixed 3 mL of sodium hypochlorite (CAS No. 7681-52-9) in 47 mL of ultra-pure water. Stored in a dark bottle and fleshly prepared before every measurement. This reagent needs to be 0.3 % available chlorine.

(4.5) Sampling procedures

Sampling for the nutrient analysis was conducted after collecting samples for other gas parameters and salinity. Seawater samples were collected in two new 10 mL polyacrylate vials, without using the sample-drawing tube typically employed for the oxygen sampling. Each vial was rinsed three times with sample water before filling and then sealed immediately without any head space. The vials were placed in a water bath maintained at 21.0 degree Celsius for more than 30 minutes prior to measurement. When the transmissometer signal (Xmiss) of a sample was below 95 %, or when particles were visually observed in the vial, the sample was centrifuged using a CN-820 centrifuge (Hsiang Tai) at approximately 3400 rpm for 2.5 minutes. The sample in the original vial was placed directly on an autosampler (AIM 4000, BL TEC K.K.) tray for analysis. All seawater samples were analyzed within 24 hours of collection.

(4.6) Data processing

Raw data from QuAAtro 39-J were processed as follows:

Checked if there were any baseline shifts.

Checked the shape of each peak and positions of peak values. If necessary, a change was made for the positions of peak values.

Conducted carry-over correction and baseline drift correction followed by sensitivity correction to apply to the peak height of each sample.

Conducted baseline correction and sensitivity correction using linear regression.

Conducted baseline correction and sensitivity correction using linear regression.
Using the salinity (from CTD data* or determined on the ship) and the laboratory room temperature (20 degree Celsius), the density of each sample was calculated. The obtained density was used to calculate the final nutrient concentration with the unit of μmol kg^{-1}.
Calibration curves to obtain the nutrient concentrations were assumed second-order equations.
* Raw CTD pre-calibrated data has been used.

(5) Certified Reference Material of nutrients in seawater
Certified reference materials (CRMs) produced by KANSO Co., Ltd. were used to ensure the comparability and traceability of nutrient measurements during this cruise. The KANSO CRMs cover inorganic nutrients (nitrate, nitrite, silicate, phosphate, and ammonia) in seawater and are produced using autoclaved natural seawater, following a quality control system based on ISO Guide 34 (JIS Q 0034). KANSO Co., Ltd. has been accredited as a CRM producer under the National Institute of Technology and Evaluation (ASNITE) System since 2011. (ASNITE 0052 R)
Certified values for the CRMs were calculated as the arithmetic means of measurements from 30 bottles per batch (measured in duplicates), performed by both KANSO Co., Ltd. and Japan Agency for Marine-Earth Science and Technology (JAMSTEC) using the colorimetric method (continuous flow analysis, CFA). The salinity of the calibration standards solution for each calibration curve was adjusted to match the CRM salinity within ± 0.5.
Each certified value of nitrate, nitrite, and phosphate in KANSO CRMs was calibrated using Japan Calibration Service System (JCSS) standard solutions for the respective ions. The JCSS standard solutions were in turn calibrated using JCSS secondary solutions, which was calibrated with primary solutions produced by the Chemicals Evaluation and Research Institute (CERI), Japan. CERI primary solutions were further calibrated with the National Metrology Institute of Japan (NMIJ) primary standards solution of nitrate, nitrite, and phosphate ions, respectively. The certified value of silicate of KANSO CRM was calibrated using a newly developed silicon standards solution (Lot. AA produced by KANSO), produced via an alkaline dissolution technique. The mass fraction of silicon in this solution was calibrated based on NMIJ CRM 3645-a Si standard solution through the technology consulting system of the National Institute of Advanced Industrial Science and Technology (AIST), providing traceability to the International System of Units (SI).
During this cruise, 15sets of CRM lots CQ, CU, CS, CW were used (Table 3.3.2.1), with serial numbers selected randomly. The CRM bottles were stored in the ship's "BIOCHEMICAL LABORATORY" at a maintained temperature of approximately 18.77 degree Celsius – 22.36 degree Celsius.

Table 3.3.2.1 Certified concentration and the uncertainty (k=2) of CRMs (μmol kg^{-1}).

Lot	Nitrate	Nitrite*	Silicate	Phosphate	Ammonia**
CQ	0.06 ± 0.03	0.075 ± 0.07	2.20 ± 0.07	0.030 ± 0.009	1.76 ± 0.07
CU	3.06 ± 0.05	0.04 ± 0.04	7.77 ± 0.09	0.262 ± 0.011	1.02 ± 0.04
CS	16.65 ± 0.16	0.18 ± 0.07	33.8 ± 0.4	1.069 ± 0.019	0.73 ± 0.06

CW	21.2 ± 0.2	0.24 ± 0.07	41.6 ± 0.5	1.45 ± 0.03	1.102

* For nitrite concentration, there is a trend that the value has been increased 0.004 ± 0.002 μmol kg^{-1} per year. The values of CQ and CS were determined by JAMSTEC in April 2025.
** Ammonia values are all reference value. The value of CQ, CU and CS were reported by KANSO. CW values were determined by JAMSTEC.

(6) Standards
To obtain the calibration curves, we prepared in-house standard solutions because (1) nutrient concentrations in seawater samples may exceed CRM, and (2) the ammonia concentrations in the CRMs are not certified values.

(6.1) Volumetric laboratory-ware of in-house standards
All volumetric glassware and polymethylpentene (PMP) volumetric flasks were gravimetrically calibrated. Plastic volumetric flasks were calibrated gravimetrically at their water temperature, within 0.4 K of approximately 19.5 degree Celsius. "Class A" volumetric flasks were used for their nominal tolerances of 0.05 % or less across the size ranges relevant to this work. Since Class A flasks are made of borosilicate glass, standard solutions were transferred to plastic bottles immediately after being made up to volume and thoroughly mixed to prevent excessive silicate dissolution from the glass. PMP volumetric flasks were also gravimetrically calibrated and used only within 1.0 K of their calibration temperature. Volume adjustments for the glass flasks at temperatures other than the calibration temperatures were calculated using the linear expansion coefficient for borosilicate crown glass. The cubic expansion coefficients for each glass and PMP volumetric flask were determined through measurements in 2023. The cubical expansion coefficient of the glass volumetric flask (SHIBATA HARIO) ranged from 0.00000975 to 0.0000172 K^{-1}, and for the PMP volumetric flask (NALGEN PMP), from 0.00038 to 0.00042 K^{-1}. Calibration weights were corrected for the water density and air buoyancy. All glass pipettes, which have nominal calibration tolerances of 0.1 % or better, were gravimetrically calibrated to verify and, where possible, improve upon their nominal tolerances.

(6.2) Reagents
For nitrate standard, we used "potassium nitrate 99.995 suprapur®" provided by Merck, Batch B1983565, CAS No. 7757-79-1. For nitrite standard solution, nitrite ion standard solutions (NO_2^- 1000) from Wako Chemicals (Lot KSK1433, Code. No. 146-06453) was used, with the certified standard solutions from Wako Chemicals. The calibration result was 1006 mg L^{-1} at 20 degree Celsius, with an expanded uncertainty of 0.8 % (k=2). For the silicate standard solution, Si standard solutions Lot. AA produced by KANSO, was used. The silicon mass fraction in the Lot. AA solution was calibrated based on NMIJ CRM 3645-a Si standard solution. For the phosphate standard, "potassium dihydrogen phosphate anhydrous 99.995 suprapur®" provided by Merck (Batch B2076208, CAS No.: 7778-77-0), was used. For the ammonia standard, we used ammonium chloride (CRM 3011-a) from NMIJ, CAS No. 12125-02-9, with a reported purity of >99.9 % by the manufacturer. The expanded uncertainty of calibration (k=2) was 0.026 %.

(6.3) Low nutrients seawater (LNSW)
Surface water with low nutrient concentrations was taken and filtered using a 0.20 μm pore capsule cartridge filter near 13°N and 136°E during the MR21-03 cruise in June 2021. The filtered seawater was drained into multiple 20 L Cubitainer (flexible containers) and stored in cardboard boxes. This water has since been used as low-nutrients seawater (LNSW) for nutrients measurements. The concentrations in each LNSW container were measured in June 2022, yielding average values of 0.01, 0.003, 1.08, 0.075, and 0.01 μmol L^{-1} for nitrate, nitrite, silicate, phosphate, and ammonia, respectively. The concentrations of nitrate, nitrite, and ammonia were below the detection limit.

(6.4) Standard solutions and calibration curves
Concentrations of nutrients for standard solutions A, B, C, and D are shown in Table 3.3.2.2. The KANSO Si standard solution was used for the A standard of silicate, which doesn't require neutralization with hydrochloric acid. The B standard was diluted from the A standard following the recipes shown in Table 3.3.2.3. To match the salinity and the density of the B standard solution to those of the LNSW, 15.00 g of sodium chloride powder was dissolved in the B standard solution, and then the final volume was adjusted to 500 mL. The C standard solution was prepared in the LNSW following the recipes shown in Table 3.3.2.4. The actual concentrations of nutrients in each standard solution were calculated based on the solution temperature and the calibrated factors of volumetric laboratory wares. Calibration curves for each run of nitrate, nitrite, silicate, and phosphate were obtained using five levels: C-2, C-3, C-5, C-6, C-8. For ammonia, calibration was achieved using four levels: C-1, C-4, C-7 C-8. C-1 was LNSW, C-2, C-3, C-5, and C-6 were the CRM of nutrients in seawater, and C-4, C-7, and C-8 were diluted using the B standard solution. The D standard solutions, used to calculate the reduction rate of the Cd coil, were diluted from the A standard solution with pure water (milli-Q). In-house standard solutions were remade according to the "renewal time" intervals listed in Table 3.3.2.5.

Table 3.3.2.2 Nominal concentrations of nutrients for A, D, B and C standards (μmol L^{-1}).

	A	B	D	C-1	C-2	C-3	C-4	C-5	C-6	C-7	C-8
NO_3	22500	670	900	-	CQ	CU	-	CS	CW	-	40
NO_2	21900	26	870	-	CQ	CU	-	CS	CW	-	1.6
SiO_2	35600	1400		-	CQ	CU	-	CS	CW	-	86
PO_4	6000	60		-	CQ	CU	-	CS	CW	-	3.7
NH_4	4000	160		LNSW	-	-	1.6	-	-	4.8	9.6

Table 3.3.2.3 B standard recipes. Final volume was 500 mL.

	A Std.
NO_3	15 mL
NO_2*	15 mL
SiO_2	20 mL
PO_4	5 mL
NH_4	20 mL

*NO_2 was D standard solution which was diluted from A standard.

Table 3.3.2.4 Working calibration standard recipes. Final volume was 500 mL.

C Std.	B Std.
C-4	5 mL
C-7	15 mL
C-8	30 mL

Table 3.3.2.5 Renewal times of in-house standards.

Standard	Renewal time
A-1 Std. (NO_3)	maximum a month
A-2 Std. (NO_2)	commercial prepared solution
A-3 Std. (SiO_2)	commercial prepared solution
A-4 Std. (PO_4)	maximum a month
A-5 Std. (NH_4)	maximum a month
D-1 Std.	maximum 8 days
D-2 Std.	maximum 8 days
B Std. (mixture of A-1, D-2, A-3, A-4 and A-5 Std.)	maximum 8 days
C Std.	every 24 hours
36 µM NO_3 (diluted D-1 Std. for reduction estimate)	when C Std. renewed
35 µM NO_2 (diluted D-2 Std. for reduction estimate)	when C Std. renewed

(7) Data quality

During this cruise, a total of 15 runs were conducted to measure samples collected by 37 casts across 34 stations. In total, 395 seawater samples were collected. The samples were collected into two vials and measured independently as replicate measurements.

(7.1) Precision

The highest-concentration standard solution (C-8) was repeatedly determined every some samples to assess the analytical precision of the nutrient analyses during this cruise. Analytical precision for each run was calculated from these C-8 results, and overall precision for this cruise were calculated from the combined precision across all runs (Table 3.3.2.6). The overall median precisions during this cruise were 0.12%, 0.21%, 0.14%, 0.18%, and 0.26% for nitrate, nitrite, silicate, phosphate, and ammonia, respectively. These values are comparable to those obtained during the previous cruises conducted from 2009 to 2025.

Table 3.3.2.6 Overall precisions (k=1)

	Nitrate CV %	Nitrite CV %	Silicate CV %	Phosphate CV %	Ammonia CV %
Median	0.12	0.21	0.14	0.18	0.26
Mean	0.12	0.21	0.13	0.16	0.27
Maximum	0.16	0.29	0.18	0.20	0.41
Minimum	0.07	0.1	0.08	0.09	0.15

n	16	16	16	16	16

(7.2) Comparability

CRM lot CW was measured during each run to evaluate the comparability across the measurements during this cruise. All measured concentrations were within the uncertainty of certified values for nitrate, nitrite, silicate, and phosphate (Table 3.3.2.7).

Table 3.3.2.7 CRM lot CW measurements (μmol kg^{-1}).

	Nitrate	Nitrite	Silicate	Phosphate	Ammonia
Median	21.22	0.24	41.71	1.451	1.14
Mean	21.22	0.24	41.72	1.451	1.14
STDEV	0.06	0.003	0.08	0.005	0.03
n	16	16	16	16	16

(7.3) Carryover

We also summarized the magnitudes of carry over, which refers to sample-to-sample contamination during flow analysis. To evaluate carryover in each run, we measured the C-8 standard solution followed by two consecutive measurements of the LNSW solution. The difference from LNSW-1 to LNSW-2 was used to estimate the carryover (%) using the following equation (1) where [ ] denotes concentrations.

Carryover (%) = ([LNSW-1] – [LNSW-2]) / ([C-8] – [LNSW-2]) * 100 (1)

The carryover (%) are shown in Table 3.3.2.8. Overall, the results indicated low carryover percentages. These low percentages suggest that there was no significant issue during this cruise.

Table 3.3.2.8 Carryovers (%)

	Nitrate	Nitrite	Silicate	Phosphate	Ammonia
Median	0.19	0.20	0.25	0.20	1.09
Mean	0.18	0.21	0.25	0.20	1.07
Maximum	0.23	0.42	0.31	0.30	1.40
Minimum	0.00	0.00	0.21	0.11	0.82
n	16	16	16	16	16

(7.4) Uncertainty (Repeatability)

Empirical equations were obtained based on 16 measurements of 16 sets of CRMs (Table 3.3.2.1) to estimate the uncertainty (repeatability) of measurements of nitrate, silicate, and phosphate, respectively . Empirical equations were obtained based on duplicate measurements of the samples to estimate the uncertainty (repeatability) of measurements of nitrite and ammonia (Table 3.3.2.9 - 10) The uncertainty formula is described in the readme.

(7.5) Detection limit and quantitative determination

The LNSW was measured every some samples to estimate the detection limit of nutrient analyses during this cruise. The detection limit was calculated based on the

LNSW results from all runs using the following equation:

Detection limit = 3 * standard deviation of repeated measurement of LNSW (7)

The estimated detection limits are shown in Table 3.3.2.9. The quantitative determination of nutrient analyses reflects concentrations with an uncertainty of 33 % as indicated in the empirical equations, eq. (2) to (6). The estimated quantitative determinations are also shown in Table 3.3.2.9.

Table 3.3.2.9 Detection limit and quantitative determination.

	Nitrate μmol kg^{-1}	Nitrite μmol kg^{-1}	Silicate μmol kg^{-1}	Phosphate μmol kg^{-1}	Ammonia μmol kg^{-1}
Detection limit	0.016	0.003	0.07	0.006	0.026
Quantitative determination	0.04	0.01	0.38	0.012	0.04

Replicate samples were taken at most of the layers. The summary of average and standard deviation of the difference between each replicate pair of analysis was shown in Table 3.3.2.10.

Table 3.3.2.10 Average and standard deviation of the difference between each replicate pair of analysis.

	Nitrate μmol kg^{-1}	Nitrite μmol kg^{-1}	Silicate μmol kg^{-1}	Phosphate μmol kg^{-1}	Ammonia μmol kg^{-1}
Average	0.01	0.002	0.04	0.004	0.02
Standard deviation	0.01	0.002	0.04	0.003	0.02
n	393	394	394	393	389

(8) Glove Material Testing During Nutrient Sampling

In previous tests, contamination of nitrogen components was detected when using Kualatec gloves (standard latex gloves, powder-free). For this reason, Clean Knoll Gloves (PVC, vinyl chloride resin, powder free) have been used instead. However, those earlier tests were conducted under conditions that did not fully reflect the actual sampling procedure. Specifically, nutrient samples were taken using new gloves directly out of the package, without prior rinsing.

In actual nutrient sampling operations, however, samples for DIC and TA (each involving approximately 20–30 seconds of overflow and sampling) and for salinity bottles (rinsed three times) are collected before nutrient samples. During these preceding steps, the gloves are likely to be sufficiently rinsed by seawater, which may reduce the risk of contamination.

Therefore, in this experiment, contamination testing was conducted out to evaluate whether the use of Kualatec gloves results in detectable contamination under realistic sampling conditions. Five new sample bottles were used, and nutrient samples were collected by five different samplers following the standard sampling sequence.

The results showed no significant difference between samples collected with Kualatec gloves and those collected with the currently used gloves. This indicates that Kualatec gloves can be safely used for nutrient sampling, provided they are adequately rinsed with seawater before use. However, it should be noted that some unexplained potential contamination was observed, possibly originating from the gloves (sample MR21-05C). Therefore, careful handling and additional testing are recommended to determine which type of gloves should be used for nutrient sampling in future work, and users should remain aware of the potential for contamination from Kualatec gloves.

(9) Problems

There is no significant issue of this data set during this cruise.

(10) List of reagents

List of reagents used in this cruise is shown in Table 3.3.2.11.

Table 3.3.2.11 List of reagents used in this cruise

IUPAC name	CAS Number	Formula	Compound Name	Manufacture	Grade
4-Aminobenzenesulfonamide	63-74-1	$C_6H_8N_2O_2S$	Sulfanilamide	FUJIFILM Wako Pure Chemical Corporation	JIS Special Grade
Ammonium chloride	12125-02-9	NH_4Cl	Ammonium Chloride	FUJIFILM Wako Pure Chemical Corporation	JIS Special Grade
Antimony potassium tartrate trihydrate	28300-74-5	$K_2(SbC_4H_2O_6)_2 \cdot 3H_2O$	Bis[(+)-tartrato]diantimonate(III) Dipotassium Trihydrate	FUJIFILM Wako Pure Chemical Corporation	JIS Special Grade
Boric acid	10043-35-3	H_3BO_3	Boric Acid	FUJIFILM Wako Pure Chemical Corporation	JIS Special Grade
Hydrogen chloride	7647-01-0	HCl	Hydrochloric Acid	FUJIFILM Wako Pure Chemical Corporation	JIS Special Grade
Imidazole	288-32-4	$C_3H_4N_2$	Imidazole	FUJIFILM Wako Pure Chemical Corporation	JIS Special Grade
L-Ascorbic acid	50-81-7	$C_6H_8O_6$	L-Ascorbic Acid	FUJIFILM Wako Pure Chemical Corporation	JIS Special Grade
N-(1-Naphthalenyl)-1,2-ethanediamine, dihydrochloride	1465-25-4	$C_{12}H_{16}Cl_2N_2$	N-1-Naphthylethylenediamine Dihydrochloride	FUJIFILM Wako Pure Chemical Corporation	for Nitrogen Oxides Analysis
Oxalic acid	144-62-7	$C_2H_2O_4$	Oxalic Acid	FUJIFILM Wako Pure Chemical Corporation	Wako Special Grade
Phenol	108-95-2	C_6H_6O	Phenol	FUJIFILM Wako Pure Chemical Corporation	JIS Special Grade
Potassium nitrate	7757-79-1	KNO_3	Potassium Nitrate	Merck KGaA	Suprapur®
Potassium dihydrogen phosphate	7778-77-0	KH_2PO_4	Potassium dihydrogen phosphate anhydrous	Merck KGaA	Suprapur®
Sodium chloride	7647-14-5	NaCl	Sodium Chloride	FUJIFILM Wako Pure Chemical Corporation	TraceSure®
Sodium citrate dihydrate	6132-04-3	$Na_3C_6H_5O_7 \cdot 2H_2O$	Trisodium Citrate Dihydrate	FUJIFILM Wako Pure Chemical Corporation	JIS Special Grade
Sodium dodecyl sulfate	151-21-3	$C_{12}H_{25}NaO_4S$	Sodium Dodecyl Sulfate	FUJIFILM Wako Pure Chemical Corporation	for Biochemistry
Sodium hydroxide	1310-73-2	NaOH	Sodium Hydroxide for Nitrogen Compounds Analysis	FUJIFILM Wako Pure Chemical Corporation	for Nitrogen Analysis
Sodium hypochlorite	7681-52-9	NaClO	Sodium Hypochlorite Solution	Kanto Chemical co., Inc.	Extra pure
Sodium molybdate dihydrate	10102-40-6	$Na_2MoO_4 \cdot 2H_2O$	Disodium Molybdate(VI) Dihydrate	FUJIFILM Wako Pure Chemical Corporation	JIS Special Grade
Sodium nitroferricyanide dihydrate	13755-38-9	$Na_2[Fe(CN)_5NO] \cdot 2H_2O$	Sodium Pentacyanonitrosylferrate(III) Dihydrate	FUJIFILM Wako Pure Chemical Corporation	JIS Special Grade
Sulfuric acid	7664-93-9	H_2SO_4	Sulfuric Acid	FUJIFILM Wako Pure Chemical Corporation	JIS Special Grade
tetrasodium;2-[2-[bis(carboxylatomethyl)amino]ethyl-(carboxylatomethyl)amino]acetate;tetrahydrate	13235-36-4	$C_{10}H_{12}N_2Na_4O_8 \cdot 4H_2O$	Ethylenediamine-N,N,N',N'-tetraacetic Acid Tetrasodium Salt Tetrahydrate (4NA)	Dojindo Molecular Technologies, Inc.	-
Synonyms: t-Octylphenoxypolyethoxyethanol 4-(1,1,3,3-Tetramethylbutyl)phenyl-polyethylene glycol Polyethylene glycol tert-octylphenyl ether	9002-93-1	$(C_2H_4O)_nC_{14}H_{22}O$	Triton®X-100	MP Biomedicals, Inc.	-

(11) Data archives

These data obtained in this cruise will be submitted to the Data Management Group of JAMSTEC, and will be opened to the public via "Data Research System for Whole Cruise Information in JAMSTEC (DARWIN)" in JAMSTEC web site. <https://www.godac.jamstec.go.jp/darwin/en/>

(12) References

Becker, S., Aoyama, M., Malcolm E., Woodward, S., Bakker, K., Coverly, S., Mahaffey, C., Tanhua, T., (2019) The precise and accurate determination of dissolved inorganic

nutrients in seawater, using Continuous Flow Analysis methods, n: The GO-SHIP Repeat Hydrography Manual: A Collection of Expert Reports and Guidelines. Available online at: http://www.go-ship.org/HydroMan.html. DOI: http://dx.doi.org/10.25607/OBP-555
Grasshoff, K. (1976). Automated chemical analysis (Chapter 13) in Methods of Seawater Analysis. With contribution by Almgreen T., Dawson R., Ehrhardt M., Fonselius S. H., Josefsson B., Koroleff F., Kremling K. Weinheim, New York: Verlag Chemie.
Grasshoff, K., Kremling K., Ehrhardt, M. et al. (1999). Methods of Seawater Analysis. Third, Completely Revised and Extended Edition. WILEY-VCH Verlag GmbH, D-69469 Weinheim (Federal Republic of Germany).
Hydes, D.J., Aoyama, M., Aminot, A., Bakker, K., Becker, S., Coverly, S., Daniel, A., Dickson, A.G., Grosso, O., Kerouel, R., Ooijen, J. van, Sato, K., Tanhua, T., Woodward, E.M.S., Zhang, J.Z., (2010). Determination of Dissolved Nutrients (N, P, Si) in Seawater with High Precision and Inter-Comparability Using Gas-Segmented Continuous Flow Analysers, In: GO-SHIP Repeat Hydrography Manual: A Collection of Expert Reports and Guidelines. IOCCP Report No. 14, ICPO Publication Series No 134.
Kimura (2000). Determination of ammonia in seawater using a vaporization membrane permeability method. 7th auto analyzer Study Group, 39-41.
Murphy, J., and Riley, J.P. (1962). Analytica Chimica Acta 27, 31-36.

3.3.3. Dissolved inorganic carbon

3.3.3.1 Bottled-water analysis

(1) Personnel
Akihiko Murata (JAMSTEC) – Principal investigator, Not on board
Masahiro Orui (MWJ)
Yasuhiro Arii (MWJ)
Nagisa Fujiki (MWJ)

(2) Objective
To clarify vertical distributions of total dissolved inorganic carbon (DIC) in water columns.

(3) Parameter
Total dissolved Inorganic Carbon (DIC)

(4) Instruments and Methods
a. Seawater sampling
Seawater samples were collected by 12 liter Niskin bottles mounted on the CTD/Carousel Water Sampling System. Seawater was sampled in a 250 mL borosilicate glass bottle with ground glass stoppers. A sampling silicone rubber tube with PFA tip was connected to the outlet of Niskin bottle for water sampling. The glass bottles were filled from their bottom gently, without rinsing, and overflowed for 20 seconds. They were sealed using ground glass stoppers with care not to leave any bubbles in the bottle. Immediately after the water sampling on the deck, the glass bottles were carried to the laboratory for the addition of saturated solution of

mercury (II) chloride ($HgCl_2$). Small volume (3 mL) of the sample (1 % of the bottle volume) was removed from the bottle and 100 µL of $HgCl_2$ was added. The bottle was then sealed with a ground glass stopper lubricated with Apiezon® Grease M. Finally, the glass stopper was secured with a clip. The samples were stored in a refrigerator at approximately 5 °C until analysis.

b. Seawater analysis
Measurements of DIC were made with a total CO2 measuring system (Nihon ANS Inc.). The system comprises of seawater dispensing unit, a CO2 extraction unit, and a coulometer (Model 3000, Nihon ANS Inc.) The seawater dispensing unit has an auto-sampler (6 ports), which dispenses the seawater from a glass bottle to a pipette of nominal 15 mL volume. The pipette was kept at 20.00 °C ± 0.05 °C by a water jacket, in which water circulated through a thermostatic water bath. The CO2 dissolved in a seawater sample is extracted in a stripping chamber of the CO2 extraction unit by adding 10 % phosphoric acid solution. The strip chamber is made approx. 25 cm long and has a fine fit at the bottom. First, a constant volume of acid is added to the stripping chamber from its bottom by pressurizing an acid bottle with nitrogen gas (99.9999 %). Second, a seawater sample kept in a pipette is introduced to the stripping chamber by the same method. The seawater and phosphoric acid are stirred by the nitrogen bubbles through a fine frit at the bottom of the stripping chamber. The stripped CO2 is carried to the coulometer through two electric dehumidifiers (kept at 2 °C) and a chemical desiccant (magnesium perchlorate) by the nitrogen gas (flow rate of 140 mL min^{-1}). Measurements of system blank (phosphoric acid blank), 1.5 % CO2 standard gas in a nitrogen base, and seawater samples (6 samples) were programmed to repeat. The variation of our own made JAMSTEC DIC reference material was used to correct the signal drift results from chemical alteration of coulometer solutions. The values of DIC were set to the assigned value of CRM (batch 209, 2060.05 ± 0.27 µmol kg^{-1}) provided by Prof. Dickson, Scripps Institution of Oceanography, Univ. of California.

(5) Observation log
Seawater samples were collected at 33 stations.

(6) Preliminary results
The repeatability was estimated to be provisionally 1.12 µmol kg^{-1} (n=54), if outliers are excluded.

(7) Data archives
These data obtained in this cruise will be submitted to the Data Management Group (DMG) of JAMSTEC, and will be opened to the public via "Data Research System for Whole Cruise Information in JAMSTEC (DARWIN)" in JAMSTEC web site.
<https://www.godac.jamstec.go.jp/darwin/en/>

3.3.3.2 Underway DIC

(1) Personnel
Akihiko Murata (JAMSTEC) – Principal investigator, Not on board
Nagisa Fujiki (MWJ)
Masahiro Orui (MWJ)

(2) Objective
To elucidate spatial variations of total dissolved inorganic carbon (DIC) concentration in sea surface water.

(3) Parameter
Total Dissolved Inorganic Carbon (DIC)

(4) Instruments and Methods
Surface seawater was continuously collected from 5th September to 2nd October 2025 (UTC) during this cruise. Surface seawater was taken from an intake placed approximately 4.5 m below the sea surface by a pump and was filled in a 250 mL glass bottle (SCHOTT DURAN) from the bottom, without rinsing, and overflowed for more than 2 times the amount. Before the analysis, the samples were put in the water bath kept about 20°C for one hour. Measurements of DIC were made with a total CO_2 measuring system (Nihon ANS Inc.). The system was comprised of seawater dispensing unit, a CO_2 extraction unit, and a coulometer (Model 3000A, Nihon ANS Inc.). The seawater dispensing unit has an auto-sampler (6 ports), which dispenses the seawater from a glass bottle to a pipette of nominal 15 mL volume. The pipette was kept at 20.00 °C ± 0.05 °C by a water jacket, in which water circulated through a thermostatic water bath. The CO_2 dissolved in a seawater sample is extracted in a stripping chamber of the CO_2 extraction unit by adding 10 % phosphoric acid solution. The strip chamber is made approx. 25 cm long and has a fine frit at the bottom. First, the certain amount of acid is taken to the constant volume tube from an acid bottle and transferred to the stripping chamber from its bottom by nitrogen gas (99.9999 %). Second, a seawater sample kept in a pipette is introduced to the stripping chamber by the same method as that for acid. The seawater and phosphoric acid are stirred by the nitrogen bubbles through a fine frit at the bottom of the stripping chamber. The stripped CO_2 is carried to the coulometer through two electric dehumidifiers (kept at 2 °C) and a chemical desiccant (Magnesium perchlorate) by the nitrogen gas (flow rate of 140 mL min^{-1}). Measurements of approx.1.5 % CO_2 standard gas in a nitrogen base, system blank (phosphoric acid blank), and seawater samples (6 samples) were programmed to repeat. CO_2 standard gas and reference material produced by JAMSTEC (batch Q41, 2034.9 ± 2.9 µmol kg^{-1}) were used to correct the signal drift results from chemical alteration of coulometer solutions. The coulometer solutions were renewed every 2 days. The values of DIC were set to the assigned value of CRM (batch 209, 2060.05 ± 0.27 µmol kg^{-1}) provided by Prof. Dickson, Scripps Institution of Oceanography, Univ. of California.

(5) Observation log
The cruise track during underway DIC observation is shown in Figure 3.3.3-1.

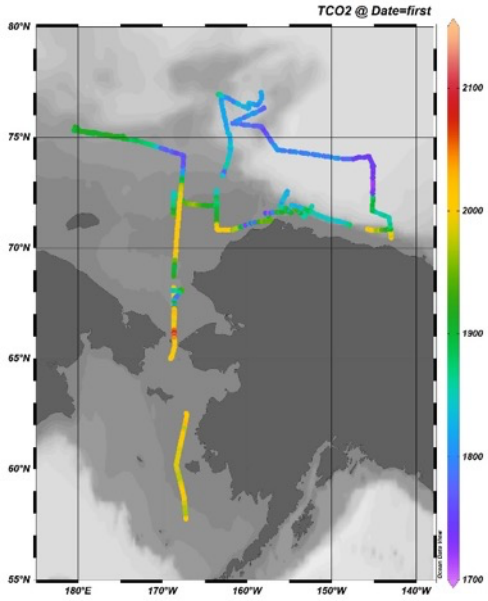

Figure 3.3.3-1. Cruise track where underway DIC was measured during the cruise.
Concentrations of DIC were shown in color.

(6) Date archives

These data obtained in this cruise will be submitted to the Data Management Group (DMG) of JAMSTEC, and will be opened to the public via "Data Research System for Whole Cruise Information in JAMSTEC (DARWIN)" in JAMSTEC web site.
<https://www.godac.jamstec.go.jp/darwin/en/>

3.3.4 Total Alkalinity

(1) Personnel
Akihiko Murata (JAMSTEC) – Principal investigator, Not on board
Nagisa Fujiki (MWJ)
Yasuhiro Arii (MWJ)
Masahiro Orui (MWJ)

(2) Objective
To survey influences of sea ice melting water and river input on carbonate system properties.

(3) Parameters
Total alkalinity (TA)

(4) Instruments and Methods
a. Seawater sampling
On this cruise, we analyzed TA in seawater collected for DIC. See the section on DIC for water sampling.

b. Seawater analysis
The total alkalinity was measured using a spectrophotometric system (Nihon ANS, Inc.) using a scheme of Yao and Byrne (1998). The calibrated volume of sample seawater (ca. 42 mL) was transferred from a sample bottle into the titration cell with its light path length of 4 cm long via dispensing unit. The TA is calculated by measuring two sets of absorbance at three wavelengths (730, 616 and 444) nm with the spectrometer (TM-UV/VIS C10082CAH, HAMAMATSU). One is the absorbance of seawater sample before injecting an acid with indicator solution (bromocresol green sodium) and another is the one after the injection. To mix the acidified-indicator solution with seawater sufficiently, the mixed solution is circulated in a circulation line by a peristaltic pump for 5 minutes. Nitrogen bubbles were introduced into the titration cell for degassing CO_2 from the mixed solution sufficiently. The TA is calculated based on the following equation:

$$TA = (-[H^+]_T V_{SA} + M_A V_A)/V_S,$$

where M_A is the molarity of the acid titrant added to the seawater sample, $[H^+]_T$ is the total excess hydrogen ion concentration in the seawater, and V_S, V_A and V_{SA} are the initial seawater volume, the added acid titrant volume, and the combined seawater plus acid titrant volume, respectively. $[H^+]_T$ is calculated from the measured absorbances based on the following equation (Yao and Byrne, 1998):

$$pH_T = -\log[H^+]_T = 4.2699 + 0.002578(35 - S) + \log((R - 0.00131)/(2.3148 - 0.1299R)) - \log(1 - 0.001005S),$$

where S is the sample salinity, and R is the absorbance ratio calculated as:

$$R = (A_{616} - A_{730})/(A_{444} - A_{730}),$$

where A_i is the absorbance at wavelength i nm.
Values of TA were corrected and reported based on certified reference material provided by Prof. Dickson, Scripps Institution of Oceanography, Univ. of California (batch 209, 2210.40 ± 0.16 μmol kg^{-1}).

(5) Observation log
Seawater samples for TA were collected at 41 stations.

(6) Preliminary results
The repeatability of this system was provisionally 1.3 μmol kg^{-1} (n = 52), which was calculated from replicate samples after excluding outliers.

(7) Date archives
These data obtained in this cruise will be submitted to the Data Management Group (DMG) of JAMSTEC, and will be opened to the public via "Data Research System for Whole Cruise Information in JAMSTEC (DARWIN)" in JAMSTEC web site.
<https://www.godac.jamstec.go.jp/darwin/en/>

3.3.5. Chlorophyll a and phytoplankton community structure
3.3.5.1. Chlorophyll a

(1) Personnel

Yuri Fukai	JAMSTEC	-Principal Investigator
Amane Fujiwara	JAMSTEC	
Misato Kuwahara	MWJ	-Operation Leader
Mariko Sano	MWJ	
Yuko Miyoshi	MWJ	
Takuya Izutsu	MWJ	

(2) Objective
Phytoplankton species are generally characterized by the cell size, and chlorophyll *a* concentration is often used to estimate their biomass. The objective of this study is to investigate the vertical and horizontal distributions of phytoplankton biomass and cell size in the Arctic Ocean based on chlorophyll *a* concentration in seawater, using the size-fractionated filtration method.

(3) Parameters
Total chlorophyll *a* concentration
Size-fractionated chlorophyll *a* concentration

(4) Instruments and methods
We collected samples for total chlorophyll *a* (chl-*a*) concentration from 6 to 9 depths and size-fractionated chl-*a* from 5 to 6 depths between the surface and 100 m depth including a chl-*a* maximum layer. The chl-*a* maximum layer was determined by a fluorometer (Seapoint Sensors, Inc.) attached to the CTD system during the downcast. Replicate water samples were taken at chl-*a* maximum depth from the

sample bottle in order to assess the precision of chl-*a* measurements.
Seawater samples for total chl-*a* were vacuum-filtrated (< 0.02 MPa) through the ADVANTEC GF-75 filter (25 mm in diameter). Seawater samples for size-fractionated chl-*a* were passed through 20 μm pore-size nylon filter (47 mm in diameter), and 2 μm pore-size polyester membrane filter (47 mm in diameter), and ADVANTEC GF-75 filter (25 mm in diameter) under gentle vacuum (< 0.02 MPa).
Each filter sample was immediately soaked in 7 ml of N,N-dimethylformamide (DMF, Wako Pure Chemical Industries Ltd.) in a polypropylene tube (Suzuki and Ishimaru, 1990). The tubes were stored at -20°C under the dark condition to extract chl-*a* at least for 24 hours.
Chl-*a* concentrations were measured by a fluorometer (10-AU, TURNER DESIGNS) following to the method of Welschmeyer (1994). The 10-AU fluorometer was calibrated against a pure chl-*a* (Sigma-Aldrich Co., LLC) prior to the analysis.

(5) Preliminary results
At each station, water samples were taken in replicate for water of chlorophyll *a* maximum layer. Results of replicate samples were shown in Table 3.3.5.1-1.

Table 3.3.5.1-1. Results of the replicate sample measurements.

	All samples	Samples over 1.00 μg L^{-1}	Samples under 1.00 μg L^{-1}
Number of replicate sample pairs	34	10	24
Standard deviation (μg L^{-1})	0.10	0.18	0.02

Table 3.3.5.1-2. Number of samples and casts.

	Number of samples	Number of casts
Total chlorophyll *a*	288	34
size-fractionated chlorophyll *a*	447	26

(6) Data archives
These data obtained in this cruise will be submitted to the Data Management Group of JAMSTEC, and will be opened to the public via "Data Research System for Whole Cruise Information in JAMSTEC (DARWIN)" in JAMSTEC web site.
<http://www.godac.jamstec.go.jp/darwin/e>

(7) Reference
Suzuki, R., & Ishimaru T. (1990). An improved method for the determination of phytoplankton chlorophyll using N, N-dimethylformamide. *J. Oceanogr. Soc. Japan*, 46, 190-194.
Welschmeyer, N. A. (1994). Fluorometric analysis of chlorophyll *a* in the presence of chlorophyll *b* and pheopigments. *Limnol. Oceanogr.* 39(8), 1985-1992.

3.3.5.2. Phytoplankton community structure
(1) Personnel
Amane Fujiwara (JAMSTEC) - Principal Investigator
Yuri Fukai (JAMSTEC)

(2) Objectives
Phytoplankton contain various pigments, such as chlorophylls, photosynthetic carotenoids, and photoprotective carotenoids. Since pigment composition varies among phytoplankton groups (e.g., diatoms, dinoflagellates, and cyanobacteria), these pigments are widely used to characterize phytoplankton community structure. Thus, we aimed to clarify the spatial distribution of the phytoplankton community structure in the Arctic Ocean by examining the horizontal and vertical variations in phytoplankton pigment concentrations.
In particular, we sought to assess the potential role of highly turbid water in transporting diatoms from the continental shelf to the slope region in the Pacific Arctic. Water samples from the turbid layer were collected, and incubation experiments were conducted to investigate the characteristics of the phytoplankton community and their photosynthetic potential.

(3) Parameters
Phytoplankton pigments
Size-fractionated chlorophyll a
Suspended particle matter
Phytoplankton DNA
Diatom cell concentration

(4) Instruments and methods
Seawater samples were collected using Niskin-X bottles mounted on the CTD/R from four to six depth layers. Seawater (2.45 L) for phytoplankton pigment analysis was filtered onto glass fiber filters (GF-75, φ47 mm, Advantec) and stored in liquid nitrogen. Pigment concentrations will be later analyzed on land using high-performance liquid chromatography (HPLC; Agilent Technologies 1300 series) following the method of Van Heukelem and Thomas (2001).
Samples for size-fractionated chlorophyll a, suspended particulate matter, phytoplankton DNA, and diatom cell concentrations were obtained only from the highly turbid water layer, except at some stations where samples were taken from the SCM layer, as identified from the beam transmission and fluorescence profiles of the CTD downcast. Seawater samples for size-fractionated chlorophyll a were sequentially filtered through a 20 μm nylon mesh (47 mm in diameter) and an Advantec GF-75 filter (25 mm in diameter). The concentration of chlorophyll a was measured using a fluorometer (10-AU, TURNER DESIGNS) as described in section 3.3.5.1. Suspended particulate matter was collected using pre-combusted glass fiber filters (GF-75, φ25 mm, Advantec) that had been pre-weighed. To collect phytoplankton for DNA analysis, 1.08 L of seawater was filtered onto either a PTFE membrane filter (pore size 0.2 μm; Merck) or a PES membrane filter (pore size 0.22 μm; Merck). Phytoplankton in the samples will be later identified on land using DNA metabarcoding. Microscopy samples (100 mL seawater) were fixed with 20% formalin at a final concentration of approximately 2%. The fixed samples were used to examine diatom communities under a light microscope. The seeding potential of phytoplankton in the highly turbid water was examined through a short-term incubation experiment. Seawater from the turbid layer was incubated under light conditions (approximately 200 μmol photons m^{-2} s^{-1}) at 2.5 °C for five days. After incubation, phytoplankton pigments and DNA were collected by filtering 500 mL of the incubated seawater. The analyses will be conducted later on land. Furthermore, using 250 mL of the incubated seawater, size-fractionated chlorophyll a was measured as described above. Additionally, microscopy samples (100 mL) were fixed as described above, and diatom images were obtained using a PlanktoScope (FairScope). For imaging

analysis, seawater (2.00–2.45 L) was concentrated to a final volume of 10–15 mL. From each concentrated sample (1.07 mL), 500 images were acquired.

(5) Station list and sampling location

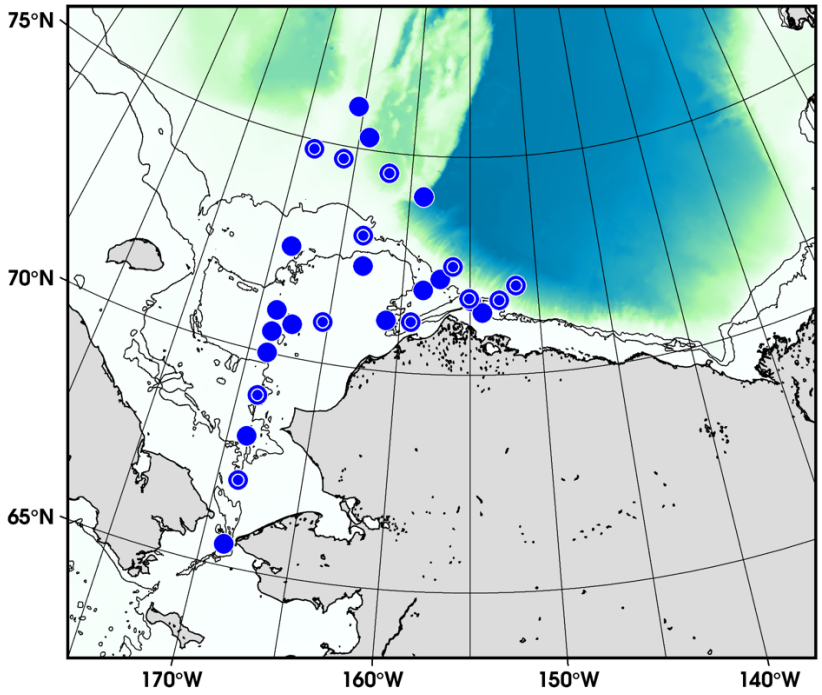

Figure 3.3.5-1. Location where phytoplankton samples were collected. Circles indicate sampling points for HPLC analysis. Double circles indicate points where samples were additionally collected from the turbid layer.

(6) Data archives

These data obtained in this cruise will be submitted to the Data Management Group of JAMSTEC, and will be opened to the public via "Data Research System for Whole Cruise Information in JAMSTEC (DARWIN)" in JAMSTEC web site.
<https://www.godac.jamstec.go.jp/darwin/en/>

(7) Reference cited

Van Heukelem, L, Thomas C. S. 2001. Computer-assisted high-performance liquid chromatography method development with applications to the isolation and analysis of phytoplankton pigments. *J Chromatogr A*, 910, 31–49.

3.3.6. $\delta^{18}O$

(1) Personnel

Daiki Nomura (Hokkaido University) – Principal Investigator
Mariko Hatta (JAMSTEC)
Ryota Akino (Hokkaido University)
Ikkan Kamiyama (Tokyo University of Marine Science and Technology)

(2) Objectives

Meltwater and river water flow into the Arctic Ocean, influencing its physical and

biogeochemical environment in ways that vary depending on the origin of the freshwater. To calculate the fraction of seawater, sea ice meltwater, and meteoric water, we have collected water, snow, ice samples to analyze the oxygen isotopic ratio ($\delta^{18}O$).

(3) Parameters
Oxygen isotopic ratio ($\delta^{18}O$)

(4) Instruments and methods
Water samples were collected in 15-mL glass vials and stored at +4˚C in the dark until analysis.

(5) Station list

Station	Collection Date (UTC)				Latitude			Longitude		
	YYYY	MM	DD	hh:mm:ss	Deg.	Min.	N/S	Deg.	Min.	E/W
St.1	2025	09	04	03:08:00	65	29.99	N	168	44.99	W
St.4	2025	09	04	23:18:00	67	0.03	N	168	45.04	W
St.7	2025	09	05	15:36:00	68	29.98	N	168	45.04	W
St.10	2025	09	06	08:05:00	69	59.99	N	168	44.98	W
St.13	2025	09	06	19:44:00	70	45.17	N	167	28.81	W
St.15	2025	09	08	22:13:00	71	41.74	N	154	55.43	W
St.16	2025	09	10	17:01:00	72	1.79	N	151	34.75	W
St.19	2025	09	11	18:10:00	71	55.11	N	158	27.73	W
St.21	2025	09	12	02:02:00	72	29.05	N	156	18.20	W
St.22	2025	09	12	16:16:00	71	45.26	N	155	3.92	W
St.24	2025	09	12	22:31:00	71	29.80	N	157	40.14	W
St.28	2025	09	13	09:16:00	71	10.04	N	160	59.85	W
St.29	2025	09	13	18:42:00	72	20.60	N	163	7.63	W
St.30	2025	09	13	23:57:00	73	22.80	N	163	26.02	W
St.31	2025	09	16	16:10:00	74	47.51	N	168	43.57	W
St.32	2025	09	16	22:27:00	74	42.46	N	166	2.68	W
St.33	2025	09	17	18:15:00	75	56.77	N	165	32.17	W
St.34	2025	09	18	00:30:00	75	16.96	N	164	6.44	W
St.35	2025	09	20	21:36:00	74	31.86	N	161	56.15	W
St.36	2025	09	21	19:08:00	74	3.50	N	158	51.79	W
St.37	2025	09	22	14:44:00	72	30.00	N	168	44.92	W
ICE1	2025	09	11	16:45:00	71	54.9	N	158	28.44	W
ICE2	2025	09	17	16:34:00	75	56.7	N	165	43.8	W
ICE3	2025	09	21	16:55:00	74	3.36	N	158	48.9	W
Snow	2025	09	14	16:30:00	72	58.68	N	163	22.98	W

(6) Data archives
Data obtained during this cruise will be submitted to the Data Management Group at JAMSTEC, and made publicly available through the “Data Research System for Whole Cruise Information in JAMSTEC (DARWIN)” on the JAMSTEC website. <http://www.godac.jamstec.go.jp/darwin/e>

3.3.7. CDOM/FDOM

(1) Personnel
Daiki Nomura (Hokkaido University) – Principal Investigator
Ryota Akino (Hokkaido University)
Amane Fujiwara (JAMSTEC)

(2) Objectives
The Arctic major rivers drain large volumes of freshwater, contributing to the freshening of the ocean surface and supplying terrestrial materials that influence hydrographic circulation and biogeochemical cycles. Additionally, river discharge has increased over the past decades. Concentrations of CDOM (Colored Dissolved Organic Matter) and FDOM (Fluorescent Dissolved Organic Matter) can serve as indicators of mixing of the water masses, as riverine waters are a primary source of high CDOM/FDOM concentrations. To understand the spread of riverine water and its impact on the oceanic environment, we collected CDOM/FDOM samples for water, snow, and ice.

(3) Parameters
Colored Dissolved Organic Matter (CDOM)
Fluorescent Dissolved Organic Matter (FDOM)

(4) Instruments and methods
Water samples were filtered through 0.2 μm PTFE Membrane filters (Merck Millipore Corporation, 47 mm) and collected into 40-mL glass vials that had been acid-washed and combusted (450°C, 4 h) before samplings. The filtered water samples were stored at +4˚C in the dark until analysis on land. We will measure the absorption coefficient of CDOM (aCDOM) using a long-path spectrophotometer (Ultrapath, World Precision Instruments, Inc.) and FDOM using a fluorometer (FluoroMax-4, HORIBA Instruments Inc.).

(5) Station list

Station	Collection Date (UTC)				Latitude			Longitude		
	YYYY	MM	DD	hh:mm:ss	Deg.	Min.	N/S	Deg.	Min.	E/W
St.1	2025	09	04	03:08:00	65	29.99	N	168	44.99	W
St.4	2025	09	04	23:18:00	67	0.03	N	168	45.04	W
St.7	2025	09	05	15:36:00	68	29.98	N	168	45.04	W
St.10	2025	09	06	08:05:00	69	59.99	N	168	44.98	W
St.13	2025	09	06	19:44:00	70	45.17	N	167	28.81	W
St.15	2025	09	08	22:13:00	71	41.74	N	154	55.43	W
St.16	2025	09	10	17:01:00	72	1.79	N	151	34.75	W
St.19	2025	09	11	18:10:00	71	55.11	N	158	27.73	W
St.21	2025	09	12	02:02:00	72	29.05	N	156	18.20	W
St.29	2025	09	13	18:42:00	72	20.60	N	163	7.63	W
St.31	2025	09	16	16:10:00	74	47.51	N	168	43.57	W
St.33	2025	09	17	18:15:00	75	56.77	N	165	32.17	W
St.35	2025	09	20	21:36:00	74	31.86	N	161	56.15	W
St.36	2025	09	21	19:08:00	74	3.50	N	158	51.79	W
St.37	2025	09	22	14:44:00	72	29.99	N	168	44.92	W
ICE1	2025	09	11	16:45:00	71	54.9	N	158	28.44	W
ICE2	2025	09	17	16:34:00	75	56.7	N	165	43.8	W
ICE3	2025	09	21	16:55:00	74	3.36	N	158	48.9	W

(6) Data archives
Data obtained during this cruise will be submitted to the Data Management Group at JAMSTEC, and made publicly available through the "Data Research System for Whole Cruise Information in JAMSTEC (DARWIN)" on the JAMSTEC website. <https://www.godac.jamstec.go.jp/darwin/en/>

3.3.8. Methane

(1) Personnel
Daiki Nomura (Hokkaido University) – Principal investigator
Ryota Akino (Hokkaido University)

(2) Objectives
In order to understand the greenhouse such as methane (CH_4) in the Arctic Ocean and their exchange process with atmosphere, we have collected samples for water, snow, and ice.

(3) Parameters
Methane (CH_4)

(4) Instruments and methods
For each sample, an aliquot of 100-mL seawater was transferred to an amber vial (120 mL). The vial was filled smoothly from the bottom with seawater using a drawing tube that extended from the Niskin or underway drain to the bottom of the vial. The seawater was allowed to overflow by an amount of approximately one and a half times the vial volume. After sampling, 0.1-mL saturated mercuric chloride was added to poison the sample. Then, the vial was crimp-sealed with a butyl-rubber stopper and aluminum cap. The samples were stored at +4°C in the dark onboard the R/V Mirai, and transported chilled to laboratories on land for analysis. The samples will be measured using a CF-IRMS analytical system in Nagoya University, Japan.

(5) Station list

Station	Collection Date (UTC)				Latitude			Longitude		
	YYYY	MM	DD	hh:mm:ss	Deg.	Min.	N/S	Deg.	Min.	E/W
St.1	2025	09	04	03:08:00	65	29.99	N	168	44.99	W
St.7	2025	09	05	15:36:00	68	29.98	N	168	45.04	W
St.13	2025	09	06	19:44:00	70	45.17	N	167	28.81	W
St.15	2025	09	08	22:13:00	71	41.74	N	154	55.43	W
St.16	2025	09	10	19:29:00	72	1.84	N	151	34.69	W
St.19	2025	09	11	18:10:00	71	55.11	N	158	27.73	W
St.21	2025	09	12	02:02:00	72	29.05	N	156	18.20	W
St.31	2025	09	16	16:10:00	74	47.51	N	168	43.57	W
St.33	2025	09	17	18:15:00	75	56.77	N	165	32.17	W
St.35	2025	09	21	00:46:00	74	31.86	N	161	56.92	W
St.36	2025	09	21	19:08:00	74	3.50	N	158	51.79	W
ICE1	2025	09	11	16:45:00	71	54.9	N	158	28.44	W
ICE2	2025	09	17	16:34:00	75	56.7	N	165	43.8	W
ICE3	2025	09	21	16:55:00	74	3.36	N	158	48.9	W

(6) Data archives

Data obtained during this cruise will be submitted to the Data Management Group at JAMSTEC, and made publicly available through the "Data Research System for Whole Cruise Information in JAMSTEC (DARWIN)" on the JAMSTEC website. <https://www.godac.jamstec.go.jp/darwin/en/>

3.3.9 Dissolved Organic Nitrogen

(1) Personnel

Ikkan KAMIYAMA (Tokyo University of Marine Science and Technology)

(2) Objectives

Dissolved Organic Matter (DOM) is produced and consumed by the biological activities. In particular, Dissolved Organic Nitrogen (DON) may play an important role as a nitrogen source in the Pacific Arctic Ocean, where nitrogen is a limiting factor for primary production. DON dynamics in this area are thought to be influenced by supply from riverine water, biological metabolism in the water column, and release from seafloor sediments. Therefore, we collected water samples from surface layer, Subsurface Chlorophyll Maximum (SCM) layer and the bottom layer (or 75 dbar, as a lower euphotic zone). These samples will contribute to understanding of DON distributions in Pacific Arctic Ocean.

(3) Parameters

Dissolved Organic Nitrogen (DON)

(4) Instruments and methods

a. Sampling

Seawater samples were collected by 12 L Niskin bottles mounted on the CTD System and a bucket at 20 stations. Seawater samples were filtered through a 0.2 μm polyethersulfone (PES) membrane capsule filter (CCS-02D-D1H, ADVANTEC) or a 0.2 μm glass fiber filter (GF-75 Φ25mm, ADVANTEC) and collected in two 10 mL polyacrylate vials after three times rinse. Samples are preserved in a freezer (-17℃)

and going to be analyzed in the laboratory.

b. Instruments and methods
The DON concentration is calculated by subtracting the Dissolved Inorganic Nitrogen (Nitrate + Nitrite + Ammonium) concentration from the Total Dissolved Nitrogen (TDN) concentration. The TDN concentration is measured by a persulfate oxidation method (Yasui-Tamura et al., 2020) with a gas-segmented continuous flow system (AutoAnalyzer QuAAtro TN-TP, BL TEC K.K.).

(5) Station list

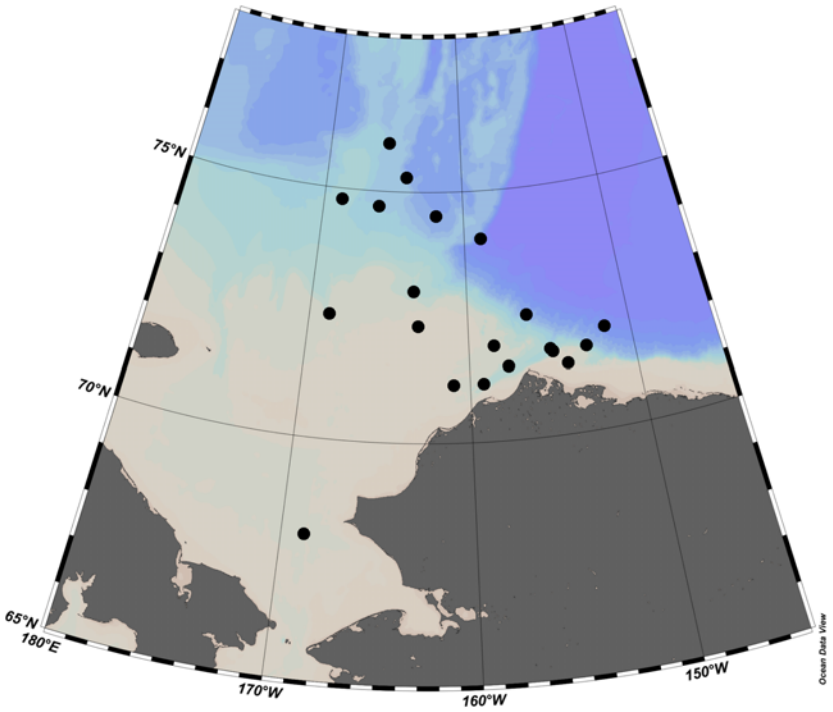

Figure 3.3.9 Sampling location

Table 3.3.9 Sample list

Station	Date (UTC)	Latitude (°N)	Longitude (°E)	Bottom depth (m)	Sampling Depth (dBar)
6	09/05/2025	68.0325	-168.833	59	SCM
15	09/08/2025	71.6957	-154.9238	111	44, 50
16	09/10/2025	72.0299	-151.5792	2426	5, SCM, B-5
17	09/10/2025	71.7121	-152.8624	229	0
18	09/11/2025	71.4282	-154.1107	42	0
19	09/11/2025	71.9185	-158.4621	57	5, SCM, B-5
21	09/12/2025	72.4841	-156.3033	1303	5, SCM, B-5
22	09/12/2025	71.7543	-155.0653	274	5, SCM, B-5
24	09/12/2025	71.4967	-157.669	83	5, SCM, B-5
27	09/13/2025	71.1734	-159.2194	95	5, SCM, B-5
28	09/13/2025	71.1673	-160.9975	48	5, SCM, B-5
29	09/13/2025	72.3434	-163.1272	41	5, SCM, B-5
30	09/13/2025	73.038	-163.4337	99	5, SCM, B-5
31	09/16/2025	74.7919	-168.7261	196	5, SCM, B-5
32	09/16/2025	74.7077	-166.0446	422	5, SCM, B-5
33	09/17/2025	75.9462	-165.5362	445	5, SCM, 75
34	09/18/2025	75.2827	-164.1073	1419	5, SCM, 75
35	09/21/2025	74.531	-161.9487	1686	5, SCM, 75
36	09/21/2025	74.0583	-158.8632	3454	5, SCM, 75
37	09/22/2025	72.4999	-168.7486	58	5, SCM, B-5

(6) Data archives

These data obtained in this cruise will be submitted to the Data Management Group of JAMSTEC, and will be opened to the public via "Data Research System for Whole Cruise Information in JAMSTEC (DARWIN)" in JAMSTEC web site.

(7) References

Saori Yasui-Tamura, Fuminori Hashihama, Hiroshi Ogawa, Takashi Nishimura, Jota Kanda, Automated simultaneous determination of total dissolved nitrogen and phosphorus in seawater by persulfate oxidation method, Talanta Open, Volume 2, 2020, 100016, ISSN 2666-8319, https://doi.org/10.1016/j.talo.2020.100016.

3.3.10. I-129, U-236, and H-3

(1) Personnel

Yuichiro Kumamoto (Principal Investigator)
Japan Agency for Marine-Earth Science and Technology (not on board)

(2) Objectives

In order to investigate the water circulation and ventilation process in the Bering Sea and Arctic Ocean, seawater samples were collected for measurements of iodine-129 (I-

129), uranium-236 (U-236), and tritium (H-3).

(3) Parameters
I-129, U-236, and H-3

(4) Instruments and methods
Seawater samples were collected from continuous pumped-up water from about 4-m depth at 15 stations. We also collected seawater samples vertically at four stations (Stns. 16, 22, 35, and 37) from the sea surface to near the bottom layer. The seawater samples were collected into a 1-L plastic bottle for I-129/H-3 and a 5-L plastic container for U-236 after a two-time rinsing. The total numbers of the seawater samples for I-129, U-236, and H-3 were 26, 26, and 15, respectively. I-129 in the seawater sample is extracted using solvent extraction with carrier iodine added. The sample is precipitated as silver iodide and I-129/I-127 is measured using accelerator mass spectrometry at the MALT (Micro Analysis Laboratory, Tandem accelerator), The University of Tokyo. 5mL aliquot of the sample is measured for I-127 by ICP-MS. U-236 in the seawater sample is co-precipitated with Fe hydroxide and purified by UTEVA® resin. The purified sample is co-precipitated as uranium oxide with 1.5 mg Fe hydroxide and U-236/U-238 is also measured using accelerator mass spectrometry at MALT. 5mL aliquot of the sample is measured for U-238 by ICP-MS. H-3 in the sample will be distilled, and enriched by an electric-enrich system, then measured by liquid scintillation counter.

(5) Station list

Table 3.3.10.-1: Sampling stations for I-129

No.	Stn		Date (UTC)	Time (UTC)	Latitude	Longitude	Sampling depth
1	16	end	2025/9/10	19:29	72-01.84N	151-34.69W	50, 99, 494, 988, 1480, 1969, 2397
2	22	end	2025/9/12	16:16	71-45.26N	155-03.92W	50, 85, 248
3	35	end	2025/9/21	00:46	74-31.86N	161-56.92W	50, 75, 494, 987, 1480, 1675
4	37	end	2025/9/22	14:44	72-29.99N	168-44.92W	20, 40, 53
5	P1	start	2025/9/04	02:23	65-27.29N	168-42.95W	4
		end	2025/9/04	02:28	65-28.05N	168-43.46W	
6	P2	start	2025/9/06	22:20	70-51.95N	166-10.26W	4
		end	2025/9/06	22:26	70-52.29N	166-06.43W	
7	P3 (16)	start	2025/9/10	19:24	72-01.84N	151-34.68W	4
		end	2025/9/10	19:29	72-01.84N	151-34.69W	
8	P4 (22)	start	2025/9/12	15:16	71-45.87N	155-06.71W	4
		end	2025/9/12	15:22	71-45.63N	155-05.82W	
9	P5 (35)	start	2025/9/21	00:26	74-31.87N	161-56.94W	4
		end	2025/9/21	00:34	74-31.89N	161-56.94W	
10	P6 (37)	start	2025/9/22	14:22	72-31.44N	168-43.14W	4
		end	2025/9/22	14:27	72-30.52N	168-43.88W	
11	P7	start	2025/9/23	16:23	67-30.00N	168-30.00W	4
		end	2025/9/23	16:29	67-30.01N	168-30.01W	

Table 3.3.10.-2: Sampling stations for U-236

No.	Stn		Date (UTC)	Time (UTC)	Latitude	Longitude	Sampling depth
1	16	end	2025/9/10	19:29	72-01.84N	151-34.69W	50, 99, 494, 988, 1480, 1969, 2397
2	22	end	2025/9/12	16:16	71-45.26N	155-03.92W	50, 125, 248
3	35	end	2025/9/21	00:46	74-31.86N	161-56.92W	50, 75, 494, 987,

							1480, 1675
4	37	end	2025/9/22	14:44	72-29.99N	168-44.92W	20, 40, 53
5	P1	start	2025/9/04	02:23	65-27.29N	168-42.95W	4
		end	2025/9/04	02:28	65-28.05N	168-43.46W	
6	P2	start	2025/9/06	22:20	70-51.95N	166-10.26W	4
		end	2025/9/06	22:26	70-52.29N	166-06.43W	
7	P3 (16)	start	2025/9/10	19:24	72-01.84N	151-34.68W	4
		end	2025/9/10	19:29	72-01.84N	151-34.69W	
8	P4 (22)	start	2025/9/12	15:16	71-45.87N	155-06.71W	4
		end	2025/9/12	15:22	71-45.63N	155-05.82W	
9	P5 (35)	start	2025/9/21	00:26	74-31.87N	161-56.94W	4
		end	2025/9/21	00:34	74-31.89N	161-56.94W	
10	P6 (37)	start	2025/9/22	14:22	72-31.44N	168-43.14W	4
		end	2025/9/22	14:27	72-30.52N	168-43.88W	
11	P7	start	2025/9/23	16:23	67-30.00N	168-30.00W	4
		end	2025/9/23	16:29	67-30.01N	168-30.01W	

Table 3.3.10.-1: Sampling stations for H-3

No.	Stn		Date (UTC)	Time (UTC)	Latitude	Longitude	Sampling depth
1	P1	start	2025/9/04	02:23	65-27.29N	168-42.95W	4
		end	2025/9/04	02:28	65-28.05N	168-43.46W	
2	P2	start	2025/9/06	22:20	70-51.95N	166-10.26W	4
		end	2025/9/06	22:26	70-52.29N	166-06.43W	
3	P3 (16)	start	2025/9/10	19:24	72-01.84N	151-34.68W	4
		end	2025/9/10	19:29	72-01.84N	151-34.69W	
4	P4 (22)	start	2025/9/12	15:16	71-45.87N	155-06.71W	4
		end	2025/9/12	15:22	71-45.63N	155-05.82W	
5	P5 (35)	start	2025/9/21	00:26	74-31.87N	161-56.94W	4
		end	2025/9/21	00:34	74-31.89N	161-56.94W	
6	P6 (37)	start	2025/9/22	14:22	72-31.44N	168-43.14W	4
		end	2025/9/22	14:27	72-30.52N	168-43.88W	
7	P7	start	2025/9/23	16:23	67-30.00N	168-30.00W	4
		end	2025/9/23	16:29	67-30.01N	168-30.01W	
8	P8	start	2025/9/24	09:38	65-23.15N	169-01.92W	4
		end	2025/9/24	09:45	65-22.07N	169-04.09W	
9	P9	start	2025/9/25	18:11	59-59.13N	177-49.05W	4
		end	2025/9/25	18:17	59-58.13N	177-50.25W	
10	P10	start	2025/9/26	02:23	58-46.70N	179-27.55W	4
		end	2025/9/26	02:28	58-46.05N	179-28.31W	
11	P11	start	2025/9/27	03:46	55-19.32N	174-56.24E	4
		end	2025/9/27	03:51	55-18.71N	174-54.76E	
12	P12	start	2025/9/28	04:27	51-54.38N	169-10.31E	4
		end	2025/9/28	04:33	51-53.37N	169-09.69E	
13	P13	start	2025/9/29	05:46	48-51.93N	165-02.41E	4
		end	2025/9/29	05:53	48-51.25N	165-00.37E	
14	P14	start	2025/9/30	07:35	45-59.05N	158-00.02E	4
		end	2025/9/30	07:43	45-57.81N	157-57.84E	
15	P15	start	2025/10/1	07:48	42-42.90N	152-15.20E	4
		end	2025/10/1	07:54	42-41.97N	152-13.85E	

(6) Data archives

These data obtained in this cruise will be submitted to the Data Management Group of JAMSTEC and will be opened to the public via “Data Research System for Whole Cruise Information in JAMSTEC (DARWIN)” in JAMSTEC web site.

<https://www.godac.jamstec.go.jp/darwin/en/>

3.3.11. Cs-137, Ra-226, and Ra-228

(1) Personnel
Yuichiro Kumamoto (Principal Investigator)
Japan Agency for Marine-Earth Science and Technology (not on board)

(2) Objectives
In order to investigate the water circulation process in the Bering Sea and Arctic Ocean, seawater samples were collected for measurements of radiocesium (Cs-137) and radium isotopes (Ra-226 and Ra-228).

(3) Parameters
Cs-137, Ra-226, and Ra-228

(4) Instruments and methods
Seawater samples were collected from continuous pumped-up water from about 4-m depth at 15 stations. We also collected seawater samples vertically at four stations (Stns. 16, 22, 35, and 37) from the sea surface to near the bottom layer. The seawater sample was collected into a 20-L plastic container after washing two times. The seawater sample was not filtered. The total number of the seawater samples was 34. Cs-137 in the seawater sample is concentrated using ammonium phosphomolybdate (AMP) that forms an insoluble compound with cesium. Cs-137 in the compound is measured using Ge detectors. Ra-free barium carrier and SO_4^{2-} are added to the supernatant seawater for Cs-137 to coprecipitate Ra-226 and Ra-228 with $BaSO_4$. After evaporating to dryness, the $BaSO_4$ fractions are compressed to disc as a mixture of $Fe(OH)_3$ and NaCl for gamma-spectrometry.

(5) Station list

Table 3.3.11.-1: Sampling stations for Cs-137, Ra-226, and Ra-228

No.	Stn		Date (UTC)	Time (UTC)	Latitude	Longitude	Sampling depth
1	16	end	2025/9/10	19:29	72-01.84N	151-34.69W	50, 99, 494, 988, 1480, 1969, 2397
2	22	end	2025/9/12	16:16	71-45.26N	155-03.92W	50, 85, 248
3	35	end	2025/9/21	00:46	74-31.86N	161-56.92W	50, 75, 494, 987, 1480, 1675
4	37	end	2025/9/22	14:44	72-29.99N	168-44.92W	20, 40, 53
5	P1	start	2025/9/04	02:23	65-27.29N	168-42.95W	4
		end	2025/9/04	02:28	65-28.05N	168-43.46W	
6	P2	start	2025/9/06	22:20	70-51.95N	166-10.26W	4
		end	2025/9/06	22:26	70-52.29N	166-06.43W	
7	P3 (16)	start	2025/9/10	19:24	72-01.84N	151-34.68W	4
		end	2025/9/10	19:29	72-01.84N	151-34.69W	
8	P4 (22)	start	2025/9/12	15:16	71-45.87N	155-06.71W	4
		end	2025/9/12	15:22	71-45.63N	155-05.82W	
9	P5 (35)	start	2025/9/21	00:26	74-31.87N	161-56.94W	4
		end	2025/9/21	00:34	74-31.89N	161-56.94W	
10	P6	start	2025/9/22	14:22	72-31.44N	168-43.14W	4

	(37)	end	2025/9/22	14:27	72-30.52N	168-43.88W	
11	P7	start	2025/9/23	16:23	67-30.00N	168-30.00W	4
		end	2025/9/23	16:29	67-30.01N	168-30.01W	
12	P8	start	2025/9/24	09:38	65-23.15N	169-01.92W	4
		end	2025/9/24	09:45	65-22.07N	169-04.09W	
13	P9	start	2025/9/25	18:11	59-59.13N	177-49.05W	4
		end	2025/9/25	18:17	59-58.13N	177-50.25W	
14	P10	start	2025/9/26	02:23	58-46.70N	179-27.55W	4
		end	2025/9/26	02:28	58-46.05N	179-28.31W	
15	P11	start	2025/9/27	03:46	55-19.32N	174-56.24E	4
		end	2025/9/27	03:51	55-18.71N	174-54.76E	
16	P12	start	2025/9/28	04:27	51-54.38N	169-10.31E	4
		end	2025/9/28	04:33	51-53.37N	169-09.69E	
17	P13	start	2025/9/29	05:46	48-51.93N	165-02.41E	4
		end	2025/9/29	05:53	48-51.25N	165-00.37E	
18	P14	start	2025/9/30	07:35	45-59.05N	158-00.02E	4
		end	2025/9/30	07:43	45-57.81N	157-57.84E	
19	P15	start	2025/10/1	07:48	42-42.90N	152-15.20E	4
		end	2025/10/1	07:54	42-41.97N	152-13.85E	

(6) Data archives
These data obtained in this cruise will be submitted to the Data Management Group of JAMSTEC and will be opened to the public via "Data Research System for Whole Cruise Information in JAMSTEC (DARWIN)" in JAMSTEC web site.
<https://www.godac.jamstec.go.jp/darwin/en/>

3.3.12 Nitrogen isotopes

(1) Responsible personnel
Aymeric P. M. Servettaz (JAMSTEC, RIGC)
Akiko Makabe (JAMSTEC, X-STAR)
Chisato Yoshikawa (JAMSTEC, MRU)
Nanako O. Ogawa (JAMSTEC, MRU)

(2) Purpose, background
The Chukchi Sea is a biological hotspot where high primary productivity is depleting nitrous nutrients. The activity of primary producers is thus limited by the amount of biologically available nitrogen, in the forms of nitrate (NO_3^-), nitrite (NO_2^-), ammonium (NH_4^+) or organic nitrogen. The balance of biologically available nitrogen is controlled by influx of nitrate rich Pacific water, efflux to the Arctic Ocean, and exchanges with atmospheric dinitrogen (N_2) (Fig. **3.3.12-1**).

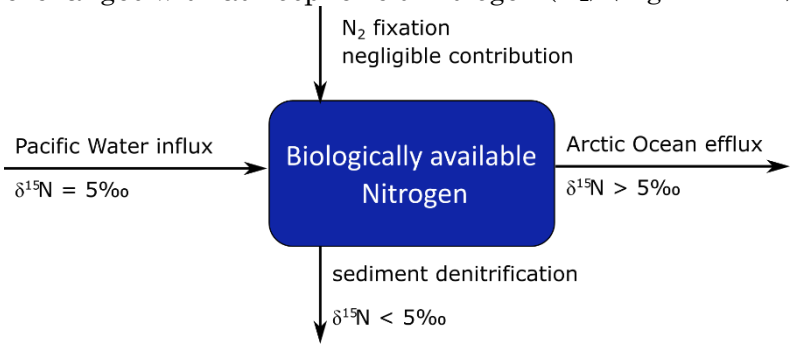

Figure 3.3.12-1. Balance of biologically available nitrogen in the Chukchi Sea, and the isotopic contribution of each flux.

In the Chukchi Sea,

sediments of the shallow shelf strongly interact with the water column. Accumulated organic matter is degraded and oxygen is rapidly consumed in the sediments, causing hypoxia in the first meters. In this oxygen-deplete environment, nitrification of NH_4^+ issued from degradation of organic matter can be coupled with denitrification, a process where NO_3^- is transformed into N_2 (Granger et al., 2011)(Brown et al., 2015). On the other hand, N_2 fixation, a process where atmospheric N_2 is incorporated into organic compounds, has been reported in the Chukchi Sea (Shiozaki et al. 2018), although it only contributes to about 1% of nitrogen assimilation.
Finding the balance of biologically available nitrogen is crucial to understanding the limitations on productivity of the Chukchi Sea. To evaluate the nitrogen loss through coupled nitrification-denitrification, we employ an isotopic approach. Nitrogen involved in denitrification in the sediment is ^{15}N depleted due to the fractionation during nitrification (Granger et al., 2011). As a result, the removal of biologically available nitrogen through this process leads to enrichment in ^{15}N of the remaining nitrogen. Measuring the $\delta^{15}N$ of various elements in the N-cycle will allow us to quantify the loss of nitrogen. For this cruise, samples will be taken for on-land analysis of the isotopic composition of NO_3^-, NO_2^-, NH_4^+, bulk particulate organic matter, and chlorophyll-specific isotopes, representing primary producers. This will also allow us to investigate sources of nitrogen for primary productivity.

(3) Sampled locations
To evaluate the nitrogen isotopes in NO_3^-, NO_2^- and NH_4^+ seawater and particulates sample were taken, mainly on the Chukchi shelf (Fig. N2). Nutrient-deplete surface layers were not sampled, with samples from a depth of 20 m in the water column, to the bottom or a maximum depth of 200 m. For sampling stations where water depth exceeds 100 m, only samples for NO_3^- and NO_2^- were taken, because NH_4^+ concentration is too low in deeper waters. A total of 26 CTD/R stations were sampled, with 98 bottles for NO_3^- and NO_2^- isotope analysis, and 80 bottles for NH_4^+ isotope analysis.
Isotopic signal of particulate matter and chlorophyll will be measured from filtered suspended particles collected with *in situ* filtration in four locations (Fig. 3.3.12-2): north of Bering Strait (St.003), central Chukchi Sea (St.008), Barrow Canyon East (St.015), and Northwind Abyssal Plain (St.035). The target depth was set to surface chlorophyll maximum.

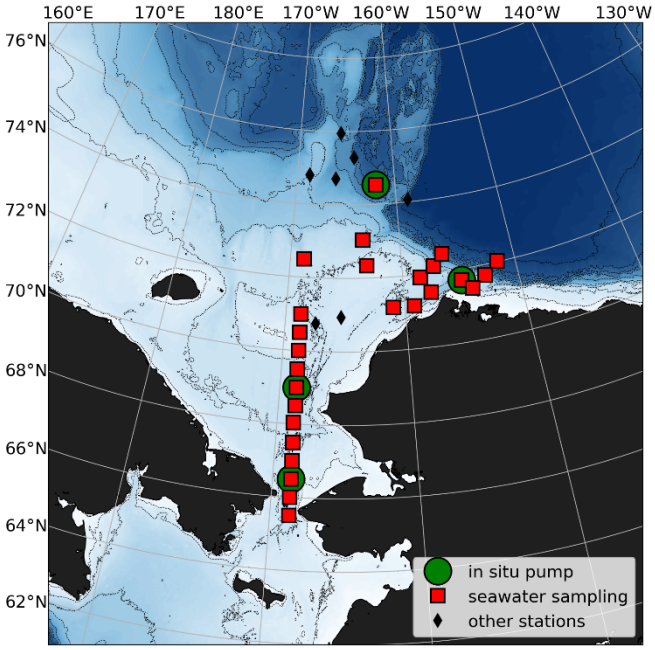

Figure 3.3.12-2. Location of CTD/R stations sampled for nitrogen isotope analysis (red squares), and *in situ* filtration station locations (green circles). Other locations where CTD cast were conducted but not sampled for nitrogen isotopes are also indicated (black diamonds). Color contour indicates bathymetry, and emerged land is in black.

(4) Methods, instruments

Seawater was collected from the Niskin bottle mounted on a CTD-equipped Rosette, and rapidly filtered using single-use 60 mL syringes with attached 0.45 μm pore size polypropylene filters to remove particulate organic matter. The collected water was split into two 25 mL centrifuge tubes for NO_3^- and NO_2^-, as well as three 50 mL i-Boy bottles for NH_4^+ analysis. Collection bottles were rinsed with the filtrate twice before filling. NO_3^- samples (centrifuge tubes) and two NH_4^+ samples (50 mL i-Boy) were frozen at -20°C to stop biological activity without chemical additives. These samples will be transported frozen until isotopic analysis on land. One NH_4^+ sample (50 mL i-Boy) was chemically treated with addition of 0.1 mL HCl 1N, 0.03 mL Ethyl Acetate and 0.03 mL dichloromethane for preservation of NH4 and suppression of biological activity, then refrigerated at 4°C until analysis on land.

In situ filtration was performed using a compact underwater particle sample Plafilt (Offshore Technologies), mounted with pre-combusted glass fiber filters of pore size 0.45 μm (GF-75). At each station sampled, two Plafilt were mounted onto Kevlar wire and lowered to target sampling depth, with filtration start scheduled. Filtration continued for 30-45 minutes, depending on the chlorophyll concentration, aiming at collecting 20-50 μg of chlorophyll. After filtration time was up, the filter was recovered, placed into aluminum foil, inside a gas-tight plastic bag with air chased and frozen at -70°C.

Isotopic analysis will be conducted following the methods described in Isaji et al. (2022). Briefly, samples for isotopic analysis are prepared by culturing a strain of denitrifying bacteria that lack N_2O-reductase activity into the sampled water (Sigman et al., 2001). Nitrate is transformed to N_2O but not assimilated for producing biogenic compounds as the growth medium is saturated with additional ammonium. The produced N_2O is collected, and its nitrogen and oxygen isotopic composition is determined by coupled Gas Chromatography-Isotope Ratio Mass Spectrometry (GC-IRMS). Chemically treated NH_4^+ samples will be analyzed following the method of (Ohno et al., 2024), where NH_4^+ is reacts with an organic

compound to form isopropoxycarbonyl-NH_2, which is then analyzed with GC-IRMS. Filters from *in situ* filtration will be extracted with acetone-water, chlorophyll will be purified using High Performance Liquid Chromatography and prepared for IRMS.

(5) References

Offshore Technologies: Compact Plankton Sampler "Plafilt" https://www.offshore-technologies.com/en/products/compact-plankton-sampler-plafilt/

Brown, Z. W., Casciotti, K. L., Pickart, R. S., Swift, J. H., and Arrigo, K. R.: Aspects of the marine nitrogen cycle of the Chukchi Sea shelf and Canada Basin, *Deep Sea Research Part II: Topical Studies in Oceanography*, **118**, 73–87, https://doi.org/10.1016/j.dsr2.2015.02.009, 2015.

Granger, J., Prokopenko, M. G., Sigman, D. M., Mordy, C. W., Morse, Z. M., Morales, L. V., Sambrotto, R. N., and Plessen, B.: Coupled nitrification-denitrification in sediment of the eastern Bering Sea shelf leads to 15N enrichment of fixed N in shelf waters, *Journal of Geophysical Research: Oceans*, **116**, C11006, https://doi.org/10.1029/2010JC006751, 2011.

Isaji, Y., Yoshikawa, C., Ogawa, N. O., Matsumoto, K., Makabe, A., Toyoda, S., Ishikawa, N. F., Ogawa, H., Saito, H., Honda, M. C., and Ohkouchi, N.: Nitrogen Sources for Phytoplankton in the Eastern Indian Ocean Determined From $\delta^{15}N$ of Chlorophyll a and Divinylchlorophyll a, *Geochem Geophys Geosyst*, **23**, e2021GC010057, https://doi.org/10.1029/2021GC010057, 2022.

Ohno, M., Takizawa, Y., and Chikaraishi, Y.: A simple and rapid method for measuring the stable nitrogen isotopic composition of ammonia in aqueous samples, *Researches in Organic Geochemistry*, **40**, 19–24, https://doi.org/10.20612/rog.40.2_19, 2024.

Sigman, D. M., Casciotti, K. L., Andreani, M., Barford, C., Galanter, M., and Böhlke, J. K.: A Bacterial Method for the Nitrogen Isotopic Analysis of Nitrate in Seawater and Freshwater, *Anal. Chem.*, **73**, 4145–4153, https://doi.org/10.1021/ac010088e, 2001.

Shiozaki, T., Fujiwara, A., Ijichi, M., Harada, N., Nishino, S., Nishi, S., et al. (2018). Diazotroph community structure and the role of nitrogenfixation in the nitrogen cycle in the Chukchi Sea (western Arctic Ocean). *Limnology & Oceanography*, **63**(5), 2191–2205. https://doi.org/10.1002/lno.10933

3.3.13 Aluminium

(1) Responsible personnel

Mariko Hatta　JAMSTEC -PI

(2) Purpose, background

Establish a shipboard aluminum monitoring system using a programmable flow injection platform, identify potential issues and implement troubleshooting protocols, and build a comprehensive dataset of dissolved aluminum concentrations in the Arctic Ocean.

Purpose: The primary objective is to set up a shipboard system for monitoring aluminum concentrations in the Arctic Ocean, an environment known for its

complexity and the challenges it poses for instrumentation. The goal is to create an analytical system that is user-friendly and suitable for shipboard use, eliminating the need for labor-intensive and complicated processes. Importantly, this system is designed to avoid the pre-concentration step (~nM). The project also aims to anticipate potential technical issues and establish troubleshooting procedures to ensure reliable data collection. By using a programmable flow injection system, the analysis of aluminum concentrations in seawater can be streamlined, making the process more efficient and accessible for research in the demanding Arctic environment. This approach responds to the need for a practical, user-friendly method to study aluminum in such a unique and sensitive ecosystem. Last year, a prototype system was deployed; and thus this year, a modified and optimized methodology with enhanced sensitivity has been implemented to test its performance at sea.

Background: Aluminum is an important element in oceanographic studies, serving as a tracer for various ocean processes. Unlike most other ocean regions, aluminum concentrations in the Arctic Ocean are higher and show unusual vertical profiles, the reasons for which remain unclear. The specific objective of this project is to monitor aluminum concentrations in the Arctic Ocean, to better understand their distribution, and to use aluminum as a tool for investigating geochemical cycles in this region. This work builds on the development of a new methodology using programmable flow injection analysis, adapted here as a shipboard analytical platform for determination of aluminum. Over the past two years, sampling equipment-including the Rosette Sampling System-was compared with trace-metal clean bottles deployed directly on a Kevlar cable. Results showed that dissolved aluminum measurements did not exhibit significant contamination from either system. Thus, this year, the focus is on obtaining a broader dataset of aluminum concentrations using the regular rosette sampling system in the Arctic Ocean in order to establish a reliable database, characterize its distribution, and identify potential sources and controlling processes.

(3) Activities (observation, sampling, development)

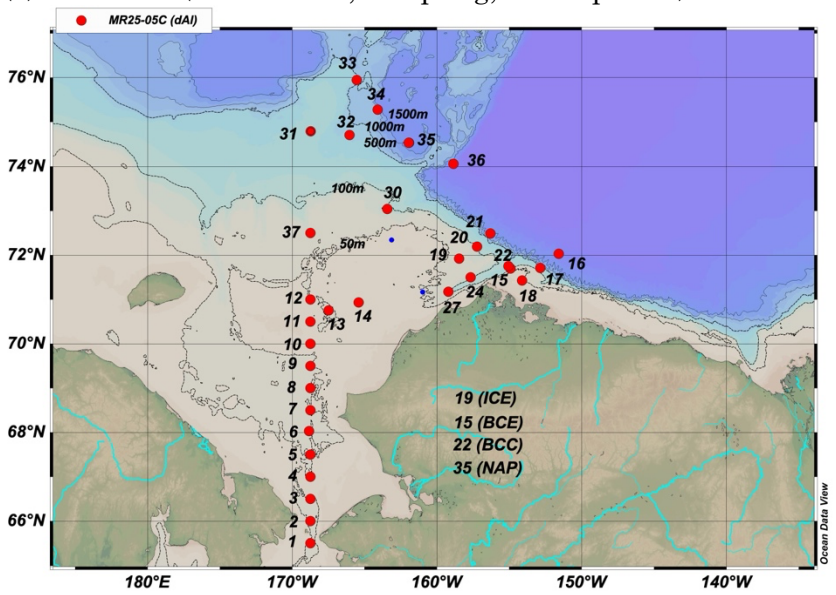

Figure 3.3.13-1. Sampling location during MR25-05C. Blue dots are all of the CTD stations, and red closed circles are the stations to collect dissolved Aluminum samples

Seawater samples were collected from the following stations, shown in the map (Figure 1):
Regular rosette system: Stations 1-14, 15(BCE),16-21, 22 (BCC), 23-27, 30-34, 35 (NAP), 36, 37. Total 33 stations.

The collected seawater samples were filtered using AcroPK200 filter (0.2um), and subjected to acidification using 500 µL of 20% trace metal clean hydrochloric acid (6M HCl) spiked into a 100 mL sample. Subsequently, the determination of dissolved aluminum content was carried out using the newly established protocol, employing the programmable flow injection technique in conjunction with a PMT detector.

(4) Methods, instruments
(4.1) Sampling system
The sampling process was executed with the use of irregular CTD rosette sampling system.

(4.2) Niskin-X bottle
In this cruise, the Niskin-X bottles were meticulously prepared to maintain the integrity of the samples. Here's a step-by-step summary of the preparation and handling process:

Before the cruise commenced, the Niskin-X bottles were coated with Teflon, and all the O-rings were replaced with Viton ones that had been pre-acid washed. No acid made contact with the external surfaces of the bottles, especially the nylon components.
At the start of this cruise, each bottle was cleaned with the following steps:
a. Each bottle was filled with a 5% detergent solution and left for one day.
b. Bottles were rinsed ten times with deionized ultra-high purity water (Milli-Q water) until there were no traces of detergent.
c. Bottles were filled with 0.1M HCl (analytical grade) for a half of days and then emptied through the spigot to rinse.
d. Bottles were rinsed five times with deionized ultra-high purity water (Milli-Q water).

(4.3) Sub-sampling for dissolved Aluminum:
Samples dissolved metal analysis, including Aluminum, were filtered through 0.2 µm Acropak filters.
Dissolved Aluminum samples were directly collected in acid-clean PMP (perfluoropolymer) bottles. Prior to the cruise, these bottles were pre-cleaned with 1M HCl.

The cleaning process for both types of bottles was as follows (if it is new):
Bottles were soaked for one day in an alkaline detergent.
Rinsed ten times with ultra-high purity water (Milli-Q water) until no traces of detergent remained.

Soaked in a 6 M reagent-grade HCl bath for more than one day.
Rinsed five times with ultra-high purity water (Milli-Q water).
Filled with 1M nitric acid (analytical grade) and heated to 80°C for 5 hours in a heated oven. Each bottle was packed with a plastic bag containing Milli-Q water in case of any spills.
Rinsed five times with ultra-high purity water (Milli-Q water) inside an ISO Class-5 laminar flow hood.
Filled the bottles with ultra-high purity water (Milli-Q water) and heated them at 80°C for 5 hours in a heated oven. Each bottle was again packed with a plastic bag containing Milli-Q water as a precaution.
Rinsed five times with ultra-high purity water (Milli-Q water) inside an ISO Class-5 laminar flow hood.
The cleaned bottles were packed in sets of six within double bags until they were ready for use.

These rigorous cleaning and preparation procedures were essential to ensure the integrity of the collected samples and to prevent any contamination during subsequent analysis.

(4.4) Shipboard dissolved Al measurement
(4.4.1) Instrumentation
The instrument, miniSIA-2 (Global FIA, Fox Island, WA, USA), comprises two high precision, synchronously refilling milliGAT pumps, two thermostated holding coils, a 6-port LOV (model COV-MANI-6, constructed from polymethyl methacrylate, Perspex®) furnished with a module for an fluoroecence flow cell (Figure 2). All tubing connections, downstream from the milliGAT pumps including the holding coils (volume 1000 µL), were made with 0.8 mm I.D. polytetrafluoroethylene (PTFE). The holding coils were thermostated at 50C for all aluminium analysis. The tubing between the carrier stream reservoirs and the milliGAT pump was made from 1.6 mm I.D. PTFE tubing to minimize degassing under reduced pressure at higher aspiration flow rates. Photon counter for fluorescence measurement with filter holder mounted for easy access (Global FIA, Fox Island, WA, USA) with a high intensity LED with filter holder mounted encased in 0.8 mm I.D. black tubing. The end of each fiber exposed to the liquid was cemented with epoxy, cut square, and polished. All assay steps were computer-controlled using commercially available software (FloZF, GlobalFIA, Fox island, WA, USA). The outlet of the flow cell was fitted with a 40-psi flow restrictor (GlobalFIA, Fox Island, WA, USA), which, by elevating the pressure within the flow path, efficiently prevented the formation of microbubbles from spontaneous outgassing.

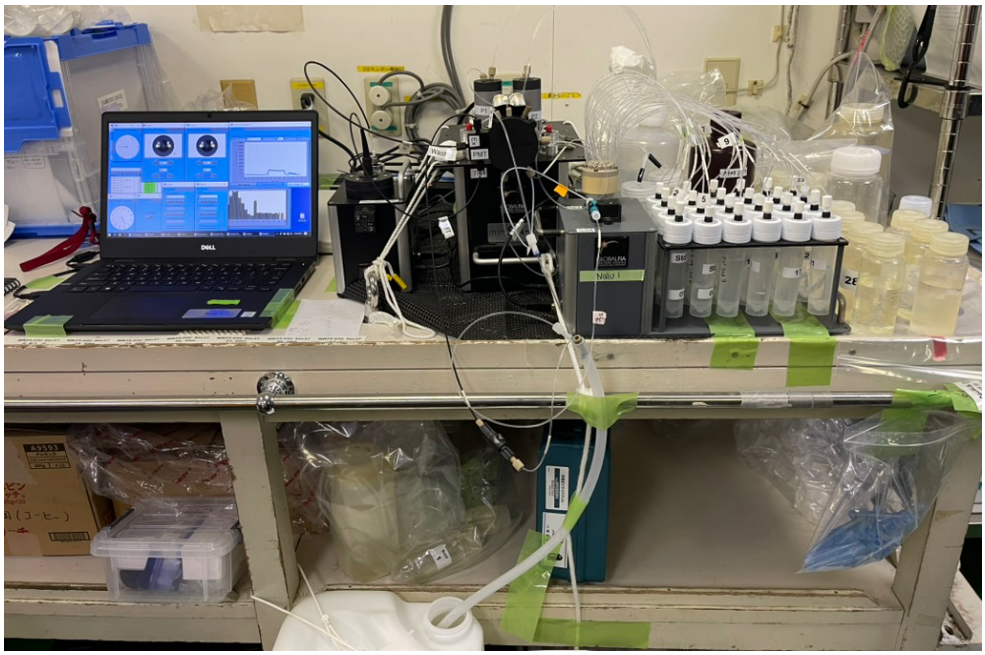

Figure 3.3.13-2. Shipboard analytical system for dissolved Aluminium determination using the programmable flow injection technique.

(4.4.2) Analytical methodology
Methodology (pFI-Al) using Programmable Flow Injection Technique:
Carrier Solution: The carrier solution used in the analysis is MilliQ water, which is known for its high purity and suitability for analytical purposes.
Stock Aluminum Standard Solution: A stock Aluminum standard solution with a concentration of 100.1 mg/L was purchased. This stock solution was then diluted with acidified MilliQ water (pH 1) to create a primary stock solution with a concentration of 3.7 µM.
Working Standards: Working standards with different concentrations were prepared using the primary stock solution and filtered seawater solution or with MilliQ water. The working standards created include: 0 nM (control), 7.41 nM, 14.78 nM, 29.45 nM, 36.79 nM. In order to obtained blank, EDTA solution (stock) was prepared and spiced 500ul in 30ml MilliQ water.
Daily constancy: AcidifedSeawater sample determined routinely across the analytical days.
Reaction Reagent: Dissolve 0.05g of Lumogalion in 30 mL of MilliQ water to create Lumogalion stock solution. Combine 1 mL of the Lumogalion solution with 100 mL of a 2M ammonium acetate buffer solution at a pH of 6.
Brij Solution:The Brij solution was stored in a 40°C oven to maintain a liquid form. To create the 2.5% Brij solution, dissolve 10 mL of Brij solution and scale it up to a total volume of 100 mL with MilliQ water.

(5) Results, Future Plans, Lists (samples, observation equipment, deployment & recovery), Local field map (dive tracks, sampling points, survey lines), etc

Results:
During the cruise, a total of 333 seawater samples were collected and analyzed using

the developed method.
The detection limit of this method was 0.35±0.27 nM, indicating its sensitivity to low concentrations of Aluminum in seawater.
Preliminary vertical profiles of dissolved Aluminum (dAl) were generated, and a subset of these profiles is shown in Figure 3.
The dAl values increased with depth, and a significant dAl difference at the deep waters were observed in the regions, suggesting a potential input into the deep waters.
Subsurface waters exhibited lower dAl values and were characterized as "winter water" (Figure 3.3.13-4).
The section plot showed that strong coastal signal with low salinity labeled with elevated dAl value (Figure 5).

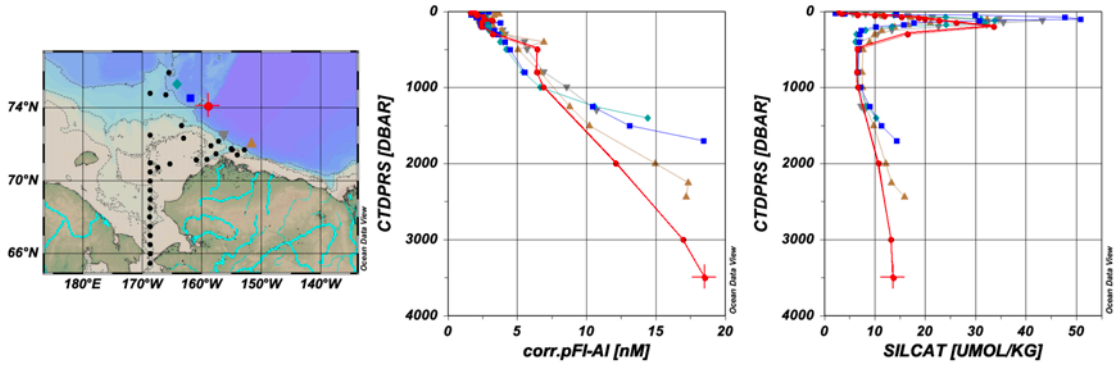

Figure 3.3.13-3. Vertical profiles of dissolved Al and silicate during MR25-05C.

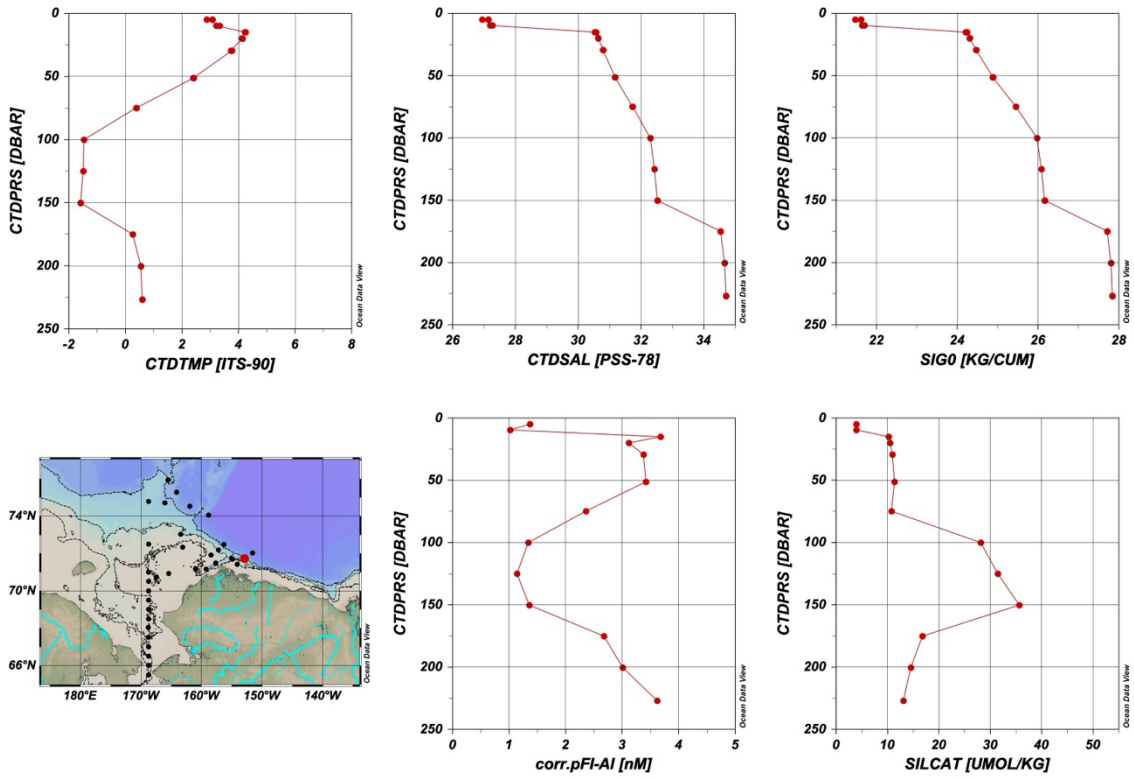

Figure 3.3.13-4. Vertical profiles at Station 17.

3.3.14 Underway surface water monitoring
3.3.14.1 TSG

(1) Personnel
Mariko Hatta (JAMSTEC): Principal Investigator
Masahiro Orui (MWJ)
Aine Yoda (MWJ)
Riho Fujioka (MWJ)

(2) Objective

Our purpose is to obtain temperature, salinity, dissolved oxygen, fluorescence, turbidity and total dissolved gas pressure data continuously in near-sea surface water.

(3) Parameters

Temperature
Salinity
Dissolved oxygen
Fluorescence
Turbidity
Total dissolved gas pressure

(4) Instruments and Methods

The Continuous Sea Surface Water Monitoring System (Marine Works Japan Co. Ltd.) is equipped with five sensors and automatically measures temperature, salinity, dissolved oxygen, fluorescence, turbidity and total dissolved gas pressure in near-sea surface water at one-miniute intervals. This system is installed in the "Sea Surface Monitoring Laboratory" and connected to the shipboard LAN-system. The measured data, along with the time and ship location, were stored on a data management PC. Seawater was continuously pumped into the laboratory from an intake placed approximately 4.5 m below the sea surface and flowed into the system through a vinyl-chloride pipe. The flow rate of the surface seawater was maintained at 10 dm^3 min^{-1}.

a. Instruments
Software

Seamoni Ver.1.2.0.0

Sensors
Specifications of each sensor in this system are listed below.

Temperature and Conductivity sensor

Model:	SBE-45, SEA-BIRD ELECTRONICS, INC.
Serial number:	4552788-0264
Measurement range:	Temperature -5 °C - +35 °C
	Conductivity 0 S m^{-1} - 7 S m^{-1}
Initial accuracy:	Temperature 0.002 °C
	Conductivity 0.0003 S m^{-1}
Typical stability (per month):	Temperature 0.0002 °C
	Conductivity 0.0003 S m^{-1}
Resolution:	Temperature 0.0001 °C
	Conductivity 0.00001 S m^{-1}

Bottom of ship thermometer

Model: SBE 38, SEA-BIRD ELECTRONICS, INC.	
Serial number:	3857820-0540
Measurement range:	-5 °C - +35 °C
Initial accuracy:	±0.001 °C
Typical stability (per 6 month):	0.001 °C
Resolution:	0.00025 °C

Dissolved oxygen sensor

Model:	RINKO II, JFE ADVANTECH CO. LTD.
Serial number:	0035
Measuring range:	0 mg L^{-1} - 20 mg L^{-1}
Resolution:	0.001 mg L^{-1} - 0.004 mg L^{-1} (25 °C)
Accuracy:	Saturation ± 2 % F.S. (non-linear) (1 atm, 25 °C)

Fluorescence & Turbidity sensor

Model:	C3, TURNER DESIGNS
Serial number:	2300707
Measuring range:	Chlorophyll in vivo 0 µg L^{-1} – 500 µg L^{-1}
Minimum Detection Limit:	Chlorophyll in vivo 0.03 µg L^{-1}
Measuring range:	Turbidity 0 NTU - 1500 NTU
Minimum Detection Limit:	Turbidity 0.05 NTU

Total dissolved gas pressure sensor

Model:	Mini TDGP, PRO OCEANUS SYSTEM, INC
Serial number:	45-450-31
Measurement range:	-5 °C - +35 °C
Resolution:	0.002% (full scale)
Accuracy:	0.1% (maximum range)

(5) Observation log

Periods of measurement, maintenance, and problems during this cruise are listed in Table 3.3.14.1.

Table 3.3.14.1 Events list of the Sea surface water monitoring during MR25-05C

System Date [UTC]	System Time [UTC]	Events
2025/09/01	00:37:00	All the measurements started and data was available.
2025/09/02	15:50:00 to 15:53:00	All the measurements stopped. (software maintenance)
2025/09/02	15:56:00	All the measurements restarted, and data was available.
2025/09/02	16:10:00 to 16:14:00	All the measurements stopped. (software maintenance)
2025/09/02	16:16:00	All the measurements restarted, and data was available.
2025/09/04	10:22:00 to 10:24:00, and 10:26:00	All the measurements stopped. (software maintenance)
2025/09/04	10:28:00	All the measurements restarted, and data was available.
2025/09/07	18:40:00 to 18:43:00	All the measurements stopped. (software maintenance)
2025/09/07	18:50:00	All the measurements restarted, and data was available.

2025/09/10	18:33:00 to 18:48:00	All the measurements stopped. (software maintenance)
2025/09/13	02:38:00 to 02:44:00	Filter Cleaning.
2025/09/20	19:44:00 to 20:18:00	Seawater flow rate has decreased.
2025/10/03	00:06:00	All the measurements stopped.

We collected surface water samples from this system once a day to compare sensor data with discreate bottle measurement of dissolved oxygen, salinity and chlorophyll a. The results are shown in fig. 3.3.14-2. All the salinity samples were analyzed by the Model 8400B "AUTOSAL" (Guildline Instruments Ltd., see 3.2.6), dissolve oxygen samples were analyzed by the Winkler method (see 3.3.1), and chlorophyll a was analyzed using the 10-AU manufactured (Turner Designs., see 3.3.5).

(a)

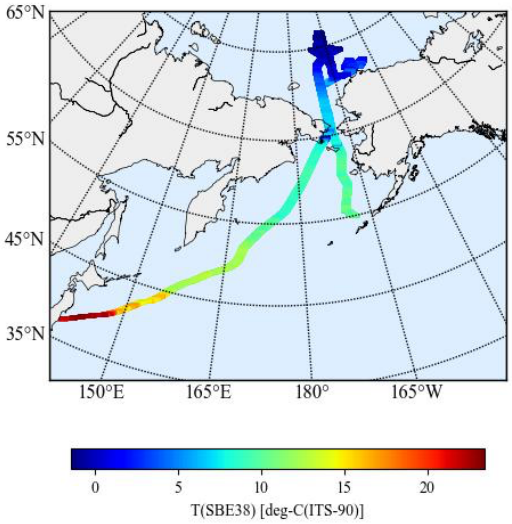

(b)

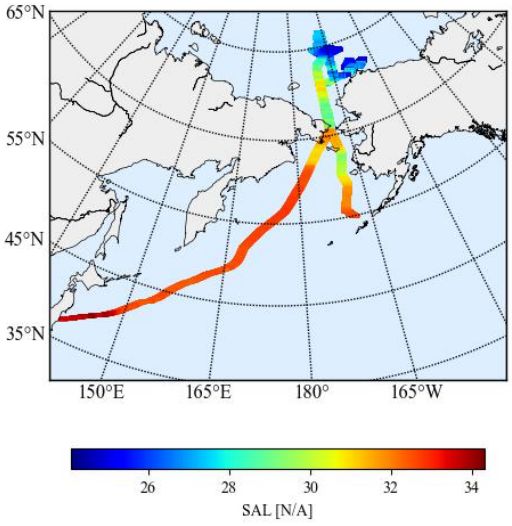

(c)

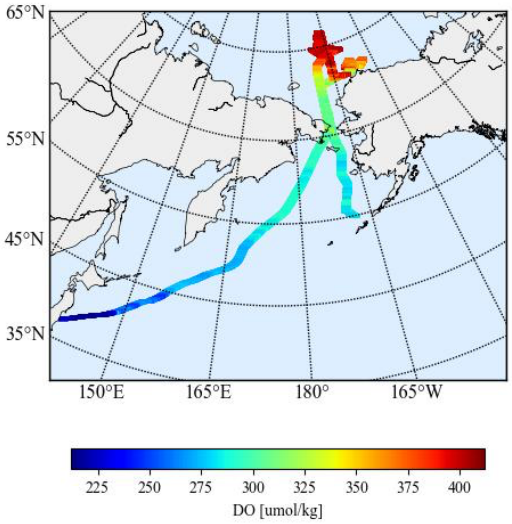

(d)

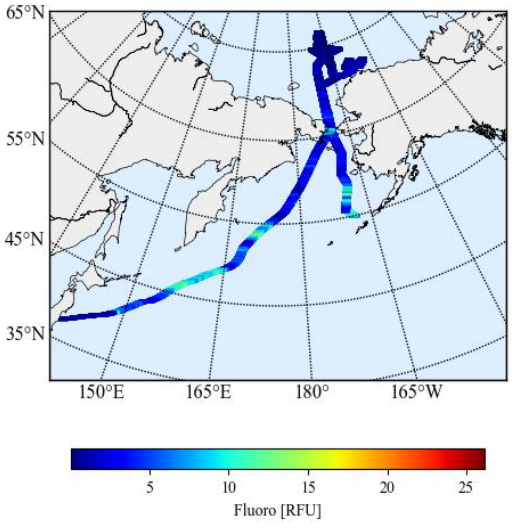

Figure 3.3.14.1-1 Spatial and temporal distribution of (a) temperature, (b) salinity, (c) dissolved oxygen, and (d) fluorescence in MR25-05C cruise.

.

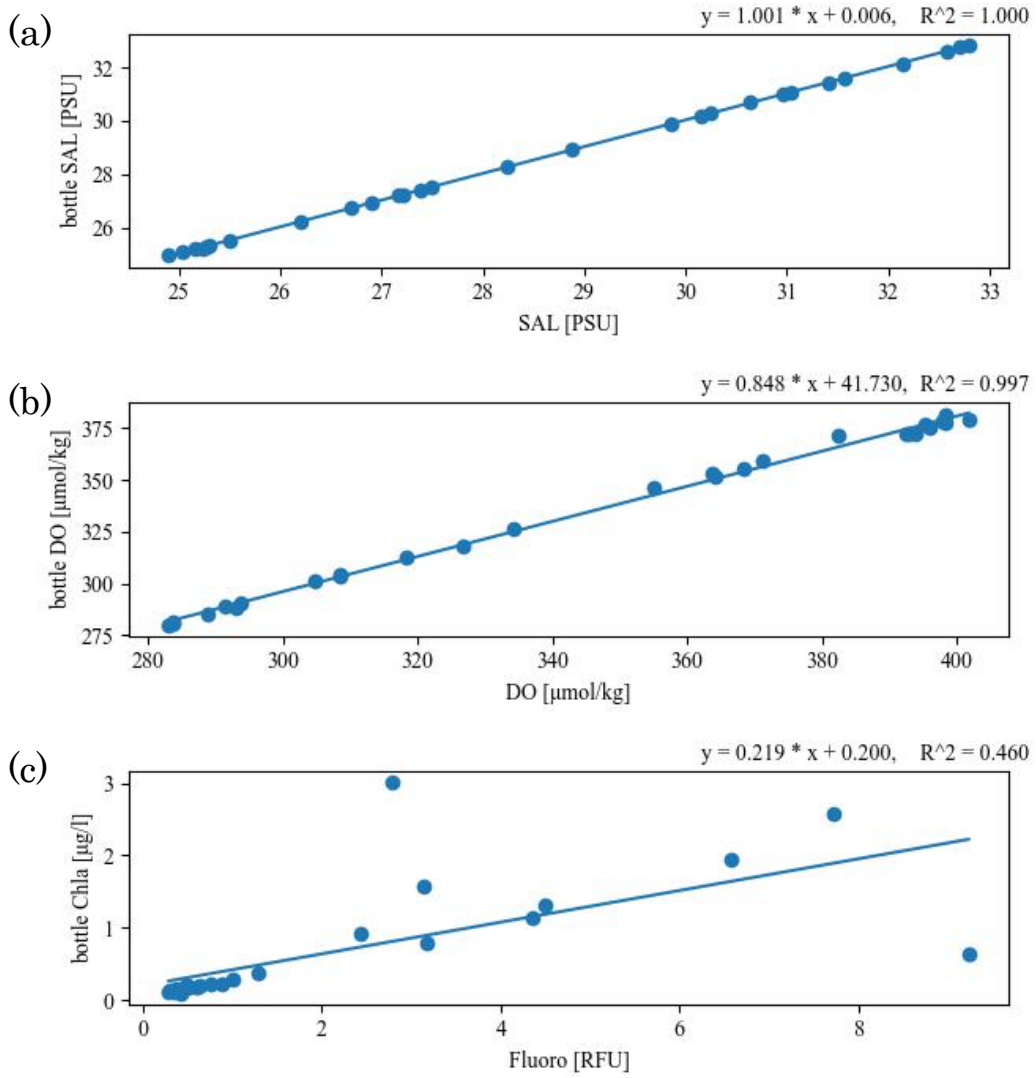

Figure 3.3.14-2 (a) Correlation of between salinity sensor data and bottle measured data, and (b) dissolved oxygen between the sensor and bottle measured data, and (c) fluorescence sensor data and bottle chlorophyll-a concentration.

(7) Data archives

These data obtained in this cruise will be submitted to the Data Management Group of JAMSTEC, and will be opened to the public via "Data Research System for Whole Cruise Information in JAMSTEC (DARWIN)" in JAMSTEC web site.
<https://www.godac.jamstec.go.jp/darwin/en/>

3.3.14.2. Discrete water samplings

(1) Personnel

Amane Fujiwara (JAMSTEC) -PI
Yuri Fukai (JAMSTEC)
Daiki Nomura (Hokkaido University)
Kohei Matsuno (Hokkaido University)
Tatsuya Kawakami (Hokkaido University)

(2) Objective and background

The ocean surface serves as a critical interface for the biogeochemical exchange between the atmosphere and the hydrosphere as well as surface and subsurface layer. In the Arctic region, this interface is further complicated by the significant influx of sea ice melt, glacial meltwater, and terrestrial riverine discharge. These various freshwater sources drastically alter the chemical composition, nutrient availability, and physical stratification of the surface layer, which in turn drive shifts in biological productivity and microbial community structures. The primary objective of this study is to quantify the mixing proportions of distinct water masses—namely seawater, sea ice melt, glacial meltwater, and river water—to evaluate their individual and synergistic impacts on the Arctic ecosystem. By integrating stable oxygen isotope ($\delta^{18}O$) analysis with a comprehensive suite of biogeochemical parameters, we aim to resolve the complex interactions between physical hydrological processes and biological responses. To this end, we conducted high-resolution sampling of nutrients, eDNA, phytoplankton pigments (HPLC), and dissolved organic matter (CDOM/FDOM), synchronized with the characterization of water mass origins. This integrated approach allows for a deeper understanding of how the ongoing "borealization" and freshening of the Arctic Ocean influence the base of the marine food web. For detailed descriptions of sampling protocols and subsequent analytical procedures, please refer to Section 3.3.2 (nutrients), 3.3.5.2 (phytoplankton community structure), 3.3.6 ($\delta^{18}O$), 3.3.7 (CDOM/FDOM), 3.3.8 (CH_4), 3.3.16.2 (phytoplankton microscopic data), and 3.3.18 (eDNA).

(3) Parameters

Methane (CH_4)
Oxygen isotopic ratio ($\delta^{18}O$)
Nutrients
CDOM
FDOM
Phytoplankton pigment (HPLC)
Phytoplankton DNA
eDNA
Phytoplankton microscopic image

(4) Sampling locations, date and time (see 3.3.17 for the eDNA information)

Table 3.3.14-1 The list of discrete water sampling from underway surface monitoring system

Date [UTC]	Time [UTC]	Latitude	Longitude	*Chemical parameters	DNA/HPLC	Phytoplankton image
2025-09-02	1:57	56-13.74N	168-56.22W	x		

2025-09-02	16:04	58-52.62N	167-33.66W	x			
2025-09-02	21:12	59-50.70N	168-10.86W	x	x		
2025-09-03	2:34	60-55.08N	168-0.36W	x			
2025-09-03	16:09	63-29.22N	167-40.14W	x	x		
2025-09-03	23:59	64-59.52N	168-25.74W	x	x		
2025-09-04	5:33	65-39.72N	168-19.86W	x	x		
2025-09-04	21:09	66-41.16N	168-45.06W	x			
2025-09-05	6:47	67-43.68N	168-46.86W	x	x		
2025-09-05	12:21	68-10.50N	168-48.48W	x			
2025-09-05	18:30	68-45.36N	168-44.76W	x	x		
2025-09-06	6:36	69-48.48N	168-44.70W	x	x		
2025-09-06	14:11	70-45.48N	168-44.64W	x			
2025-09-06	22:17	70-51.78N	166-12.18W	x	x		
2025-09-07	4:33	71-7.68N	162-59.34W	x			
2025-09-07	17:03	71-17.10N	161-0.00W	x			
2025-09-08	1:48	71-9.72N	159-51.72W	x	x		
2025-09-08	6:18	71-22.68N	156-58.80W	x			
2025-09-08	16:37	71-47.76N	155-20.76W	x			
2025-09-09	2:02	71-47.46N	155-22.38W	x	x		
2025-09-10	2:12	71-49.44N	155-56.16W	x	x		
2025-09-10	22:07	71-50.76N	152-17.10W	x			
2025-09-11	2:25	71-32.28N	153-35.58W	x			
2025-09-12	0:27	72-25.44N	156-30.12W	x			
2025-09-12	19:01	71-40.74N	156-18.96W	x			
2025-09-13	3:02	71-14.28N	158-5.64W	x			
2025-09-13	16:02	71-55.38N	163-27.42W	x			
2025-09-13	21:13	72-41.64N	163-16.68W	x			
2025-09-14	5:50	72-53.04N	163-26.76W	x			
2025-09-14	22:04	73-17.40N	163-18.84W	x			
2025-09-16	0:16	73-27.72N	164-6.72W	x			
2025-09-16	6:24	74-3.84N	166-5.70W	x	x		
2025-09-16	19:34	74-45.06N	167-24.06W	x			
2025-09-17	6:10	75-12.60N	165-58.56W	x			
2025-09-17	21:39	75-35.04N	164-44.64W	x			
2025-09-18	5:29	75-42.96N	164-3.42W	x			
2025-09-18	16:13	76-22.68N	164-25.38W	x			
2025-09-19	0:06	76-22.38N	164-34.26W	x			
2025-09-19	6:46	75-9.78N	165-10.02W	x			
2025-09-19	15:57	74-25.62N	163-23.64W	x			
2025-09-22	2:13	73-55.08N	162-18.72W	x	x		
2025-09-22	10:52	73-8.70N	167-36.48W	x			
2025-09-22	20:35	71-37.86N	168-44.82W	x	x		
2025-09-23	4:04	70-0.30N	168-39.06W	x	x	x	
2025-09-23	16:02	67-30.00N	168-30.00W	x	x	x	
2025-09-24	2:00	66-47.88N	168-23.34W	x	x	x	
2025-09-24	8:30	65-33.30N	168-39.84W	x	x	x	
2025-9-24	8:57	65-29.41N	168-48.42W				
2025-09-24	17:00	64-16.38N	171-27.18W	x	x	x	
2025-09-24	23:04	63-17.40N	173-21.66W	x	x	x	
2025-09-25	5:00	62-12.72N	174-54.90W	x	x	x	
2025-09-25	18:00	60-0.96N	177-46.86W	x	x	x	
2025-09-26	0:00	59-4.00N	178-57.82W	x		x	
2025-09-26	6:02	58-18.06N	179-57.23E	x		x	
2025-09-26	19:00	56-24.09N	177-25.28E	x		x	
2025-09-27	1:00	55-38.80N	175-42.86E			x	
2025-09-27	7:00	54-53.27N	173-59.27E			x	
2025-09-27	20:00	53-7.53N	170-48.95E			x	
2025-09-28	2:00	52-14.44N	169-34.55E			x	
2025-09-28	8:00	51-22.57N	168-51.83E			x	
2025-09-28	13:06	50-42.45N	168-29.16E			x	

2025-09-28	21:00	49-42.13N	167-16.71E	x
2025-09-29	3:00	49-7.06N	165-49.54E	x
2025-09-29	9:00	48-34.18N	164-3.98E	x
2025-09-29	14:45	48-4.10N	162-35.30E	x
2025-09-29	22:00	47-9.82N	160-40.55E	x
2025-09-30	4:00	46-32.00N	159-0.40E	x
2025-09-30	10:00	45-37.29N	157-22.76E	x
2025-09-30	15:50	44-43.03N	156-7.16E	x
2025-09-30	23:00	43-40.93N	154-29.45E	x
2025-10-01	4:55	43-5.93N	152-56.48E	x
2025-10-01	11:00	42-14.00N	151-31.18E	x
2025-10-01	16:00	41-31.23N	150-20.07E	x
2025-10-01	23:00	40-33.67N	148-37.81E	x
2025-10-02	4:00	40-0.58N	147-16.21E	x
2025-10-02	12:10	39-8.08N	145-10.81E	x

*chemical parameters: $\delta^{18}O$, nutrients, CDOM, FDOM

(5) Data archives

These data obtained in this cruise will be submitted to the Data Management Group of JAMSTEC, and will be opened to the public via "Data Research System for Whole Cruise Information in JAMSTEC (DARWIN)" in JAMSTEC web site.
<https://www.godac.jamstec.go.jp/darwin/en/>

3.3.14.3. Silicate

(1) Responsible personnel
Mariko Hatta JAMSTEC

(2) Purpose, background

Establish the shipboard system using a programmable flow injection system and identify potential trouble and establish the troubleshooting protocol:

Purpose: The primary purpose of this study is to develop a compact and automated microfluidic analyzer for nutrient analysis. This innovative system is designed to meet specific criteria for efficient, unsupervised operation, including durability, minimal reagent consumption, and computer-controlled manipulations. In essence, it aims to create a state-of-the-art tool for analyzing nutrients in ocean samples with a focus on practicality and precision.
Background: The background provides essential context for the study: ***Current Knowledge Gap:*** It is established that there's a significant gap in our understanding of ocean biogeochemical data. This knowledge gap is attributed to the complexity and intricacy of the analytical procedures involved in both at-sea and on-land sample analysis.

Identify the water mass characteristics with shipboard silicate data with the other physical parameters (i.e. Temperature, salinity, oxygen) obtained from the underway surface water monitoring system:

Purpose: This goal aims to collect and analyze data related to water mass

characteristics. It mentions specific parameters such as silicate and phosphate concentrations along with temperature, salinity, and oxygen levels. The purpose is to understand the composition and characteristics of the water masses the ship encounters during its journey.
Background: ***Arctic Ocean Significance***: The study highlights the significance of the Arctic Ocean, which experiences dynamic changes in freshwater influx due to factors such as sea ice melt and river inputs. These changes have substantial effects on the surface ocean. ***Continental Shelves:*** The Arctic Ocean's unique geographical characteristics, notably its extensive continental shelves, play a vital role in the transport of geochemical substances from the continental boundary to the Arctic interior. These processes are influenced by climate change, making it increasingly important to understand the Arctic's geochemical cycles.

In summary, the study aims to address the existing knowledge gap by developing an advanced microfluidic analyzer that facilitates nutrient analysis in ocean samples and expands the database. This innovation is particularly important given the intricate nature of existing analytical procedures and the unique environmental changes occurring in the Arctic Ocean. Understanding the geochemical cycles in the Arctic region has broad implications, making this research significant in the context of oceanography and environmental science.

(3) Activities (observation, sampling, development)

The activities described in this section involve the process of collecting and analyzing seawater samples for real-time determination of Silicate (SiO_2) using a programmable flow injection technique. Here's a breakdown of the activities:

Seawater Sample Collection: Samples were aspirated into the analysis system using an underway water sampling pump system, waters were collected approximately at 4.5m depth.
Real-Time Analysis: The collected seawater samples are then subjected to real-time analysis. The analysis focuses on Silicate (SiO_2).
Programmable Flow Injection Technique: The analysis technique being employed is the programmable flow injection technique. This technique involves the controlled injection of samples and reagents into a flowing stream. It allows for precise and automated measurements and is valuable for continuous monitoring.

(4) Methods, instruments
4.1. Instrumentation
The instrument, miniSIA-2 (Global FIA, Fox Island, WA, USA), comprises two high precision, synchronously refilling milliGAT pumps, two thermostated holding coils, a 6-port LOV (model COV-MANI-6, constructed from polymethyl methacrylate, Perspex®) furnished with a module for an external flow cell (Figure 4.1). All tubing connections, downstream from the milliGAT pumps including the holding coils (volume 1000 µL), were made with 0.8 mm I.D. polytetrafluoroethylene (PTFE). The holding coils were thermostated at 40C temperature for all silicate and phosphate analysis. The tubing between the carrier stream reservoirs and the milliGAT pump was made from 1.6 mm I.D. PTFE tubing to minimize degassing under reduced pressure at higher aspiration flow rates. A spectrophotometer (Flame, Ocean Insight,

Orlando, FL, USA) and a light source were connected to the flow cells by using optical fibers with 500-µm silica cores encased in 0.8 mm I.D. green PEEK tubing. The end of each fiber exposed to the liquid was cemented with epoxy, cut square, and polished. An Ocean Optics Tungsten Halogen (HL-2000, Ocean Insight, Orlando, FL, USA) light source was used. All assay steps were computer-controlled using commercially available software (FloZF, GlobalFIA, Fox island, WA, USA). The Linear Light Path (LLP) flow cell was purchased from Global FIA. The outlet of the LLP flow cell, was fitted with a 40-psi flow restrictor (GlobalFIA, Fox Island, WA, USA), which, by elevating the pressure within the flow path, efficiently prevented the formation of microbubbles from spontaneous outgassing.

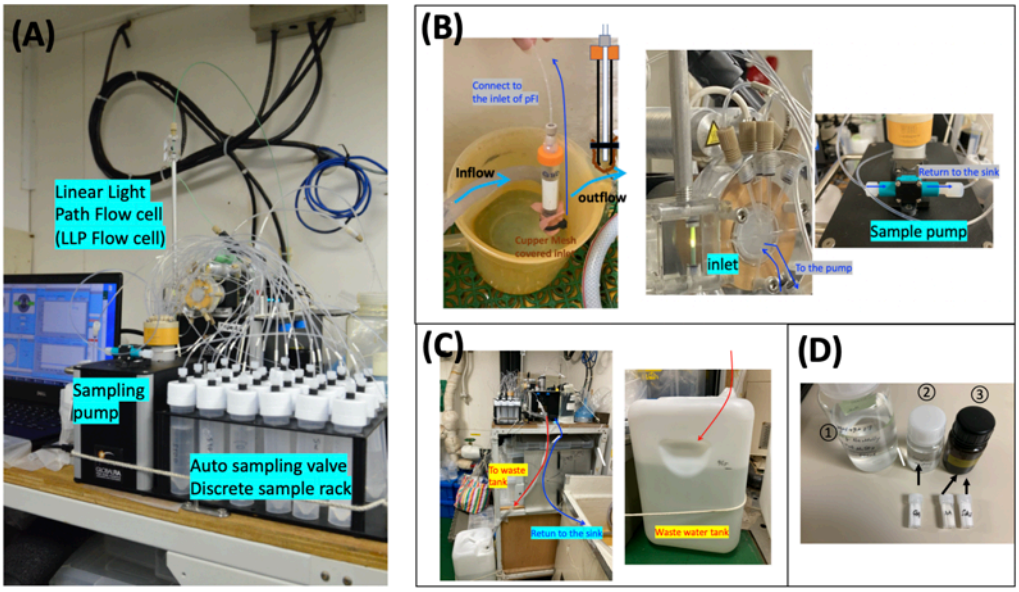

Figure 3.3.14-3. Shipboard analytical system for continuous silicate determination using the programmable flow injection technique. (A) the mini-SIA2 system and the autosampler. (B) Newly established sampling inlet. (C) The waste water drains system (D) Preparation for the reagents for the Silicate analysis during the cruise.

Remarks:
Flow Cell Length: This year, a flow cell with a length of 10 centimeters was utilized. The flow cell is a key component of the analysis system and is used to pass the seawater samples through for analysis.
Sample Collection Frequency: Surface water samples were collected approximately every 5 minutes. This frequent sampling interval allows for more detailed temporal resolution in the data.
Sample Aspiration: Samples were aspirated into the analysis system using a sample pump for a duration of 20 seconds. Aspiration is the process of drawing the seawater samples into the system for analysis.
Temperature Adjustment: Maintaining a consistent temperature is important for accurate and reproducible analysis, but the room temperature changes significantly during the analysis time or date. Thus, the heating coil has been adjusted to 40 degrees C during this cruise to meet the constant determination throughout the cruise.
Return of Flushed Surface Samples: Samples that weren't analyzed, which are

referred to as "flushed surface samples". Since they were not mixed with any reagent, these samples were directly returned to the sink, indicating that they were not retained after analysis.

Waste Handling: Any waste samples and reagents generated during the analysis process were drained into a waste tank. These waste materials were stored in the waste tank until the end of the cruise. Proper waste management is crucial for environmental and safety reasons.

(4.2) Analytical methodology

The detailed the methodology using programmable flow injection technique was published in Hatta et al., 2021. The detailed of each reagent and standards were made as follow: Carrier solution: MilliQ water. Certified reference materials (KANSO) have been analyzed as a standard solution for this cruise (see Table 3.3.14-1).

Table 3.3.14-1. The certified reference materials

CRMs	Reported silicate value
CQ	2.20±0.07
CR	14.0±0.3
CS	34.0±0.3
CP	61.1±0.3

Silicate analysis:

The acidified molybdate reagent was prepared by dissolving 2 g of ammonium molybdate tetrahydrate crystalline in 500 mL of acidified MilliQ water (2.5 mL of conc. sulfuric acid was added). This solution was stable for 2 months. The mixed solution of ascorbic acid and SDS solution was prepared by dissolving 4 g of L (+)-ascorbic acid in 200 mL of MilliQ water, and then 4 g of solid of ultrapure sodium dodecyl sulfate was added into this ascorbic acid solution, and then 4 g of solid of oxalic acid was added into this mixture.

(5) Results and Future Plans

Results:

During the cruise, the surface samples for continuous determination were collected every 5 minutes. Over 2952 samples were determined during this cruise. There was no significant air bubble issue was detected.

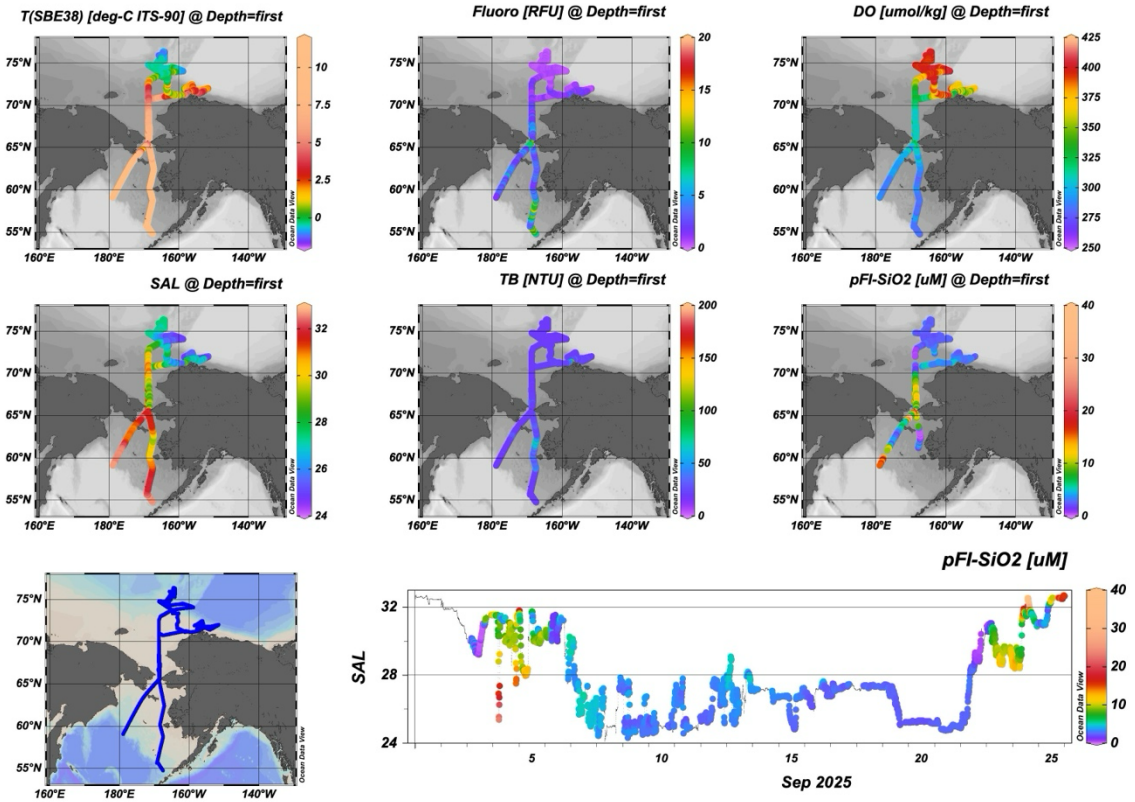

Figure 3.3.14-4 The surface distribution of temperature, salinity, fluorescence, turbidity, dissolved oxygen, and silicate during the cruise. The scatter plot shows trajectory for the salinity with silicate value.

Future Plans:

Further analysis and interpretation of the entire dataset to provide a comprehensive view of silicate in the study area.

Investigation of the factors influencing the observed silicate anomalies, such as riverine inputs and water mass dynamics.

Comparisons and validations with other data sources and cruises to refine the understanding of the spatiotemporal distribution of silicate in the region.

Refining the analytical methodology, especially sample introducing system.

Continued monitoring and data collection to build on the insights gained during this cruise and contribute to a better understanding of oceanographic processes in the Arctic Ocean.

(6) Data archives

These data obtained in this cruise will be submitted to the Data Management Group of JAMSTEC, and will be opened to the public via "Data Research System for Whole Cruise Information in JAMSTEC (DARWIN)" in JAMSTEC web site.
<https://www.godac.jamstec.go.jp/darwin/en/>

(7) References

Hatta et al., 2021. Programmable flow injection in batch mode: Determination of nutrients in seawater by using a single, salinity-independent calibration line, obtained with standards prepared in distilled water, Talanta.

https://doi.org/10.1016/j.talanta.2021.122354.
Hatta et al., 2024. Autocalibration based on dilution of a single concentrated standard is used for the determination of silicate in sea water by the modified molybdenum blue method, Talanta 276 (2024) 126183. https://doi.org/10.1016/j.talanta.2024.126183.

3.3.15. Continuous measurement of pCO_2 and pCH_4

(1) Personnel

Akihiko Murata (JAMSTEC) – Principal investigator, Not on board
Yuta Oda (MWJ)
Masahiro Orui (MWJ)
Nagisa Fujiki (MWJ)

(2) Objective

To survey spatial distributions of surface seawater pCO_2 in the western Arctic Ocean.

(3) Parameters

Partial pressures of CO_2 (pCO_2) and CH_4 (pCH_4)

(4) Methods, Apparatus and Performance

Atmospheric and surface seawater pCO_2 and pCH_4 were measured with a system having the off-axis integrated-cavity output spectroscopy gas analyzer (Off-Axis ICOS; 911-0011, Los Gatos Research). Standard gases were measured every about 4 hours, and atmospheric air taken from the bow of the ship (approx.13 m above the sea level) were measured every about 3 hours. Seawater was taken from an intake placed at the approximately 4.5 m below the sea surface and introduced into the equilibrator at the flow rate of (4 - 5) L min^{-1} by a pump. The equilibrated air was circulated in a closed loop by a pump at flow rate of (0.6 - 0.7) L min^{-1} through two electric cooling units, a starling cooler, and the Off-Axis ICOS.

(5) Preliminary result

Distributions of atmospheric and surface seawater CO_2 were shown in Figure 3.3.15-1, along with those of sea surface temperature (SST). Distributions of atmospheric and surface seawater CH_4 were displayed in Figure 3.3.15-2, along with those of SST.

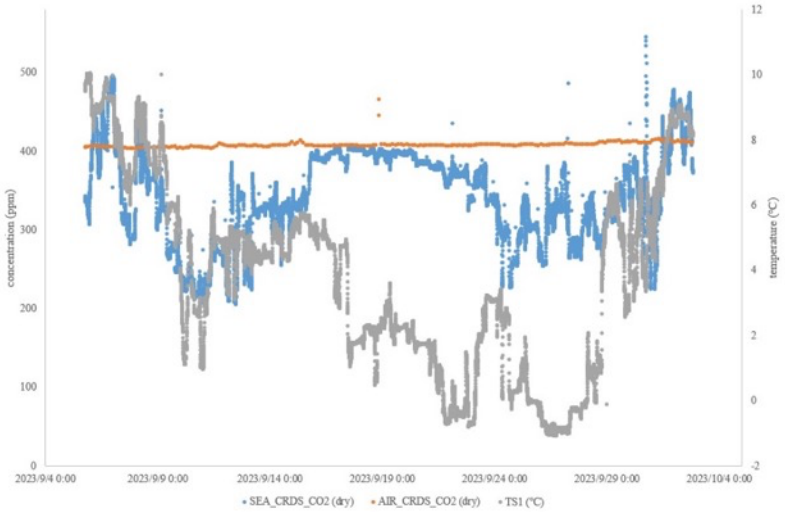

Figure 3.3.15-1. Distributions of atmospheric (orange) and surface seawater CO_2 (blue), and SST (grey) as a function of observation time.

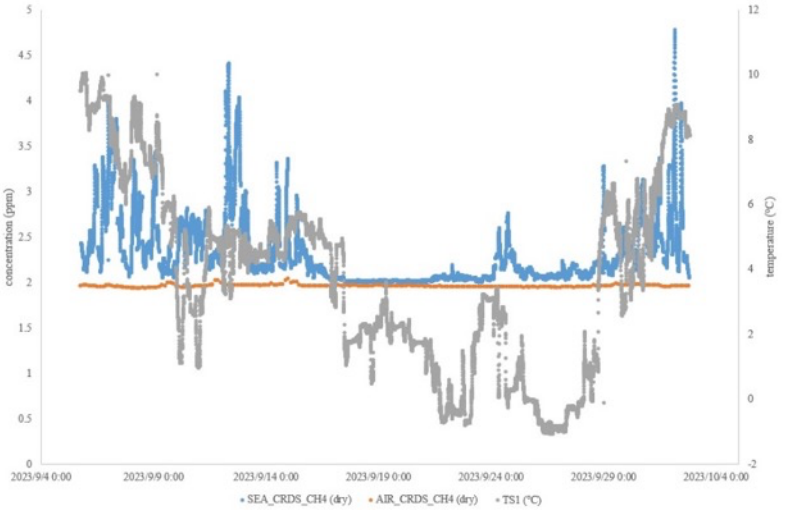

Figure 3.3.15-2. Distributions of atmospheric (orange) and surface seawater CH_4 (blue), and SST (grey) as a function of observation time.

(6) Date archives

These data obtained in this cruise will be submitted to the Data Management Group (DMG) of JAMSTEC, and will be opened to the public via "Data Research System for Whole Cruise Information in JAMSTEC (DARWIN)" in JAMSTEC web site.
<https://www.godac.jamstec.go.jp/darwin/en/>

3.3.16. Plankton

3.3.16.1. Zooplankton

(1) Personnel

Kohei Matsuno (Hokkaido University) - Principal Investigator

(2) Objectives

The goals of this study are following:

Clarifying spatial changes of mesozooplankton community using plankton net and *in-situ* camera

Evaluation physiological conditions (fatty acids) of the Pacific and Arctic zooplankton

Comparison population structure, fatty acids and metabolic activity of dominant copepod *Calanus glacialis/marshallae* between different populations examined by haplotype analysis

(3) Parameters

Mesozooplankton abundance

Fatty acids

Haplotypes of *Calanus glacialis/marshallae*

(4) Sampling and treatment

(4-1) Plankton net sampling

Zooplankton samples were collected by vertical hauls of a Quad-NORPAC net at 24 stations in the Pacific Arctic Ocean. Quad-NORPAC net (mesh sizes: 335, 150 and two 63 μm with large cod-end, mouth diameter: 45 cm) was towed between surface and 150 m depth or bottom -7 m (stations where the bottom shallower than 150 m) at all stations (Fig. 3.3.16.1-1 and Table 3.3.16.1-1). The volume of water filtered through the net was estimated from the reading of a flow-meter mounted in the mouth ring. The zooplankton samples collected by the NORPAC net with 335 and 150 μm mesh were immediately fixed with 5% buffered formalin for zooplankton community structure analysis. Samples collected with 63 μm mesh were used for evaluation of the zooplankton physiological parameters (i.e., fatty acids composition). 80 cm ring net (mesh: 335 μm, mouth diameter: 80 cm) was towed between surface and 150 m or bottom -7 m at 9 stations (Fig. 3.3.16.1-1 and Table 3.3.16.1-2). Fresh samples were used for evaluation of individual fatty acid composition and haplotype for *Calanus glacialis*, and the remaining sub-samples were preserved in methanol for analysis of total fatty composition in zooplankton community.

(4-2) PTZ camera

To examine vertical distribution of macrozooplankton, vertical tow of Pan-Tilt-Zoom camera with LED lights was conducted (Fig. 3.3.16.1-1 and Table 3.3.16.1-1). PTZ camera was casted at 0.2 m s^{-1} winch speed down to the sea bottom or 100 m depth. Camera angle fixed to see bottom.

(4-3) On-board treatment

Firstly, I added with 10% soda water (CO_2 water) for anesthesia into a sample collected by 63 μm NORPAC net or 335 μm ring net after net sampling. I sorted out all stages of *C. glacialis/marshallae* under dissecting microscope. C5 and C6F stages were moved on a slide glass and was cut their antenules by needles. The antenules were preserved in a 1.5 mL tube filled with 99% ethanol for haplotype (16s

rRNA) and Mig-seq analysis (by Dr. Junya Hirai in The University of Tokyo). Remaining body was transferred into a small plastic case (3 mL), and stored in –80°C for fatty acid composition analysis (by Dr. Yasuhiro Ando in Hokkaido University). Additionally, five specimen of C5 stage were moved 2 mL cryo tube and frozen at –80°C for measure of their metabolic activity (ETS, total ATP etc.) (by Dr. Jose M. Landeira in Norwegian University of Science and Technology). The other stages were individually preserved into the small plastic case and stored in –80°C. Several large copepods (e.g., *Calanus hyperboreus*, *Metridia longa*) were treated same procedure for fatty acids sample as written above for inter-species comparison on fatty acid composition. After these procedures, the remaining sub-samples were fixed with 99.5% ethanol as backup samples for haplotype analysis of *Calanus glacialis*.

Fresh zooplankton was randomly picked up by a small pipet, moved into 2 mL cryo tube filled with antifreezes and stored in –80°C with controlled freezing system for survival experiments in the antifreezes (by Dr. Yuya Kumagai in Hokkaido University). Sea water from the remaining samples was removed by 63 μm nylon mesh, and preserved in 99.5% ethanol for DNA analysis of Radiolaria (by Dr. Takahito Ikenoue in JAMSTEC).

Fresh samples collected by 80 cm ring net with 335 μm mesh was primally used for picking up *C. glacialis/marshallae* as mentioned above. The remaining sub-samples were preserved in methanol for analysis of total fatty composition in zooplankton community (by Dr. Fumiaki Beppu in Hokkaido University).

(5) Station list

Table 3.3.16.1-1. Data on plankton samples collected by vertical hauls with a Quad-NORPAC net. PTZ camera observation is remarked in the table.

Station no.	Position Lat. (N)	Position Lon.	S.M.T. Date	S.M.T. Hour	Length of wire (m)	Angle of wire (°)	Depth estimated by wire angle (m)	Mesh size (μm)	Flowmeter No.	Flowmeter Reading	Estimated volume of water filtered (m^3)	Remark
1	65 29.97	168 45.01 W	3 Sep.	19:42 - 19:45	48	4	48	335	3994	440	6.62	5)
								150	2446	345	4.92	5)
								63				1)
								63				1)
2	66 0.13	168 44.89 W	4 Sep.	0:11 - 0:14	46	1	46	335	3994	401	6.03	5)
								150	2446	335	4.77	5)
								63				1)
								63				2)
4	67 0.07	168 45.06 W	4 Sep.	14:46 - 14:49	39	6	39	335	3994	388	5.84	
								150	2446	383	5.46	
								63				1)
								63				1)
6	68 1.96	168 50.07 W	5 Sep.	2:40 - 2:45	53	4	53	335	3994	540	8.12	3)
								150	2446	507	7.23	
								63				1)
								63				1)
8	69 0.00	168 44.93 W	5 Sep.	13:41 - 13:45	47	1	47	335	3994	576	8.66	3)
								150	2446	578	8.24	
								63				1)
								63				2)
10	70 0.00	168 45.01 W	6 Sep.	0:34 - 0:36	34	2	34	335	3994	357	5.37	3)
								150	2446	372	5.30	
								63				1)
								63				1)
12	71 0.00	168 44.96 W	6 Sep.	8:16 - 8:19	38	1	38	335	3994	422	6.35	3)
								150	2446	405	5.77	
								63				1)
								63				1)
14	70 56.0	165 24 W	6 Sep.	16:13 - 16:17	36	2	36	335	3994	390	5.87	3)
								150	2446	417	5.94	
								63				1)
								63				1)
15	71 42.34	154 52.58 W	8 Sep.	14:55 - 14:59	106	4	106	335	3994	1004	15.10	3)
								150	2446	1059	15.09	
								63				1)
								63				1)
16	72 1.82	151 34.79 W	10 Sep.	10:06 - 10:13	151	7	150	335	3994	1395	20.98	
								150	2446	1250	17.81	
								63				1)
								63				2)
17	71 42.59	152 50.75 W	10 Sep.	16:18 - 16:27	152	9	150	335	3994	1397	21.01	
								150	2446	1298	18.50	
								63				1)
								63				2)
18	71 25.64	154 6.98 W	10 Sep.	19:36 - 19:38	34	1	34	335	3994	403	6.06	3)
								150	2446	395	5.63	
								63				1)
								63				1)
19	71 55.11	158 27.67 W	11 Sep.	10:44 - 10:47	50	1	50	335	3994	490	7.37	3)
								150	2446	467	6.66	
								63				1)
								63				2)
21	72 29.05	156 18.18 W	11 Sep.	18:43 - 18:50	150	1	150	335	3994	1321	19.87	
								150	2446	980	13.97	5)
								63				1)
								63				2)
27	71 10.4	159 13.24 W	12 Sep.	21:39 - 21:45	88	1	88	335	3994	955	14.36	3)
								150	2446	828	11.80	
								63				1)
								63				2)
29	72 20.64	163 7.53 W	13 Sep.	11:08 - 11:11	34	8	34	335	3994	349	5.25	3)
								150	2446	318	4.53	
								63				1)
								63				2)
30	73 2.29	163 26.05 W	13 Sep.	15:23 - 15:28	92	1	92	335	3994	830	12.48	3)
								150	2446	715	10.19	
								63				1)
								63				2)

S.M.T. is UTC-8h
1) Samples was used for experiments on board
2) Experiment, remaining was preserved in ethanol
3) PTZ camera observation was conducted
4) High wave and strong wind
5) Phytoplankton abundant
6) Large mudusa clogged

Table 3.3.16.1-1. (Continued).

Station no.	Position Lat. (N)	Position Lon.	S.M.T. Date	S.M.T. Hour	Length of wire (m)	Angle of wire (°)	Depth estimated by wire angle (m)	Mesh size (μm)	Flowmeter No.	Flowmeter Reading	Estimated volume of water filtered (m^3)	Remark
31	74 47.56	168 43.63 W	16 Sep.	9:08 - 9:16	150	1	150	335	3994	1280	19.25	3)
								150	2446	1248	17.79	
								63				1)
								63				2)
32	74 42.47	166 2.94 W	16 Sep.	13:45 - 13:52	150	1	150	335	3994	1280	19.25	3)
								150	2446	1260	17.96	6)
								63				1)
								63				2)
33	75 56.79	165 32.1 W	17 Sep.	11:25 - 11:32	150	1	150	335	3994	1347	20.26	3)
								150	2446	1324	18.87	
								63				1)
								63				2)
34	75 16.98	164 6.4 W	17 Sep.	15:44 - 15:52	151	6	150	335	3994	1328	19.97	3)
								150	2446	1360	19.38	
								63				1)
								63				2)
35	74 31.88	161 56.16 W	20 Sep.	14:42 - 14:50	150	1	150	335	3994	1463	22.00	3),4)
								150	2446	1405	20.02	4)
								63				1)
								63				2)
36	74 3.49	158 51.72 W	21 Sep.	13:06 - 13:12	150	1	150	335	3994	1379	20.74	3)
								150	2446	1307	18.63	
								63				1)
								63				2)
37	72 30.02	168 45.06 W	22 Sep.	7:28 - 7:31	51	4	51	335	3994	590	8.87	3)
								150	2446	599	8.54	
								63				1)
								63				2)

S.M.T. is UTC-8h
1) Samples was used for experiments on board
2) Experiment, remaining was preserved in ethanol
3) PTZ camera observation was conducted
4) High wave and strong wind
5) Phytoplankton abundant
6) Large mudusa clogged

Table 3.3.16.1-2. Data on plankton samples collected by vertical hauls with ring net. GG54: 0.335 mm mesh size.

Station no.	Position Lat. (N)	Position Lon.	S.M.T. Date	S.M.T. Hour	Length of wire (m)	Angle of wire (°)	Depth estimated by wire angle (m)	Kind of cloth	Remark
1	65-29.97	168-45.01 W	3 Sep.	19:50	48	2	48	GG54	Experiment
15	71-42.34	154-52.58 W	8 Sep.	15:05	108	2	108	GG54	Experiment, remaining in ethanol
16	72-1.82	151-34.79 W	10 Sep.	10:19	150	1	150	GG54	Experiment
17	71-42.59	152-50.75 W	10 Sep.	16:35	150	8	149	GG54	Experiment
21	72-29.05	156-18.18 W	11 Sep.	18:51	150	1	150	GG54	Experiment
31	74-47.56	168-43.63 W	16 Sep.	9:21	150	1	150	GG54	Experiment
32	74-42.47	166-2.94 W	16 Sep.	13:45	150	1	150	GG54	Experiment
35	74-31.88	161-56.16 W	20 Sep.	14:55	150	1	150	GG54	Experiment
36	74-3.49	158-51.72 W	21 Sep.	13:16	150	1	150	GG54	Experiment

S.M.T. is UTC-8h

(6) Preliminary results

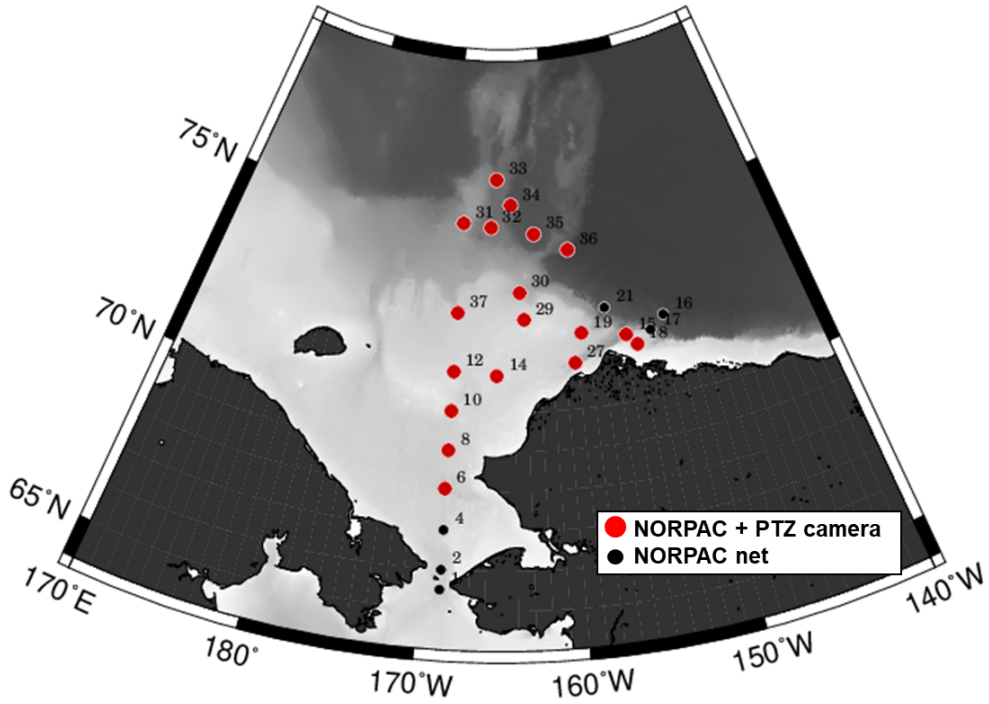

Fig. 3.3.16.1-1. Location of the sampling stations in the Pacific Arctic Ocean from 1 September to 5 October in 2025. Vertical hauls by a Quad-NORPAC net was made at all stations.

(7) Data archives

These data obtained in this cruise will be submitted to the Data Management Group of JAMSTEC, and will be opened to the public via "Data Research System for Whole Cruise Information in JAMSTEC (DARWIN)" in JAMSTEC web site.
<https://www.godac.jamstec.go.jp/darwin/en/>

3.3.16.2. Microplankton

(1) Personnel

Kohei Matsuno (Hokkaido University) - Principal Investigator

(2) Objective

The goals of this study are following:

Clarifying spatial distribution of microplankton assemblages by a microscopy and a PlanktoScope

Evaluating photosynthetic activity by a pulse-amplitude modulated fluorometer

(3) Parameters

Microplankton community in cell number

Size structure of microplankton cells

Fv/Fm

alpha

ETRm

IK

(4) Sampling and treatment

(4-1) Spatial distribution by Niskin sampler and bucket

Sea water samples (2 L) were collected from 0 and chlorophyll *a* maximum layer (SCM) by bucket and Niskin water sampler at 24 stations (Fig. 3.3.16.2-1, Table 3.3.16.2-1). Microplankton in the water was concentrated with reverse filtration using 20 μm mesh and a siphon tube. 3-5 mL of the concentrated sample was filtered through a GF/F filter, and the filter extracted with 3 mL of N,N-dimethylformamide. After one-day extracting, the chlorophyll *a* concentration was measured by the method of Holm-Hansen et al. (1965) using a Trilogy fluorometer.

1-1.5 mL of the concentrated sample was insert into a 20 mL syringe attached a PlanktoScope. Sample information was registered, sample filled into a glass cell by slow vacuum rate, and started to taking 100-250 photos, which was adjusted to the number of cells in a first view. After taking the photos, segmentations was conducted for checking data.

Additionally, using the concentrated samples, maximum photochemical efficiency (Fv/Fm) was measured with a pulse-amplitude modulated fluorometer (Water-PAM; Walz, Effeltrich, Germany) in the sediment preservation room (3-5ºC). After light-acclimatation in the dark bottle for over 15 minutes, samples (4 mL) were placed in a quartz cuvette. Fv/Fm of each sample was determined by a red LED with a peak illumination at 650 nm. The initial fluorescence (Fv) was measured by applying a weak measuring light, and a saturating pulse was applied to determine the maximum fluorescence (Fm). Then, the samples in the measuring cuvette were light-acclimated for 15 minutes by turning off the internal actinic light source of the PAM fluorometer. After the acclimation, rapid light curve was obtained by illuminating the samples for 10 s before each ΔF/Fm measurement at each of a series of eight irradiances that increased in steps from 136 to 2122 μmol photons m^{-2} s^{-1}. The remaining samples were fixed by glutaraldehyde (1% final concentration) in draft, and kept in a dark glass bin in a refrigerator.

(4-2) Surface monitoring

Surface water samples (2 L) from the underway system three to four times a day to

examine cell density, size structure and photosynthetic activity from the Bering Sea and the North Pacific Ocean (Fig. 3.3.16.2-1, Table 3.3.16.2-1). Procedure of sample was same as mentioned above. Subsequent to the microplankton sampling, seawater was collected in a plastic tube and frozen for measuring macronutrients.

(5) Station list

Table 3.3.16.2-1. Data on water samples collected by Niskin water sampler, bucket and surface monitoring system.

St.	Date (UTC)	Latitude (°N)		Longitude			Sampling depth (m)
1	2025/9/4 2:52	65	30.02	168	45.08	W	0, 15
2	2025/9/4 8:19	66	0.09	168	44.88	W	0, 30
4	2025/9/4 23:05	67	0.05	168	45.11	W	0, 10
6	2025/9/5 9:56	68	1.96	168	49.94	W	0, 25
8	2025/9/5 20:54	69	0.07	168	45.06	W	0, 15
10	2025/9/6 7:55	69	59.98	168	44.97	W	0, 23
12	2025/9/6 15:26	70	59.53	168	44.6	W	0, 27
14	2025/9/6 23:35	70	56.21	165	24.32	W	0, 20
15	2025/9/8 21:58	71	41.63	154	55.82	W	0, 10
16	2025/9/10 19:01	72	1.82	151	34.83	W	0, 18
17	2025/9/10 23:19	71	42.72	152	51.73	W	0, 15
18	2025/9/11 4:04	71	25.71	154	6.72	W	0, 20
19	2025/9/11 17:53	71	55.1	158	27.75	W	0, 25
21	2025/9/12 3:42	72	29.05	156	18.09	W	0, 35
27	2025/9/13 4:51	71	10.4	159	12.84	W	0, 33
29	2025/9/13 18:25	72	19.99	163	8.64	W	0, 20
30	2025/9/13 23:43	73	2.29	163	26.01	W	0, 35
31	2025/9/16 15:53	74	47.52	168	43.65	W	0, 35
32	2025/9/16 21:48	74	42.47	166	2.94	W	0, 42
33	2025/9/17 17:54	75	56.71	165	32.7	W	0, 50
34	2025/9/17 23:53	75	16.98	164	6.45	W	0, 50
35	2025/9/21 0:21	74	31.85	161	56.91	W	0, 40
36	2025/9/21 17:54	74	2.58	158	49.93	W	0, 58
37	2025/9/22 14:26	72	30.67	168	43.75	W	0,20
Sur1(TSG44)	2025/9/23 4:04	70	0.85	168	39.06	W	0
Sur2(TSG45)	2025/9/23 16:00	67	30	168	29.99	W	0
Sur3(TSG46)	2025/9/24 2:00	66	47.81	168	23.35	W	0
Sur4(TSG47)	2025/9/24 8:30	65	33.415	168	39.544	W	0
Sur5(TSG48)	2025/9/24 17:00	64	16.384	171	27.167	W	0
Sur6(TSG49)	2025/9/24 23:00	63	18.07	173	20.437	W	0
Sur7(TSG50)	2025/9/25 5:00	62	12.44	174	55.27	W	0
Sur8(TSG51)	2025/9/25 18:00	60	1.15	177	46.62	W	0
Sur9(TSG52)	2025/9/26 0:00	59	2.88	178	59.37	W	0
Sur10(TSG53)	2025/9/26 6:00	58	18.25	179	57.42	E	0
Sur11(TSG54)	2025/9/26 19:00	56	24.15	177	25.41	E	0
Sur12(TSG55)	2025/9/27 1:00	55	38.80	175	42.86	E	0
Sur13(TSG56)	2025/9/27 7:00	54	53.27	173	59.27	E	0
Sur14(TSG57)	2025/9/27 20:00	53	7.53	170	48.95	E	0
Sur15(TSG58)	2025/9/28 2:00	52	14.44	169	34.55	E	0
Sur16(TSG59)	2025/9/28 8:00	51	22.57	168	51.83	E	0
Sur17(TSG60)	2025/9/28 13:06	50	42.45	168	29.16	E	0
Sur18(TSG61)	2025/9/28 21:00	49	42.13	167	16.71	E	0
Sur19(TSG62)	2025/9/29 3:00	49	7.06	165	49.54	E	0
Sur20(TSG63)	2025/9/29 9:00	48	34.18	164	3.98	E	0
Sur21(TSG64)	2025/9/29 14:45	48	4.1	162	35.3	E	0
Sur22(TSG65)	2025/9/29 22:00	47	9.82	160	40.55	E	0
Sur23(TSG66)	2025/9/30 4:00	46	32	159	0.4	E	0
Sur24(TSG67)	2025/9/30 10:00	45	37.29	157	22.76	E	0
Sur25(TSG68)	2025/9/30 15:50	44	43.03	156	7.16	E	0
Sur26(TSG69)	2025/9/30 23:00	43	40.93	154	29.45	E	0
Sur27(TSG70)	2025/10/1 4:55	43	5.93	152	56.48	E	0
Sur28(TSG71)	2025/10/1 11:00	42	14	151	31.18	E	0
Sur29(TSG72)	2025/10/1 16:00	41	31.23	150	20.07	E	0
Sur30(TSG73)	2025/10/1 23:00	40	33.67	148	37.81	E	0
Sur31(TSG74)	2025/10/2 4:00	40	0.58	147	16.21	E	0
Sur32(TSG75)	2025/10/2 12:10	39	8.08	145	10.81	E	0

(6) Preliminary results

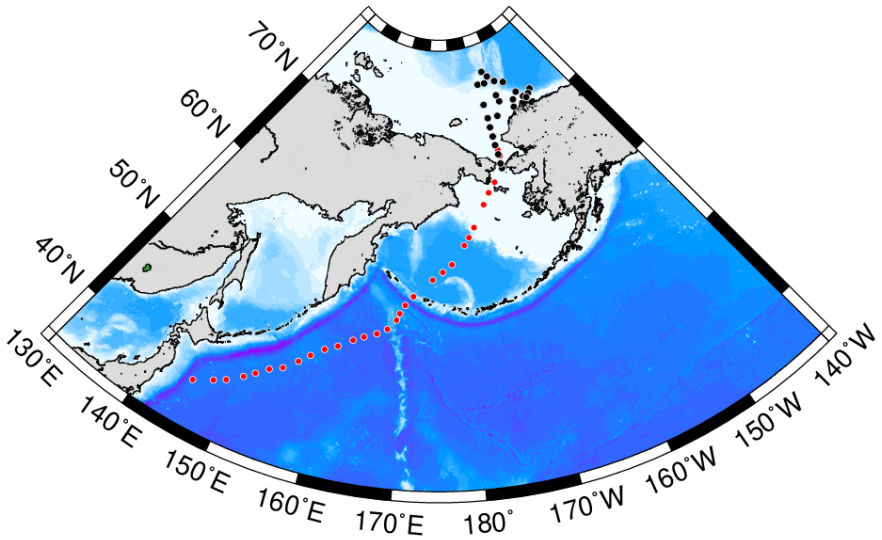

Fig. 3.3.16.2-1. Location of the water sampling stations from the Pacific Arctic Ocean to north Pacific Ocean (black circles: CTD+bucket, red circles: TSG).

(7) Data archives

These data obtained in this cruise will be submitted to the Data Management Group of JAMSTEC, and will be opened to the public via "Data Research System for Whole Cruise Information in JAMSTEC (DARWIN)" in JAMSTEC web site.
<https://www.godac.jamstec.go.jp/darwin/en/>

3.3.17. Environmental DNA

(1) Personnel

Tatsuya Kawakami (Hokkaido University)
Akihide Kasai (Hokkaido University)
Hiromichi Ueno (Hokkaido University)

(2) Objectives

In the Arctic Ocean, poleward shifts of fish species associated with increasing water temperatures and sea-ice reduction have been observed (Fossheim et al., 2015). Focusing on cod species, which are representative taxa in Arctic and subarctic regions, previous studies have reported northward distribution shifts of polar cod (*Boreogadus saida*) and walleye pollock (*Gadus chalcogrammus*) in the Chukchi Sea under warmer conditions (Levine et al., 2023).

With continued warming and sea-ice decline, it is predicted that the suitable habitat of polar cod will shrink, while walleye pollock will further expand their range from the Bering Sea into the Chukchi Sea. As these species are key components of the Arctic food web, such distributional changes are expected to have major impacts on the entire ecosystem by altering interspecific relationships and energy transfer pathways. However, the present distribution patterns and the environmental factors driving these changes remain poorly understood, particularly under the unprecedentedly warm conditions of the 2020s.

Detecting environmental DNA (eDNA), which is genetic material shed by macro-

organisms and remaining in the environment, has proven to have great potential for describing Arctic fish distribution and diversity (Kawakami et al., 2023a; 2023b). Analyzing the fish diversity and distribution using eDNA collected during this cruise will provide a great opportunity to add complementary information to those from previous Mirai Arctic cruises, thereby allowing us to comprehensively understand the annual changes in fish diversity and distribution and their environmental drivers.
Despite its usefulness, one of the technical limitations to broadly applying the eDNA technique for large-scale biomonitoring in the ocean is the need for the collection of large volumes of water and time-consuming filtration. Passive eDNA sampling, utilizing the adsorption of suspended particles in seawater, is now considered a promising approach to drastically reduce the laborious work involved in eDNA sampling (Jeunen et al., 2024).

Based on this background, we set the following objectives:
To clarify the spatial distribution of cod species in the Arctic region and its relationship with the oceanographic environment using eDNA.
To clarify the fish community structure and find species boundaries in the open ocean across the western North Pacific to the Arctic using eDNA.
To evaluate the efficiency of novel eDNA collection methods such as passive sampling.

(3) Parameters
Fish environmental DNA

(4) Instruments and methods
(4.1) eDNA collection from seawater
In the Arcitic Ocean, eDNA samples were basically obtained from seawater collected using 12 L Niskin bottles mounted on the CTD/Carousel Water Sampling System (Table 3.3.17-1). Depths for water collection were basically determined as 5 m, the subsurface chlorophyll maximum (SCM), and the bottom layer. If the stations were located on the shelf slope or the Canada basin, seawater was additionally collected at middle depth deeper than 50 m. To enhance spatial resolution, the supplementary sampling was conducted in the regions where CTD was scarcely performed by collecting seawater continuously pumped up from about 5 m depth for the underway sea-surface monitoring. During the transit to Japan, the pumped seawater was continually collected in the same manner approximately 1–1.5° intervals (Table 3.3.17-1).
For each water sample, a clean, plastic tank or foldable plastic bag was filled with collected seawater. At each site and depth, the 5 L of water sample was filtered through a 0.45 μm pore size cartridge filters (Sterivex HV, Millipore, Billerica, MA, USA) in two replicates using a peristaltic tubing pump (Masterflex 07528-10, Cole-Parmer, IL, USA) at a flow rate of 100 mL/min. Filtration was halted when the 5 L of water was completely filtered or clogging became severe. After filtration, the filters were filled with 2.0 ml of RNAlater and then stored at −20 °C.
To prevent cross-contaminations, all equipment used for eDNA sampling was soaked in a 2% bleach solution (approximately 0.12% NaOCl) for at least 30 min and subsequently rinsed three times with Milli-Q water. The workspace was decontaminated using bleach disinfectant spray (approximately 0.1% NaOCl). For each water collection and filtration, disposable gloves and masks were used. Further,

1 L of Milli-Q water was also filtered as a negative control for every five sites as a basic to check for cross-contamination during the filtration process.
At Stations 1–5, eDNA collection specifically targeting microbial DNA was also conducted. In this case, 8 L of seawater collected from both the SCM and the bottom layer using a Niskin water sampler was filtered in two replicates onto 0.22 μm pore size cartridge filters (Sterivex GP, Millipore, Billerica, MA, USA), following the same procedure described above. The filters were subsequently stored at −80°C.

(4.2) Passive sampling
Cellulose sponges (Sponge-Stick, Neogen) were submerged in a 1.3 L plastic flow-through tank supplied with pumped seawater. Prior to deployment, the sponges were prepared by cutting them into approximately 1 cm cubes using sterile scissors. The sponge pieces were then either fixed to the bottom of the tank by inserting them into cable ties wrapped around a silicone tube or were left to float freely in the tank. The sponge pieces were generally deployed in the tank between eDNA sampling stations described in 4.1 (Table 3.3.17-2). Consequently, the deployment time varied from approximately 3 hours to 62 hours (median: 8.3 hours). The average flow rate was 3.4 L/min (standard deviation: 0.3 L/min), indicating that the total volume of water per deployment varied from 575 L to 12,670 L (median: 1,685 L).
During the transit to Japan, more porous cellulose sponges (AsOne), also cut into approximately 1 cm cubes, were submerged in the tank in parallel to investigate differences in sampling efficiency based on the substrate. Passive eDNA samples were stored at −20°C after removing excess water on a clean paper towel.
To prevent carry-over contamination, the tank was replaced before every sampling occasion with a sterilized one that had soaked in a 2% bleach solution and was subsequently rinsed with Milli-Q water.

(4.3) Evaluation of filtration efficiency
Two types of cartridge filters, Sterivex HV (PVDF, 0.45 μm) and Sterivex GP (PES, 0.22 μm), which differ in membrane material and pore size, were used for eDNA collection to compare their sampling efficiency. In addition, QuickConc and QuickConc Vacuum (AdvanSentinel, Osaka) were tested in parallel to evaluate their potential to enhance eDNA collection efficiency. This test was conducted at four sites, though the combinations of methods varied across these sites (Table 3.3.17-3).
Prior to filtration, approximately 80 L of pumped seawater was collected into eight 10 L foldable plastic bags. An equal volume of seawater was then dispensed into 5 L plastic tanks (for cartridge filters) or 5 L foldable plastic bags (for the QuickConc products) after gentle mixing to homogenize the eDNA composition. Five replicates were created for each method at each test site.
Filtration using the cartridge filters was performed according to Section 4.1. Processing seawater samples using the QuickConc products was carried out following the manufacturer's protocol. This protocol involves adding the QC solution and the glass fiber sheet (both included in the kit) to the sampled seawater, followed by a filtration through a provided disk filter.

(5) Station list

Table 3.3.17-1 Sampling sites for eDNA collection aimed at analyzing fish diversity and distribution.

Site name	Date (UTC)	Time (UTC)	Latitude	Longitude	Bottom depth (m)	Sampling depth (m)
St01	9/4	3:08:00	65-29.99N	168-44.99W	54.7	5, 15, 50
St02	9/4	8:30:00	66-00.07N	168-44.88W	53.2	5, 30, 48
St03	9/4	18:22:00	66-30.05N	168-45.19W	54	5, 49
St04	9/4	23:18:00	67-00.03N	168-45.04W	46	5, 10, 40
St05	9/5	4:06:00	67-29.99N	168-45.01W	50	5, 14, 44
St06	9/5	10:06:00	68-01.95N	168-49.98W	59	5, 25, 54
St07	9/5	15:36:00	68-29.97N	168-45.03W	53.8	5, 10, 49
St08	9/5	21:06:00	69-00.01N	168-44.89W	54	5, 15, 48
St09	9/6	4:28:00	69-30.01N	168-45.03W	52	5, 11, 46
St10	9/6	8:05:00	69-59.99N	168-44.97W	41	5, 23, 36
St11	9/6	12:24:00	70-29.98N	168-45.08W	38.3	6, 33, 34
St12	9/6	15:45:00	71-00.00N	168-44.90W	45	5, 27, 39
St13	9/6	19:44:00	70-45.17N	167-28.81W	55	5, 22, 49
St14	9/6	23:46:00	70-56.15N	165-24.33W	43	5, 20, 37
COMAI1	9/7	17:46:00	71-17.07N	160-59.99W	48.8	5
St15	9/8	22:13:00	71-41.73N	154-55.44W	111	5, 10, 50, 107
St16-cast1	9/10	17:01:00	72-01.79N	151-34.75W	2413	1001, 1999, 2436
St16-cast2	9/10	19:29:00	72-01.83N	151-34.69W	2426	5, 18, 50, 100
St17	9/10	23:32:00	71-42.73N	152-51.77W	229	5, 15, 51, 150, 227
St18	9/11	4:21:00	71-25.69N	154-06.63W	42	5, 20, 34
ICE1	9/11	17:45:00	71-55.10N	158-27.71W	57.2	5
St19	9/11	18:10:00	71-55.11N	158-27.72W	57.1	5, 25, 51
St20	9/11	22:20:00	72-11.35N	157-13.80W	122	5, 33, 50, 116
St21-cast1	9/12	2:02:00	72-29.04N	156-18.19W	1303	1001, 1303
St21-cast2	9/12	4:08:00	72-29.05N	156-18.07W	1299	5, 35, 51, 101
St22	9/12	16:16:00	71-45.25N	155-03.91W	274	6, 20, 51, 271
St24	9/12	22:31:00	71-29.80N	157-40.13W	82.8	6, 25, 51, 81
St27	9/13	5:06:00	71-10.40N	159-13.16W	95	5, 33, 50, 91
St28	9/13	9:16:00	71-10.03N	160-59.85W	48	5, 18, 43
St29	9/13	18:42:00	72-20.60N	163-07.63W	41	5, 22, 35
St30	9/13	23:57:00	73-02.27N	163-26.01W	98.8	5, 35, 50, 98
St31	9/16	16:10:00	74-47.51N	168-43.55W	196	5, 35, 50, 193
St32	9/16	22:27:00	74-42.46N	166-02.68W	422	5, 42, 50, 413
St33	9/17	18:15:00	75-56.77N	165-32.17W	445	5, 50, 436
St34	9/18	0:30:00	75-16.95N	164-06.44W	1466	5, 50, 100, 499, 1000, 1406
COMAI4	9/18	20:40:00	76-24.28N	164-28.29W	600	5
St35-cast1	9/20	21:36:00	74-31.86N	161-56.14W	1688	1000, 1250, 1501, 1699
St35-cast2	9/21	0:46:00	74-31.86N	161-56.92W	1686	5, 40, 100, 203, 500
St36	9/21	19:08:00	74-03.49N	158-51.79W	3454	5, 58, 100, 200, 499, 3504
WP	9/22	6:16:00	73-45.03N	165-03.09W	154.1	5
XCTD41	9/22	12:37:00	72-52.77N	168-24.37W	57.8	5
St37	9/22	14:44:00	72-29.99N	168-44.90W	58	6, 20, 53
XCTD43	9/22	21:16:00	71-29.11N	168-44.97W	48.6	5
BS01	9/24	12:12:00	65-00.37N	169-52.36W	49.9	5
BS02	9/24	19:30:00	63-54.86N	172-12.67W	55.6	5
BS03	9/25	3:05:00	62-32.64N	174-27.39W	70.7	5
BS04	9/25	9:36:00	61-26.44N	175-56.90W	100	5
BS05	9/25	18:05:00	60-00.14N	177-47.84W	139.5	5
BS06	9/26	0:07:00	59-03.03N	178-59.11W	3158	5
BS07	9/26	8:25:00	57-59.54N	179-32.26E	3742	5

BS08	9/26	18:57:00	56-24.46N	177-26.06E	3808	5
BS09	9/27	2:51:00	55-26.16N	175-12.55E	3877	5
BS10	9/27	10:17:00	54-25.66N	173-00.56E	3893	5
BS11	9/27	20:09:00	53-06.04N	170-46.52E	729	5
NP01	9/28	3:30:00	52-02.40N	169-18.23E	4747	5
NP02	9/28	11:17:00	50-57.57N	168-39.81E	2658	5
NP03	9/28	21:04:00	49-41.53N	167-15.63E	5316	5
NP04	9/29	5:08:00	48-55.66N	165-13.35E	5737	5
NP05	9/29	13:23:00	48-12.61N	162-55.59E	5718	5
NP06	9/29	22:01:00	47-09.48N	160-39.92E	5266	5
NP07	9/30	6:21:00	46-10.51N	158-20.17E	4860	5
NP08	9/30	13:55:00	45-01.16N	156-29.13E	4988	5
NP09	9/30	20:47:00	43-59.39N	155-02.89E	5332	5
NP10	10/1	5:53:00	42-58.90N	152-42.32E	5161	5
NP11	10/1	12:41:00	41-59.92N	151-07.04E	5097	5
NP12	10/1	21:05:00	40-48.72N	149-07.77E	5283	5
NP13	10/2	4:13:00	39-59.15N	147-12.57E	5307	5
NP14	10/2	12:50:00	39-04.05N	145-01.15E	5501	5
NP15	10/2	22:09:00	37-56.97N	142-41.08E	1307	5

Table 3.3.17-2 Summary of deployment locations (start/end coordinates) and elapsed time for passive samplings.

Sample ID	Latitude (start)	Longitude (start)	Latitude (end)	Longitude (end)	Elapsed time (h)	Total volume of water (L)
Passive01	65-29.99N	168-45.02W	66-00.05N	168-44.90W	5	1015
Passive02	66-00.05N	168-44.90W	66-43.76N	168-53.14W	8	1624
Passive03	66-43.76N	168-53.14W	67-00.05N	168-45.11W	7	1353
Passive04	67-00.05N	168-45.11W	67-29.99N	168-45.02W	5	1049
Passive05	67-29.99N	168-45.02W	68-01.95N	168-50.00W	6	1184
Passive06	68-01.95N	168-50.00W	68-33.46N	168-45.14W	6	1319
Passive07	68-33.46N	168-45.14W	68-59.99N	168-44.91W	4	913
Passive08	68-59.99N	168-44.91W	69-34.83N	168-44.62W	8	1675
Passive09	69-34.83N	168-44.62W	69-59.99N	168-44.96W	3	575
Passive10	69-59.99N	168-44.96W	70-29.98N	168-45.08W	4	846
Passive11	70-29.98N	168-45.08W	71-00.00N	168-44.89W	3	660
Passive12	71-00.00N	168-44.89W	70-45.17N	167-28.82W	4	812
Passive13	70-45.17N	167-28.82W	70-56.47N	165-19.51W	5	1032
Passive14	70-56.47N	165-19.51W	71-17.06N	160-59.99W	17	3451
Passive15	71-17.06N	160-59.99W	71-47.79N	155-27.20W	32	6580
Passive16	71-47.79N	155-27.20W	71-49.50N	155-55.41W	24	4906
Passive17	71-49.50N	155-55.41W	72-01.85N	151-34.80W	16	3349
Passive18	72-01.85N	151-34.80W	71-25.69N	154-06.65W	9	1928
Passive19	71-25.69N	154-06.65W	72-29.05N	156-18.08W	24	4787
Passive20	72-29.05N	156-18.08W	71-10.38N	159-23.78W	27	5396
Passive21	71-10.38N	159-23.78W	72-53.95N	163-26.35W	21	4195
Passive22	72-53.95N	163-26.35W	74-47.56N	168-43.64W	62	12670
Passive23	74-47.56N	168-43.64W	76-24.28N	164-28.30W	51	10370
Passive24	76-24.28N	164-28.30W	74-29.45N	161-56.79W	29	5921
Passive25	74-29.45N	161-56.79W	74-03.50N	158-51.78W	41	8424
Passive26	74-03.50N	158-51.78W	67-29.96N	168-30.05W	49	10042
Passive27	67-29.96N	168-30.05W	62-32.48N	174-27.61W	30	6147
Passive28	62-32.48N	174-27.61W	61-26.36N	175-57.00W	6	1120
Passive29	61-26.36N	175-57.00W	59-59.43N	177-48.69W	9	1736
Passive30	59-59.43N	177-48.69W	59-02.99N	178-59.19W	6	1211
Passive31	59-02.99N	178-59.19W	57-59.47N	179-32.17W	8	1685
Passive32	57-59.47N	179-32.17E	56-24.45N	177-26.03E	11	2138

Passive33	56-24.45N	177-26.03E	55-26.11N	175-12.43E	8	1604
Passive34	55-26.11N	175-12.43E	54-25.65N	173-00.55E	7	1509
Passive35	54-25.65N	173-00.55E	53-05.93N	170-46.34E	10	2003
Passive36	53-05.93N	170-46.34E	52-02.44N	169-18.23E	7	1492
Passive37	52-02.44N	169-18.23E	50-57.57N	168-39.81E	8	1580
Passive38	50-57.57N	168-39.81E	49-41.50N	167-15.59E	10	1986
Passive39	49-41.50N	167-15.59E	48-55.60N	165-13.17E	8	1638
Passive40	48-55.60N	165-13.17E	48-12.54N	162-55.43E	8	1675
Passive41	48-12.54N	162-55.43E	47-09.47N	160-39.89E	9	1753
Passive42	47-09.47N	160-39.89E	47-09.47N	160-39.89E	8	1692
Passive43	47-09.47N	160-39.89E	45-01.07N	156-29.03E	8	1536
Passive44	45-01.07N	156-29.03E	43-59.37N	155-02.87E	7	1394
Passive45	43-59.37N	155-02.87E	42-58.71N	152-41.94E	9	1827
Passive46	42-58.71N	152-41.94E	41-59.85N	151-06.93E	7	1401
Passive47	41-59.85N	151-06.93E	40-48.66N	149-07.65E	8	1705
Passive48	40-48.66N	149-07.65E	39-59.12N	147-12.49E	7	1448
Passive49	39-59.12N	147-12.49E	39-03.95N	145-00.91E	9	1749
Passive50	39-03.95N	145-00.91E	37-56.96N	142-41.07E	9	1891

Table 3.3.17-3 Summary of filtration trials for the evaluation of eDNA collection efficiency.

Site name	Date (UTC)	Time (UTC)	Latitude	Longitude	Bottom depth (m)	Trial		
						Sterivex HV	Sterivex GP	QuickConc
Test-A	9/1	22:42:00	55-39.28N	169-16.16W	2456	x		x
Test-B	9/9	22:15:00	71-44.56N	154-57.82W	185.4	x	x	x
Test-C	9/19	23:35:00	74-32.35N	161-55.81W	1701	x	x	
Test-D	9/23	20:48:00	67-29.96N	168-30.05W	48.6	x	x	x

(6) Preliminary results

During the cruise, eDNA samples for fish distribution analysis were obtained from a total of 40 sites, including 34 CTD stations in the Arctic Ocean and the vicinity of the Bering Strait (Table 3.3.17-1, Fig. 3.3.17-1). Samples were collected from multiple depths at the CTD stations, yielding 140 unique samples in total that covered all representative water masses present in the Pacific Arctic. These samples will be analyzed to estimate the distribution of cod species and other Arctic fish, thereby clarifying their distributional changes during the recent warming period.

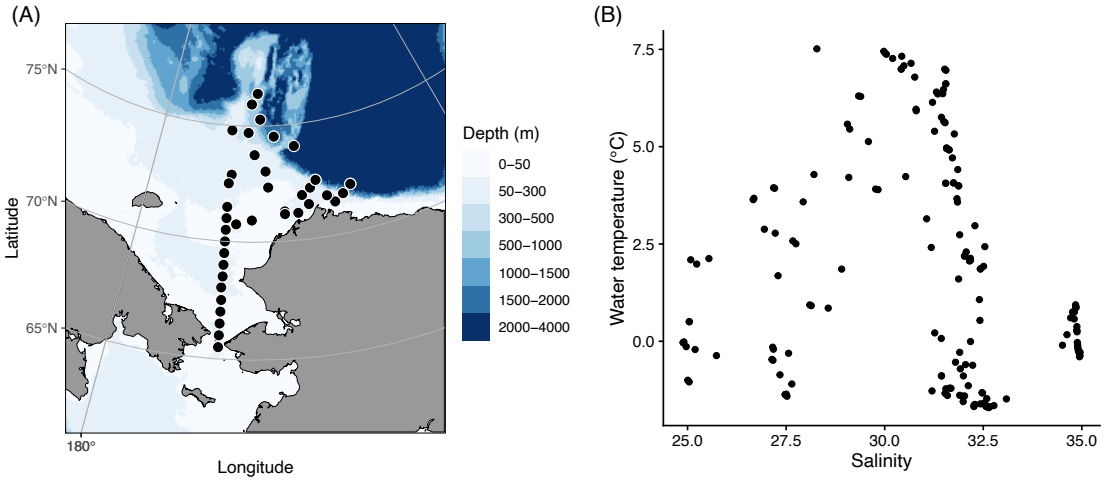

Fig. 3.3.17-1 (A) Locations of the sampling stations within the Arctic Ocean and the vicinity of the Bering Strait and (B) TS diagram for those stations.

We were also able to collect latitudinal eDNA samples across the Bering Sea and the western North Pacific (Table 3.3.17-1, Fig. 3.3.17-2). These collection sites effectively captured the latitudinal differences in water temperature and salinity, enabling us to investigate the species boundaries of pelagic fish across various water masses.

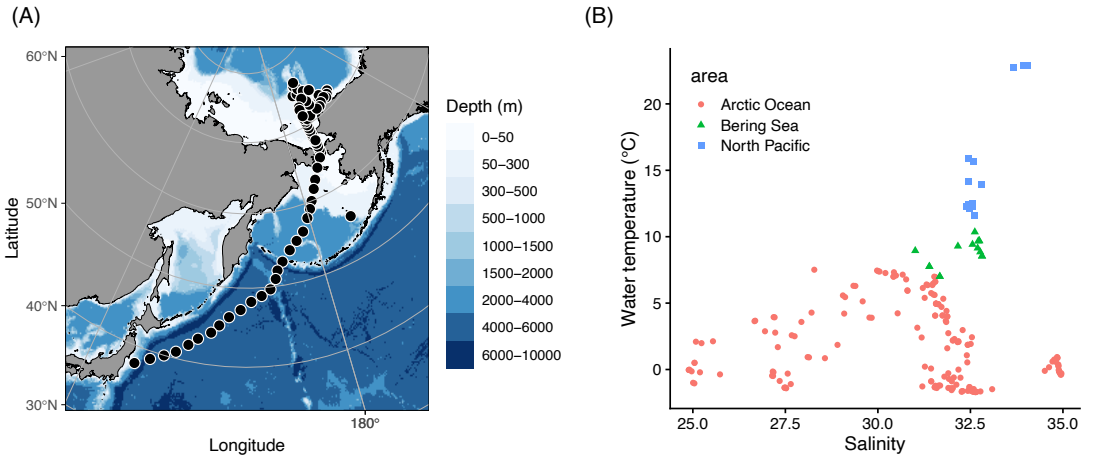

Fig. 3.3.17-2 (A) Locations of the sampling stations during the whole cruise and (B) TS diagram for those stations.

Along with the eDNA sampling, we also conducted several trials aimed at further improving onboard eDNA sampling in the Arctic Ocean (Tables 3.3.17-2, 3.3.17-3). The collection efficiency of these sampling methods will be evaluated by comparing them with the usual filtration method across various aspects, such as required effort and costs, extent of PCR inhibition, total amount of eDNA, amount of target eDNA, taxonomic diversity yielded by metabarcoding, and performance in detecting overall diversity change.

(5) Data archives

These data obtained in this cruise will be submitted to the Data Management

Group of JAMSTEC, and will be opened to the public via “Data Research System for Whole Cruise Information in JAMSTEC (DARWIN)” in JAMSTEC web site.
<https://www.godac.jamstec.go.jp/darwin/en/>

(6) References
Fossheim, M., Primicerio, R., Johannesen, E., Ingvaldsen, R. B., Aschan, M. M., & Dolgov, A. V. (2015). Recent warming leads to a rapid borealization of fish communities in the Arctic. Nature Climate Change, 5(7), 673–677. https://doi.org/10.1038/nclimate2647
Jeunen, G.-J., Mills, S., Mariani, S., Treece, J., Ferreira, S., Stanton, J.-A. L., et al. (2024). Streamlining large-scale oceanic biomonitoring using passive eDNA samplers integrated into vessel’s continuous pump underway seawater systems. Science of the Total Environment, 946, Article 174354. https://doi.org/10.1016/j.scitotenv.2024.174354
Kawakami, T., Yamazaki, A., Asami, M., Goto, Y., Yamanaka, H., Hyodo, S., et al. (2023a). Evaluating the sampling effort for the metabarcoding-based detection of fish environmental DNA in the open ocean. Ecology and Evolution, 13(3), Article e9921. https://doi.org/10.1002/ece3.9921
Kawakami, T., Yamazaki, A., Jiang, H.-C., Ueno, H., & Kasai, A. (2023b). Distribution and habitat preference of polar cod (*Boreogadus saida*) in the Bering and Chukchi Seas inferred from species-specific detection of environmental DNA. Frontiers in Marine Science, 10, Article 1193083. https://doi.org/10.3389/fmars.2023.1193083
Levine, R. M., De Robertis, A. D., Grünbaum, D., Wildes, S., Farley, E. V., Stabeno, P. J., et al. (2023). Climate-driven shifts in pelagic fish distributions in a rapidly changing Pacific Arctic. Deep Sea Research Part II: Topical Studies in Oceanography, 208, Article 105244. https://doi.org/10.1016/j.dsr2.2022.105244

3.3.18 Carbon fixation

3.3.18.1 Carbon fixation from surface water to the bottom

(1) Personnel
Takuhei Shiozaki (AORI, The University of Tokyo) - Principal Investigator

(2) Objective
This study aims to examine carbon fixation and nitrification from surface to the bottom water of the Arctic Ocean.

(3) Methods
Water samples were collected from depths corresponding to 100%, 10, 1, and 0.1% of surface light intensity, as well as from 500m, 1000m, 3000m, and near-bottom depth using Niskin-X bottles and a bucket for surface samples. The depth profiles of light intensity were obtained using a CTD-attached PAR sensor just before the sampling. We collected samples for the analysis of DNA, nutrient and chlorophyll *a* concentrations, and incubation experiments from all depth.
Samples for DNA (4–10 L) were filtered onto 0.2-μm pore Sterivex-GP pressure filters (Millipore). Samples for nutrient concentration were collected into duplicate 10-mL tubes. Samples for chlorophyll *a* (290 mL) were filtered onto GF/F filters (Advantec). Chlorophyll *a* concentrations were determined fluorometrically onboard

using a 10-AU fluorometer (Turner Designs, San Diego, CA, USA) on board after extraction with N,N-dimethylformamide.
Samples for determining carbon fixation rate were collected into duplicate 1.2-L polycarbonate bottles from depths corresponding to 100%, 10, 1, and 0.1% of surface light intensity and into 2.3-L polypropylene bottles from other depths. Then, they were added ^{13}C-labeled sodium bicarbonate at a final concentration of 200 μmol L^{-1}. Samples for determining nitrification rate were collected into duplicate 0.3-L polycarbonate bottles. Then, ^{15}N-labeled ammonium was added to the bottles to reach final concentration of 99 nmol N L^{-1}. Additionally, ammonium and amino acids were introduced into separate water samples at the 0.1% light depth and at 1000 m to assess their effects on carbon fixation. Samples collected 100%, 10%, and 1% light depths were covered with neutral-density screens to adjust the light intensity and incubated in an on-deck incubator which filled with flowing surface seawater. Samples collected from other depths were incubated temperature-controlled incubator at 0ºC under dark condition. The incubation time was 24 hr.
The incubations for carbon fixation were terminated by filtration onto pre-combusted GF/F filters (Advantec). The samples for nitrification were filtered through a 0.2-μm pore size cellulose acetate in-line filter (Dismic, Advantec MFSTM), and the filtrates were collected in 50-mL polypropylene bottles for isotope measurement and in 10-mL acrylic tubes for measurement of the nitrate + nitrite concentration. The filters and filtrates were frozen at −20ºC and transported to an onshore laboratory.

(3) Data archive
These data obtained in this cruise will be submitted to the Data Management Group of JAMSTEC when ready.

3.3.18.2 Carbon fixation linked to atmosphere-ocean interactions

(1) Personnel
Yuri Fukai (JAMSTEC) - Principal Investigator
Amane Fujiwara (JAMSTEC)
Fumikazu Taketani (JAMSTEC)

(2) Objectives
We aimed to investigate the potential contribution of nitrogen nutrients from snow to primary production in surface waters. On-deck incubation experiments simulating snowfall were conducted to examine atmosphere–ocean interactions.

(3) Parameters
Carbon uptake rate
Nitrate uptake rate

(4) Instruments and methods
Seawater for incubation experiments was collected from surface using a bucket. Aliquots of 500 mL of seawater were transferred into polycarbonate bottles, and $NaH^{13}CO_3$ was added to a final concentration of 0.02 g L^{-1} as a tracer to measure carbon uptake. Snow collected as described in Section 3.1.4 or $Na^{15}NO_3$ was added to the bottles as nutrient sources for primary production, except for control bottles. Snow was added at approximately 1% of the seawater volume, and $Na^{15}NO_3$ was

added to final concentrations of 1 μmol L^{-1} or 0.1 μmol L^{-1}. Incubations were conducted on deck for approximately 24 hours under in situ sea surface temperature and light conditions. After the incubation, phytoplankton were collected on pre-combusted glass fiber filters (GF-75, φ25 mm, Advantec). Carbon and nitrate uptake rates will be later analyzed using an elemental analyzer/isotope ratio mass spectrometer (EA/IRMS; Elementar).

(5) Experiment location

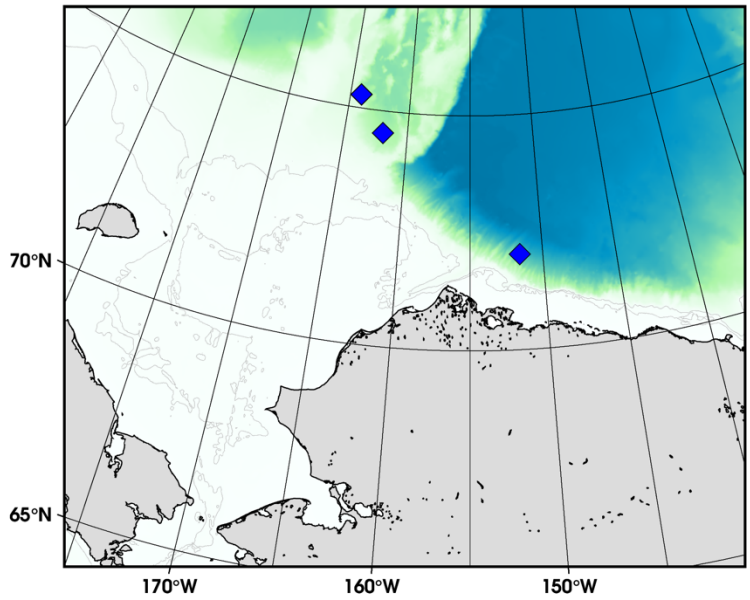

Figure 3.3.18.2-1. Location where the incubation experiments were conducted.

(6) Data archives

These data obtained in this cruise will be submitted to the Data Management Group of JAMSTEC, and will be opened to the public via "Data Research System for Whole Cruise Information in JAMSTEC (DARWIN)" in JAMSTEC web site.
<https://www.godac.jamstec.go.jp/darwin/en/>

3.3.19. Sediment dynamics and paleoceanography: sampling of sediments, near-bottom water, and brash sea ice

(1) Personnel

Jean-Carlos Montero-Serrano (Institut des sciences de la mer-ISMER, Université du Québec à Rimouski-UQAR, Canada) - Principal investigator
Takuhei Shiozaki (Atmosphere and Ocean Research Institute-AORI, The University of Tokyo)
Yusuke Yokoyama (Atmosphere and Ocean Research Institute- AORI, The University of Tokyo) - Not on board
Guillaume St-Onge (Institut des sciences de la mer-ISMER, Université du Québec à Rimouski-UQAR, Canada) - Not on board

(2) Context and objectives

The Arctic Ocean is experiencing rapid environmental change driven by anthropogenic warming. Key impacts include reduced summer sea ice, permafrost thaw, increased river discharge, and rising sea levels. These changes are intensifying coastal erosion, enhancing ice rafting, and altering sediment transport pathways, ultimately reshaping marine sedimentary dynamics. To place these recent changes in a longer-term perspective, scientists employ marine sediment cores to reconstruct past environmental conditions and elucidate the responses of Arctic systems to natural climate variability. During the MR25-05C expedition, sediment sampling using the Ashura multi-corer was carried out to investigate the origin, transport, and dynamics of detrital sediments in the Bering Strait and Chukchi Sea, in relation to climate variability over the past two millennia. Near-bottom water samples were sampled to characterize the mineralogical and geochemical composition of suspended matter and to assess the role of the benthic nepheloid layer in the lateral transport of fine sediments across these regions. Additionally, three brash sea ice samples from different stations were collected to determine the provenance of sediment-laden sea ice and to calibrate sediment transport proxies in sea-ice–derived material within sediment cores.

(3) Parameters
-The sedimentological framework of the cores will be established through physical (X-ray radiography, high-resolution imaging, bulk density, color, magnetic susceptibility) and chemical (pXRF) analyses, along with grain-size measurements.
-Sediment provenance, both modern and past, will be assessed using quantitative mineralogy and elemental geochemistry on bulk and clay fractions from cores.
-Mineralogical and trace-element signatures, including Rare Earth Elements, will be determined on near-bottom suspended particles.
-Grain size and mineralogical composition will also be analyzed in sediment-laden sea ice.

(4) Instruments and methods
Sediment cores. - A multi-corer system (ASHURA) was used to collect short sediment cores (Figure 3.3.19-1A-B). During the MR25-05C expedition, this system was only suitable for sampling at water depths less than 200 meters, due to the limited length of the winch cable onboard the *R/V Mirai*. The system is designed to minimize disturbance at the sediment-water interface. It consists of a main body weighing 60 kg and three acrylic core tubes. Each core barrel is 60 cm long with an inner diameter of 7.4 cm. However, because of its design, the system can only retrieve cores up to 32 cm in length.

During the expedition, the ASHURA multiple-corer system was operated by the joint team from ISMER-UQAR (Jean-Carlos Montero-Serrano) and AORI (Takuhei Shiozaki). Core sampling sites were strategically selected near CTD stations, with a focus on areas previously identified as having significant Late Holocene sediment accumulation (e.g., Trefry et al., 2014; Lisé-Pronovost et a;., 2019; Astakhov et al. 2019; Su et al., 2023; Ren et al., 2025).

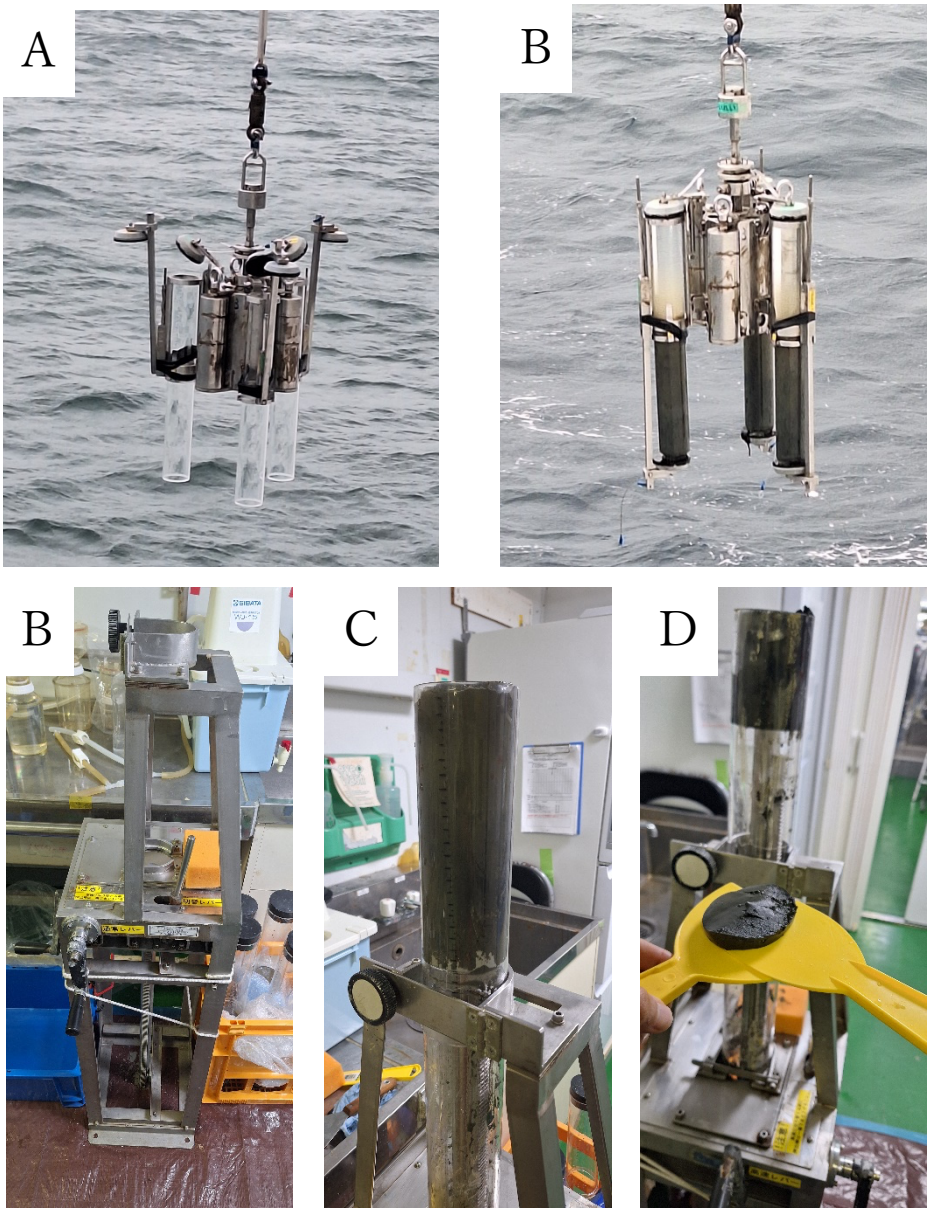

Figure 3.3.19-1. (A-B) Deployment of the ASHURA multi-corer during the MR25-05C expedition. (C–D) Core extrusion in the laboratory. (D) highlights a 1 cm sediment layer. (Photos: J.-C. Montero-Serrano).

The ASHURA corer system was deployed following the standardized JAMSTEC protocol to minimize disturbance of the sediment-water interface. The system was lowered at an initial speed of 0.5-1.0 m $\cdot s^{-1}$. Upon reaching approximately 10 m above the seafloor, the descent was paused for stabilization—30 seconds at stations 3, 4, 6, 7, 9, 11, and 12, and 90 seconds at the remaining stations—to reduce pendulum motion. Most uniform sediment cores and better penetration were obtained after a 90-second pause. Following stabilization, the descent resumed at a reduced speed of 0.3 m $\cdot s^{-1}$ while monitoring the tension meter for bottom contact. Once contact was confirmed, an additional 3-5 m of slack was introduced to allow wire bowing.

Recovery began at a dead-slow speed (0.3 m·s^{-1}) to minimize disturbance, then increased to 0.5-1.0 m·s^{-1} for the remainder of the retrieval.

At each station, three sediment cores were retrieved. The longest of the three was preserved for physical property analyses, while the remaining two were extruded onboard (Figure 3.3.19-1B-D). The upper 12 cm of each core were sliced at 1 cm intervals, and the remaining sections was cut every 2 cm down to the base using a plastic spatula. Samples were placed in plastic bags. Each core and sediment subsamples were stored at 4 °C in the geology store refrigerator to preserve sample integrity for subsequent laboratory analyses.

Near-bottom water sampling and filtration procedure. – Water sampling and vertical profiling were conducted using a rosette system equipped with multiple sensors capable of measuring conductivity, temperature, pressure, dissolved oxygen, fluorescence, beam transmission, turbidity, nitrate concentration, and photosynthetically active radiation or PAR (Figure 3.3.19-2A). The system included 36 Niskin bottles of 12 liters each (Sea-Bird Electronics, Inc.), allowing for the collection of water samples at targeted depths. This setup enabled the acquisition of high-resolution data on various physico-chemical parameters throughout the water column, supporting the characterization of water masses and suspended particulate matter. Approximately 4 L of water were collected on the shelf (up to ~ 100 m) and 8–17 L in deeper areas, from 5 and 10-20 m above the seafloor, respectively, to characterize suspended particulate matter near the bottom. Samples were transferred directly from the Niskin bottles into two 2 L Nalgene bottles that had been pre-rinsed with Milli-Q water (18.2 MΩ·cm) and subsequently rinsed twice with sample water prior to collection. Filtration was immediately performed using 0.45 µm Sartorius cellulose acetate filters mounted on a Thermo Scientific™ Nalgene™ polycarbonate filter holder (500 mL capacity), coupled with a Sibata WJ-15 vacuum aspirator to ensure consistent suction during the process (Figure 3.3.19-2B). The entire setup (filter holder and filter) was rinsed twice with Milli-Q water prior to filtering the samples. Each sample required between 2 and 3 hours to filter. Blank controls using Milli-Q water from the onboard system of the *R/V Mirai* were performed at various stations to monitor potential contamination during filtration and to verify the overall cleanliness of the procedure. After filtration, the filters were rinsed with 500 mL of Milli-Q water to remove sea salts, dried in a laboratory oven at 40 °C for 48 hours, photographed (Figure 3.3.19-2C), and stored in sterile Petri dishes until further analysis. Filters will be weighed in the laboratory to determine suspended particulate matter concentrations.

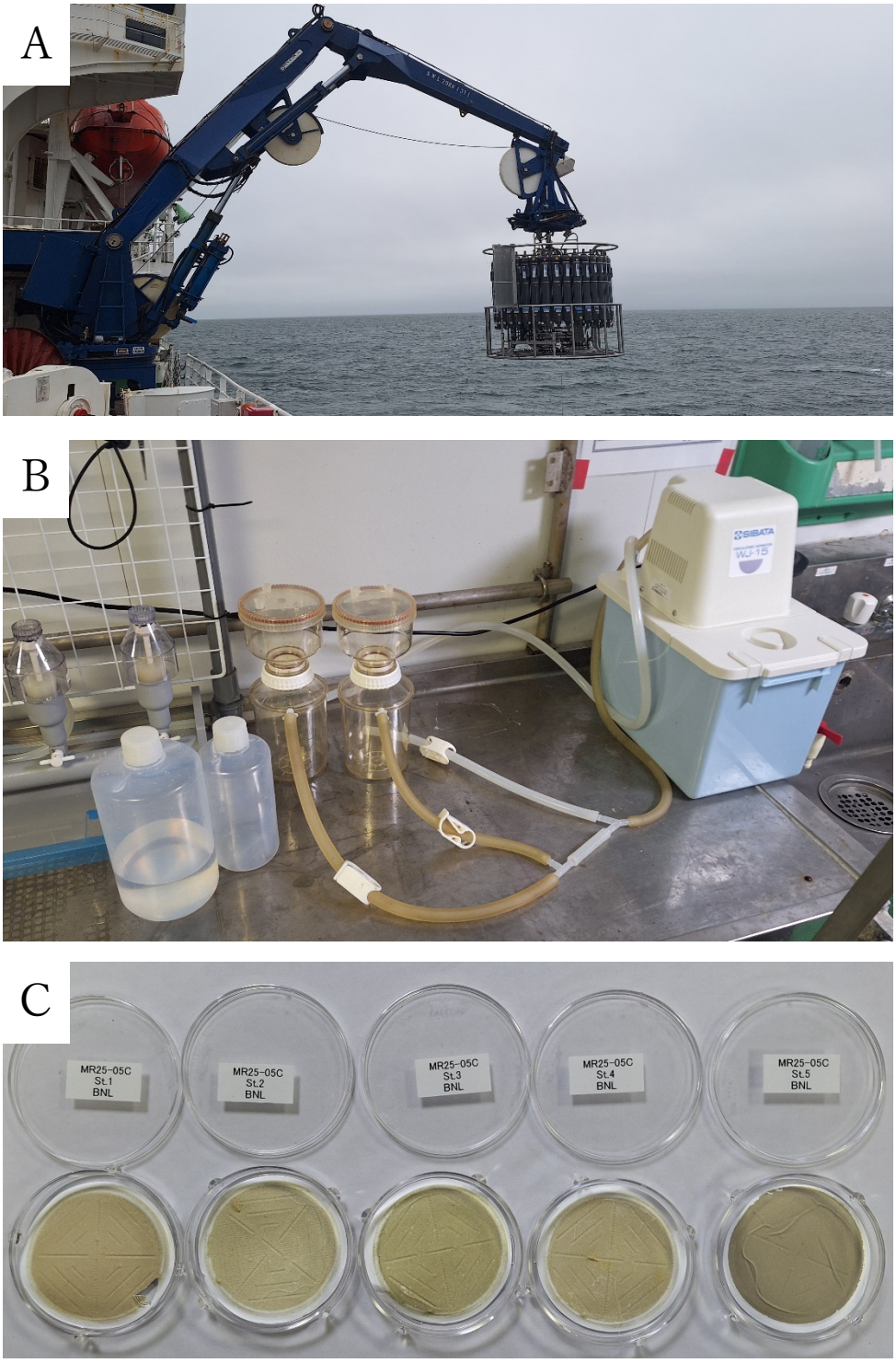

Figure 3.3.19-2. (A) Deployment of the rosette system during the MR25-05C expedition. (B) Laboratory setup for water sample filtration. (C) Examples of filtered water samples from stations 1 to 5. (Photos: J.-C. Montero-Serrano).

Brash sea ice sampling. – Sea-ice samples (each ~1 m^3) were collected using a wire mesh pallet cage (1.2 × 1.0 × 0.9 m) deployed with the ship's crane (Figure 3.3.19-

3A-B). A subsample (~20-30 cm^3) was placed in double plastic bags and melted in a container with hot water. The resulting meltwater was filtered through 0.45 µm Sartorius cellulose acetate filters mounted on a Thermo Scientific™ Nalgene™ polycarbonate filter holder (500 mL capacity), connected to a Sibata WJ-15 vacuum aspirator. After filtration, the filters were rinsed with 500 mL of Milli-Q water to remove sea salts, dried in a laboratory oven at 40 °C for 48 hours, photographed (Figure 3.3.19-3C-D), and stored in sterile Petri dishes until further analysis.

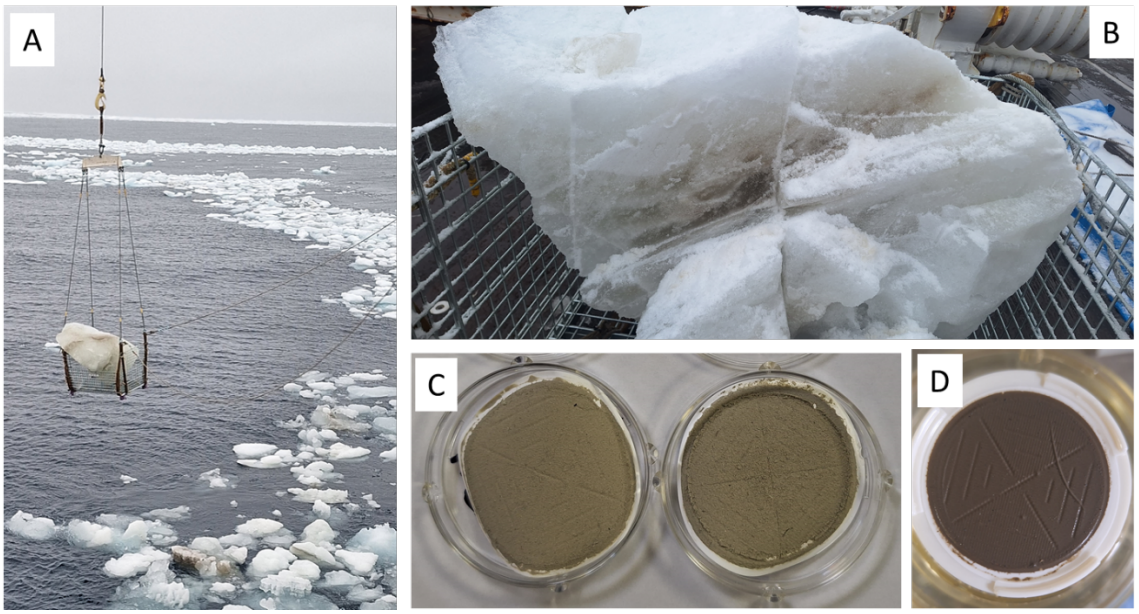

Figure 3.3.19-3. (A) Collection of brash ice using a wire mesh pallet cage near station 36 during the MR25-05C expedition. (B) Brash ice sample on the bridge prior to subsampling. (C-D) Filters from stations 19 and 36 showing sediments incorporated into the ice. (Photos: J.-C. Montero-Serrano).

(5) Preliminary results and future plans

Sediment cores were collected at 15 sites across the Bering Strait, Chukchi Shelf and Slope (Figure 3.3.19-4; Table 3.3.19-1). The median length of the longest cores recovered at each station was approximately 27 cm. At stations 3 and 11, the seabed was predominantly sandy, with minimal accumulation of fine-grained sediments. In stations 3 and 31, small rock fragments were observed at the top of the cores. The sediments primarily consist of dark olive gray sandy mud (Munsell color: 5Y 3/2 to 3/1). Toward the base of the cores, the sediment becomes slightly darker, denser, and more compact. With the exception of stations 3, 9, 20 and 31, all cores contain different intervals with shell fragments. Two live mollusks (likely *Macoma calcarea;* Koch et al., 2025) were retrieved from surface sediments at station 19 (west of Barrow Canyon; Figure 3.3.19-5). These specimens will be useful for validating reservoir radiocarbon ages in a region where only two data points currently exist (McNeely et al., 2006). Based on previously reported sedimentation rates in similar coring sites within the region (0.4 to 1.5 mm/yr; Trefry et al., 2014; Astakhov et al. 2019; Su et al., 2023; Ren et al., 2025), it is likely that many of the cores collected

during this expedition span the last two millennia.

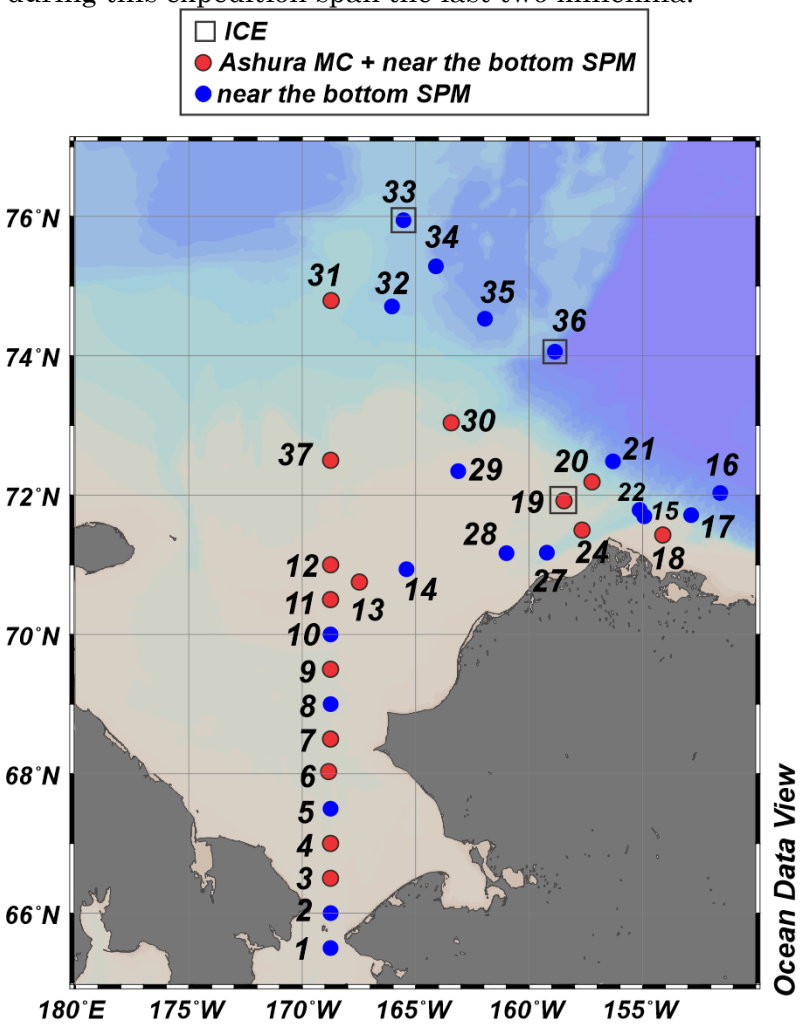

Figure 3.3.19-4. Location of the all samples collected during the MR25-05C expedition. For samples details see Tables 3.3.19-1 to 3.

Figure 3.3.19-5. Photograph of the telinid clam *Macoma calcarea* found alive in the surface sediments of Station 19 in west of Barrow Canyon. (Photo: J.-C. Montero-Serrano).

All of these sediment core samples will be analyzed in detail in the laboratory at

ISMER-UQAR to achieve the objectives of this expedition. Briefly, sediment samples will be studied for their physical (X-ray radiography, high-resolution images, bulk density, sediment color, and magnetic susceptibility), mineralogical (bulk and clay fraction), geochemical (majors and trace elements), and siliciclastic grain-size signatures. The chronology of sediment cores will be established using ^{210}Pb-^{137}Cs measurements and radiocarbon (^{14}C) dating on shell fragments. Such studies will to provide foundational information to improving our understanding on the past and present seafloor sediment composition, sediment transport processes, and sedimentation history of the Bering Strait and Chukchi Shelf/Slope over the past two millennia.

Table 3.3.19-1. Summary of recovered core samples. Site numbers correspond to the locations shown in Figure 3.3.19-4.

MR25-05C St. #	Short-ID	Date [yyyy/mm/dd]	Time UTC [hh:mm]	Latitude [°N]	Longitude [°W]	Water depth [m]	Length [cm]			Cores extruded	Instervals with shell fragments [cm]
							A	B	C		
3	St.03-MC	2025-09-04	19:07	66.500	-168.753	54	10	8	Failed	A, B, C	Not observed
4	St.04-MC	2025-09-04	23:01	67.001	-168.751	46	22	10	7.5	A, B, C	A: 4-5; 5-6; 8-9; 12-14 // B: 2-3; 6-7; 7-8 // C: 2-3; 4-5
6	St.05-MC	2025-09-05	10:06	68.033	-168.833	59	31	19	20.5	B, C	B: 8-9; 12-14; 18-19 // C: 6-7; 8-9; 12-14; 14-16; 16-18; 18-20
7	St.07-MC	2025-09-05	15:36	68.500	-168.751	54	31	21	17	B, C	C: 6-7; 10-11
9	St.09-MC	2025-09-06	04:06	69.500	-168.750	52	19	16.5	13	B, C	Not observed
11	St.11-MC	2025-09-06	12:01	70.500	-168.750	38	12.5	9	9	A, B, C	A: 7-8 // B: 5-6; 6-7 // C: 6-7; 7-8
12	St.12-MC	2025-09-06	16:41	71.000	-168.749	45	25	13	16	B, C	C: 7-8
13	St.13-MC	2025-09-06	19:19	70.753	-167.481	54	27	21	19	B, C	B: 12-14 // C: 0-1;7-8; 11-12; 14-16
18	St.18-MC	2025-09-11	03:58	71.429	-154.112	41	36	21.5	23	B, C	B: 5-6 // C: 9-10, core bioturbated
19	St.19-MC	2025-09-11	19:09	71.919	-158.462	57	26	21.5	16	B, C	B: 4-5 (live); 5-6; 16-18 // C: 0-1 (live); 5-6
20	St.20-MC	2025-09-11	21:54	72.189	-157.229	122	34	32	28	B, C	Not observed
24	St.24-MC	2025-09-12	23:10	71.497	-157.668	82	29.5	26	26.5	A, B	Surface very bioturbaded. Less bioturbation below 5-6 cm (A) and 6-7 cm (B)
30	St.30-MC	2025-09-13	23:33	73.038	-162.434	98	29.5	19.5	19.5	B, C	B: 8-9
31	St.31-MC	2025-09-16	17:32	74.794	-168.728	201	33.5	31.5	31	C	A: surface remobilized by a rock fragment
37	St.37-	2025-09-22	15:36	72.500	-168.750	58	25.5	26	26	B, C	B: 1-2; 6-7

	MC										

Near-bottom suspended particles were collected at 36 sites across the Bering Strait, Chukchi Shelf, Barrow Canyon, and Northwind Abyssal Plain regions (Figure 3.3.19-4; Table 3.3.19-2). Samples were taken 5 m above the seafloor on the shelf and 10–20 m above the seafloor on the slope and in the deep basin. Dried filters from near-bottom water samples exhibit a range of colors, from light beige (Munsell: 10YR 8/2) to greenish (5GY 6/4–5GY 5/4) and darker beige/tan (10YR 6/3) hues (Figure 3.3.19-2C). This variation in coloration likely reflects differences in inorganic and organic particulate matter among sampling sites. The greenish tint observed on several filters is likely associated with chlorophyll pigments, which are abundant in Arctic shelf waters. All filter samples will be analyzed at ISMER-UQAR for their mineralogical and trace element (including rare earth elements) signatures.

Table 3.3.19-2. Summary of recovered near-bottom suspended particles samples. Site numbers correspond to the locations shown in Figure 3.3.19-4.

MR25-05C St. #	Date [yyyy/mm/dd]	Time [hh:mm]	Latitude [°N]	Longitude [°W]	Water depth [m]	Water depth sampled [m]	Filtered volume [L]
1	2025-09-04	03:08	65.500	-168.750	55	50	4.0
2	2025-09-04	08:30	66.001	-168.748	53	48	4.3
3	2025-09-04	18:22	66.501	-168.753	54	49	4.0
4	2025-09-04	23:18	67.001	-168.751	46	40	4.3
5	2025-09-05	04:06	67.500	-168.750	50	45	4.5
6	2025-09-05	10:06	68.033	-168.833	59	54	4.4
7	2025-09-05	15:36	68.500	-168.751	54	49	4.0
8	2025-09-05	21:06	69.000	-168.748	54	48	4.2
9	2025-09-06	04:28	69.500	-168.751	52	46	4.5
10	2025-09-06	08:05	70.000	-168.750	41	36	4.1
11	2025-09-06	12:24	70.500	-168.751	40	34	4.4
12	2025-09-06	15:45	71.000	-168.748	45	39	4.4
13	2025-09-06	19:44	70.753	-167.480	55	49	4.3
14	2025-09-06	23:46	70.936	-165.406	43	37	4.3
15	2025-09-08	22:13	71.696	-154.924	111	107	4.4
16	2025-09-10	17:01	72.030	-151.579	2436	2413	8.5
17	2025-09-10	23:32	71.712	-152.862	229	227	8.1
18	2025-09-11	4:21	71.428	-154.111	42	34	4.5
19	2025-09-11	18:10	71.919	-158.462	57	51	4.5
20	2025-09-11	22:20	72.189	-157.230	122	116	4.4
21	2025-09-12	2:02	72.484	-156.303	1303	1293	8.3
22	2025-09-12	16:16	71.754	-155.065	274	271	4.4
24	2025-09-12	22:31	71.497	-157.669	83	81	4.5
27	2025-09-13	5:06	71.173	-159.219	95	91	4.5
28	2025-09-13	9:16	71.167	-160.998	48	43	4.6
29	2025-09-13	18:42	72.343	-163.127	41	35	4.5
30	2025-09-13	23:57	73.038	-163.434	99	98	4.6
31	2025-09-16	16:10	74.792	-168.726	196	193	9.0

32	2025-09-16	22:27	74.708	-166.045	422	413	8.8
33	2025-09-17	18:15	75.946	-165.536	445	436	8.5
34	2025-09-18	0:30	75.283	-164.107	1419	1406	16.7
35	2025-09-20	21:36	74.531	-161.936	1699	1688	17.1
36	2025-09-21	19:08	74.058	-158.863	3504	3454	17.1
37	2025-09-22	14:44	72.500	-168.749	58	53	7.5
37	2025-09-22	14:44	72.500	-168.749	58	53	1.1
37	2025-09-22	14:44	72.500	-168.749	58	53	0.4

Brash sea-ice samples were collected at three sites: near station 19 in the Barrow Canyon and near stations 33 and 36 in the Northwind Abyssal Plain (Figure 3.3.19-4; Table 3.3.19-3). Filter images from stations 19 and 36 reveal distinct color differences (Figure 3.3.19-3C-D). Sediments from station 19 appear coarser and light brown, whereas those from station 36 are finer-grained and darker, suggesting two different sediment sources. Very little sediments were found in the ice sample from station 33.

Table 3.3.19-3. Summary of recovered brash sea ice samples. Site numbers correspond to the locations shown in Figure 3.3.19-4.

MR25-05C St. #	Short-ID	Date [yyyy/mm/dd]	Time [hh:mm]	Latitude [°N]	Longitude [°W]
19	St. 19-ICE-1	2025-09-11	16:45	71.915	-158.474
33	St. 33-ICE-1	2025-09-17	16:34	75.945	-165.730
	St. 33-ICE-3				
36	St. 36-ICE-2	2025-09-21	16:55	74.056	-158.815

(6) References

Astakhov, A.S., Bosin, A.A., Liu, Y.G., Darin, A.V., Kalugin, I.A., Artemova, A.V., Babich, V.V., Melgunov, M.S., Vasilenko, Yu P., Vologina, E.G. (2019). Reconstruction of ice conditions in the northern Chukchi Sea during recent centuries: geochemical proxy compared with observed data. Quat. Int. 522, 23–37. https://doi.org/ 10.1016/j.quaint.2019.05.009.

Koch, C.W., Sonsthagen, S.A., Cooper, L.W., Grebmeier, J.M., Riddle-Berntsen, A.E., Cornman, R.S. (2025). Prevalence of pelagic diatoms and harmful algae in tellinid bivalve diets during record low sea ice in the Pacific Arctic determined by DNA metabarcoding. Front. Mar. Sci. 12:1480327. doi: 10.3389/fmars.2025.1480327

Lisé-Pronovost, A., St-Onge, G., Brachfeld, S., Barletta, F., Darby, D. (2009). Paleomagnetic constraints on the Holocene stratigraphy of the Arctic Alaskan margin. Global and Planetary Change 68: 85–99. https://doi.org/10.1016/j.gloplacha.2009.03.015

McNeely, R., Dyke, A.S., Southon, J.R. (2006). Canadian marine reservoir ages, preliminary data assessment, Open File 5049, pp. 3. Geological Survey Canada.

Ren, P., Hillaire-Marcel, C., Wang, M., Shan, S., Zhao, S., Song, T., Dong, L., Wang, X., & Liu, Y. (2025). Sources, transport, age, and evolution of terrestrial organic carbon across the Chukchi Sea margin, Arctic Ocean. Global and Planetary Change, 253, 104978. https://doi.org/10.1016/j.gloplacha.2025.104978

Su, L., Ren, J., Sicre, M.-A., Bai, Y., Zhao, R., Han, X., Li, Z., Jin, H., Astakhov, A. S., Shi, X., & Chen, J. (2023). Changing sources and burial of organic carbon in the Chukchi Sea sediments with retreating sea ice over recent centuries, Climate of the Past 19, 1305–1320, https://doi.org/10.5194/cp-19-1305-2023
Trefry, J. H., Trocine, R. P., Cooper, L. W., & Dunton, K. H. (2014). Trace metals and organic carbon in sediments of the northeastern Chukchi Sea. Deep-Sea Research Part II: Topical Studies in Oceanography, 102, 18–31. https://doi.org/10.1016/j.dsr2.2013.07.018.

(7) Data archives
These data obtained in this cruise will be submitted to the Data Management Group (DMG) of JAMSTEC, and will opened to the public via "Data Research System for Whole Cruise Information in JAMSTEC (DARWIN)" in JAMSTEC web site: https://www.godac.jamstec.go.jp/darwin/en/

3.3.20. Sea ice biogeochemistry

(1) Personnel
Amane Fujiwara (JAMSTEC) – Principal investigator
Daiki Nomura (Hokkaido University)
Yuri Fukai (JAMSTEC)
Satoshi Kimura (JAMSTEC)
Mariko Hatta (JAMSTEC)
Aymeric Servettaz (JAMSTEC)
Ryota Akino (Hokkaido University)
Tatsuya Kawakami (Hokkaido University)
Jean-Carlos Montero-Serrano (Université du Québec à Rimouski)
Ikkan Kamiyama (Tokyo University of Marine Science and Technology)
Aymeric Servettaz (JAMSTEC)

(2) Objective
Arctic sea ice is undergoing significant alterations, characterized by rapid reductions in summer sea ice extent and a transition toward a predominance of younger, thinner first-year ice instead of thick multi-year ice. While the influence of sea ice formation and melting on biogeochemical cycles in the ocean has been previously explored, the specific impacts of sea ice melt processes on the biogeochemistry of the surface waters remain inadequately understood. Consequently, this study involved the collection of sea ice samples during the melt season.

(3) Parameters
Ice temperature
Ice salinity
carbonate chemistry (DIC and TA)
Oxygen isotopic ratio
Dissolved nitrogen isotopic ratio
Nutrient concentration
Chl-a concentration
Organic/Inorganic Particle weight

Algal community structure and seed
Environmental DNA
Particulate organic carbon/nitrogen
CDOM/FDOM
Particle Organic Carbon (POC)
Suspended Particulate Matter (SPM)
Scanning Electron Microscope (SEM)
Transparent Expolymer Particle (TEP)
Thick/Thin section

(4) Instruments and methods
Floating sea ice samples were collected at an ice-edge site (Table 3.3.20-1 and Figures 3.3.20-1) utilizing a wire mesh pallet cage (1.2 x 1.0 x 0.9 m) deployed via the ship's crane. The temperatures of the ice samples were measured immediately post-collection using a needle-type temperature sensor.
The collected sea ice samples were cut into smaller pieces using ice thaw, with some allocated for the measurement of vertical profiles of biogeochemical properties on board. These samples were melted under dark and cool conditions (temperature = ~2 °C), and subsequent analyses will be conducted on the melted water for salinity, nutrient concentrations, chlorophyll-a, and particulate weight. The remaining samples were stored frozen for later analysis of the aforementioned biogeochemical parameters on land.

(5) Observation log and the sampling sites
Table 3.3.20-1 List of ice sampled location and time

Ice ID	Sampled date & time [UTC]	Sampled location
ICE1-1	2025/9/11 16:45	71-54.92379N, 158-28.44495W
ICE1-2	2025/9/11 17:25	71-54.90301N, 158-28.36658W
ICE2-1	2025/9/17 16:26	75-56.73745N, 165-43.69423W
ICE2-2	2025/9/17 16:51	75-56.70236N, 165-43.86357W
ICE2-3	2025/9/17 17:26	75-56.59659N, 165-43.19952W
ICE3-1	2025/9/21 16:54	74-03.38159N, 158-48.90039W
ICE3-2	2025/9/21 17:14	74-03.35852N, 158-48.91943W

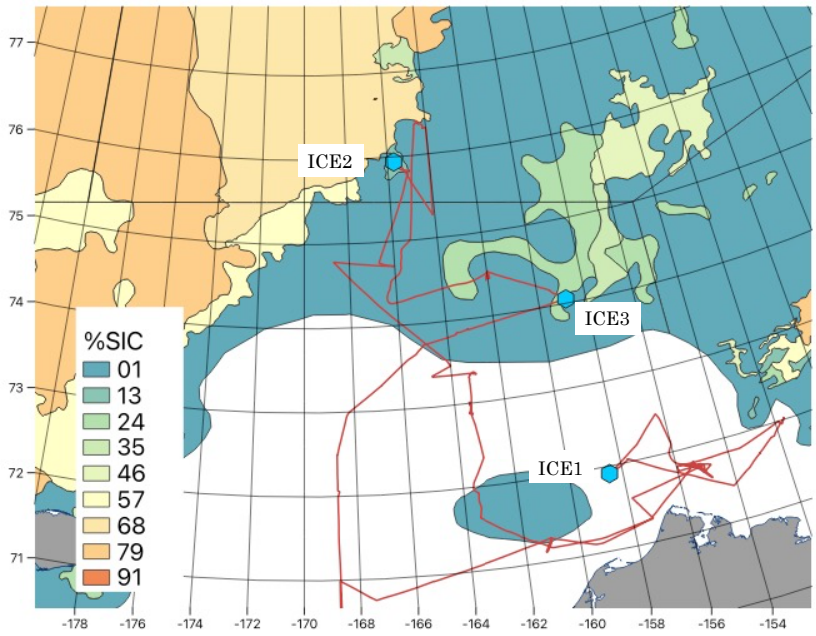

Figure 3.3.20-1 Location where the floating ice samplings were conducted. The background color indicates sea ice concentration from NOAA on Sep 19.

Figure 3.3.20-2. Photos of the collected sea ice samples.

(6) Data archives

These data obtained in this cruise will be submitted to the Data Management Group of JAMSTEC, and will be opened to the public via "Data Research System for Whole Cruise Information in JAMSTEC (DARWIN)" in JAMSTEC web site <https://www.godac.jamstec.go.jp/darwin/en/>.

3.4. Under Ice Drone Trials

3.4-1. Science Party

Shojiro Ishibashi (JAMSTEC) – Engineer and the COMAI system integrator
Kiyotaka Tanaka (JAMSTEC) – Engineer and console operator
Makoto Sugesawa (JAMSTEC) – Engineer and field operator
Hiroshi Yoshida (JAMSTEC) – Engineer and field operator
Satomi Ogawa (NME) – Observational technician and console operator
Satoshi Kimura (JAMSTEC) – Scientist and tether handling master
Ryo Oyama (NME) – Chief observational technician and tether handler
Haruki Doi (NME) – Observational technician and tether handler
Seika Takai (NME) – Observational technician and tether handler
Nobuyuki Yamaoka (MOL) – Officer and tether handler
Amane Fujiwara (JAMSTEC) – Principal scientist and operation supporter
Tatsuhiro Fukuba (JAMSTEC) – Engineer (Not on board)
Yosaku Maeda (JAMSTEC) – Engineer (Not on board)
Hiroshi Matsumoto (JAMSTEC) – Engineer (Not on board)

3.4-2. Objective

The under-ice drone named COMAI (Fig. 3.4.1) is a middle size autonomous underwater vehicle (AUV) for observations under ice in the Arctic. The drone will autonomously cruise and observe environment under ice in coverage area planned of 15 km. The completion of fully autonomous operation under ice is more complex than operation in open sea because of two big breakthrough items: positioning and emergency recovery. At high latitudes, performance of magnetic compasses or inertial navigation systems (INS) degrades, and navigation errors increase. In the latest cruise, we tested the performance of navigation and autonomous cruise (single function), and attempted observations under sea ice using a manual operation mode. This year we try the fully autonomous cruise with a scenario in high latitude area, and sea ice observation using the multi beam sonar with semi-autonomous cruising mode.

Figure 3.4.1. A recovery scene of COMAI. (Photo by Kato)

The test items are followings:
fully autonomous cruising with scenario which includes 3D-passing points, cruising modes, speeds and so on, and
under sea ice observation with the multi beam sonar cruising by a single function autonomous mode (w/o scenario).
All tests are carried out with a thin tether cable for safety.

3.4-3. Instruments and Methods

The drone is a platform of observation sensors. It will autonomously cruise and survey under sea- ice without a tether cable (At this time a tether cable is used in all trials). Specifications of the drone are listed in Table 3.4.1. The maximum cruising range designed is about 30 km or endurance is about 16 hours (at cruising speed of 1 kt). The drone utilizes a hybrid navigation system consisting of a MEMS inertial measurement unit, a magnetic compass, a depth sensor and a Doppler velocity log (DVL) as shown in Fig. 3.4.2. The drone has four operation modes: 1) an untethered, which means that the connection is made with a thin optical fiber instead of a thick cable, remotely operated vehicle mode (UROV), 2) an acoustic ROV mode (AROV), 3) a radio wave ROV mode (RROV), and 4) an autonomous underwater vehicle (AUV) mode, and an initial mode for individual test of the functions. In the AUV mode, three cruising patterns (heading-depth control, way-point control, and way-line control) are selectable. It has a special cruising mode named “escape mode” (the ability to exit the sea ice zone in the event of a system anomaly under sea ice). If one of the navigation devices is down, the drone automatically changes the control mode to the heading-depth control with an acoustic super short baseline navigation toward an acoustic light house pre-deployed as shown in Fig. 3.4.3.

Table 3.4.1: Specifications of COMAI.

Items	Specifications	Remarks
Size	2.3 x 0.6 x 0.7 m	
Weight	330 kg	in air
Depth rating	300 m	
Cruising speed	2 kt max.	
Cruising range	30 km	
Power	Li-ion battery （5.7 kWh）	
Actuators	Horizontal thrusters (100 W) x 2 Vertical thruster (100 W) x 1 Rudders	
Scientific payloads	CTD (conductivity, temperature, depth) Turbidity and chlorophyll meter Snapshot camera Multi beam sonar eDNA sampler	 installed on top side installed on top side (New item)

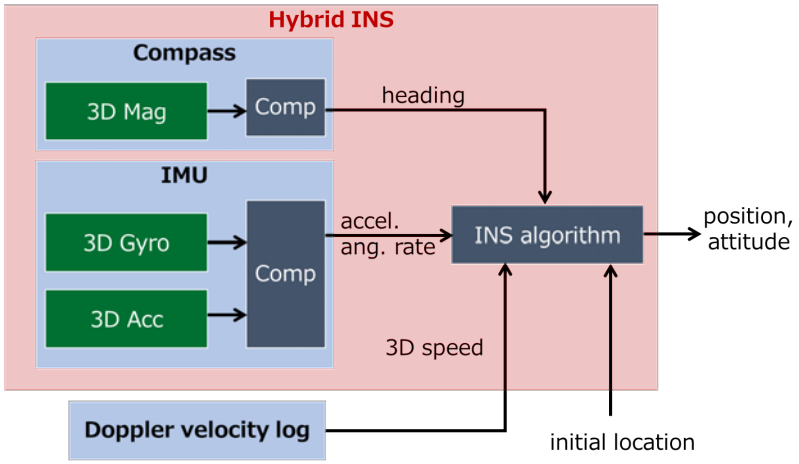

Figure 3.4.2 Block diagram of the hybrid navigation system.

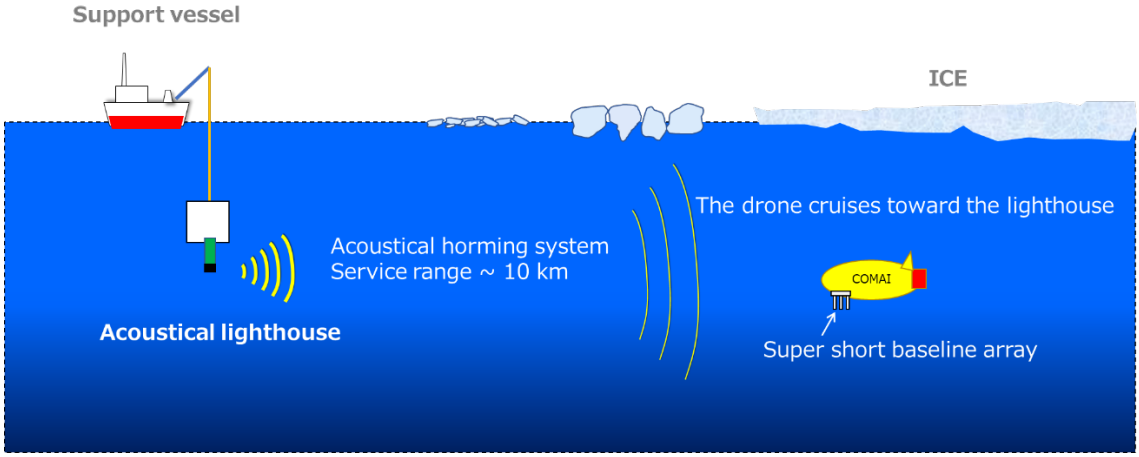

Figure 3.4.3. A working image of the heading-depth control with the acoustic super short baseline navigation in the escape mode.

COMAI is equipped with scientifical sensors: a CTD sensor (miniCTD, Valeport), a turbidity and chlorophyll meter (ECO FLUNTU, WET Labs), a snapshot camera (2592 x 1944 pixels, F2.2) with LED strobe lights, and a 260 kHz multi beam sonar (837B Delta T, IMAGENEX). The camera and the multi beam sonar are mounted on top side of the body because of ice bottom observations. All data obtained are automatically logged in a drone internal memory and a hard disk of the personal computer of the ship-side console (if each ROV mode). In the 2025 trial, an eDNA sampler is newly installed and used.

3.4-4. Test log

We carried out five dives in this cruise. Table 3.4.2 and Figure 3.4.4 show the dive points and trial information.

Table 3.4.2: Dive list of COMAI.

Dive No.	Theme	Date UTC	SMT (UTC-8)	JST (UTC+9)	Area	Launch Lat.	Launch Lon.	Depth (m)	HoistUp (SMT)	Launch (SMT)	HoistUp (SMT)	On Deck (SMT)
–	Ballast Adj.	9/7/25	9/7/25	9/8/25	Off Barrow	71-17.05N	160-59.95N	49	9:09	9:11	9:18	9:21
–	Training	9/7/25	9/7/25	9/8/25	Off Barrow	71-17.05N	160-59.95N	49	9:45	9:47	10:36	10:39
Dive1	Scenario	9/7/25	9/7/25	9/8/25	Off Barrow	71-17.12N	161-00.10	49	13:36	13:39	15:33	15:36
Dive2	Ice Survey	9/14/25	9/14/25	9/15/25	Arctic Ocean	73-17.41N	163-18.86W	93	14:03	14:05	15:08	15:10
Dive3	Ice Survey	9/15/25	9/15/25	9/16/25	Arctic Ocean	73-21.41N	163-10.60W	94	9:12	9:15	10:25	10:28
Dive4	Ice Survey	9/18/25	9/18/25	9/19/25	Chukchi sea	76-23.52N	164-28.36W	614	10:17	10:20	11:41	11:43
Dive5	Scenario	9/23/25	9/23/25	9/24/25	Chukchi sea	67-30.00N	168-30.00W	49	9:24	9:26	10:47	10:50

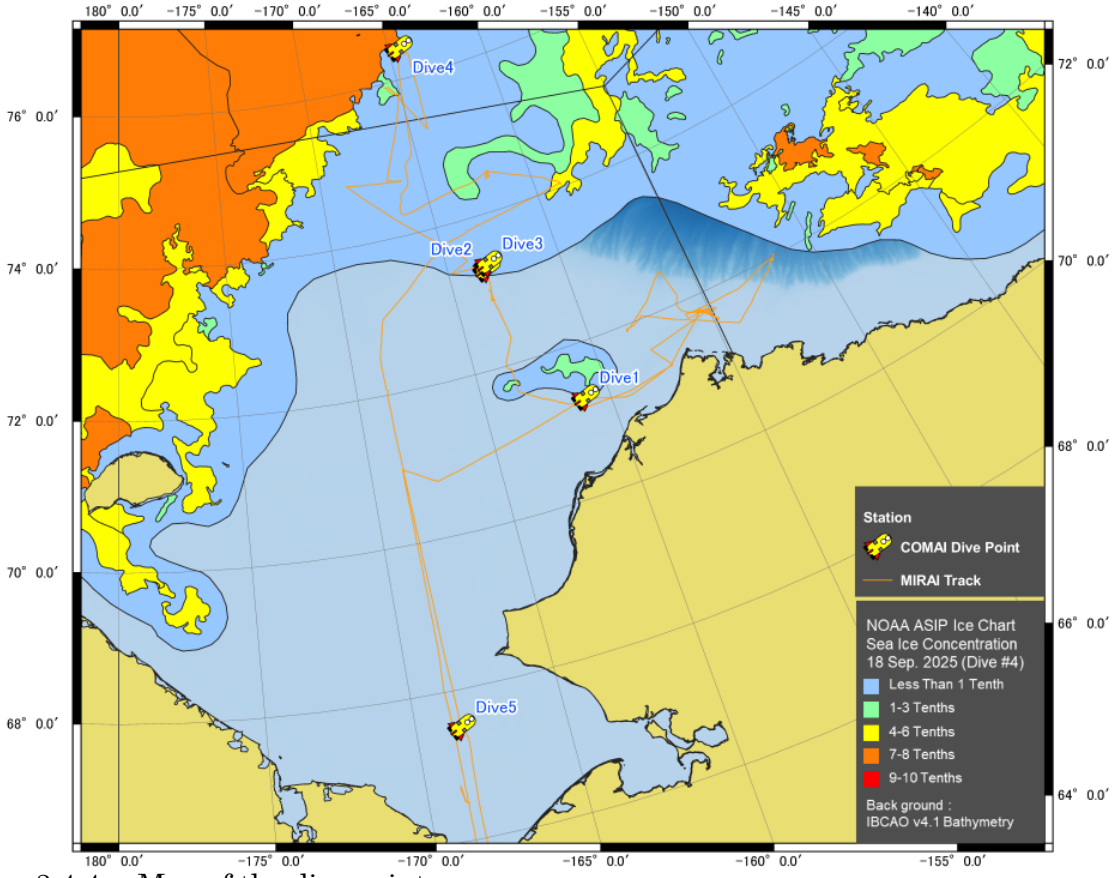

Figure 3.4.4. Map of the dive points.

3.4-5. Preliminary results

1) Fully autonomous cruising with scenarios

Dives 1 and 5 were autonomous cruising tests in open sea. In these tests, we evaluated scenario cruising errors caused by environmental disturbance and navigation system errors in high attitude areas. Contents of a scenario are multiple way points (longitude, latitude, depth), control modes, vehicle speeds and so on. In launch of COMAI, the support ship keeps its position for keeping distance from the 1st way point described in the scenario. After launching COMAI and then starting the scenario, the support ship and COMAI cruise side by side because COMAI is connected by a tether cable (~1 km long). A scenario start command is sent by acoustic communication for realizing real autonomous control. This means that the tether cable including optical fiber is connected but does not use optical communication. In navigation bottom tracking mode of the DVL was available so that the trial area was shallow.

Fig. 3.4.5 shows COMA cruising track and the waypoints described in the scenario in Dive 1. COMAI followed the scenario until the waypoint 2, and after passing through that its heading was abnormally spun during depth shift (Figure 3.4.6). An operator monitored it aborted the test because ongoing of the test has a risk. The cause of the spin is under investigation. Dive 5 is retry of the scenario cruising. We prepared new scenario (1 km travel with 6 waypoints, two control modes (way point and way line), and shifting depth and heading). After launching COMAI, it started with the scenario via acoustic communication, normally cruised via all waypoints,

and then automatically surfaced. The test achieved complete scenario cruising. The data in dive 5 are not shown here because of writing and publishing research articles.

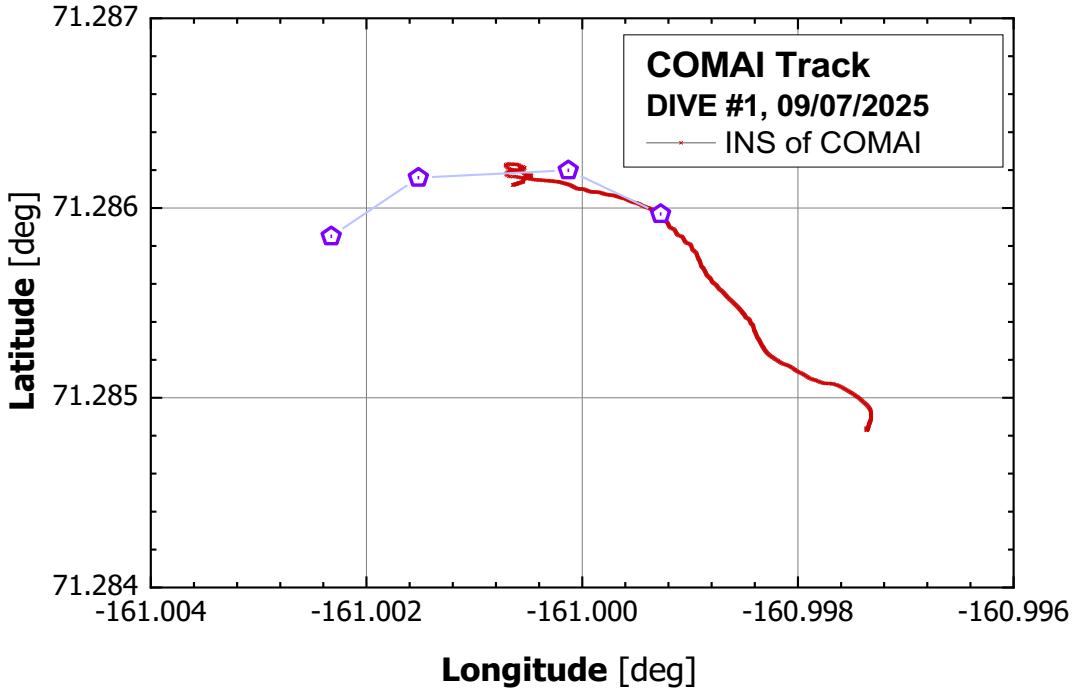

Figure 3.4.5. The drone track in Dive 1. Red dots and purple mark denote INS track measured and way points defined in the scenario, respectively.

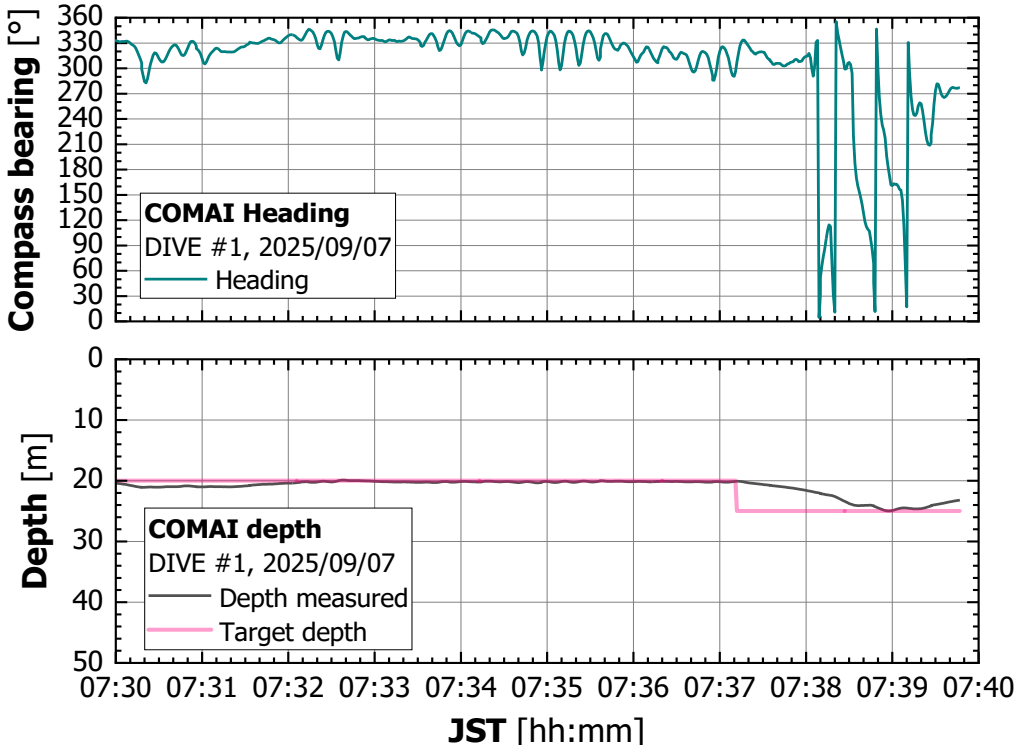

Figure 3.4.6. Time-series data of compass bearing (upper) and depth (lower) in Dive 2.

2) Observation performance

The depth dependences of fluorescence and turbidity in Dives 1 and 2 are shown in Figure 3.4.7. In Dive 1, there are two layers of density discontinuity around 5 meters and 15 meters. And region of chlorophyll dominance was observed at depths around 20 m. Below depth of 25 meters, turbidity increased due to roll up seafloor sediments. A density discontinuity is around 17 meters in Dive 2. We also obtained the data in Dive 3~5 which would be reported in research papers.

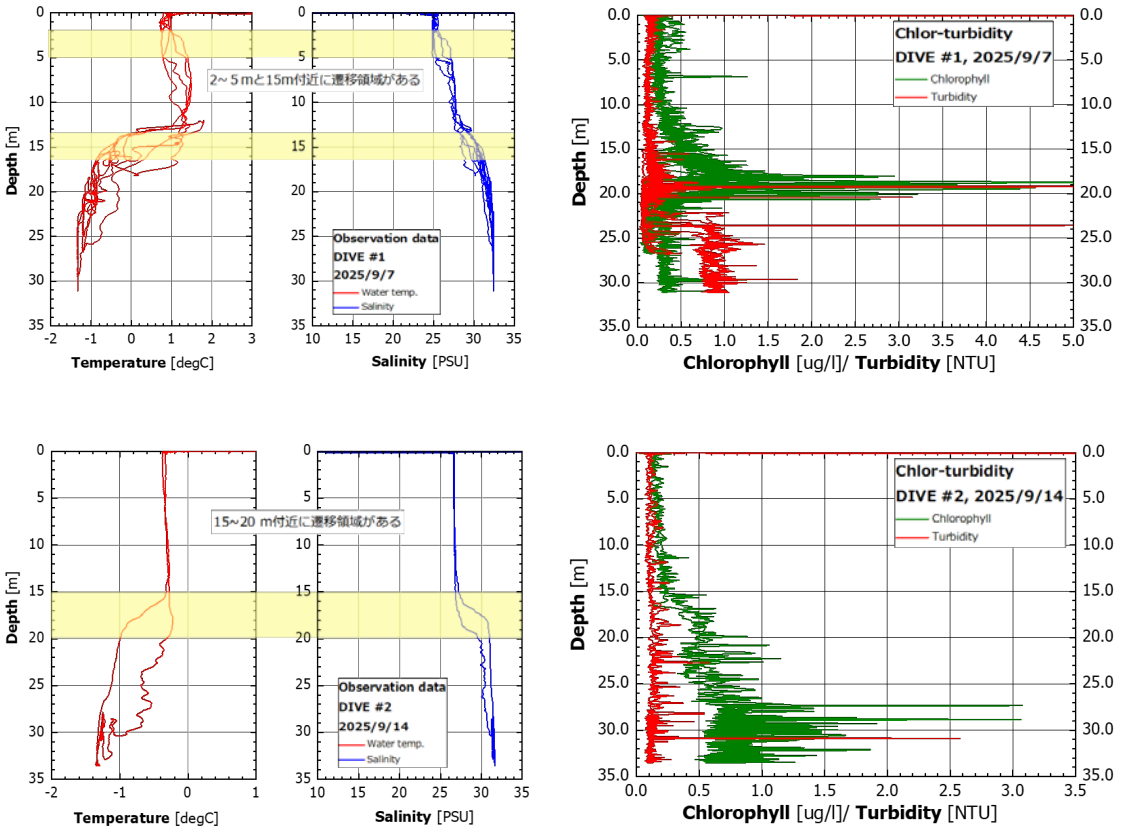

Figure 3.4.7. Depth vs. water temperature, salinity, fluorescence and turbidity in Dive 1 (upper) and 2 (lower).

In Dive 2 and Dive 3, we tried to obtain sonar images and snapshots, but COMAL could not reach to the bottom of sea-ice due to sea current. In Dive 4, we had luck with under-ice cruise and obtained images. COMAI cruised under 20-m class ice kept depth of about 30 m. Snapshot image is shown in Figure 3.4.8. The detail of this trial will be presented in a conference in next year.

.

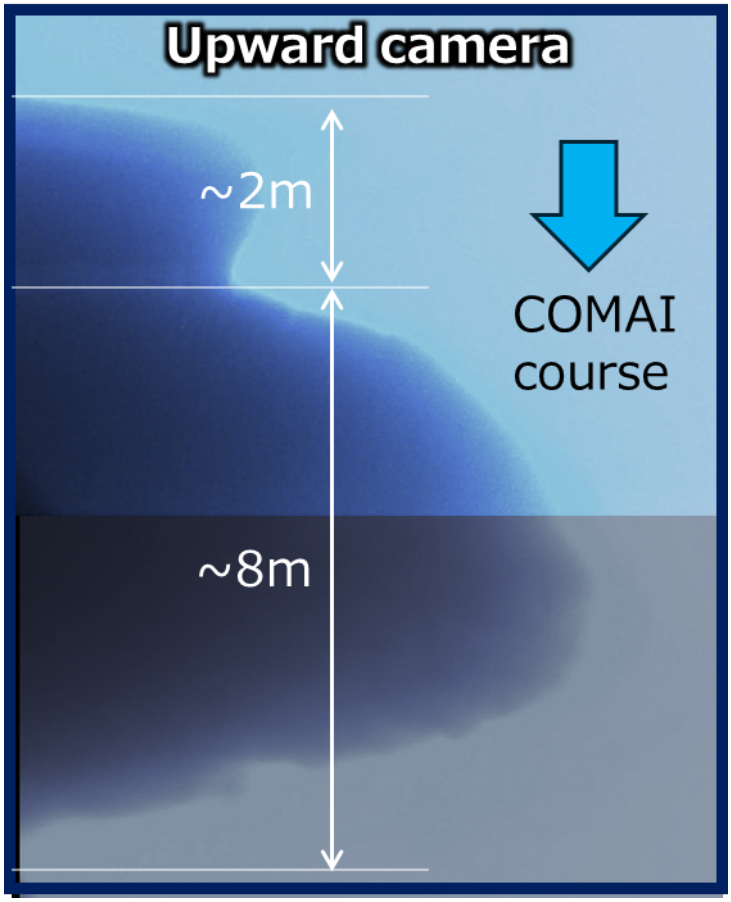

Figure 3.4.8. Snapshot image of part of sea-ice bottom in dive 4.

3) Summary of trials
We successfully achieved:
fully autonomous scenario cruise in high attitude area, and
under-ice autonomous cruise according to the design concept and ice bottom image observation.
We had good luck obtaining the latter result, because COMAI does not have a way to find ice from a distance horizontally. In this trial, the ice happened passing through the setting course of COMAI. Next trials are planned in 2027 using the new R/V MIRAI 2 which can approach ice edge and then we will conduct tether-less diving.
During this year's cruise, the captain and the ice navigator gave us a lot of advice on testing in icy waters. We also thank the Chief Scientist for arranging nice situations of COMAI's diving. We would like to express my sincere appreciation.

3.4-6. Data archives

This data obtained on this cruise will be submitted to the Data Management Group (DMG) of JAMSTEC, and will be opened to the public via "Data Research System for Whole Cruise Information in JAMSTEC (DARWIN)" in JAMSTEC web site.
<https://www.godac.jamstec.go.jp/darwin/en/>

3.5 Geology

3.5.1. Sea bottom topography measurements

(1) Personnel

Amane Fujiwara	JAMSTEC	-PI
Ryo Oyama	NME(Nippon Marine Enterprises, Ltd.)	
Satomi Ogawa	NME	
Haruki Doi	NME	
Seika Takai	NME	
Masanori Murakami	MIRAI Crew	

(2) Objectives

R/V MIRAI is equipped with the Multi Beam Echo Sounding system (MBES; SEABEAM 3012 (L3 Communications ELAC Nautik, Germany)) and Sub-Bottom Profiler (SBP), Bathy 2010 (SyQwest). The objective of MBES and SBP is to collect bathymetric data and sub-bottom profiling data especially for geological and geophysical studies.

(3) Parameters

MBES: Depth [m]
SBP: Sub-bottom profiling [m]

(4) Instruments and Methods

The "SEABEAM 3012" on R/V MIRAI was used for bathymetry mapping during this cruise. To get accurate sound velocity of water column for ray-path correction of acoustic beams, we determined sound velocities at the depth of 6.62 m, the bottom of the ship, by the surface sound velocimeter. We made sound velocity profiles based on the observations of CTD, XCTD and Argo float conducted in this cruise by the equation in Del Grosso (1974).
The "Bathy 2010" system was used for determining physical properties of the sea floor and for imaging and characterizing geological information several tens of meters below the sea floor. Its sound velocity was fixed 1,500 m/s during operations.

Table 3.5.1-1 and 3.5.1-2 show system configuration and performance of SEABEAM 3012 and Bathy2010 system.

Table 3.5.1-1: SEABEAM 3012 System configuration and performance

Frequency:	12 kHz
Transmit beam width:	2.0 degree
Transmit power:	4 kW
Transmit pulse length:	2 to 20 msec.
Receive beam width:	1.6 degree
Depth range:	50 to 11,000 m
Number of beams:	301 beams (Spacing mode: Equi-angle)
Beam spacing:	1.5 % of water depth (Spacing mode: Equi-distance)
Swath width:	60 to 150 degrees
Depth accuracy:	< 1 % of water depth (average across the swath)

Table 3.5.1-2: Bathy2010 System configuration and performance

Frequency:	3.5 kHz (FM sweep)

Transmit beam width: 30 degree
Transmit pulse length: 0.5 to 50 msec
Strata resolution: Up to 8 cm with 300 m of bottom penetration according to bottom type
Depth resolution: 0.1 feet, 0.1 m
Depth accuracy: ±10 cm to 100 m, ± 0.3% to 6,000 m
Sound velocity: 1,500 m/s (fix)

(5) Observation log
i) MBES: 00:27UTC 01 Sep. 2025 - 21:41UTC 01 Sep. 2025
22:45UTC 01 Sep. 2025 - 02:28UTC 02 Sep. 2025
02:40UTC 10 Sep. 2025 - 01:54UTC 11 Sep. 2025
22:56UTC 11 Sep. 2025 - 08:44UTC 12 Sep. 2025
02:28UTC 16 Sep. 2025 - 18:07UTC 18 Sep. 2025
19:20UTC 18 Sep. 2025 - 01:47UTC 22 Sep. 2025
18:49UTC 25 Sep. 2025 - 23:49UTC 02 Oct. 2025

ii) SBP: Stn.03 (18:47UTC 04 Sep. 2025 - 19:58UTC 04 Sep. 2025)
Stn.04 (23:09UTC 04 Sep. 2025 - 23:17UTC 04 Sep. 2025)
Stn.12 (16:42UTC 06 Sep. 2025 - 16:50UTC 06 Sep. 2025)
Stn.13 (19:22UTC 06 Sep. 2025 - 19:27UTC 06 Sep. 2025)
Stn.30 (23:33UTC 13 Sep. 2025 - 23:41UTC 13 Sep. 2025)
Stn.31 (17:33UTC 16 Sep. 2025 - 17:43UTC 16 Sep. 2025)

(6) Preliminary Results
The results will be published after primary processing.

(7) Data archives
These data obtained in this cruise will be submitted to the Data Management Group of JAMSTEC, and will be opened to the public via "Data Research System for Whole Cruise Information in JAMSTEC (DARWIN)" in JAMSTEC web site.
< https://www.godac.jamstec.go.jp/darwin/en/ >

3.5.2. Sea surface gravity measurements

(1) Personnel

Amane Fujiwara	JAMSTEC -PI
Ryo Oyama	NME(Nippon Marine Enterprises, Ltd.)
Satomi Ogawa	NME
Haruki Doi	NME
Seika Takai	NME
Masanori Murakami	MIRAI Crew

(2) Objective
The local gravity is an important parameter in geophysics and geodesy. The gravity data were collected during this cruise.

(3) Parameters
Relative Gravity [CU: Counter Unit]
[mGal] = (coef.: 0.9946) * [CU]

(4) Instruments and Methods

The relative gravity using LaCoste and Romberg air-sea gravity meter S-116 (Micro-g LaCoste, LLC) was measured during the cruise. To convert the relative gravity to absolute one, we measured gravity, using the portable gravity meter (Scintrex gravity meter CG-5), at Sekinehama and Shimizu port as the reference points.

(5) Observation log
31 Aug. 2025 - 06 Oct. 2025

(6) Preliminary Results
Absolute gravity table is shown in Table 3.5.2-1

Table 3.5.2-1: Absolute gravity table of the MR25-05C cruise

No.	S-116 Date [m/d]	UTC	Port	Absolute Gravity [mGal]	Sea Level [cm]	Ship Draft [cm]	Gravity at Sensor *1 [mGal]	Gravity [mGal]
#1	7/23	23:56	Sekinehama	980371.88		341	643	
	980373.19		12647.07					
#2	8/29	21:21	Dutch Harbor	unknown		330	642	
	unknown		13807.45					
#3	10/6	03:44	Shimizu (Sodeshi)	979728.98		245	590	
	979729.87		12001.27					

*1: Gravity at Sensor = Absolute Gravity + Sea Level*0.3086/100 + (Draft-530)/100*0.2222

(7) Data archives
These data obtained in this cruise will be submitted to the Data Management Group of JAMSTEC, and will be opened to the public via "Data Research System for Whole Cruise Information in JAMSTEC (DARWIN)" in JAMSTEC web site.
< https://www.godac.jamstec.go.jp/darwin/en/ >

3.5.3. Surface magnetic field measurement

(1) Personnel

Amane Fujiwara	JAMSTEC	-PI
Ryo Oyama	NME(Nippon Marine Enterprises, Ltd.)	
Satomi Ogawa	NME	
Haruki Doi	NME	
Seika Takai	NME	
Masanori Murakami	MIRAI Crew	

(2) Objective
Measurement of magnetic force on the sea is required for the geophysical investigations of marine magnetic anomaly caused by magnetization in upper crustal structure. We measured geomagnetic field using a three-component magnetometer during this cruise.

(3) Parameters
Three components of a magnetic field vector on-board, Hx, Hy, Hz [nT]
Hx : A magnetic field component in the bow/stern direction on the vessel

horizontal plane. “To bow” is positive.
Hy : A magnetic field component in the port/starboard direction on the vessel horizontal plane. “To starboard” is positive.
Hz : A perpendicular magnetic field component to the vessel horizontal plane. “upward” is positive.

(4) Instruments and Methods
A shipboard three-components magnetometer system (SFG2018, Tierra Tecnica) is equipped on-board R/V MIRAI. Three-axes flux-gate sensors with ring-cored coils are fixed on the fore mast. Outputs from the sensors are digitized by a 20-bit A/D converter (1 nT/LSB) and sampled at 8 times per second. Yaw (heading), Pitch and Roll are measured by the Inertial Navigation Unit (INU) for controlling attitude of a Doppler radar. Ship's position, speed over ground (Differential GNSS) and gyro data are taken from LAN every second.
The relation between a magnetic-field vector observed on-board, H_{ob}, (in the ship's fixed coordinate system) and the geomagnetic field vector, F, (in the Earth's fixed coordinate system) is expressed as:

$$H_{ob} = \tilde{A}\,\tilde{R}\,\tilde{P}\,\tilde{Y}\,F + H_p \qquad (a)$$

where $\tilde{R}$, $\tilde{P}$ and $\tilde{Y}$ are the matrices of rotation due to roll, pitch and heading of a ship, respectively. $\tilde{A}$ is a 3 x 3 matrix which represents magnetic susceptibility of the ship, and H_p is a magnetic field vector produced by a permanent magnetic moment of the ship's body. Rearrangement of Eq. (a) makes

$$\tilde{B}\,H_{ob} + H_{bp} = \tilde{R}\,\tilde{P}\,\tilde{Y}\,F \qquad (b)$$

where $\tilde{B} = \tilde{A}^{-1}$, and $H_{bp} = -\tilde{B}\,H_p$. The magnetic field, F, can be obtained by measuring, $\tilde{R}$, $\tilde{P}$, $\tilde{Y}$ and H_{ob}, if $\tilde{B}$ and H_{bp} are known. Twelve constants in $\tilde{B}$ and H_{bp} can be determined by measuring variation of H_{ob} with, $\tilde{R}$, $\tilde{P}$, and, $\tilde{Y}$ at a place where the geomagnetic field, F, is known.

(5) Observation log
31 Aug. 2025 - 05 Oct. 2025

(6) Preliminary Results
The results will be published after the primary processing.

(7) Data archives
These data obtained in this cruise will be submitted to the Data Management Group of JAMSTEC, and will be opened to the public via “Data Research System for Whole Cruise Information in JAMSTEC (DARWIN)” in JAMSTEC web site.
< https://www.godac.jamstec.go.jp/darwin/en/ >

(8) Remarks
For calibration of the ship’s magnetic effect, “figure-eight” turns (a pair of clockwise and anti-clockwise rotation) were held at the following periods and positions.
01:57UTC 10 Sep. 2025 - 02:18UTC 10 Sep. 2025 (71-49N, 155-57W)
00:23UTC 20 Sep. 2025 - 00:45UTC 20 Sep. 2025 (74-31N, 161-56W)
23:30UTC 03 Oct. 2025 - 23:52UTC 03 Oct. 2025 (34-51N, 138-39E)

3.6. Public outreach

(1) Responsible personnel

Akiko Mohri	NIPR	- Principal Investigator
Amane Fujiwara	JAMSTEC	
Mariko Hatta	JAMSTCE	
Yuri Fukai	JAMSTCE	
Eiji Watanabe*	JAMSTCE	
Motoyo Ito*	JAMSTEC	
Shigeto Nishino*	JAMSTEC	
Aya Mikami*	JAMSTEC	
Yoshiyuki Ogita*	JAMSTEC	
Motoyo Kudo*	JAMSTEC	
Kana Sugimoto*	NIPR	
Jun Ono*	NIPR	
Jun Inoue*	NIPR	

*: onshore members

(2) Purpose/background

Purpose

To stimulate public interest in the Arctic and Arctic research by sharing up-to-date information and unique content available only from on board R/V *Mirai*.

The final live streaming was presented as a special edition, featuring a summary of the MR25-05C cruise and a retrospective on R/V *Mirai*'s history and achievements of the Arctic cruises.

Background

To commemorate the final Arctic cruise of the R/V *Mirai*, the first live streaming from the Arctic Ocean was expected.

A science communicator responsible for public outreach had extensive experience in planning, organizing, and executing live streaming.

(3) Activities

(3-1) Live streaming from R/V *Mirai*

As part of the public outreach activities of the ArCS III project, live streaming from on board the vessel was carried out during MR25-05C. For each onboard research project, interviews were conducted, and both photographic and video documentation were collected before and during the cruise. Observation activities and daily life on board were live-streamed via a high-speed internet connection (Starlink).

Live streaming method for each program

A Starlink Maritime antenna was secured to the handrail above Wet Lab 1, and the cable from the antenna was routed into the semi dry lab or No.1 mooring body shed. Live streaming was carried out from the semi dry lab and the area around No.1 mooring body shed, where a stable network connection could be ensured.

Live! R/V *Mirai* Arctic Cruise #Mirai the FINAL (YouTube Live Streaming)

URL: https://www.arcs3.nipr.ac.jp/event/2045/

A zoom meeting connecting the onboard and the onshore members was streamed via JAMSTEC's official YouTube channel.

URL: https://www.youtube.com/channel/UCapekjAa9x29a-gZNsWci1Q
Questions from viewers were collected in advance through a Google form, and additional questions were accepted during each live streaming via chat or verbal interaction.
Announcements regarding the live streaming was made through the official SNS accounts (X, Facebook, Instagram) of JAMSTEC and NIPR.
The live-streamed videos were made available on JAMSTEC's official YouTube channel for a limited time and will be re-edited and archived for future use.

(3-2) NIPR– Public Open Day
URL: https://www.nipr.ac.jp/tanken2025/program1/
JAMSTEC– Marine Discovery Lab
URL: https://www.jamstec.go.jp/j/pr/events/mdl20250927/
A zoom meeting connecting the onboard and the onshore members was projected onto a screen at the live event venue.
Questions from the audience at the venue were addressed directly in real time.

(3-3) "Messages from the Arctic Ocean" (blog)
Onboard members wrote blogs on the theme of *Mirai*'s Arctic cruise, which were disseminated via the ArCS III website and the official JAMSTEC X account.
ArCS III website https://www.arcs3.nipr.ac.jp/report/category/cruise/mirai2025/message/
Official JAMSTEC X https://x.com/jamstec_pr

(3-4) Cruise Track of R/V *Mirai* during MR25-05C
During MR25-05C, images of the vessel's route and sea-ice extent map —provided by Arctic and Anterctic Data archive System (ADS) and Arctic Sea Ice Information Center in support of the cruise—were posted on the ArCS III website.
ArCS III website https://www.arcs3.nipr.ac.jp/report/1544/

(4) Results

(4-1) Live! R/V *Mirai* Arctic Cruise #Mirai the FINAL (YouTube Live Streaming)
Planner / Navigator: Akiko Mohri (NIPR)
Guests: Onboard and onshore researchers
Onshore supporters: Eiji Watanabe, Motoyo Ito, Aya Mikami, Yoshiyuki Ogita, Motoyo Kudo, Takamasa Tamura (JAMSTEC)

#	Thumbnail	Streaming Date and Time (UTC)	Guests	Contents	Views (As of Nov. 9, 2025)
1		2025-9-3 9:00-9:15	Eiji Watanabe, Amane Fujiwara (JAMSTEC)	Introduction of *Mirai* and ArCS III *Mirai*'s road to departure	4846

2		2025-9-10 9:00-9:20	Mariko Hatta (JAMSTEC), Kohei Matsuno (Hokkaido Univ.)	This week's *Mirai* Water sampling Plankton	1620
3		2025-9-17 9:00-9:20	Fumikazu Taketani (JAMSTEC), Daiki Nomura (Hokkaido Univ.)	This week's *Mirai* Tethered balloon Sea ice	2771
4		2025-9-24 9:00-9:20	Jonaotaro Onodera (JAMSTEC), Tatsuya Kawakami (Hokkaido Univ.)	This week's *Mirai* Mooning system Environmental DNA	1208
5		2025-9-30 9:00-10:00	Takuhei Shiozaki (The Univ. of Tokyo), Shojiro Ishibashi, Amane Fujiwara, Eiji Watanabe, Shigeto Nishino, Motoyo Ito, Yuri Fukai, Takashi Kikuchi (JAMSTEC), Ryota Akino (Hokkaido Univ.), Ikkan Kamiyama (TUMSAT)	Carbon sequestration COMAI *Mirai*'s history and achievements ECS Dialogue	1656

Delivering the latest updates from on board

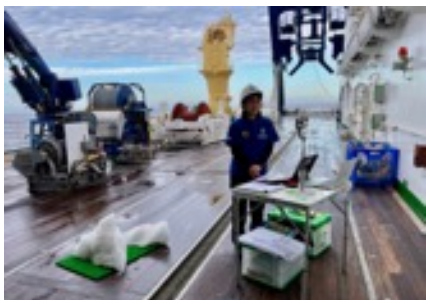
Live streaming studio setup

Sharing on-site exclusives

Real-time answering questions from viewers

Reflecting on achievements of *Mirai*

A retrospective on the *Mirai* cruise with ECS

Selected questions submitted through the online form

- What is the Arctic Ocean like this year? Japan experienced an extremely hot summer.
- What differences have you observed between the past and now?
- How many people are on board *Mirai* to conduct research during the cruise?
- Does most of the sea ice melt in the Arctic during summer?
- Did you see seals, clione, or white whales?
- Due to global warming, are marine species from warmer regions beginning to move into the Arctic?
- What kind of food do you eat on board the ship?
- What is the first thing you would like to do when you return to Japan?

(4-2) NIPR– Public Open Day
Title: Live streaming! R/V *Mirai* Arctic Cruise 2025
Streaming Date and Time (UTC): 2025-9-27 2:45-3:15
Planners / Navigators: Akiko Mohri, Jun Inoue (NIPR)
Guests: Daiki Nomura (Hokkaido Univ.), Amane Fujiwara (JAMSTEC)
Onshore supporters: Jun Ono, Takara Teramura (NIPR)
Contents: The Arctic quiz, This month's *Mirai*, Tethered balloon, Sea ice, and Daliy life on *Mirai*

At the venue (NIPR)

Sea ice cutting demonstration

Event Participant Survey

During the NIPR Open Day, the live streaming from R/V *Mirai* received high engagement from participants. In the "Science Café / Live Programs" category of the participant survey, the live streaming ranked second out of 10 programs. Many free-response comments highlighted the program positively, noting that the live streaming conveyed a strong sense of presence, introduced *Mirai* to new audiences, and made the Arctic field research feel accessible. For example, we received comments such as the following:

- I was glad to be able to touch real sea ice. (Sea ice collected in the Arctic Ocean was displayed at the venue.)
- I want to smell the 'stinky' sea ice.
- Watching the sea-ice catching demonstration was fascinating.
- The live streaming from R/V *Mirai* made me feel as if I were actually in the Arctic Ocean.
- These results indicate that the outreach activity effectively enhanced public interest and awareness of the Arctic and Arctic research.

(4-3) JAMSTEC– Marine Discovery Lab

Title: What is happening in the Arctic Ocean.
Streaming Date and Time (UTC): 2025-9-24 4:50-5:10
Planners / Navigators: JAMSTEC PR officers
Guests: Mariko Hatta (JAMSTEC), Akiko Mohri (NIPR)
Contents: Q&A session and introduction of observation instruments on board R/V *Mirai*

Locations of the live streaming

Date	Program (*)	Position
2025-9-3	JAMSTEC#1	Lat. 62°N Long. 167°W
2025-9-10	JAMSTEC #2	Lat. 72°N Long. 151°W
2025-9-17	JAMSTEC #3	Lat. 75°N Long. 165°W
2025-9-24	JAMSTEC #4	Lat. 65°N Long. 168°W
2025-9-27	NIPR JAM-MDL	Lat. 55°N Long. 175°E
2025-9-30	JAMSTEC #5	Lat. 45°N Long. 157°E

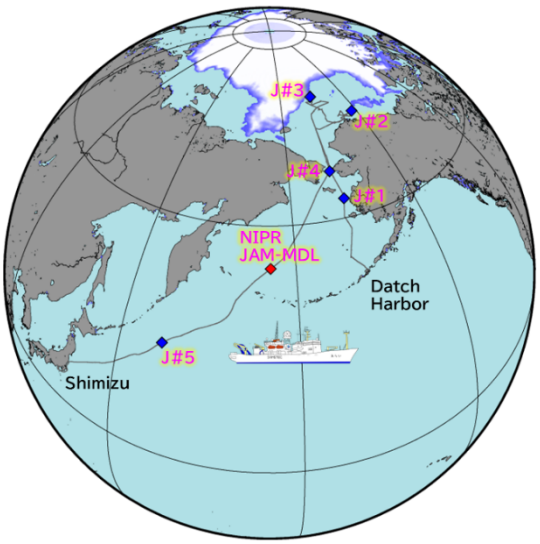

Modified from figures provided by A. Fujiwara

* JAMSTEC#1~5: Live! R/V *Mirai* Arctic Cruise #Mirai the FINAL #1~5
NIPR: NIPR– Public Open Day
JAM-MDL: JAMSTEC– Marine Discovery Lab

(4-4) Internet connection environment

By using a high-speed internet connection, real-time communication and the sharing of photo slideshows between onboard and onshore members were possible with minimal time lag. However, when sharing video files, temporary disruptions (stuttering of the video) were observed.

During the live streaming from the Arctic Ocean and the northern Bering Sea, communication between onboard and onshore members was occasionally interrupted for approximately 1 minute. These interruptions occurred twice in the first live streaming, several times in the second and third live streaming and once in the fourth one.

When communication was interrupted, the onshore supporter maintained the flow of the program by reading comments from the chat and responding to questions. Once the connection with R/V *Mirai* was restored, the supporter guided the program to resume smoothly from the point where it had been interrupted.

(4-5) Future plan

These next steps will support more accessible, engaging, and sustainable live streaming from the Arctic research cruise.

Strengthen the live streaming environment, including improving the stability and reliability of the internet connection.

Expand the range of onboard locations used for live streaming.

Schedule live streaming to align with daytime on board.

Plan and develop a framework that enables live streaming to be conducted during future Arctic cruises on a continuing basis.

(4-5) “Messages from the Arctic ocean” (blog)
A total of 22 articles have been posted on ArCS III website, official JAMSTEC X and YouTube channel. One of the most highly engaged posts on X was about a polar bear, which received over 8,238 “likes” and recorded more than 275,000 views. (https://x.com/JAMSTEC_PR/status/1982756274128425251) (as of November 9, 2025)

(4-6) Cruise Track of R/V *Mirai* during MR25-05C
A total of 41 images were posted on ArCS III website.

(5) Acknowledgements
I would like to express my sincere appreciation to everyone who contributed to our real-time outreach activities, including the onboard researchers, vessel crew, observation technicians, onshore supporters, and public communication staff. I am also grateful for the cooperation and interest of all participants and viewers. These outreach activities were made possible through your support.

4. Cruise Log

Table 4-1 Cruise Log of MR25-05C

Date & Time [UTC]	Stn info	Activities
2025/8/31 2:00		Departed the port of Dutch Harbor
2025/8/31 23:55		Started continuous monitoring of sea surface water properties
2025/9/1 0:04		XCTD cast1
2025/9/1 14:30		Releaser and CTD test cast
2025/9/2 18:30		radiosonde launch
2025/9/2 22:30		radiosonde launch
2025/9/4 3:00	Stn.1	CTD/water-sampling
2025/9/4 3:41		NORPAC-net tow
2025/9/4 3:50		80cm ring-net tow
2025/9/4 5:22		XCTD cast2
2025/9/4 5:38		XCTD cast3
2025/9/4 5:55		XCTD cast4
2025/9/4 6:12		XCTD cast5
2025/9/4 6:29		XCTD cast6
2025/9/4 6:50		XCTD cast7
2025/9/4 8:10	Stn.002	NORPAC-net tow
2025/9/4 8:24		CTD/water-sampling
2025/9/4 16:00	Stn.003	radiosonde launch
2025/9/4 17:06	TB-1	tethered balloon launch
2025/9/4 18:14		CTD/water-sampling
2025/9/4 19:03		sediment coring
2025/9/4 19:16		in-situ filtration
2025/9/4 22:46	Stn.004	NORPAC-net tow
2025/9/4 22:56		sediment coring
2025/9/4 23:11		CTD/water-sampling
2025/9/5 3:58	Stn.005	CTD/water-sampling
2025/9/5 10:00	Stn.006	CTD/water-sampling
2025/9/5 10:40		NORPAC-net tow
2025/9/5 10:50		PTZ camera lowering
2025/9/5 11:06		sediment coring
2025/9/5 15:06	Stn.007	sediment coring
2025/9/5 15:26		CTD/water-sampling
2025/9/5 19:01		radiosonde launch
2025/9/5 20:59	Stn.008	CTD/water-sampling
2025/9/5 21:40		NORPAC-net tow
2025/9/5 21:50		PTZ camera lowering
2025/9/5 22:03		In-situ filtration
2025/9/6 4:01	Stn.009	sediment coring
2025/9/6 4:20		CTD/water-sampling
2025/9/6 8:00	Stn.010	CTD/water-sampling
2025/9/6 8:33		NORPAC-net tow
2025/9/6 8:43		PTZ camera lowering
2025/9/6 12:00	Stn.011	sediment coring
2025/9/6 12:16		CTD/water-sampling
2025/9/6 15:38	Stn.012	CTD/water-sampling
2025/9/6 16:15		NORPAC-net tow
2025/9/6 16:27		PTZ camera lowering
2025/9/6 16:40		sediment coring
2025/9/6 19:19	Stn.013	sediment coring
2025/9/6 19:36		CTD 観測開始
2025/9/6 20:12		CTD/water-sampling
2025/9/6 23:40	Stn.014	CTD/water-sampling
2025/9/7 0:16		NORPAC-net tow
2025/9/7 0:23		PTZ camera lowering
2025/9/7 17:09	COMAI-1	COMAI dive
2025/9/7 21:00		RINKO profiler cast
2025/9/7 21:36		COMAI dive
2025/9/8 16:09	BCW	mooring recovery (BCW-24)
2025/9/8 18:02	BCC	mooring recovery (BCC-24)
2025/9/8 21:10	BCE	mooring recovery (BCE-24)

2025/9/8 22:06	Stn.015	CTD/water-sampling
2025/9/8 22:54		NORPAC-net tow
2025/9/8 23:04		Ring-net tow
2025/9/8 23:30		radiosonde launch
2025/9/8 23:34		PTZ camera lowering
2025/9/8 23:50		In-situ filtration
2025/9/9 2:48		XCTD cast8
2025/9/9 3:19		XCTD cast9
2025/9/9 3:40		XCTD cast10
2025/9/9 3:56		XCTD cast11
2025/9/9 4:11		XCTD cast12
2025/9/9 4:26		XCTD cast13
2025/9/9 4:41		XCTD cast14
2025/9/9 4:56		XCTD cast15
2025/9/9 5:13		XCTD cast16
2025/9/9 16:20	BCW	mooring deployment (BCW-25)
2025/9/9 18:07	BCC	mooring deployment (BCC-25)
2025/9/9 21:12	BCE	mooring deployment (BCE-25)
2025/9/9 22:21		radiosonde launch
2025/9/9 23:18	TB-2	tethered balloon launch
2025/9/10 1:56		figure-eight maneuver
2025/9/10 16:18	Stn.016	CTD/water-sampling
2025/9/10 16:41		XCTD cast17
2025/9/10 18:06		NORPAC-net tow
2025/9/10 18:17		Ring-net tow
2025/9/10 19:08		CTD/water sampling
2025/9/10 21:58		XCTD cast18
2025/9/10 23:23	Stn.017	CTD/water-sampling
2025/9/11 0:17		NORPAC-net tow
2025/9/11 0:34		Ring-net tow
2025/9/11 2:13		XCTD cast19
2025/9/11 3:36	Stn.018	NORPAC-net tow
2025/9/11 3:45		PTZ camera lowering
2025/9/11 3:57		sediment coring
2025/9/11 4:14		CTD/water-sampling
2025/9/11 16:40	Stn.019	sea ice sampling
2025/9/11 18:02		CTD/water-sampling
2025/9/11 18:43		NORPAC-net tow
2025/9/11 18:54		PTZ camera lowering
2025/9/11 19:08		sediment coring
2025/9/11 21:53	Stn.020	sediment coring
2025/9/11 22:13		CTD/water-sampling
2025/9/11 23:50		XCTD cast20
2025/9/12 1:33	Stn.021	CTD/water-sampling
2025/9/12 1:52		XCTD cast21
2025/9/12 2:04		XCTD cast22
2025/9/12 2:42		NORPAC-net tow
2025/9/12 2:52		Ring-net tow
2025/9/12 3:47		CTD/water-sampling
2025/9/12 15:59	Stn.022	CTD/water-sampling
2025/9/12 21:31	Stn.023	CTD
2025/9/12 22:02		XCTD cast23
2025/9/12 22:23	Stn.024	CTD/water-sampling
2025/9/12 23:09		sediment coring
2025/9/12 23:37		XCTD cast24
2025/9/13 0:13	Stn.025	CTD
2025/9/13 0:50		XCTD cast25
2025/9/13 1:09	Stn.026	CTD
2025/9/13 1:43		XCTD cast26
2025/9/13 4:58	Stn.027	CTD/water-sampling
2025/9/13 5:38		NORPAC-net tow
2025/9/13 5:51		PTZ camera lowering
2025/9/13 9:10	Stn.028	CTD/water-sampling
2025/9/13 14:30		XCTD cast27
2025/9/13 18:35	Stn.029	CTD/water-sampling
2025/9/13 19:08		NORPAC-net tow

2025/9/13 19:17		PTZ camera lowering
2025/9/13 23:06	Stn.030	PTZ camera lowering
2025/9/13 23:22		NORPAC-net tow
2025/9/13 23:32		sediment coring
2025/9/13 23:49		CTD/water-sampling
2025/9/14 22:03	COMAI-2	COMAI dive
2025/9/15 17:12	COMAI-3	COMAI dive
2025/9/15 19:15		Drone flight
2025/9/15 22:00	TB-3	radiosonde launch
2025/9/15 22:44		tethered balloon launch
2025/9/15 22:54		XCTD cast28
2025/9/16 0:28		radiosonde launch
2025/9/16 0:53		radiosonde launch
2025/9/16 16:01	Stn.031	CTD/water-sampling
2025/9/16 16:50		PTZ camera lowering
2025/9/16 17:08		NORPAC-net tow
2025/9/16 17:20		RING-net tow
2025/9/16 17:31		sediment coring
2025/9/16 21:25	Stn.032	PTZ camera lowering
2025/9/16 21:44		NORPAC-net tow
2025/9/16 21:55		RING-net tow
2025/9/16 22:08		radiosonde launch
2025/9/16 22:12		CTD/water-sampling
2025/9/16 23:29	TB-4	tethered balloon launch
2025/9/17 1:05		radiosonde launch
2025/9/17 16:25	Stn.033	sea ice sampling
2025/9/17 16:35		Drone flight
2025/9/17 18:00		CTD/water-sampling
2025/9/17 19:06		PTZ camera lowering
2025/9/17 19:24		NORPAC-net tow
2025/9/17 19:35		radiosonde launch
2025/9/17 23:24	Stn.034	PTZ camera lowering
2025/9/17 23:42		NORPAC-net tow
2025/9/18 0:00		CTD/water-sampling
2025/9/18 0:17		XCTD cast29
2025/9/18 16:53	COMAI-4	XCTD cast30
2025/9/18 18:17		COMAI dive
2025/9/18 22:30		towing CTD
2025/9/19 19:30	Stn.035	radiosonde launch
2025/9/19 21:34		mooring recovery (NAP24t)
2025/9/20 0:23		figure-eight maneuver
2025/9/20 16:23		mooring deployment (NAP25t)
2025/9/20 21:03		CTD/water-sampling
2025/9/20 21:22		XCTD cast31
2025/9/20 22:24		PTZ camera lowering
2025/9/20 22:41		NORPAC-net towing
2025/9/20 22:53		Ring-net tow
2025/9/20 23:08		In-situ filtration
2025/9/21 0:25		CTD/water-sampling
2025/9/21 3:02		XCTD cast32
2025/9/21 4:02		XCTD cast33
2025/9/21 5:01		XCTD cast34
2025/9/21 16:40	Stn.036	sea ice sampling
2025/9/21 16:43		Drone flight
2025/9/21 18:09		CTD/water-sampling
2025/9/21 18:33		XCTD cast35
2025/9/21 20:48		PTZ camera lowering
2025/9/21 21:05		NORPAC-net tow
2025/9/21 21:15		Ring-net tow
2025/9/21 21:30		radiosonde launch
2025/9/21 22:52		XCTD cast36
2025/9/22 0:08		XCTD cast37
2025/9/22 1:25		XCTD cast38
2025/9/22 2:43		XCTD cast39
2025/9/22 3:30		radiosonde launch
2025/9/22 4:19		XCTD cast40
2025/9/22 9:30		radiosonde launch

2025/9/22 12:12		XCTD cast41
2025/9/22 14:36	Stn.037	CTD/water-sampling
2025/9/22 15:14		PTZ camera lowering
2025/9/22 15:27		NORPAC-net tow
2025/9/22 15:36		sediment coring
2025/9/22 18:30		radiosonde launch
2025/9/22 18:52		XCTD cast42
2025/9/22 21:11		XCTD cast43
2025/9/23 15:54	COMAI-5	XCTD cast44
2025/9/23 17:24		COMAI dive
2025/9/23 20:47		radiosonde launch
2025/9/23 21:34	TB-5	tethered balloon launch
2025/9/23 23:16		radiosonde launch
2025/9/24 3:14		Crossed 65N
2025/9/25 0:30		radiosonde launch
2025/9/26 22:36		XCTD cast45
2025/9/27 2:30		radiosonde launch
2025/9/27 10:30		radiosonde launch
2025/9/28 3:30		radiosonde launch
2025/10/3 6:30		Ended continuous monitoring of sea surface water properties
2025/10/3 23:30		figure-eight maneuver
2025/10/5 0:00		Arrived at the port of Shimizu

5. Notice on using

This cruise report is a preliminary documentation as of the end of the cruise. This report is not necessarily corrected even if there is any inaccurate description (i.e., taxonomic classifications). This report is subject to be revised without notice. Some data in this report may be raw or unprocessed. If you are going to use or refer to the data in this report, it is recommended to ask the Chief Scientist for the latest status. Users of information on this report are requested to submit Publication Report to JAMSTEC.

https://www.godac.jamstec.go.jp/darwin/en/note.html#report
E-mail: submit-rv-cruise@jamstec.go.jp